SUSTAINABLE AND ADHESIVE-FREE LIGNOCELLULOSIC FIBERBOARDS FROM STEAM EXPLODED ARUNDO DONAX L.

Federica Vitrone

FEDERICA VITRONE

SUSTAINABLE AND ADHESIVE-FREE LIGNOCELLULOSIC FIBERBOARDS FROM STEAM EXPLODED *ARUNDO DONAX* L.

DOCTORAL THESIS

SUPERVISED BY

DR. JOAN SALVADÓ ROVIRA,
DEPARTMENT OF CHEMICAL ENGINEERING
DR. DIEGO RAMOS ROMERO,
DEPARTMENT OF MECHANICAL ENGINEERING

UNIVERSITAT ROVIRA i VIRGILI

TARRAGONA, 2023

DEPARTAMENT
D'ENGINYERIA QUÍMICA
Universitat Rovira i Virgili

Avinguda dels Països Catalans, 26
43007 Tarragona

Statement of supervision

Dr. Joan Salvadó Rovira, Professor at the Department of Chemical Engineering, and Dr. Diego Ramos Romero, Professor at the Department od Mechanical Engineering, both from the Rovira i Virgili University,

STATE that the present study, entitled "Sustainable and adhesive-free lignocellulosic fiberboards from steam exploded *Arundo donax* L.", presented by Federica Vitrone for the award of the degree of Doctor, has been carried out under their supervision at the Department of Chemical Engineering of this university, and that it fulfills all the requirements to be eligible for the International Doctorate Mention.

Tarragona, May 8, 2023

Dr. Joan Salvadó Rovira

Dr. Diego Ramos Romero

Acknowledgements

I would like to express my sincere gratitude to my supervisors Dr. Joan Salvadó, and Dr. Diego Ramos, for their guidance, patience, and valuable support throughout my doctoral research. Without their help and encouragement, this work would have not been possible.

I am also grateful to the members of my thesis committee and the other examiners, Dr. Francesc Ferrando, Dr. Carsten Mai, Dr. Fabiola Vilaseca, Dr. Markus Euring for their insightful comments and feedback on my research.

I am grateful to the staff and faculty of the Department of Chemical engineering at the University Rovira i Virgili, for their assistance and support during my doctoral studies, especially the administrative staff and Núria Juanpere Mitjana who provided me with the necessary resources and help when I needed it.

I would also like to thank the staff and faculty of the Department of Wood Biology and Wood Products at the University of Göttingen who, during the three months of my stay welcomed and helped me with great professionalism.

I would like to acknowledge my friends for their moral support, and motivation during the course of my studies. Their encouragement has been instrumental in my success.

I am grateful to my parents for their unwavering love and support throughout my life, and for instilling in me the importance of education. To my siblings, thank you for your love and encouragement. Their belief in me and my abilities has been instrumental in helping me achieving this significant milestone in my life.

To everyone who has contributed to my journey, big or small, thank you, your help has made all the difference.

Summary

The objective of this thesis is to optimize a sustainable process for making lignocellulosic fiberboards without the addition of synthetic adhesive, also avoiding the exploitation of forest resources.

Indeed, the production of wood-based panels (WBP) has increased dramatically in recent years, and it is estimated to increase further in the next years. The growing demand has led the wood industry to face two main problems: on the one hand, the use of forest resources as raw materials, leading to increasing deforestation; and on the other hand, the use of synthetic adhesives, mostly formaldehyde-based, which, although easy to use and high-performance, lead to pollution due to their emissions that pose a hazard to both the environment and human health.

This is the context for the present study, which explores the possibility of making sustainable lignocellulosic binderless fiberboards from the *Arundo donax* L. plant, through a process involving the following steps: pretreatment of the raw material with steam explosion, milling of the dried fibers, hot pressing of the milled material, and final heat treatment.

Arundo donax L. is a perennial cane to which investigation has devoted special attention in recent years, thanks in part to the European project “Giant Reed Network” (FAIR962028, European Commission), which promotes the use of *Arundo donax* L. for biomass production. The interest stems from the ease of cultivation and growth of this plant, which is also very common in Mediterranean areas, growing wild in different climatic environments. Accordingly, since this project, many others have followed that do not limit its use to bioenergy technologies, but explores a variety of other fields in which *Arundo donax* L. can be a valuable resource. In the field of construction, for instance, *Arundo donax* L. has been used as structural material for many years, used in its natural form to make beams or panels, generally consisting of parallel canes stiffened with perpendicular elements. Its chemical characteristics make it a material with high potential even in the production of binderless fiberboards, especially because of its lignin content (i.e., between about 19% and 24%), which competes with the lignin content of some softwood (e.g. spruce with a lignin content of about 25%). Indeed, although studies on self-bonding mechanism is still active and not entirely comprehensive, it is clear that lignin plays a key

role and provides better mechanical performance and reduces the water absorption.

However, to obtain the expected results, it is necessary to pretreat the material to break down the chain of primary elements in lignocellulosic material, resulting in defibrillated fibers that can be pressed into rigid three-dimensional panels. The pretreatment used in this study is steam explosion, which has been claimed to be one of the most effective and valuable methods to achieve the desired results. Through steam explosion, the material undergoes a controlled high-pressure, high-temperature treatment in a batch reactor for the desired period of time. Afterward, the pressure is suddenly released, causing the polymer chain to break down, the hydrolyzation of hemicellulose, and the distribution of lignin over the surface of the fibers. This results in a pulp that is first dried, then milled, hot pressed to obtain panels, and finally subjected to a final heat treatment to improve some of the properties, especially the behavior against water.

Given the above steps, this study particularly investigates the effects of pretreatment and final heat treatment parameters, while also considering the effect of pressing parameters, especially pressing pressure. In addition, the effect of geometric parameters, specifically panel thickness and size, is studied. The former is studied in the context of high density boards, and the latter for medium density boards.

With the goal of optimizing parameters, the most suitable pretreatment and final heat treatment conditions for high density boards made from *Arundo donax* L. are first identified, by analyzing the response data obtained for mechanical properties (i.e., modulus of elasticity MOE, modulus of rupture MOR, and internal bond IB), and physical properties (i.e., density, thickness swelling TS, and water absorption WA). Additionally, the influence of thickness on the same type of high density board is studied. Medium density boards with larger size are also made, thus studying the effect of changing density and geometric characteristics, and comparing the results with panels made with the same procedure but with synthetic adhesive. The latter results were obtained at the University of Göttingen during a research stay, and are those for which changes in the process need to be implemented to improve the results. However, in the case of the high density, small thickness panels, the results obtained largely meet the standards, although the smaller size of the specimens has to be taken into account when drawing conclusions.

Finally, a sustainability perspective is developed by conducting an initial study of the environmental impact of the production process,

through life cycle assessment and the calculation of environmental impact indicators. The analysis is conducted with the main objective of comparing with the closest market product to that proposed here, for which the best results were obtained. Thus, high density panels made by the process of steam explosion, hot pressing, and final heat treatment are compared with high density panels made using synthetic adhesives, whose environmental impact is obtained from Ecoinvent database. Overall, the results show that binderless fiberboards have a lower impact when compared to conventional panels, despite involving additional steps such as steam explosion pretreatment of the material.

This last result, together with the good performance obtained with certain manufacturing conditions, reveals the effectiveness and sustainability of the process and the value of *Arundo donax* L. as a raw material to be used in this field.

Resum

L'objectiu d'aquesta tesi és optimizar un procés sostenible d'elaboració de taulers de fibres lignocel·lulósiques sense l'addició d'adhesiu sintètic, evitant també, l'explotació dels recursos foresals.

De fet, la producció de taulers a base de fusta ha augmentat espectacularment en els darrers anys, i s'estima que augmentarà encara més en els propers anys. La demanda creixent ha fet que la indústria de la fusta s'enfronti a dos problemes principals: d'una banda, l'aprofitament dels recursos forestalscom a matèries primeres, que comporta un augment de la deforestació; i d'altra banda, l'ús d'adhesius sintètics, majoritàriament a base de formaldehid, que, tot i ser fàcils d'utilitzar i d'alt rendiment, provoquen contaminacions per les seves emissions que constitueixen un perill tant per al medi ambient com per a la salut humana.

Aquest és el context del present estudi, que explora la possibilitat de fabricar taulers sostenibles de fibra lignocel·lulòsic sense aglutinant, a partir de la planta *Arundo donax* L. mitjançant un procés que inclou els següents passos: pretractament de la matèria primera amb explosió de vapor, fresat de les fibres seques, premsat en calent del material fresat, i tractament tèrmic final.

Arundo donax L. és una canya perenne a la qual la investigació ha dedicat una atenció especial en ela darrers anys, gràcies en part al projecte europeu "Giant Reed Network" (FAIR962028, Comissió Europea), que promou l'ús d'*Arundo donax* L. per a la producció de biomassa. L'interès neix de la facilitat de cultiu i creixement d'aquesta planta, que també és molt freqüent a les zones mediterrànies, creixen silvestre en diferents ambients climàtics. En conseqüència, des d'aquest projecte, n'han seguit molts altres que no limiten el seu ús a les tecnologies bioenergètiques, sinó que explora una varietat d'altres camps en els cuals *Arundo donax* L. por ser un resurs valuós. En l'àmbit de la construcció, per exemple, *Arundo donax* L. és un material estructural des de fa molts anys, utilizat en la seva forma natural per fer bigues o panells, generalment formats per canyes paral·leles endurides amb elements perpendiculars. Les seves característiques químiques el converteixen en un material amb u alt potencial fins i tot en la producció de taulers de fibres sense aglutinant, sobretot pel seu contingut en lignina (i.e., entre un 19% i un 24%), que competeix amb el contingut en lignina d'algunes coníferes (e.g. l'avet amb un contingut en lignina d'un 25%). De fet, tot i que els estudis sobre el mecanisme d'autounió encara

són actius i no del tot exhaustius, és evident que la lignina té un paper clau i proporciona un millor rendiment mecànic i redueix l'absorció d'aigua.

No obtant això, per obtenir els resultats esperats, és necessari un pretractament del material per trencar la cadena d'elements primaris de material lignocel·lulòsic, a partir del cual es produeixen fibres desfibril·lades que es poden pressionar en taulers tridimensionals rígids. El pretractament utilizat en aquest estudi és l'explosió de vapor, que s'ha afirmat com un dels més efectius i valuosos per aconseguir els resultats desitjats. Mitjançant l'esplosió de vapor, el material se sotmet a un tractament controlat d'alta pressió i alta temperatura en un reactor "batch" durant el període de temp desitjats, despré del cual la pressió s'allibera sobtadament provocant la ruptura de la cadena del polímer, la hidrolització de l'hemicel·lulosa, i la distribució de la lignina a la superficie de les fibres. D'aquesta manera, el material es converteix en una polpa que primer s'asseca, després es mòlta, es premsa en calent per obtenir taulers, i finalment se sotmet a un tractament tèrmic final per millorar algunes de les proprietats, especialment el comportament davant l'aigua.

Tenint en compte els passos esmentats ateriorment, aquí s'investiga especialment els efectes del pretractament i els paràmetres del tractament tèrmic final, atès que també es desenvolupen algunes consideracions pel que fa a l'efecte dels paràmetres de premsat, especialment la pressió de premsat. Seguint la línea d'investigació, tampoc s'havia investigat l'efecte dels paràmetres geomètrics, i en particular el gruix i la mida del tauler. El primer es va estudiar en el context de taulers d'alta densitat, i el segon per a taulers de densitat mitjana.

Amb l'objectiu d'optimizar els paràmetres, primer identifiquem les condicions de pretractament i tractament tèrmic final més adequades per a taulers d'alta densitat fets amb *Arundo donax* L., mitjaçant l'anàlisi de les dades de resposta obtingudes per a les proprietats mecàniques (i.e., mòdul d'elasticitat MOE, mòdul de ruptura MOR, i enllaç intern IB) i proprietats físiques (i.e., densitat, inflor de gruix TS, i absorció d'aigua WA). A partir d'aquestes mateixes proprietats, també s'estudia la influència del gruix sobre el mateix tipus de tauler d'alta densitat. També es frabriquen taulers de densitat mitjana amb mida més gran, estudiant així l'efecte del canvi de densitat i característiques geomètriques, i comparant els resultats amb taulers amb el mateix procediment però amb adhesiu sintètic. Els resultats d'aquesta darrera part s'han obtingut a la universitat de Göttingen durant una estada de

recerca, i són aquells per als quals cal implementar canvis en el procés per millorar els resultats, mentre que en el cas dels taulers d'alta densitat i de petit gruix, els resultats ontinguts compleixen en gran mesura els estàndards, tot i que la mida més petita de les mostres s'ha de tenir en compte a l'hora d'extreure conclusions.

Finalment, la perspectiva de la sostenibilitat es concreta mitjaçant el desenvolupament d'un estudi inicial d'impacte ambiental del procés productiu, per mitjà de l'avaluació del cicle de vida i el càlcul d'indicadors d'impacte ambiental. L'anàlisi es desenvolupa amb l'objectiu principal de comparar amb el producte de mercat més proper al que aquí es proposa, pel qual s'an obtingut els millors resultats. Així, els taulers d'alta densitat realitzats pel procés d'explosió de vapor, premsat en calent i tractament tèrmic final es comparen amb els taulers d'alta densitat fets amb adhesius sintètics, l'impacte ambiental dels quals s'obté de la base de dades Ecoinvent. En general, els resultats mostren que els taulers de fibra sense aglutinant tenen un impacte menor en comparació amb els taulers convencionals, tot i implicar alguns passos addicionals com el pretractament per explosió de vapor del material.

Aquest darrer resultat, juntament amb el bon rendiment obtingut amb determinades condicions de fabricació, posa de manifest l'eficàcia i la sostenibilitat del procés, i el valor d'*Arundo donax* L. com a marèria primera a utilizar en aquest camp.

Table of Contents

Index of Abbreviations

Materials, compounds, and products

LM	Lignocellulosic material
AD	*Arundo donax* L.
WF	Wood fibers
NWF	Non-wood fibers
FBA	Formaldehyde-based adhesive
UF	Urea formaldehyde
PF	Phenol formaldehyde
MF	Melamine formaldehyde
MUF	Melamine urea formaldehyde
MDI	Methylene diphenyl diisocyanate
pMDI	Polymeric methylene diphenyl diisocyanate
BBA	Bio-based adhesive
WBP	Wood-based panels
BF	Binderless fiberboard
LDF	Low density fiberboard
MDF	Medium density fiberboard
HDF	High density fiberboard

Properties, instruments, and techniques

MOE	Modulus of elasticity
MOR	Modulus of rupture
IB	Internal bond
TS	Thickness swelling
WA	Water absorption
RH	Relative humidity
CY	Char yield
LOI	Limiting oxygen index
STEX	Steam explosion
CP	Cold pressing
HP	Hot pressing
FHT	Final heat treatment
R_0/logR_0	Severity factor of steam explosion
Tr	Reaction temperature (steam explosion)
tr	Reaction time (steam explosion)
Tp	Pressing temperature
tp	Pressing time (tp_1 1st step, tp_b breathing, tp_2 2nd step)

Pp	Pressing pressure (Pp_1 first step, Pp_2 second step)
Tc	Curing temperature (final heat treatment)
tc	Curing time (final heat treatment)
SEM	Scanning electron microscopy
FT-IR	Fourier transform infrared
TGA	Thermogravimetric analysis
dTGA	First derivative of thermogravimetric curve
VDP	Vertical density profile
WFP	Wet forming process
DFP	Dry forming process

Other abbreviations

ANOVA	Analysis of variance
HSD	Honestly significance difference
St.Dev.	Standard deviation
R-squared	Coefficient of determination
LCA	Life cycle assessment
LCI	Life cycle inventory
LCIA	Life cycle impact assessment

List of Tables

Annexes

List of Figures

Chapter 6. Medium density boards: comparison between self-bonded and pMDI-bonded boards

Introduction and objectives

Introduction

The term fiberboards generally refers to a wide range of products made from fibers bound together to form a three-dimensional element. Restricting the field to wood fibers or fibers from other lignocellulosic materials, fiberboards covers several uses, especially in the field of construction, such as indoor and outdoor furniture, insulation, and soundproofing. Their versatility has led to an ever-increasing demand, and to a consequent overexploitation of natural resources. For instance, Sala et al., reported that the fabrication of fiberboards in Europe has increased from 8.4 to 18 Mm^3 between 2000 and 2018 (Sala et al., 2020), and the European "EUwood" study stated that the deficit of wood is expected to be 300 million m^3 by 2030 (Mantau et al., 2010). Added to this is the issue of the use of synthetic adhesives. Indeed, the manufacture of fiberboards is consolidated in industry with the use of formaldehyde-based adhesives, which on the one hand result in a significative environmental footprint, and on the other hand are associated with emissions harmful to both the environment and human health (Binetti et al., 2006; UE Ordinance N° 605, 2014; Salthammer, 2015; Salthammer et al., 2010). In recent decades, these challenges have led research to move on both of them to find alternative materials meeting the high demand without compromising the stability of the ecosystem and to produce eco-friendly fiberboards by partially substituting or totally removing the synthetic adhesive. Both topics are part and parcel to the concept of sustainability, which is becoming increasingly important, and thus the main objective of many research applications. Sustainability is in some ways an abstract concept, strongly linked to the local area. Indeed, the sustainability is defined not only from an ecological point of view, but also from social and economic perspectives.

In this context, the present manuscript explores an alternative to conventional fiberboards, using a material very common in the Spanish peninsula, i.e., the *Arundo donax* L. (AD) reeds. As perennial grass, AD is widespread and can grow spontaneously in different kind of environments. It is fast-growing, adaptable to different climatic conditions, and has low input requirements. The adaptability of its cultivation in marginal lands has also been extensively studied with good results (Bosco et al., 2016; Curt et al., 2017; Impagliazzo et al., 2017; Pari et al., 2016; Schmidt et al., 2015; Scordia et al., 2021). As a

result, the use of AD reeds can be economically favorable, considering that their cultivation does not need complex infrastructures and does not compete with food crops. This situation generally prompted attempts to take advantage of it for biogas production (De Bari et al., 2020; Dell'omo & Spena, 2020), papermaking (Shatalov & Pereira, 2006), extraction of chemical compounds (Corno et al., 2014), musical instruments (Ukshini & Dirckx, 2020), and phytoremediation of contaminated soils (Ferrarini et al., 2021).

Recently, our studies have focused on the use of this multipurpose material for the production of binderless fiberboards (BF), i.e., fiberboards without the addition of any type of adhesive. To make this possible, it is necessary to pretreat the material to obtain fibers that can easily be pressed and bonded together into a rigid structure. Steam explosion (STEX) pretreatment has been shown to be particularly effective. This results in the separation of lignocellulosic materials into their major components (Nasir et al., 2019), via high pressure steam and sudden decompression. This process is known as "Masonite process", which by applying high temperature and high steam pressure, enables the processing of lignocellulosic fibers in order to obtain the hemicellulose degradation and the lignin softening (H. Luo et al., 2014).

In this framework, the general and specific objectives of this work outlined below are identified, and in the following chapters each topic pointed out in this brief introduction will be further explored.

Objectives

The main topic of this work is to produce BF from AD of such quality as to fulfill European standards. Hence, the main objective is to verify whether it is possible to produce good quality and binder-free panels through STEX pretreatment of AD chips.

Related to this, the specific objective on which the following chapters will focus are:

- Analysis of the effects of STEX parameters on BF properties, and identification of optimal parameters for AD fibers;
- Analysis of the effects of final heat treatment (FHT) parameters, and identification of optimal parameters for BF from steam exploded AD fibers;
- Analysis of the effects of variation in panel size on final performance;
- Identification of the relationship between the main steps of the production process and how they affect each other;

- Analysis of the environmental impact of the manufacturing process and calculation of the impact indexes by a life cycle assessment study.

References

Binetti, R., Costamagna, F. M., & Marcello, I. (2006). Development of carcinogenity classifications and evaluations: the case of formaldehyde. *Annali Dell'Istituto Superiore Di Sanità*, 42(2), 132–143.

Bosco, S., Nassi o Di Nasso, N., Roncucci, N., Mazzoncini, M., & Bonari, E. (2016). Environmental performances of giant reed (Arundo donax L.) cultivated in fertile and marginal lands: A case study in the Mediterranean. *European Journal of Agronomy*, 78, 20–31. https://doi.org/10.1016/j.eja.2016.04.006

Corno, L., Pilu, R., Adani, F., & Ricicla, G. (2014). Arundo donax L.: A non-food crop for bioenergy and bio-compound production. *Biothechnology Advances*, 32, 1535–1549. https://doi.org/10.1016/j.biotechadv.2014.10.006

Curt, M. D., Mauri, P. V, Sanz, M., Cano-Ruiz, J., Del Monte, J. P., Aguado, P. L., & Sánchez, J. (2017). The ability of the Arundo donax crop to compete with weeds in central Spain over two growing cycles. *Industrial Crops and Products*, 108, 86–94. https://doi.org/10.1016/j.indcrop.2017.06.015

De Bari, I., Liuzzi, F., Ambrico, A., & Trupo, M. (2020). Arundo donax Refining to Second Generation Bioethanol and Furfural. *Processes*, 8(12), 1591. https://doi.org/10.3390/pr8121591

Dell'Omo, P. P., & Spena, V. A. (2020). Mechanical pretreatment of lignocellulosic biomass to improve biogas production: Comparison of results for giant reed and wheat straw. *Energy*, 203, 117798. https://doi.org/10.1016/j.energy.2020.117798

Ferrarini, A., Fracasso, A., Spini, G., Fornasier, F., Taskin, E., Fontanella, M. C., Beone, G. M., Amaducci, S., & Puglisi, E. (2021). Bioaugmented phytoremediation of metal-contaminated soils and sediments by hemp and giant reed. *Frontiers in Microbiology*, 12, 645893. https://doi.org/10.3389/fmicb.2021.645893

Impagliazzo, A., Mori, M., Fiorentino, N., Di Mola, I., Ottaiano, L., De Gianni, D., Nocerino, S., & Fagnano, M. (2017). Crop growth analysis and yield of a lignocellulosic biomass crop (Arundo donax L.) in three marginal areas of Campania region. *Italian Journal of Agronomy*, 12(1), 1–7. https://doi.org/10.4081/ija.2016.755

Luo, H., Zhang, H., & Lu, X. (2014). Manufacture of binderless fiberboard made from bamboo processing residues by steam explosion pretreatment. *Wood Research*, 59(5), 861–870. https://www.researchgate.net/publication/279098113

Mantau, U., Saal, U., Prins, K., Steierer, F., Lindner, M., Verkerk, H., Eggers, J., Leek, N., Oldenburger, J., Asikainen, A., & Anttila, P. (2010). EUwood – Real potential for changes in growth and use of EU forests. Final report. Hamburg/Germany, June 2010. 160 p.

Nasir, M., Khali, D. P., Jawaid, M., Tahir, P. M., Siakeng, R., Asim, M., & Khan, T. A. (2019). Recent development in binderless fiber-board fabrication from agricultural residues: A review. *Construction and Building Materials* 211, 502–516. https://doi.org/10.1016/j.conbuildmat.2019.03.279

Pari, L., Curt, M. D., Sánchez, J., & Santangelo, E. (2016). Economic and energy analysis of different systems for giant reed (Arundo donax L.) harvesting in Italy and Spain. *Industrial Crops and Products*, 84, 176–188. https://doi.org/10.1016/j.indcrop.2016.01.036

Sala, C. M., Robles, E., & Kowaluk, G. (2020). Influence of the addition of spruce fibers to industrial-type high-density fiberboards produced with recycled fibers. *Waste and Biomass Valorization*, 12, 4033 – 4042. https://doi.org/10.1007/s12649-020-01250-8

Salthammer, T. (2015). The formaldehyde dilemma. *International Journal of Hygiene and Environmental Health* 218(4), 433–436. https://doi.org/10.1016/j.ijheh.2015.02.005

Salthammer, T., Mentese, S., & Marutzky, R. (2010). Formaldehyde in the indoor environment. *Chemical Reviews*, 110, 2536–2572. https://doi.org/10.1021/cr800399g

Schmidt, T., Fernando, A. L., Monti, A., & Rettenmaier, N. (2015). Life Cycle Assessment of bioenergy and bio-based products from perennial grasses cultivated on marginal land in the Mediterranean region. *Bioenergy Research*, 8(4), 1548–1561. https://doi.org/10.1007/s12155-015-9691-1

Scordia, D., D'agosta, G. M., Mantineo, M., Testa, G., & Cosentino, S. L. (2021). Life cycle assessment of biomass production from lignocellulosic perennial grasses under changing soil nitrogen and water content in the Mediterranean area. *Agronomy*, 11(5), 988. https://doi.org/10.3390/agronomy11050988

Shatalov, A. A., & Pereira, H. (2006). Papermaking fibers from giant reed (Arundo donax L.) by advanced ecologically friendly pulping and bleaching technologies. *BioResources*, 1(1), 45–61. https://www.researchgate.net/publication/26460087

Ukshini, E., & Dirckx, J. J. J. (2020). Longitudinal and transversal elasticity of natural and artificial materials for musical instrument reeds. *Materials*, 13(20), 1–13. https://doi.org/10.3390/ma13204566

Chapter 1. Background

Chapter content

This chapter discusses the literature review in the field of wood-based panels with and without adhesives. It covers the types lignocellulosic materials and adhesives commonly used in the industry, as well as new research on both topics. The pretreatments that lignocellulosic materials undergo before board manufacture, as well as other steps related to the manufacturing process, are presented. European reference standards are identified for the classification of panels, and their introduction into the market by meeting the minimum requirements indicated by the standards is also discussed. In addition, the Chapter presents some of the current applications based on the literature review are given. Finally, an overview of studies concerning the environmental footprint and the life cycle assessment is provided at the end of the Chapter.

1.1. Lignocellulosic raw materials

Lignocellulose is the most abundant complex of polymers on earth, and it is mainly composed of lignin, cellulose, and hemicellulose. Lignocellulosic material (LM), including both wood and non-wood materials (grass, straw, and other agricultural residues), consists of varying ratios the aforementioned polymers, according to the plant species (Naraian & Gautam, 2018).

The ranges in which the percentages of each component use to change are reported to be: 35%-55% cellulose, 25%-40% hemicellulose, and 15%-25% lignin with a small fraction of extractives, protein, and ash (Adhikari et al., 2018).

Owing to their abundance, underutilization and low cost, LMs appear as one of the best alternatives that could be converted in value-added materials such as biofuel, chemicals, and bio-based materials like binderless fiberboards (BF). Many wood based panel (WBP) industries increased their interest in the replacement of wood fibers (WF), due to the low cost of the worldwide available LM, although total costs depend on the location, quality, harvesting, and transport costs.

In the context of the valorization of LMs for the production of BF, the chemical composition is an important issue since the lack of binder makes the percentage of each component affecting the panel properties to a greater extent. Research into the field of LM fiberboards largely explored the behavior of different fiber sources, as well as the influence of the chemical components on the physico-mechanical properties of the panels.

Some studies showed that a smaller amount of *hemicellulose* leads to a better resistance to water as hemicellulose is hydrophilic and has a high absorption rate (Pelaez-Samaniego et al., 2013; Suchsland et al., 1987). It is most responsible for moisture sorption and biological degradation (Anglés et al., 2001). However, the low hemicellulose content may lead to weak bonding strength as it helps in better fibers to fibers binding (Nasir et al., 2019).

Lignin is the component that permits adhesion in wood structure. At the same time, it is also responsible for ultraviolet degradation (Anglés et al., 2001). High amount of cellulose and lignin but low hemicellulose is generally found in WF. On the other hand, non-wood fibers (NWF) contain a higher amount of hemicellulose which usually leads to poorer dimensional stability (Zhang et al., 2015).

Extractives help to solve this drawback but, at the same time, their evaporation during hot pressing (HP) may cause delamination (Migneault et al., 2011). Other studies (Alvarez et al., 2015) revealed

how extractable components of NWF play a critical role in the development of mechanical strength of self-bonded fiberboards. In this study, organic extractives decreased the reactivity of the surface of the fibers, resulting in less bonding ability and, consequently, less mechanical properties of fiberboards. On the contrary, water extractives serve as catalysts of fiber degradation reaction during thermo-compression, thus leading to the formation of covalent bonds and increasing the mechanical properties.

The percentage of *ash* in LMs is generally small, and it is reported as an indicator of non-fibrous proportion. However, even in low quantities, it has an abrasive effect on cutting tools and affects the processability of the wood products (Migneault et al., 2011).

The following subsections include some studies that paid attention on the valorization of residual or alternative LMs for the WBP industry sector. For the sake of simplicity, LMs were divided into three categories:

- Forestry and agricultural residues;
- Industrial by-products;
- Other alternative materials.

Moreover, a specific paragraph about *Arundo donax* L. (AD), which is the material used in the study presented later, is discussed at the end of this Chapter.

1.1.1. Forestry and agricultural residues

In recent decades, research has paid an increasing interest in the use of forestry and agricultural residues in the production of fiberboards.

Among others, *oil and date palm residues* proceeding from their plantations, are not used completely and have a great potential to be converted into value-added products, thanks to their availability (Baskaran et al., 2011; Laemsak et al., 2000). Palm trunk is considered as a renewable and sustainable natural resource and it has been utilized as a cellulosic raw material in the production of WBP including particleboard, medium density fiberboards (MDF), cement bonded particleboard, blockboard, plywood, and in the development of BF (Lamaming et al., 2014). Hence, oil and date palm showed a great potential in BF manufacturing and many different by-products of this plant can be used for this purpose such as core-parts, mid-parts, fronds, bark, and leaves (Hashim et al., 2011; Saadaoui et al., 2013), although dimensional stability remains the biggest drawback.

Within agricultural residues, there has been in recent years an increasing interest in *cereals* as raw material for fiberboard production. Cereal crops are worldwide available and harvesting residues may be a

valuable resource for fiberboard production. Among the cereals, *wheat* accounted for 34% of total production. Available wheat residues are estimated at 875x106 Mg worldwide in 2001 (Lal, 2005). Research shows that wheat straw is one of the most suitable agricultural residues for producing pulp and paper (Dahy, 2019), thus constituting a viable alternative also for fiberboards. Such is the example of Domínguez-Robles et al., who developed fully biobased LM fiberboards from wheat straw fibers (Domínguez-Robles et al., 2020). The wheat straw biomass was refined by either enzymatic pretreatment or mechanical pretreatment, and the results were compared. They obtained fiberboards of good quality for both mechanical and enzymatic pretreatment, even though obtaining a lower thickness swelling (TS) than commercial fiberboards.

Analogously to wheat, *rice* is one of the most important agricultural products in the world both in terms of food and production volume. Rice straw is estimated at 890x106 Mg worldwide in 2001 (Lal, 2005). Most straw is used for landfilling or is burned, resulting in environmental issues (Kurokochi & Sato, 2015). In BF production, it was found that rice straw silica content contributed to water resistance while the wax-like substances negatively affect self-bonding (Kurokochi & Sato, 2020).

As an abundant agricultural waste product, *Vitis vinifera pruning* have also been used for fiberboard manufacture. After the pruning season, a large quantity of pruning remains in the fields. The average pruning yield per hectare is about five tons (Mancera et al., 2012). Part of the pruning waste is used as fuel, but copious quantities remain unused in the fields, thus increasing the risks of infestations and fire. Moreover, its chemical composition revealed medium cellulose and high lignin percentages that suggested its suitability as an alternative source of WF used in fiberboards production (Mancera, el Mansouri, et al., 2011; Mancera et al., 2012; Mancera, Mansouri, et al., 2011; Wong et al., 2020).

Kenaf has attracted special interest in fiberboard production too, especially for its rapid growth: it can reach a height of 3.6–4.2 m during a growing season (Okuda & Sato, 2004). The stalk contains two types of fiber: an outer bast and an inner core. Kenaf fibers have gained popularity mainly for use in automotive application like head restrains, back pads and seat bottoms (Sreenivas et al., 2020), but the core remains underused and often discarded. Great attention has been devoted to the properties of fiberboards made by this natural fiber also for construction applications, especially for its use as insulation material. For instance, Xu et al. produced low-density fiberboard made

from kenaf core, obtaining a thermal conductivity quite similar to the insulation materials generally used in construction like rock wool, and also showing good mechanical properties and dimensional stability for the purpose considered (Xu et al., 2004).

The abundance and availability of the material is the necessary conditions for its feasible use in panel production. In this instance, *Cynara cardunculus* represents a viable alternative. The plant is available in the Mediterranean area and generally cultivated for nutritional purposes. The stalk could be used as source in fiberboard production, thus helping to halt deforestation. Mencera et al., used *Cynara cardunculus* to produce BF. They obtained boards of good quality which can be used for interior applications, even if their lower lignin and higher ash content led to poorer results compared to other materials (Mancera et al., 2008).

1.1.2. Industrial by-products

The WBP industry sector usually take advantage of industrial residues from wood itself. Indeed, solid wood processing involves the production of several scraps that are often further processed to manufacture adhesive-bonded fiberboards or particleboards.

Referring to industrial by-products proceeding from other fields, *sugarcane bagasse* is probably one of the oldest non-wood resources used for the fiberboard production. It is a by-product of sugarcane processing, and it is considered one of the most promising non-wood resource, since massive quantities of this waste are still left unused or burnt (Widyorini et al., 2005). Sugarcane is an annual plant native to Latin America, but its cultivation has been imported into Europe for centuries. Sugarcane has a full cycle in 12 months, whereas trees take years to grow. Its rapid growth cycle makes it a more available resource compared to wood. Besides, the stockpiling of this material may cause spontaneous combustion of the stored bagasse, representing a serious environmental risk (Hoareau et al., 2006). Based on Table 1.1., the boards manufactured by steam-injection pressing of sugarcane bagasse showed a high quality in terms of TS, but a worse performance in terms of mechanical strength when compared to panels made from other materials.

1.1.3. Other alternative materials

Grasses represent one of the best alternatives to wood in term of final performance, currently under study. They showed a great adaptability to different climatic conditions, as well as rapid growth, low agronomic input, low production costs, thus increasing the interest of

research in cane-type plants. They normally have a higher percentage of lignin which is expected to have a positive effect on bonding strength and dimensional stability, as well as having a high-speed growth when comparing to wood resources. For instance, some studies focused on bamboo (H. Luo et al., 2014; Shao et al., 2009) or Miscanthus sinensis (Velásquez et al., 2002, 2003).

The lignin percentage is even higher in fruit shells. Some interesting results have been held with walnut or almond shell. Thanks to its characteristic of being hydrophobic, lignin could represent a way to overcome one of the major problems arising from the lack of adhesive, though in many cases TS still need to be improved (Ferrandez-Villena et al., 2019; Pirayesh et al., 2012). Shells could play a key role in the manufacture of value-added panels from alternative LMs, and it may be an efficient use of them. In this concern, Hidayat et al., studied the potential of the seed cake of *Jatropha curcas* proceeding by mechanical pressing of the seeds (shell and kernel) followed by deoiling with hexane for the preparation of BF, but the better results were obtained with exceedingly high pressing pressure, thus making the production high energy consuming (H. Hidayat et al., 2014).

Looking at the results obtained mainly in the field of high density fiberboards (HDF) or hardboards (HB) (Table 1.1.), mechanical properties and dimensional stability showed competitiveness compared to commercial ones, especially when the fibers are properly treated. These studies show that the use of alternative NWF is both viable and promising and sustainable in the WBP industry.

1.1.4. *Arundo Donax* L.

As mentioned, perennial grasses represent a viable alternative in the searching of suitable alternative raw materials for fiberboard production, as they are generally widespread and can grow spontaneously in different kinds of environments (Corno et al., 2014; e Silva et al., 2015). This is the case of AD, also known as giant reed, which is considered a multipurpose crop (Carnevale et al., 2021). Along with its features of fast-growing rate, adaptability to different climatic conditions, and low input requirements (Zegada-Lizarazu et al., 2020), AD is also considered one of the world's 100 most invasive species and it has been included in the Spanish Catalogue of Invasive Species (Ferrandez-Villena, Ferrandez-Garcia, Garcia-Ortuño, Ferrandez-Garcia, & Ferrandez-Garcia, 2020). Due to its vegetative reproduction, it easily occupies new areas by forming dense masses, thus causing the alteration of the ecosystem, and affecting the abundance of native species (Ferrandez-Villena, Ferrandez-Garcia, Garcia-Ortuño,

Ferrandez-Garcia, & Ferrandez-Garcia, 2020; Hardesty-Moore et al., 2020). This situation triggered attempts to take advantage of AD by using it for biogas production (De Bari et al., 2020; Dell'omo & Spena, 2020), papermaking (Shatalov & Pereira, 2006), extraction of chemical compounds (Corno et al., 2014), musical instruments (Ukshini & Dirckx, 2020), and phytoremediation of contaminated soils (Ferrarini et al., 2021). Recently, it has also gained popularity in the production of particleboards and fiberboards for WBP industry.

AD was already used as a structural material in traditional architecture. Its mechanical properties starting from the traditional structural use have been studied, finding a similar behavior to various species of bamboo used in construction (Molari et al., 2021). This showed the potentiality of AD use as construction structural material.

Nonetheless, research in the field of BF made by giant reed is still scarce. For instance, (Ferrandez-Villena, Ferrandez-Garcia, Garcia-Ortuño, Ferrandez-Garcia, & Ferrandez-Garcia, 2020) evaluated mechanical and physical properties of BF made by giant reed rhizome, achieving stunning results with a modulus of rupture (MOR) of 14.2 N mm^{-2}, a modulus of elasticity (MOE) of 2052.45 N mm^{-2}, and an internal bonding (IB) of 1.12 N mm^{-2}. An interesting study developed an eco-friendly board from AD and citric acid as a natural binder, proving its suitability as insulating material, since it has a thermal conductivity ranging between 0.081-0.093 W/m K (Ferrandez-Garcia et al., 2019).

Previous studies of the same research line of the present manuscript investigated the steam explosion (STEX) pretreatment of AD for BF production. In these studies, the STEX led to high quality boards, having a MOE of 7439 N mm^{-2}, a MOR of 40.4 N mm^{-2}, an IB of 1.28 N mm^{-2}, a water absorption (WA) of 17.6wt%, and a TS of 13.3wt%. This showed the feasibility of AD. as raw material for self-bonded boards, provided that a pretreatment is carried out (Ramos et al., 2017, 2018, 2020).

1.2. Adhesives

Notwithstanding the main purpose of the present manuscript is to give a comprehensive overview of the possibilities within the fabrication of BF, it is appropriate to mention a few types of adhesives normally used in the WBP industry.

An adhesive can be defined as a substance able to hold together permanently two or more surfaces (Gonçalves et al., 2021). A wide variety of adhesives are currently used in the WBP industry, although the most used are petroleum-based adhesives containing formaldehyde. In this field, formaldehyde emissions are still a major concern when producing WBP and during their service life . Indeed, the

use of formaldehyde-based adhesives (FBA) has been widely associated with the release of formaldehyde, which causes a serious hazard for human and environmental health (Ordinance 605 EU Commission, 2014). Thus, both academia and industry devoted a special effort towards sustainable WBP, aiming at lowering the hazardousness, but still being qualitatively comparable to current industrial products (Gouveia et al., 2018).

To all intent, the bonding of solid wood and wood particles is a key factor in achieving the standards imposed by the regulations (Solt et al., 2019). From this viewpoint, the total replacement of FBA is still challenging. This is due to the low reactivity of bio-based adhesives (BBA), which consequently leads to an increase in production time and costs, as well as the lower mechanical properties and dimensional stability (Balea (Paul) et al., 2022).

An overview of the most widely used synthetic adhesives in the WBP industry is given in the following subsections, as well as some research dealing with the optimization in the use of them and in the use of BBA.

1.2.1. Conventional synthetic adhesives

The extensive application of FBA is due to the ease of use, the economic efficiency, and the rapid development. Adhesives such as urea-formaldehyde (UF), phenol-formaldehyde (PF), and melamine-urea-formaldehyde (MUF) based are the preferred ones in the WBP industry. In such adhesives, formaldehyde acts as a crosslinker and the reaction with the monomers leads to the production of phenoplast or aminoplast thermosetting resins (Gonçalves et al., 2021). During their production some free formaldehyde remains unreacted, causing both positive and negative effect: on the one hand, the free formaldehyde induces the hardening reaction, but at the same time it causes formaldehyde emission during the HP and even during boards life cycle (Dunky, 2003; Dunky & Pizzl, 2002). The main challenge for researchers in the past 50 years, has been the reduction of the formaldehyde content in adhesives formulation without major changes in their properties.

Table 1.1 *Literature review of mechanical and physical properties of fiberboards from different pretreated fiber sources, with a density between 800 and 1300 kg m^{-3}.*

	Fiber source	Treatment	MOR N mm^{-2}	MOE N mm^{-2}	IB N mm^{-2}	TS %	Reference
Forestry/Agricultural residues	Date palm**	milling	6.1-12.9	430-1257	0.02-0.14	230-150	Saadaoui, N. et al 2013
	Oil palm**	milling	2-14	-	0.05-0.70	100-20	Hashim, R. et al 2011
		milling	1.50-12	-	0.05-0.55	80-20	Hashim, R. et al 2012
		milling	5-25	-	0.50-1.10	50-40	Hashim, R. et al 2010
		milling	3-6	-	0.20-0.40	65-20	Hashim, R. et al 2011
	Wheat straw	hydrothermal pretreatment	3.92-8.76	-	0.17-1.10	111-23	Lamaming, J. et al 2014
		enzymatic refining	95	5000	1.5	50	Domínguez-Robles, J. et al 2020
		mechanical refining	100	6500	1.6	40	Domínguez-Robles, J.et al 2020
		chemical pretreatment	7-27	1800-4500	0.20-0.80	190-70	Halvarsson, S. et al 2008
	Rice straw	milling	-	-	0.02-0.17	40-15	Kurokochi, Y. et al 2015
		extrusion	27.90-50.30	4200-7700	-	35-10	Theng D. et al 2019
	Vitis Vinifera	steam-explosion	25-55	4000-7000	0.17-1.20	9-2	Mancera C. et al 2012; Mancera C et al 2011
	Cotton	milling	26-78	-	-	24-10	Fahmy T. et al 2013
	Cynara cardunculus	Steam explosion and grinding	20-55	2527-7123	0.20-1.30	39-4	Mancera C. et al 2008
Industrial by-products	Sugarcane bagasse	Steam injection pressing	1-6	400-800	0.05-0.20	21-7	Widyorini R et al 2005
Other materials	*Arundo donax*	Steam Explosion, Grinding, and final heat treatment	21-42	3254-6249	2.10-3.25	11.13-5.84	Ramos D et al 2020
	Bamboo	Milling, steam explosion	3-16	-	0.20-0.80	50-5	Luo H et al 2014
	Miscanthus sinensis	Steam Explosion, grinding	25-45	3090-4630	1.07-2.80	38-8	Velásquez J et al 2002; Velásquez J et al 2003
	Almond shell	shredding	7.64-14.01	1362-2295	0.59-1.27	33-18	Ferrandez-Villena M et al 2019
	Jatropha curcas	oil extraction	22.8	5100	-	19	Hidayat H et al 2014
Commercial HDF			41.70-42.25	2670-4299	0.39-0.47	13-66	Domínguez-Robles J et al 2018; Ramos D et al 2018; Theng D et al 2015; Khedari J et al 2004

UF adhesives have the advantages of curing at relatively low temperatures, they are cheaper compared to other FBA, such as PF, and

they have a good resistance to fire. The boards bonded with UF resins are mainly used indoor, in dry conditions, as they do not have a sufficient resistance against moisture. Whilst *PF* resins provide a higher resistance to moisture and the formaldehyde emissions after hardening in this case are lower. On the other hand, they need longer pressing times and higher temperatures for curing, as well as being more expensive. Moreover, phenol is a known carcinogenic and represents a hazard to human health. *Melamine-formaldehyde (MF)* resins also provide a better resistance to moisture. Nevertheless, they are the most expensive ones, and this limits their application in WBP industry in favor of PF or UF. To lower the cost, melamine can be used in combination with urea for the MUF adhesives, which ensure the higher resistance to water but at a lower cost.

As outlined above, although UF, PF, MF, and MUF based adhesives have the advantages of good adhesion and technological maturity, they release formaldehyde during manufacturing and use of the wood composites. This led to the use of formaldehyde-free binders.

Among the formaldehyde-free synthetic adhesives, methylene diphenyl diisocyanate (MDI) gained an increasing popularity as it shows a higher affinity to wood and non-wood materials than FBA (Li et al., 2010; Pędzik et al., 2021). It is mainly used as polymeric MDI (pMDI) and has the advantage of reacting with the naturally occurred moisture inside the fibers to form polyurea networks (Das et al., 2007; P. Luo et al., 2020), although the reactions that contribute to bond formation have not yet been fully elucidated. Moreover, other benefits associated with pMDI are the fast curing rate, the good moisture tolerance, and the excellent dry and wet bonding strength (H. Chen & Yan, 2018; P. Luo et al., 2020). On the other hand, certain drawbacks need to be addressed. Firstly, the potential health hazard and carcinogenity is still under study (H. Chen & Yan, 2018; Tupciauskas et al., 2021). Furthermore, its cost is higher than conventional FBA, thus leading to more expensive final products (Asafu-Adjaye et al., 2020; Pan et al., 2006). Because of its prohibitive cost, the use of pMDI in the WBP industry is still challenging in Europe, together with the need for specialized equipment, and a safety control during the production due to the toxicity of isocyanate particles that may be released during manufacturing. Thus, it is not clear weather pMDI resins are an environmental-friendly alternative to FBA or not.

In this framework, research focused attention on the formulation of new adhesives obtained by combining pMDI and bio-adhesives for both reducing the amount of pMDI, thereby the cost and impact of boards

manufacturing, and increasing the reactivity and water resistance of natural binders. Some works (W. Hidayat et al., 2022), studied the feasibility of natural rubber latex (NRL) as adhesive by adding 5% of pMDI to the adhesive formulation. They showed the feasibility of producing particleboards with 20% NRL/pMDI related to dry fiber mass, although the enhancement of mechanical and physical properties needed further studies and they attributed the poor properties to the low percentage of pMDI in the adhesive formulation. Moreover, others (Asafu-Adjaye et al., 2020) used the pMDI in the amount of 2wt% and 4wt% to dry particles, partially substituting it with 12% and 15% of soy flour. They compared the results obtained with the different amounts of soy flour plus pMDI, with pure pMDI bonded boards in the same amount. The mixing of soy flour and pMDI resulted in the improvement of all the properties for both strand boards, MDF, and particleboards. By using the same amounts of pMDI, it has been showed the improvement in IB and a sufficient performance against moisture by doubling its amount in boards made of thermomechanical pulp fibers of spruce and silver fir, kraft lignin (i.e. technical lignin) as adhesive, and pMDI as crosslinker (Ostendorf et al., 2021). Finally, other studies (Hemmilä et al., 2019) compared the effect of two different crosslinkers, i.e. pMDI and furfuryl alcohol (FA), in combination with ammonium lignosulfonate (ALS). They used a ratio of 6% for both pMDI or FA to ALS for a total amount of 12% of adhesive (wt% to dry particles), thus aiming to reduce it to 8%. Hence, they showed the superiority of pMDI as a crosslinker for ALS in achieving a higher IB, with further improvements by adding tannin to the adhesive formulation.

1.2.2. Bio-based adhesives

The need to incorporate the concepts of sustainability and circular economy into the industry have moved research toward the development of adhesives from natural sources. Nowadays, industries must include the environmental footprint of their products in their usual marketing. BBA have the advantage of being widespread and renewable. Indeed, the focus of research lies on abundant biomolecules obtained from renewable resources and materials that would otherwise be industrial residues, such as LMs. There has been an increasing interest in BBA derived from soy, lignin, and tannin, among others (Gonçalves et al., 2021). Although there is a great interest in reducing the industrial dependency on oil, BBA have not yet achieved a significant importance in WBP industry. The main problem connected with the use of BBA, is their low reactivity, which lead to an increasing in production time and cost. Moreover, their strength and water

resistance are generally lower when compared to synthetic conventional binders (Balea (Paul) et al., 2022). The following are some natural compounds studied by research for making adhesives in the WBP industry.

Tannins are the fourth most abundant compound in the plant tissue next to cellulose, hemicellulose, and lignin (Niaz & Khan, 2020). They are polyphenolic materials, soluble in water, alcohols, acetone and can coagulate proteins (Dunky & Pizzl, 2002). The attractiveness of using tannins in wood adhesives is due to the similar behavior with formaldehyde, phenol, and resorcinol (Gonçalves et al., 2021). The main issue in using tannin in the adhesive formulation is that it generally requires the addition of a hardener, which is usually formaldehyde. Some alternatives lie with the use of proteins, lignin, and starches as crosslinkers. Some studies (Oktay et al., 2021), proposed a greener approach with a BBA containing corn starch, tannin, sugar, and citric acid, and obtaining the expected crosslinked adhesive network.

Lignin is the second most abundant biological macromolecule (Gonçalves et al., 2021). In the natural form of wood and LM, lignin acts as a glue, as the matrix that binds cellulose and hemicellulose, thus giving rigidity and water resistance to the wood structure. Technical lignin is considered one of the most promising alternatives to synthetic binders, and it has already been studied for the formulation of formaldehyde-free binders for boards production (Mansouri et al., 2007). Some review papers (Gendron et al., 2022; Karthäuser et al., 2021), explored the lignin application in wood adhesives and wood modification, drawing the attention on the gap between the potential of this abundant natural polymer and its actual use at pilot scale. Indeed, the lignin valorization is not yet run after at industrial scale due to the need in first developing cost-effective and greener extraction methodologies and supply lines (Gonçalves et al., 2021). The increasing interest in lignin in the field of adhesives is due to its polyphenolic structure, which can partially substitute the phenol in PF resin (Antov et al., 2021; Bekhta et al., 2021; Karthäuser et al., 2021). However, technical lignin differs significantly depending on the extraction method used and requires some chemical modification to increase the reactivity of the BBA. Various researchers studied fiberboard properties made with a percentage of lignin as natural binder obtaining considerable results. For instance, the effect of the addition of lignosulphonate and kraft lignin in fiberboard made by STEX softwood has been studied (Anglés et al., 2001). In this study, the authors gained an increasing improvement for both mechanical properties and dimensional stability,

especially with kraft lignin, with the increase of lignin amount from 0% to 20% by fibers weight. Velásquez et al., set the maximum amount of added lignin at 20% for pretreated Miscanthus sinensis, as they observed a negative effect on physico-mechanical properties with higher quantities (Velásquez et al., 2003). Other researchers obtained equally satisfactory results by using alkaline lignin (Glasser & Wright, 1998). Some studies (Theng et al., 2017), also detected an improvement in mechanical properties of fiberboard made from thermomechanically processed corn residues by adding about 20wt% of purified kraft lignin, thus obtaining excellent results in mechanical strength. Domínguez-Robles et al. used the lignin obtained from the pulping process of the wheat straw employed for fiberboard production itself, achieving flexural strength values always above the ones found in literature or even including commercial fiberboard (Domínguez-Robles et al., 2018). As a result, lignin-based adhesives showed potentials for engineering applications and their abundance makes them even more attractive (Hamidreza Ghaffar & Fan, 2014).

1.3. Production methods

In fiberboards manufacturing, two methods have been developed: wet-forming process (WFP), and dry-forming process (DFP). In WFP less or no binders are needed (Zhang et al., 2015), due to the hydrogen bonds formation and adhesive behavior of lignin which occur during heating and drying processes (Zhang et al., 2015). In DFP the dried fibers are blended with binder, the mixture is distributed into a mat, and then hot pressed (Domínguez-Robles et al., 2020).

When it comes to BF, a pretreatment may improve fiberboard properties in many cases, especially for dimensional stability. The mechanisms that occur during the pretreatment and contribute to the enhancement of the panel's properties are varied and still not fully explained. A recognized interpretation of the results normally obtained in this field believes that the fiberboard production process serves to activate the lignin bonding ability. In turn, lignin contained in the WF or NWF serves to bond fiber itself without any added synthetic or natural adhesive. As highlighted previously, lignin already acts as a binder, but it is stuck in a polymer chain with cellulose and hemicelluloses, which together give to the wood its natural resistance to loads and moisture, with some differences depending on the resource considered. However, there are many theories and demonstrations that also show the key role of sugars in the self-bonding process. Despite this, to date, self-bonding mechanism has not been fully elucidated. Some potential explanations have been reported such has lignin-furfural linkages,

condensation reaction in lignin, and furfural self-polymerization, as well as thermal softening of lignin (Zhang et al., 2015). Indeed, the self-bonding mechanism can vary depending on LM used and the manufacturing process. All the mechanism recognized to play a role in self-bonding are attainable, so far. This means that the mechanism itself may change according to the raw material used, the pretreatment, and the other steps of the manufacturing process.

The following subsections discuss the main phases in the production of BF, trying to elucidate the most likely mechanisms occurring during the manufacturing process which lead to the achievement of properties fulfilling the standards.

1.3.1. Pretreatments

Different treatments can be carried out in BF production. Raw materials are generally subjected to a prior mechanical treatment (sawing, chipping, shredding, grinding, and milling) before any other treatment, through which particle size is reduced. Overall, LMs are always further treated after milling, but in certain cases a good quality BF can be obtained without any further treatment.

The following subsections include some studies that paid attention on different pretreatments of LMs. For the purpose, the pretreatments considered fall into four categories:

- Mechanical treatment;
- Chemical treatments (acid or alkaline hydrolysis, and oxidation agents);
- Hydrothermal treatments (thermomechanical pulping and STEX);
- Biological treatments (microbiological and enzymatic).

Table 1.2. summarizes and compares the effect of pretreatments on fiber and board properties, as well as it outlines the advantages and disadvantages of each pretreatment, by considering results obtained in the field of BF.

Of all the pretreatment considered, we will focus on STEX, which is the treatment used for the study presented in the following chapters.

1.3.1.1. Mechanical pretreatment

Mechanical pretreatment increases the total accessible surface area thus improving the accessibility of constituents and leading to better bonding strength (Barakat et al., 2014). Milling reduces crystallinity of cellulose, the substrate particle size, and the degree of polymerization (Cheng & Timilsina, 2011). Most researchers combine mechanical pretreatment with others since it does not modify the chemical composition or the structure of the raw material. When only a

mechanical pretreatment is carried out fiberboard properties are deeply dependent on raw chemical composition, and it is more difficult to overcome the main drawbacks like the high hydrophilicity. It has been clearly showed the dependency between chemical composition and the properties of the panels (Hidalgo-Cordero et al., 2020). In this study, the authors observed quite different results for fiberboards made by shredded fibers of totora stem, pith, and rind, as they have different amount of the main chemical components, i.e. cellulose, hemicellulose, and lignin. As a result, the general trend is to use mechanical treatment before, and sometimes also after, other treatments.

1.3.1.2. Chemical pretreatments

Chemical pretreatments can be at low, neutral, or high pH (Kumar et al., 2009). Typically, low pH pretreatments (acid pretreatment) remove most of the hemicellulose and a small portion of lignin. Neutral pH pretreatments (controlled pH) remove much of the hemicellulose but leave most of the cellulose and lignin intact. High pH pretreatments (alkali pretreatments) remove a large fraction of lignin and some hemicelluloses (Kumar et al., 2009).

In *acid pretreatment* method, acids are used as catalysts to hydrolyze lignocellulose components (Baskaran et al., 2011). Common chemicals used are sulfuric acid, hydrochloric acid, or acetic acid (Amin et al., 2017). Acid pretreatment results in the disruption of van der Waals forces, hydrogen bonds and covalent bonds that hold together the biomass components, which consequently cause the solubilization of hemicellulose (Miyamoto et al., 2002). Acid pretreatments can be carried out with both concentrated and diluted acids. The use of concentrated acid may cause corrosion of the equipment, high consumption of the acid, toxicity to the environment, and energy demand for acid recovery (Miyamoto et al., 2002). Dilute acid hydrolysis presents the advantage of lower acid consumption but in return, a higher temperature is required (Baskaran et al., 2011). It can be performed in combination with other treatments to reach a further hydrolysis of hemicellulose. It has been proven that the addition of sulfuric acid during STEX improves the solubilization effect as well as a wider redistribution of lignin, thus leading to a better resistance to water (Anglés et al., 2001; Cheng & Timilsina, 2011). However, fiber length decreases when acid catalyst is used, thus leading to poorer mechanical strength (Cheng & Timilsina, 2011).

Alkaline pretreatment of LMs originates from soda pulping patented in 1854 (Rabemanolontsoa & Saka, 2015). The main alkaline reagents are sodium hydroxide, potassium hydroxide, aqueous ammonia,

calcium hydroxide and oxidation reagents. This pretreatment consists in adding a base to biomass and leads to an increase of internal surface area by a swelling of cell wall, a decrease of polymerization degree and crystallinity, a destruction of links between lignin and other polymers, and lignin breakdown (Badiei et al., 2014). Compared to other chemical pretreatment technologies, alkaline hydrolysis can be conducted at a lower temperature and pressure, causing less sugar degradation than acid pretreatment, but the reaction times take several hours, days, or even weeks for softwood. Indeed, the yield of alkaline pretreatment depends on the lignin amount: the lower the lignin content, the better the treatment effect. It turns out that the alkaline pretreatment is more effective on hardwoods and agricultural residues than softwoods, as softwoods normally have a lignin content higher than hardwoods (Badiei et al., 2014). Ahmad et al. implemented an alkaline treatment with sodium hydroxide on rattan furniture waste to produce binderless particleboards. The treatment hugely increased MOR and IB values and demonstrated to be helpful in hydrolyzing hemicellulose, improving dimensional stability too. However, sodium discharge in the process effluent is difficult to be recycled and it limits its application on the pilot scale (Ahmad et al., 2018). Lastly, oxidation agent as Fenton's reagent is being studied (Zhang et al., 2015). Fenton's reagent is composed of ferrous chloride and hydrogen peroxide which could activate the fiber surface and facilitate the adhesive bonding between fibers. Some studies (Halvarsson et al., 2008) produced BF from wheat straw by using oxidative activation of wheat straw fibers performed by adding hydrogen peroxide during defibration. They obtained an improvement in fiberboard properties by increasing the added hydrogen peroxide from 2.5% to 4% by weight.

1.3.1.3. Hydrothermal pretreatments

Hydrothermal pretreatments are wet treatments generally developed at high temperature. Several papers have been published on hydrothermal treatments. They generally lead to a more condensed lignin that has a high average molecular weight and contribute to the self-bonding formation of LM (Xiao et al., 2014). Steam treatments and thermomechanical pulping are analyzed here. The first can be carried out before forming a mattress (STEX), during HP (steam injection pressing), and after HP (post treatment steaming). Among these, the *STEX* pretreatment is considered to be particularly effective in improving all fiberboard properties. With this treatment, biomass is subjected to high pressure steam followed by a sudden decompression in a batch reactor. When the pressure is released, the steam expands

within the LM matrix, causing the separation of individual fibers and the disruption of cell wall structure (Agbor et al., 2011). This method is industrially practiced in the Masonite process (Glasser & Wright, 1998). The LM results in a pulp in which most of hemicellulose is hydrolyzed and which can be subjected to HP to produce fiberboard without using binders (Laemsak et al., 2000; Velásquez et al., 2003). Temperature and pressure are two important parameters of STEX. The reaction temperature (Tr) generally ranges between 160-260°C with the corresponding saturated steam pressure of 5-50 bar (Agbor et al., 2011). Tr and reaction time (tr) are combined in the severity factor (R_0), which is a commonly used parameter in STEX, defined as follow:

$R_0 = \int_0^{tr} \exp[\frac{Tr-100}{14.75}]dt$ (Mobarak et al., 1982; Overend et al., 1987)

Some studies demonstrated that boards made from fibers exploded under too high severe conditions (high Tr or long tr) become brittle and show low MOR and MOE (Anglés et al., 2001; Velásquez et al., 2002). An increase in the R_0 can improve the physical properties of the panels but there is an optimum value with no further improvement. The advantages of STEX are reported to be the recovery of all constitutive wood components without the destructive degradation components, the lower environmental impact, the lower capital investment, the higher potential for energy efficiency, and less hazardous process chemicals and conditions (Avellar & Glasser, 1998). However, it has been observed that STEX has a high effectiveness for pretreatment of agricultural residues and hardwood, but it is less effective for softwood. In such cases, using an acid catalyst during STEX process becomes significant (Badiei et al., 2014).

It is appropriate to also mention the *thermomechanical process*. In a thermomechanical treatment the pulp is made by heating the chips at Tr above 100°C and by mechanically separating the fibers in a pressurized refiner. Thermomechanical pulping process has become one of the major processes for the manufacturing of pulps, accounting for 20% of the world pulp production together with other mechanical pulps (Kortekaas et al., 1998). Refining pressure and time are the two main manufacturing parameters which consequently influence almost all properties of the panels (Aisyah et al., 2012). Gao et al. compared thermomechanical treatment and grinding process. They showed that the thermomechanical treatment of bark via refining lowers the required pressing temperature (Tp) and shortens the pressing time (tp) needed for manufacturing BF from bark (Gao et al., 2011).

On the other hand, e*xtrusion* is a promising thermomechanical pretreatment for use in biomass conversion because it is cheap, the

monitoring of temperature and screw speed is good, and it has high shear and excellent processing capacities. The main advantages are that the twin-screw extruder used for the pretreatment of fibers is cheaper than the other fiber-removing technologies, and it does not change the chemical and thermal properties of the raw biomass (Theng et al., 2019).

Among all these pretreatments of LMs, STEX has been claimed as particularly successful. It results in the separation of LMs into their major components (Nasir et al., 2019). By applying elevated Tr and high steam pressure, STEX processes LM and leads to the hemicellulose degradation and the lignin softening (H. Luo et al., 2014). This permits the redistribution of lignin onto the surface of the fibers (Mejía et al., 2014), thus enhancing the self-bonding and the improvement of dimensional stability. Previous research studied the employment of STEX in the production of BF and the effect of Tr and tr on the properties of the boards. For example, Kurokochi and Sato studied the effect of STEX carried out at 200°C for 10 or 20 min, on rice straw BF. They obtained a significant improvement in IB, and TS and justified it by the hemicellulose hydrolyzation, cellulose decomposition, and lignin degradation occurring during the treatment (Kurokochi & Sato, 2020). Other studies (Mejía et al., 2014) compared mechanical and physical results of BF made by oil palm empty fruit bunches treated by STEX and oxidated by Fenton's reagent. Their study showed that high performance of BF can be achieved by STEX carried out at a $\log R_0$ of 4.0 which led to optimum values of MOE 3100 N mm^{-2}, MOR 28.49 N mm^{-2}, TS 11.80 %, and WA 22.74 %. Luo et al. studied the effect of increasing tr from 60 s to 180 s, with a steam pressure of 30 bar, in BF properties made by bamboo processing residues. The increasing in tr produce an improvement in all mechanical and physical properties and they were able to obtain panels with maximum value of 15.9 N mm^{-2} for MOR, 0.48 N mm^{-2} for IB, and 12 % for TS (H. Luo et al., 2014). the effect of STEX on the physico-mechanical responses of BF made by banana bunch was also studied, as well as the effect of HP conditions (Quintana et al., 2008). The authors found the optimum values with a $\log R_0$ of 3.55, a Tp of 200°C, and a pressing pressure (Pp) of 14 N mm^{-2}. The high consumption of energy may be the main drawback when carrying out STEX. For this reason, it may be necessary to define a limit of R_0 beyond which there are no further improvement in term of physico-mechanical properties of BF.

1.3.1.4. Biological pretreatments

Biological pretreatment is an eco-friendly process that requires low energy input, low disposal costs, and milder operating conditions against other pretreatment strategies (Mishra et al., 2018). It usually refers to the deconstruction of lignin structures in the cell wall using microbes or enzymes as catalysts.

Within biological pretreatments, *fungi* have gained popularity as sources of commercial plant cell wall degrading enzymes (Badiei et al., 2014). White-rot fungi can selectively metabolize low molecular weight lignin and hemicellulose while leaving cellulose relatively unaffected (Saritha et al., 2012). This results in increasing the mechanical properties of BF since it increases the number of hydroxyl groups, crystallinity, polysaccharide, and laccase content (J. Wu et al., 2011, 2019). However, the rate of biological pretreatment is slow for industrial purposes. Indeed, fungi treatment needs long residence time (10-14 days) and precise growth conditions to be effective (Saritha et al., 2012). There is no suitability for wood industrial application so far.

Also *enzymatic treatment* can be included into biological pretreatments. It often involves mild reaction condition, low by-products, and low environmental impact. Laccase is an oxido-reductase agent, as it removes the lignin molecule from LM and helps polymerization of lignin through free radical reactions (Nasir et al., 2014). During the fiber treatments, laccase hardly penetrated into fibers and mainly oxidized the lignin on the surface (Mishra et al., 2018). As a result, free radicals are generated on the fiber surface, acting as potential reactive sites for further cross-linking reactions in the production of fiberboards (Zhang et al., 2015). Laccase treatment can improve bonding properties thanks to the surface modification which occurs with the precipitation of lignin extractives on the surface (Felby et al., 2004). Typically, laccase treatment led to an improvement in both mechanical and physical properties, although the concentration of laccase is less effective on MOR, MOE and IB (Alvarez et al., 2015; Zhang et al., 2015). On the other hand, the different concentrations can largely affect thermal properties: fibers treated with a higher concentration showed higher thermal stability, probably due to the grafting reaction of low molecular weight components on the fiber with the lignin (Álvarez et al., 2011). However, the high cost of laccase made it difficult to be applied on a large scale (J. G. Wu et al., 2016).

Table 1.2. *Literature review of the effects of pretreatments on fiberboards properties, pros, and cons.*

Pretreatment	Effect on fiber and board properties	Pre-treatment pros and cons	References
Mechanical (sawing, milling, grinding, shredding)	It increases the total accessible surface area, increasing the bulk density and porosity, and IB.	It may require a large amount of energy. It is generally combined with other treatments.	Barakat A et al 2014; Cheng JJ et al 2011; Velásquez J et al 2003; Wu J et al 2011.
Acid pretreatment	It removes most of the hemicellulose and a small portion of lignin. Combined with STEX pretreatment it improves WA and TS.	Concentrated acid may cause corrosion of the equipment, toxicity to the environment, and energy demand for acid recovery.	Kumar R et al 2009; Miyamoto K et al 2002; Anglés M et al 2001; Baskaran M et al 2011.
Alkaline pretreatment	It removes a large fraction of lignin and some hemicelluloses and leads to an improvement in all fiberboard properties.	It can be conducted at a lower temperature and pressure, causing less sugar degradation, but reaction times take several hours or days.	Kumar R et al 2009; Zheng M et al 2009; Badiei M et al 2014; Amin F et al 2017.
Oxidation agents	It facilitates the adhesive bonding between fibers, thus improving mechanical properties, WA, and TS.	It is believed to have a harmful effect because of the instability of board quality and insufficient mechanical strength obtained.	Zhang D et al 2015; Halvarsson S et al 2008.
Steam explosion	It is known for being particularly effective for improving all fiberboard properties, especially dimensional stability, if carried out in a certain severity factor range.	It does not lead to a destructive degradation of components, non-hazardous process chemicals and conditions. Potential energy consumption is the main drawback.	Velásquez J et al 2002; Avellar B et al 1998.
Microbiological pretreatment	It can metabolize low molecular weight lignin and hemicellulose while leaving cellulose unaffected. It has a beneficial effect on mechanical properties.	It needs a long residence time (10-14 days), extremely precise growth conditions and the need for a large space	Saritha M et al 2012; Wu J et al 2011.
Enzymatic pretreatment with laccase	It help polymerization of lignin. It can improve fiberboard properties, both mechanical and physical.	It involves mild reaction condition, and less by-products. In turn, the prohibitive cost of laccase makes it less feasible	Nasir M et al 2014; Zhang D et al 2015; Felby C et al 2004; Álvarez C et al 2011; Wu J et al 2016.

1.3.2. Grinding and fiber size

Many studies showed the importance of particle size, which may have a significant effect on boards properties. The range of particle size is expected to have a great influence on the binding capacity of BF (Ferrandez-Villena, Ferrandez-Garcia, Garcia-Ortuño, Ferrandez-Garcia, & Ferrandez-Garcia, 2020). Finer particles have been associated to an improved water resistance, while bonding strength is generally enhanced by larger particles (Hashim et al., 2010; Miyamoto et al., 2002).

Some studies (Ferrandez-Villena, Ferrandez-Garcia, Garcia-Ortuño, Ferrandez-Garcia, & Ferrandez-Garcia, 2020; Hashim et al., 2010) showed the importance of particle size which affect the mechanical performance to a large extent. Ferrandez-Villena et al. found the optimal range of particle size between 0.25 and 1 mm for BF manufactured from AD rhizomes. Flores et al. also studied the effect of particle size in UF bonded boards made from AD. They found optimal results using 2 mm and 4 mm sieves (Flores et al., 2011). On the other hand, Kurokochi and Sato worked on BF from various parts of rice straw, also showing the influence of grinding step, using a screen of 1 mm (Kurokochi & Sato, 2015). Grinding showed to be particularly effective in increasing IB if carried out on STEX pulp (Velásquez et al., 2003). However, fine grinding requires a large amount of energy. Therefore, more studies could be devoted to maintain a balance between efficiency improvement and cost.

1.3.3. Hot pressing conditions

The HP is the stage at the end of which the board is obtained in its final form. This is where the chemical changes obtained in pretreatment come into play to activate the self-bonding mechanism. The main parameters of HP are the temperature (Tp), the time (tp), and the pressure (Pp). If heated at high Tp, the lignin of the pretreated biomass surrounds and bonds the fibers (Anglés et al., 2001; Nasir et al., 2019). Moreover, the water loss produced during the HP may contribute to the formation of covalent bonds between chemical components of LM (Domínguez-Robles et al., 2020). Tp has a major influence on BF properties, as well as tp and Pp. As the Tp and tp increase, MOR, IB, and TS are observed to improve (Hashim et al., 2011; Hidalgo-Cordero et al., 2020; Zhang et al., 2015). Okuda et al. studied chemical changes of kenaf core BF after HP and its influence on fiberboard properties. In this study, part of the lignin and hemicellulose decomposed during the HP process, and this led to a condensation reaction in lignin (Okuda et al.,

2006). Other studies indicated that the increasing in Tp, tp, and Pp, increased the stability against moisture, mechanical strength, and the resistance of microorganisms' decays of the specimens (Boon et al., 2013). Nonaka et al. investigated the effect of high Tp on binderless particleboards made by sugarcane bagasse and recycled wood chips. They found an improvement in mechanical properties and dimensional stability by using high Tp for both bagasse and wood chips (Nonaka et al., 2013).

Commonly Tp ranges from 110°C and 230°C, while tp values varying among 10 min and 50 min were found in literature. Many authors divided the HP into three steps when producing BF: a first HP step at controlled Tp, Pp, and tp; a breathing time during which the pressure is released; and a last shorter HP step, generally with a higher Pp (Anglés et al., 2001; Mancera et al., 2008; Theng et al., 2015; Velásquez et al., 2003). The three-steps HP helps to avoid the formation of blisters on the surface of the specimens, which may compromise the mechanical properties of fiberboard (Ramos et al., 2017).

Recently steam injection has gained attention as a manufacturing process for fiberboards (Pintiaux et al., 2015). As mentioned, it can be considered as a combination of STEX pretreatment and HP, as it consists of injecting steam directly into the material while it is being pressed in the mold. Thus, all fractions are formed during treatment and remain in the fibers (Alvarez et al., 2015), while in STEX the degraded components are solubilized in water and can be removed after processing. There are some researchers studying steam injection process to produce low density fiberboards (LDF), especially with kenaf core (Widyorini et al., 2005; Xu et al., 2003). In one of these studies, BF of relatively good quality have been obtained, as they showed an improved IB and TS when comparing with the HP method (Xu et al., 2003).

1.4. Fiberboards classification

The classification of fiberboards can refer to different criteria, as indicated by the reference standard EN 316:2009 (Figure 1.3.). Fiberboards can be classified according to the production process, to the density, to the thickness, to specific properties, and to the application.

Figure 1.1. *Summary scheme of the classification of fiberboards, according to current European standards (EN 316:2009).*

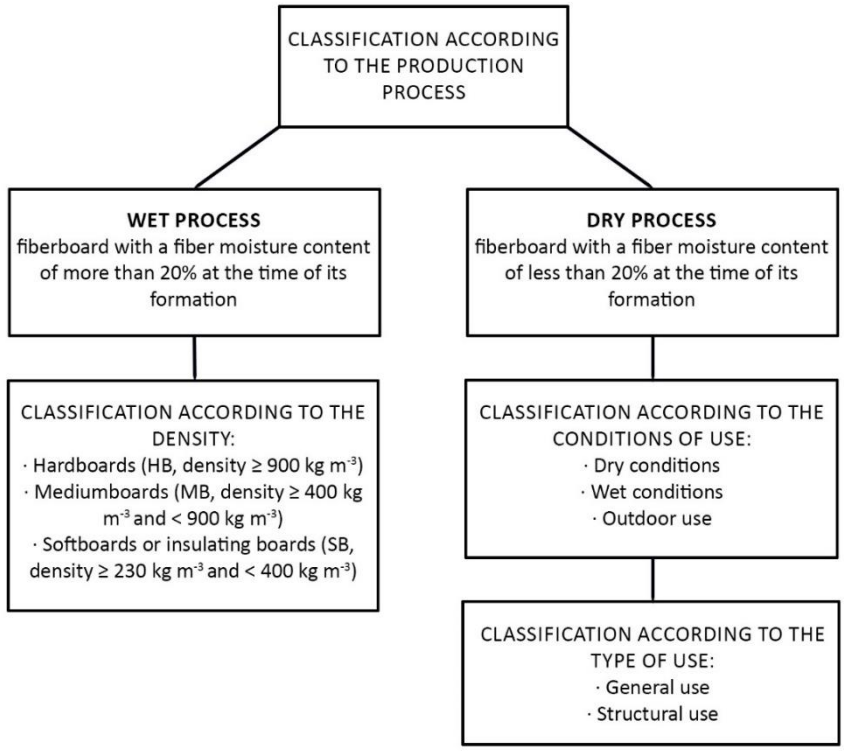

According to the production process, fiberboards can be divided in two groups: boards made by WFP or boards made by DFP. Within this category they are further divided into density-dependent subcategories. Thus, panels derived from WFP can have a high density above 900 kg/m^3 (hardboards HB), a medium density between 400 and 900 kg/m^3 (medium boards MB), and a low density from 230 to 400 kg/m^3 (softboards SB). The density ranges are the same for boards made by DFP. On the other hand, the boards manufactured by DFP can be classified according the conditions of use: dry conditions, wet conditions, and outdoor use. Moreover, they can be divided depending on whether they are used for general or structural use (Figure 1.1.).

Other standards define the minimum mechanical and physical requirements for their application under the above conditions. In particular, the series EN 622 defines the requirements for HB, MB, SB, and for the dry-formed boards, and more details will be presented in Chapter 2.

Current applications

The construction industry makes extensive use of WBP, causing environmental problems both in terms of meeting the high demand for wood and emissions from the use of synthetic adhesives (Viel et al., 2019). BF could be a solution to both problems if manufactured from alternative LMs. On the one hand, the use of alternative fibers supports the concept of forest protection and on the other hand, the absence of FBA makes these panels particularly suitable for indoor use applications such as wall partitions, false ceilings, and furniture (Nasir et al., 2019).

To date, many studies investigated the feasibility of BF for example for thermal insulation. Natural fibers generally have good thermal properties (Ramlee et al., 2021) and this has motivated many researchers to investigate their behavior into this field. Some examples available in the literature reviewed use renewable materials such as sunflower (Evon et al., 2014), coconut husks and bagasse (Panyakaew & Fotios, 2011), cotton stalk fibers (Zhou et al., 2010) eucalyptus leaves and wheat straw fibers (Ali et al., 2020), and hemp and corn residues (Viel et al., 2019). A recent review (Madurwar et al., 2013) investigated the use of agro-waste for sustainable construction, also considering BF.

Despite their potential, BF are struggling to break into the building materials market. Literature results offer a few application examples and there are still many gaps that it is not possible to have a clear idea of the competitiveness of these products on the market. Beforehand, WA and TS are major concern and need further study and improvement (Nasir et al., 2019). In addition, there is almost a complete lack of economic information.

As a result, more studies could address:

- Improving the physico-mechanical characteristics of the BF;
- Finding new and viable ways for the real use of BF;
- Studying the economic competitiveness on the construction materials market, considering the influence of the raw material and the manufacturing process on the product;
- Studying the environmental impact and benefit compared to current fiberboards.

There are few studies evaluating the impact of BF. This might be due to their use, while potentially beneficial, is not yet fully contemplated in the WBP industry. Despite this, some environmental impact studies found in the literature are reported in the following subsection.

1.5. Carbon footprint and life cycle assessment studies

Nowadays, the environmental impact of the products is a major issue. Forest industry, associated with the production of panels, is responsible for high energy consumption and environmental pollution

(Yuan & Guo, 2017), as for the emission of formaldehyde and volatile organic compounds (VOC) during the production, use, and after disposal of panel product. Besides, building sector plays an essential role in the global energy scenario, and its environmental impact could be reduced by introducing more sustainable materials (Casas-Ledón et al., 2020; Scrucca et al., 2020).

Life cycle assessment (LCA) is a methodology that proved to be appropriate for assessing the environmental impact of products (Iritani et al., 2015), since it considers the entire life cycle, i.e. the sourcing of raw material, its processing, the manufacturing of the product and its marketing, up to the end of its life. A number of studies focusing on environmental assessment of WBP pointed out that the high environmental impact is mainly due to the use and processing of wood resources, and the formaldehyde emissions related to the use of synthetic adhesives (Dos Santos et al., 2014; González-García et al., 2009; Rivela et al., 2006, 2007).

Nevertheless, very few studies concerning green BF are available at the present day. As an example, González-García et al. carried out an environmental assessment of green hardboards made by a two-component adhesive based on laccase activated system and demonstrated their industrial viability (González-García et al., 2011). Also, Freire et al. evaluated the environmental impact of green MDF and HDF comparing their results with commercial UF bonded boards. They showed the environmental superiority of the first boards in most of impact categories (climate change, acidification, land use, particulate matter, water depletion, and freshwater eutrophication) (Freire et al., 2017).

Aforementioned research provides useful information on the potential role of BF in the building sector, but the literature is still too scarce to draw appropriate conclusions. For this reason, further studies considering the environmental impact and the principles of circular economy are needed.

References

Adhikari, S., Nam, H., & Chakraborty, J. P. (2018). Chapter 8 – Conversion of solid wastes to fuels and chemicals through pyrolysis. *Waste Biorefinery. Potential and Perspectives*, Elsevier, 239–263. https://doi.org/10.1016/B978-0-444-63992-9.00008-2

Agbor, V. B., Cicek, N., Sparling, R., Berlin, A., & Levin, D. B. (2011). Biomass pretreatment: Fundamentals toward application. *Biotechnology Advances* 29(6), 675–685. https://doi.org/10.1016/j.biotechadv.2011.05.005

Ahmad, Z., Tajuddin, M., Salim, N. F. F., & Halim, Z. (2018). Effect of alkaline treatment on properties of rattan waste and fabricated binderless particleboard. *IIUM Engineering Journal*, 19(1), 185–196. https://doi.org/10.31436/iiumej.v19i1.879

Aisyah, H. A., Paridah, M. T., Sahri, M. H., Astimar, A. A., & Anwar, U. M. K. (2012). Influence of thermomechanical pulping production parameters on properties of medium density fiberboard made from kenaf bast. *Journal of Applied Science*, 12(6), 575–580.

Ali, M., Alabdulkarem, A., Nuhait, A., Al-Salem, K., Iannace, G., Almuzaiqer, R., Al-turki, A., Al-Ajlan, F., Al-Mosabi, Y., & Al-Sulaimi, A. (2020). Thermal and acoustic characteristics of novel thermal insulating materials made of Eucalyptus Globulus leaves and wheat straw fibers. *Journal of Building Engineering*, 32, 101452. https://doi.org/10.1016/j.jobe.2020.101452

Álvarez, C., Rojano, B., Almaza, O., Rojas, O. J., & Gañán, P. (2011). Self-bonding boards from plantain fiber bundles after enzymatic treatment: adhesion improvement of lignocellulosic products by enzymatic pre-treatment. *Journal of Polymers and the Environment*, 19(1), 182–188. https://doi.org/10.1007/s10924-010-0260-6

Alvarez, C., Rojas, O. J., Rojano, B., & Gañán, P. (2015). development of self-bonded fiberboards from fiber of leaf plantain: effect of water and organic extractives removal. *BioResources*, 10(1), 672–683.

Amin, F. R., Khalid, H., Zhang, H., Rahman, S., Zhang, R., Liu, G., & Chen, C. (2017). Pretreatment methods of lignocellulosic biomass for anaerobic digestion. *AMB Express*, 7, 72. https://doi.org/10.1186/s13568-017-0375-4

Anglés, M. N., Ferrando, F., Farriol, X., & Salvadó, J. (2001). Suitability of steam exploded residual softwood for the production of binderless panels. Effect of the pre-treatment severity and lignin addition. *Biomass and Bioenergy*, 21, 211–224.

Antov, P., Savov, V., Krišťák, L., Réh, R., & Mantanis, G. I. (2021). Eco-friendly, high-density fiberboards bonded with urea-formaldehyde and ammonium lignosulfonate. *Polymers*, 13(2), 1–13. https://doi.org/10.3390/polym13020220

Asafu-Adjaye, O., Via, B., & Banerjee, S. (2020). Soy flour substitution in polymeric methylene diphenyl diisocyanate resin for composite panel applications. *Forest Products Journal*, 70(3), 350–355. https://doi.org/10.13073/FPJ-D-20-00014

Avellar, B. K., & Glasser, W. G. (1998). Steam-assisted biomass fractionation. I. Process considerations and economic evaluation. *Biomass and Bioenergy*, 14(3), 205–2018.

Badiei, M., Asim, N., Jahim, J. M., & Sopian, K. (2014). Comparison of chemical pretreatment methods for cellulosic biomass. *APCBEE Procedia*, 9, 170–174. https://doi.org/10.1016/J.APCBEE.2014.01.030

Balea (Paul), G., Lunguleasa, A., Zeleniuc, O., & Coşereanu, C. (2022). Three adhesive recipes based on magnesium lignosulfonate, used to manufacture particleboards with low formaldehyde emissions and good mechanical properties. *Forests*, 13(5), 737. https://doi.org/10.3390/f13050737

Barakat, A., Mayer-Laigle, C., Solhy, A., Arancon, R. A. D., de Vries, H., & Luque, R. (2014). Mechanical pretreatments of lignocellulosic biomass: towards facile and environmentally sound technologies for biofuels production. *RSC Advances*, 4, 48109. https://doi.org/10.1039/c4ra07568d

Baskaran, M., Hashim, R., Said, N., Raffi, M., Balakrishnan, K., Sudesh, K., Sulaiman, O., Arai, T., Kosugi, A., Mori, Y., Sugimoto, T., & Sato, M. (2011). Properties of binderless particleboard from oil palm trunk with addition of polyhydroxyalkanoates. *Composites: Part B*, 43, 1109–1116. https://doi.org/10.1016/j.compositesb.2011.10.008

Bekhta, P., Noshchenko, G., Réh, R., Kristak, L., Sedliačik, J., Antov, P., Mirski, R., & Savov, V. (2021). Properties of eco-friendly particleboards bonded with lignosulfonate-urea-formaldehyde adhesives and PMDI as a crosslinker. *Materials*, 14(17), 4875. . https://doi.org/10.3390/ma14174875

Boon, J. G., Hashim, R., Sulaiman, O., Hiziroglu, S., Sugimoto, T., & Sato, M. (2013). Influence of processing parameters on some properties of oil palm trunk binderless particleboard. *European Journal of Wood and Wood Products*, 71(5), 583–589. https://doi.org/10.1007/s00107-013-0712-5

Carnevale, M., Longo, L., Gallucci, F., & Santangelo, E. (2021). Influence of the harvest time and the airflow rate on the characteristics of the Arundo biochar produced in a pilot updraft reactor. *Biomass Conversion and Biorefinery*, 12, 2525 – 2539. https://doi.org/10.1007/s13399-020-01241-8

Casas-Ledón, Y., Daza Salgado, K., Cea, J., Arteaga-P Erez, L. E., & Fuentealba, C. (2020). Life cycle assessment of innovative insulation panels based on eucalyptus bark fibers. *Journal of Cleaner Production*, 249, 119356. https://doi.org/10.1016/j.jclepro.2019.119356

Chen, H., & Yan, N. (2018). Application of Western red cedar (Thuja plicata) tree bark as a functional filler in pMDI wood adhesives. *Industrial Crops and Products*, 113, 1–9. https://doi.org/10.1016/j.indcrop.2018.01.005

Cheng, J. J., & Timilsina, G. R. (2011). Status and barriers of advanced biofuel technologies: A review. *Renewable Energy*, 36, 3541–3549. https://doi.org/10.1016/j.renene.2011.04.031

Corno, L., Pilu, R., Adani, F., & Ricicla, G. (2014). Arundo donax L.: A non-food crop for bioenergy and bio-compound production. *Biothechnology Advances*, 32, 1535–1549. https://doi.org/10.1016/j.biotechadv.2014.10.006

Dahy, H. (2019). Natural fibre-reinforced polymer composites (NFRP) fabricated from lignocellulosic fibres for future sustainable architectural applications, case studies: Segmented-shell construction, acoustic panels, and furniture. *Sensors (Switzerland)*, 19(3), 738. https://doi.org/10.3390/s19030738

Das, S., Malmberg, M. J., & Frazier, C. E. (2007). Cure chemistry of wood/polymeric isocyanate (PMDI) bonds: Effect of wood species. *International Journal of Adhesion and Adhesives*, 27(3), 250–257. https://doi.org/10.1016/j.ijadhadh.2006.05.002

De Bari, I., Liuzzi, F., Ambrico, A., & Trupo, M. (2020). Arundo donax refining to second generation bioethanol and furfural. *Processes*, 8(12), 1591. https://doi.org/10.3390/pr8121591

Dell'omo, P. P., & Spena, V. A. (2020). Mechanical pretreatment of lignocellulosic biomass to improve biogas production: Comparison of results for giant reed and wheat straw. *Energy*, 203, 117798. https://doi.org/10.1016/j.energy.2020.117798

Domínguez-Robles, J., Tarrés, Q., Alcalà, M., Mansouri, N.-E. el, Rodríguez, A., Mutjé, P., & Delgado-Aguilar, M. (2020). Development of high-performance binderless fiberboards from wheat straw residue. *Construction and Building Materials*, 232, 117247. https://doi.org/10.1016/j.conbuildmat.2019.117247

Domínguez-Robles, J., Tarrés, Q., Delgado-Aguilar, M., Rodríguez, A., Espinach, F. X., & Mutjé, P. (2018). Approaching a new generation of fiberboards taking advantage of self lignin as green adhesive. *International Journal of Biological Macromolecules*, 108, 927–935. https://doi.org/10.1016/j.ijbiomac.2017.11.005

Dos Santos, F. M. N., Battistelle, A. G., Stolte Bezerra, B., & Varum, H. S. A. (2014). Comparative study of the life cycle assessment of particleboards made of residues from sugarcane bagasse (Saccharum spp.) and pine wood shavings (Pinus elliottii). *Journal of Cleaner Production*, 64, 345–355. https://doi.org/10.1016/j.jclepro.2013.06.039

Dunky, M. (2003). Chapter 47 – Adhesives in the wood industry. *Handbook of Adhesive Technology, third edition*. CRC Press. https://doi.org/10.1201/9780203912225.ch47

Dunky, M., & Pizzl, A. (2002). Chapter 23 - Wood adhesives. *Adhesion Science and Engineering*, 2, 1039–1103. https://doi.org/10.1016/B978-044451140-9/50023-8

e Silva, C. F. L., Schirmer, M. A., Maeda, R. N., Barcelos, C. A., & Pereira, N. (2015). Potential of giant reed (Arundo donax L.) for second generation ethanol production. *Electronic Journal of Biotechnology*, 18(1), 10–15. https://doi.org/10.1016/J.EJBT.2014.11.002

Evon, P., Vandenbossche, V., Pontalier, P.-Y., & Rigal, L. (2014). New thermal insulation fiberboards from cake generated during biorefinery of sunflower whole plant in a twin-screw extruder. *Industrial Crops and Products*, 52, 354–362. https://doi.org/10.1016/j.indcrop.2013.10.049

Felby, C., Thygesen, L. G., Sanadi, A., & Barsberg, S. (2004). Native lignin for bonding of fiberboards-evaluation of bonding mechanisms in boards made from laccase-treated fibers of beech (Fagus sylvatica). *Industrial Crops and Products*, 20, 181–189. https://doi.org/10.1016/j.indcrop.2004.04.020

Ferrandez-Garcia, M. T., Ferrandez-Garcia, C. E., Garcia-Ortuño, T., Ferrandez-Garcia, A., & Ferrandez-Villena, M. (2019). Experimental evaluation of a new giant reed (Arundo donax L.) composite using citric acid as a natural binder. *Agronomy*, 9(12), 882. https://doi.org/10.3390/agronomy9120882

Ferrandez-Villena, M., Ferrandez-Garcia, C. E., Garcia-Ortuño, T., Ferrandez-Garcia, A., & Ferrandez-Garcia, M. T. (2020). The influence of processing and particle size on binderless particleboards made from Arundo donax L. Rhizome. *Polymers*, 12(3), 696. https://doi.org/10.3390/polym12030696

Ferrandez-Villena, M., Ferrandez-Garcia, C. E., Ortuño, T. G., Ferrandez-Garcia, A., & Ferrandez-Garcia, M. T. (2019). Study of the utilisation of almond residues for low-cost panels. *Agronomy*, 9(12), 811. https://doi.org/10.3390/agronomy9120811

Ferrarini, A., Fracasso, A., Spini, G., Fornasier, F., Taskin, E., Fontanella, M. C., Beone, G. M., Amaducci, S., & Puglisi, E. (2021). Bioaugmented phytoremediation of metal-contaminated soils and sediments by hemp and giant reed. *Frontiers in Microbiology*, 12, 645893. https://doi.org/10.3389/fmicb.2021.645893

Flores, J. A., Pastor, J. J., Martinez-Gabarron, A., Gimeno-Blanes, F. J., Rodríguez-Guisado, I., & Frutos, M. J. (2011). Arundo donax chipboard based on urea-formaldehyde resin using under 4 mm particles size meets the standard criteria for indoor use. *Industrial Crops and Products*, 34, 1538–1542. https://doi.org/10.1016/j.indcrop.2011.05.011

Freire, A. L. F., Araújo Júnior, C. P. de, Rosa, M. de F., Figueirêdo, M. C. B. de, & Almeida Neto, J. A. de. (2017). Environmental assessment of bioproducts in development stage: The case of fiberboards made from coconut residues. *Journal of Cleaner Production*, 153, 230–241. https://doi.org/10.1016/j.jclepro.2017.03.100

Gao, Z., Wang, X.-M., Wan, H., & Brunette, G. (2011). Binderless panels made with black spruce bark. *BioResources*, 6(4), 3960–3972.

Gendron, J., Stambouli, I., Bruel, C., Boumghar, Y., & Montplaisir, D. (2022). Characterization of different types of lignin and their potential use in green adhesives. *Industrial Crops and Products*, 182, 114893. https://doi.org/10.1016/j.indcrop.2022.114893

Glasser, W. G., & Wright, R. S. (1998). Steam-assisted biomass fractionation. II. Fractionation behavior of various biomass resources. *Biomass and Bioenergy*, 14(3), 219–235.

Gonçalves, D., Bordado, J. M., Marques, A. C., & dos Santos, R. G. (2021). Non-formaldehyde, bio-based adhesives for use in wood-based panel manufacturing industry—a review. *Polymers* 13(23), 4086. MDPI. https://doi.org/10.3390/polym13234086

González-García, S., Feijoo, G., Heathcote, C., Kandelbauer, A., & Moreira, M. T. (2011). Environmental assessment of green hardboard production coupled with a laccase activated system. *Journal of Cleaner Production*, 19(5), 445–453. https://doi.org/10.1016/j.jclepro.2010.10.016

González-García, S., Feijoo, G., Widsten, P., Kandelbauer, A., Zikulnig-Rusch, E., & Moreira, M. T. (2009). Environmental performance assessment of hardboard manufacture. *International Journal of Life Cycle Assessment*, 14(5), 456–466. https://doi.org/10.1007/s11367-009-0099-z

Gouveia, S., Otero, L. A., Fernández-Costas, C., Filgueira, D., Sanromán, Á., & Moldes, D. (2018). Green binder based on enzymatically polymerized eucalypt kraft lignin for fiberboard manufacturing: A preliminary study. *Polymers*, 10(6), 642. https://doi.org/10.3390/polym10060642

Halvarsson, S., Edlund, H., & Norgren, M. (2008). Manufacture of non-resin wheat straw fibreboards. *Industrial Crops and Products*, 29, 437–445. https://doi.org/10.1016/j.indcrop.2008.08.007

Hamidreza Ghaffar, S., & Fan, M. (2014). Lignin in straw and its applications as an adhesive. *International Journal of Adhesion and Adhesives*, 48, 92–101. https://doi.org/10.1016/j.ijadhadh.2013.09.001

Hardesty-Moore, M., Orr, D., & McCauley, D. J. (2020). Invasive plant Arundo donax alters habitat use by carnivores. *Biological Invasions*, 22(6), 1983–1995. https://doi.org/10.1007/s10530-020-02234-4

Hashim, R., Saari, N., Sulaiman, O., Sugimoto, T., Hiziroglu, S., Sato, M., & Tanaka, R. (2010). Effect of particle geometry on the properties of binderless particleboard manufactured from oil palm trunk. *Materials and Design*, 31, 4251–4257. https://doi.org/10.1016/j.matdes.2010.04.012

Hashim, R., Said, N., Lamaming, J., Baskaran, M., Sulaiman, O., Sato, M., Hiziroglu, S., & Sugimoto, T. (2011). Influence of press temperature on the properties of binderless particleboard made from oil palm trunk. *Materials and Design*, 32, 2520–2525. https://doi.org/10.1016/j.matdes.2011.01.053

Hemmilä, V., Adamopoulos, S., Hosseinpourpia, R., & Ahmed, S. A. (2019). Ammonium lignosulfonate adhesives for particleboards with pMDI and furfuryl alcohol as crosslinkers. *Polymers*, 11(10). https://doi.org/10.3390/polym11101633

Hidalgo-Cordero, J. F., García-Ortuño, T., & García-Navarro, J. (2020). Comparison of binderless boards produced with different tissues of totora (Schoenoplectus californicus (C.A. Mey) Soják) stems. *Journal of Building Engineering*, 27, 100961. https://doi.org/10.1016/j.jobe.2019.100961

Hidayat, H., Keijsers, E. R. P., Prijanto, U., van Dam, J. E. G., & Heeres, H. J. (2014). Preparation and properties of binderless boards from Jatropha curcas L. seed cake. *Industrial Crops and Products*, 52, 245–254. https://doi.org/10.1016/j.indcrop.2013.10.024

Hidayat, W., Aprilliana, N., Asmara, S., Bakri, S., Hidayati, S., Banuwa, I. S., Lubis, M. A. R., & Iswanto, A. H. (2022). Performance of eco-friendly particleboard from agro-industrial residues bonded with formaldehyde-free natural rubber latex adhesive for interior applications. *Polymer Composites*, 43(4), 2222–2233. https://doi.org/10.1002/PC.26535

Hoareau, W., Oliveira, F. B., Grelier, S., Siegmund, B., Frollini, E., & Castellan, A. (2006). Fiberboards based on sugarcane bagasse lignin and fibers. *Macromolecular Materials and Engineering*, 291(7), 829–839. https://doi.org/10.1002/mame.200600004

Iritani, D. R., Silva, D. A. L., Saavedra, Y. M. B., Grael, P. F. F., & Ometto, A. R. (2015). Sustainable strategies analysis through Life Cycle Assessment: a case study in a furniture industry. *Journal of Cleaner Production*, 96, 308–318. https://doi.org/10.1016/j.jclepro.2014.05.029

Karthäuser, J., Biziks, V., Mai, C., Militz, H., Charrier, B., & Kowaluk, G. (2021). Lignin and lignin-derived compounds for wood applications-A review. *Molecules*, 26, 2533. https://doi.org/10.3390/molecules26092533

Kortekaas, S., Wijngaarde, R. R., Klomp, J.-W., Lettinga, G., & Field, J. A. (1998). Anaerobic treatment of hemp thermomechanical pulping wastewater. *Water Research*, 32(11), 3362–3370.

Kumar, R., Mago, G., Balan, V., & Wyman, C. E. (2009). Physical and chemical characterizations of corn stover and poplar solids resulting from leading pretreatment technologies. *Bioresources Technology*, 100, 3948–3962. https://doi.org/10.1016/j.biortech.2009.01.075

Kurokochi, Y., & Sato, M. (2015). Properties of binderless board made from rice straw: The morphological effect of particles. *Industrial Crops and Products*, 69, 55–59. https://doi.org/10.1016/j.indcrop.2015.01.044

Kurokochi, Y., & Sato, M. (2020). Steam treatment to enhance rice straw binderless board focusing hemicellulose and cellulose decomposition products. *Journal of Wood Science*, 66(1), 1–8. https://doi.org/10.1186/s10086-020-1855-8

Laemsak, N., Okuma, M., Laemsak, N., & Okuma, M. (2000). Development of boards made from oil palm frond II: properties of binderless boards from steam-exploded fibers of oil palm frond. *Journal of Wood Science*, 46, 322–326.

Lal, R. (2005). World crop residues production and implications of its use as a biofuel. *Environment International*, 31, 575–584. https://doi.org/10.1016/j.envint.2004.09.005

Lamaming, J., Hashim, R., Sulaiman, O., Sugimoto, T., Sato, M., & Hiziroglu, S. (2014). Measurement of some properties of binderless particleboards made from young and old oil palm trunks. *Measurement*, 47, 813–819. https://doi.org/10.1016/j.measurement.2013.10.007

Li, X., Cai, Z., Winandy, J. E., & Basta, A. H. (2010). Selected properties of particleboard panels manufactured from rice straws of different geometries. *Bioresource Technology*, 101, 4662–4666. https://doi.org/10.1016/j.biortech.2010.01.053

Luo, H., Zhang, H., & Lu, X. (2014). Manufacture of binderless fiberboard made from bamboo processing residues by steam explosion pretreatment. *Wood Research*, 59(5), 861–870. https://www.researchgate.net/publication/279098113

Luo, P., Yang, C., Li, M., & Wang, Y. (2020). Manufacture of thin rice straw particleboards bonded with various polymeric methane diphenyl diisocyanate/urea formaldehyde resin mixtures. *BioResource*s, 15(1), 935–944.

Madurwar, M. v, Ralegaonkar, R. v, & Mandavgane, S. A. (2013). Application of agro-waste for sustainable construction materials: A review. *Construction and building materials*, 38, 872–878. https://doi.org/10.1016/j.conbuildmat.2012.09.011

Mancera, C., el Mansouri, N.-E., Ferrando, F., & Salvadó, J. (2011). The suitability of steam exploded Vitis vinifera and alkaline lignin for the manufacture of fiberboard. *BioResources*, 6(4), 4439–4453. https://doi.org/10.15376/biores.6.4.4439-4453

Mancera, C., Ferrando, F., & Salvadó, J. (2008). Cynara cardunculus as raw material for the production of binderless fiberboards: Optimization of pretreatment and pressing conditions. *Journal of Wood Chemistry and Technology*, 28(3), 207–226. https://doi.org/10.1080/02773810802347024

Mancera, C., Mansouri, N.-E. el, Angels Pelach, M., Francesc, F., & Salvadó, J. (2012). Feasibility of incorporating treated lignins in fiberboards made from agricultural waste. *Waste Management*, 32, 1962–1967. https://doi.org/10.1016/j.wasman.2012.05.019

Mancera, C., Mansouri, N.-E. el, Vilaseca, F., Ferrando, F., & Salvadó, J. (2011). The effect of lignin as a natural adhesive on the physico-mechanical properties of Vitis vinifera fiberboards. *BioResources*, 6(3), 2851–2860.

Mansouri, E., Pizzi, A., Salvadó, J., Mansouri, N.-E. El, Salvadó, J, & Pizzi, A. (2007). Lignin-based wood panel adhesives without formaldehyde. *Holz Roh Werkst*, 65, 65–70. https://doi.org/10.1007/s00107-006-0130-z

Mejía, E. H., Quintana, G. C., & Ogunsile, B. O. (2014). Development of binderless fiberboards from steam exploded and oxidized oil palm wastes. *BioResources*, 9(2), 2922–2936. https://doi.org/10.15376/biores.9.2.2922-2936

Migneault, S., Koubaa, A., Riedl, B., Nadji, H., Deng, J., & Zhang, T. (2011). Binderless fiberboard made from primary and secondary pulp and paper sludge. *Wood and Fiber Science*, 43 (2), 180 – 193.

Mishra, S., Singh, P. K., Dash, S., & Pattnaik, R. (2018). Microbial pretreatment of lignocellulosic biomass for enhanced biomethanation and waste management. 3 Biotech, 8, 458. https://doi.org/10.1007/s13205-018-1480-z

Miyamoto, K., Nakahara, S., & Suzuki, S. (2002). Effect of particle shape on linear expansion of particleboard. *Journal of Wood Science*, 48, 185–190.

Mobarak, F., Fahmy, Y., & Augustin, H. (1982). Binderless lignocellulose composite from bagasse and mechanism of self-bonding. *Holzforschung*, 36(3), 131–136. https://doi.org/10.1515/hfsg.1982.36.3.131

Molari, L., Coppolino, F. S., & García, J. J. (2021). Arundo donax: A widespread plant with great potential as sustainable structural material. *Construction and Building Materials*, 268, 121143. https://doi.org/10.1016/j.conbuildmat.2020.121143

Naraian, R., & Gautam, R. L. (2018). Chapter 6 – Penicillium enzymes for the saccharification of lignocellulosic feedstocks. new and future developments in microbial biotechnology and bioengineering: penicillium system properties and applications. *New and Future Developments in Microbial Biotechnology and Bioengineering*, 121–136, Elsevier. https://doi.org/10.1016/B978-0-444-63501-3.00006-5

Nasir, M., Gupta, A., Dalour, M., Beg, H., Chua, G. K., & Asim, M. (2014). Laccase application in medium density fibreboard to prepare a bio-composite. *RSC Advances*, 4, 11520. https://doi.org/10.1039/c3ra40593a

Nasir, M., Khali, D. P., Jawaid, M., Tahir, P. M., Siakeng, R., Asim, M., & Khan, T. A. (2019). Recent development in binderless fiber-board fabrication from agricultural residues: A review. *Construction and Building Materials* 211, 502–516. https://doi.org/10.1016/j.conbuildmat.2019.03.279

Niaz, K., & Khan, F. (2020). Chapter 3 – Analysis of polyphenolics. *Recent Advances in Natural Products Analysis*, 39–197, Elsevier. https://doi.org/10.1016/B978-0-12-816455-6.00003-2

Nonaka, S., Umemura, K., & Kawai, S. (2013). Characterization of bagasse binderless particleboard manufactured in high-temperature range. *Journal of Wood Science*, 59(1), 50–56. https://doi.org/10.1007/s10086-012-1302-6

Oktay, S., Kızılcan, N., & Bengü, B. B. (2021). Development of bio-based cornstarch-mimosa tannin-sugar adhesive for interior particleboard production. *Industrial Crops and Products*, 170, 113689. https://doi.org/10.1016/j.indcrop.2021.113689

Okuda, N., Hori, K., & Sato, M. (2006). Chemical changes of kenaf core binderless boards during hot pressing (I): Influence of the pressing temperature condition. *Journal of Wood Science*, 52(3), 244–248. https://doi.org/10.1007/s10086-005-0761-4

Okuda, N., & Sato, M. (2004). Manufacture and mechanical properties of binderless boards from kenaf core. *Journal of Wood Science*, 50(1), 53–61. https://doi.org/10.1007/s10086-003-0528-8

Ostendorf, K., Ahrens, C., Beulshausen, A., Tayo, J. L. T., & Euring, M. (2021). On the feasibility of a pMDI-reduced production of wood fiber insulation boards by means of kraft lignin and ligneous canola hulls. *Polymers*, 13(7). https://doi.org/10.3390/polym13071088

Overend, R. P., Chornet, E., & Gascoigne, J. A. (1987). Fractionation of lignocellulosics by steam-aqueous pretreatments [and Discussion]. *Philosophical Transactions of the Royal Society of London. Series A, Mathematical and Physical Sciences*, 321(1561), 523–536. http://www.jstor.org/stable/37798

Pan, Z., Cathcart, A., & Wang, D. (2006). Properties of particleboard bond with rice bran and polymeric methylene diphenyl diisocyanate adhesives. *Industrial Crops and Products*, 23, 40–45. https://doi.org/10.1016/j.indcrop.2005.03.004

Panyakaew, S., & Fotios, S. (2011). New thermal insulation boards made from coconut husk and bagasse. *Energy and Buildings*, 43(7), 1732–1739. https://doi.org/10.1016/j.enbuild.2011.03.015

Pędzik, M., Janiszewska, D., & Rogozi´nski, R. (2021). Alternative lignocellulosic raw materials in particleboard production: A review. *Industrial Crops and Products*, 174, 114162. https://doi.org/10.1016/j.indcrop.2021.114162

Pelaez-Samaniego, M. R., Yadama, V., Lowell, E., & Espinoza-Herrera, R. (2013). A review of wood thermal pretreatments to improve wood composite properties. *Wood Science and Technology,* 47(6), 1285–1319. Springer Verlag. https://doi.org/10.1007/s00226-013-0574-3

Pintiaux, T., Viet, D., Vandenbossche, V., Rigal, L., & Rouilly, A. (2015). Binderless materials obtained by thermos-compressive processing of lignocellulosic fibers: A comprehensive review. *BioResources*, 10(1), 1915–1963.

Pirayesh, H., Khazaeian, A., & Tabarsa, T. (2012). The potential for using walnut (Juglans regia L.) shell as a raw material for wood-based particleboard manufacturing. *Composites: Part B*, 43, 3276–3280. https://doi.org/10.1016/j.compositesb.2012.02.016

Quintana, G., Velasquez, J., Betancourt, S., & Gañán, P. (2008). Binderless fiberboard from steam exploded banana bunch. *Industrial Crops and Products*, 29, 60–66. https://doi.org/10.1016/j.indcrop.2008.04.007

Rabemanolontsoa, H., & Saka, S. (2015). Various pretreatments of lignocellulosics. *Bioresource Technology,* 199, 83 – 91. https://doi.org/10.1016/j.biortech.2015.08.029

Ramlee, A., Naveen, J., & Jawaid, M. (2021). Potential of oil palm empty fruit bunch (OPEFB) and sugarcane bagasse fibers for thermal insulation application-A review. *Construction and Building Materials*, 271, 121519. https://doi.org/10.1016/j.conbuildmat.2020.121519

Ramos, D., Ferrando, F., Farriol, X., & Salvadó, J. (2020). Optimization of the production factors of boards obtained from Arundo Donax L. Fibers without added adhesives. *Molecules*, 25(7), 1660. https://doi.org/10.3390/molecules25071660

Ramos, D., Mansouri, N. E. El, Ferrando, F., & Salvadó, J. (2018). All-lignocellulosic fiberboard from steam exploded Arundo donax L. *Molecules*, 23(9), 2088. https://doi.org/10.3390/molecules23092088

Ramos, D., Salvadó, J., & Ferrando, F. (2017). High mechanical performance boards made from fibers of Arundo donax without added adhesives. *BioResources*, 12(3), 5383–5394.

Rivela, B., Hospido, A., Moreira, M. T., & Feijoo, G. (2006). Life cycle inventory of particleboard: A case study in the wood sector. *International Journal of Life Cycle Assessment*, 11(2), 106–113. https://doi.org/10.1065/lca2005.05.206

Rivela, B., Moreira, M. T., & Feijoo, G. (2007). Life cycle inventory of medium density fibreboard. *International Journal of Life Cycle Assessment*, 12(3), 143–150. https://doi.org/10.1065/lca2006.12.290

Saadaoui, N., Rouilly, A., Fares, K., & Rigal, L. (2013). Characterization of date palm lignocellulosic by-products and self-bonded composite materials obtained thereof. *Materials and Design*, 50, 302–308. https://doi.org/10.1016/j.matdes.2013.03.011

Saritha, M., Arora, A., & Lata, •. (2012). Biological Pretreatment of Lignocellulosic Substrates for Enhanced Delignification and Enzymatic Digestibility. *Indian Journal of Microbiology*, 52(2), 122–130. https://doi.org/10.1007/s12088-011-0199-x

Scrucca, F., Ingrao, C., Maalouf, C., Moussa, T., Polidori, G., Messineo, A., Arcidiacono, C., & Asdrubali, F. (2020). Energy and carbon footprint assessment of production of hemp hurds for application in buildings. *Environmental Impact Assessment Review*, 84, 106417. https://doi.org/10.1016/j.eiar.2020.106417

Shao, S., Jin, Z., Wen, G., & Iiyama, K. (2009). Thermo characteristics of steam-exploded bamboo (Phyllostachys pubescens) lignin. *Wood Science and Technology*, 43(7–8), 643–652. https://doi.org/10.1007/s00226-009-0252-7

Shatalov, A. A., & Pereira, H. (2006). Papermaking fibers from giant reed (Arundo donax L.) by advanced ecologically friendly pulping and bleaching technologies. *BioResources*, 1(1), 45–61. https://www.researchgate.net/publication/26460087

Solt, P., Konnerth, J., Gindl-Altmutter, W., Kantner, W., Moser, J., Mitter, R., & van Herwijnen, H. W. G. (2019). Technological performance of formaldehyde-free adhesive alternatives for particleboard industry. *International Journal of Adhesion and Adhesives*, 94, 99–131. https://doi.org/10.1016/j.ijadhadh.2019.04.007

Sreenivas, H. T., Krishnamurthy, N., & Arpitha, G. R. (2020). A comprehensive review on light weight kenaf fiber for automobiles. *International Journal of Lightweight Materials and Manufacture*, 3(4), 328–337. https://doi.org/10.1016/J.IJLMM.2020.05.003

Suchsland, O., Lansing, E., & Woodson, G. E. (1987). Fiberboard Manufacturing Practices in the United States, US Department of Agriculture, Forest service, p. 263.

Theng, D., Arbat, G., Delgado-Aguilar, M., Ngo, B., Labonne, L., Mutjé, P., & Evon, P. (2019). Production of fiberboard from rice straw thermomechanical extrudates by thermopressing: influence of fiber morphology, water and lignin content. *European Journal of Wood and Wood Products*, 77(1), 15–32. https://doi.org/10.1007/s00107-018-1358-0

Theng, D., Arbat, G., Delgado-Aguilar, M., Vilaseca, F., Ngo, B., & Mutjé, P. (2015). All-lignocellulosic fiberboard from corn biomass and cellulose nanofibers. *Industrial Crops and Products*, 76, 166–173. https://doi.org/10.1016/j.indcrop.2015.06.046

Theng, D., Mansouri, N.-E. el, Arbat, G., Ngo, B., Delgado-Aguilar, M., Àngels Pèlach, M., Fullana-I-Palmer, P., Mutjé, P. (2017). Fibreboards made from corn stalk thermomechanical pulp and kraft lignin as a green adhesive. *BioResources*, 12(2), 2379 – 2393.

Tupciauskas, R., Rizhikovs, J., Brazdausks, P., Fridrihsone, V., & Andzs, M. (2021). Influence of steam explosion pre-treatment conditions on binder-less boards from hemp shives and wheat straw. *Industrial Crops and Products*, 170, 113717. https://doi.org/10.1016/j.indcrop.2021.113717

Ukshini, E., & Dirckx, J. J. J. (2020). Longitudinal and transversal elasticity of natural and artificial materials for musical instrument reeds. *Materials*, 13(20), 1–13. https://doi.org/10.3390/ma13204566

Velásquez, J. A., Ferrando, F., & Salvadó, J. (2002). Binderless fiberboard from steam exploded Miscanthus sinensis: The effect of a grinding process. *Holz Als Roh - Und Werkstoff*, 60(4), 297–302. https://doi.org/10.1007/s00107-002-0304-2

Velásquez, J. A., Ferrando, F., & Salvadó, J. (2003). Effects of kraft lignin addition in the production of binderless fiberboard from steam exploded Miscanthus sinensis. *Industrial Crops and Products*, 18, 17–23. https://doi.org/10.1016/S0926-6690(03)00016-5

Viel, M., Collet, F., & Lanos, C. (2019). Development and characterization of thermal insulation materials from renewable resources. *Construction and Building Materials*, 214, 685–697. https://doi.org/10.1016/j.conbuildmat.2019.04.139

Widyorini, R., Xu, J., Umemura, K., & Kawai, S. (2005). Manufacture and properties of binderless particleboard from bagasse I: Effects of raw material type, storage methods, and manufacturing process. *Journal of Wood Science*, 51(6), 648–654. https://doi.org/10.1007/s10086-005-0713-z

Wong, M. C., Hendrikse, S. I. S., Sherrell, P. C., & Ellis, A. v. (2020). Grapevine waste in sustainable hybrid particleboard production. *Waste Management*, 118, 501–509. https://doi.org/10.1016/j.wasman.2020.09.007

Wu, J., Chen, C., Zhang, H., Xia, L., Huang, Y., Huang, H., Wang, Y., Qian, D., Wang, J., Wang, X., & Zhang, T. (2019). Eco-friendly fiberboard production without binder using poplar wood shavings bio-pretreated by white rot fungi Coriolus versicolor. *Construction and Building Materials*, 236, 117620. https://doi.org/10.1016/j.conbuildmat.2019.117620

Wu, J. G., Zhang, X., Liu, J., Xiong, M., Lu, X. Y., Fan, H. D., Wang, X. F., & Zhang, X. Y. (2016). Medium density fibreboard production by hot pressing without adhesive using Triarrhena sacchariflora residue bio-pretreated by white-rot fungus Coriolus versicolor. *Journal of Applied Microbiology*, 121(2), 415–421. https://doi.org/10.1111/JAM.13148

Wu, J., Zhang, X., Wan, J., Ma, F., Tang, Y., & Zhang, X. (2011). Production of fiberboard using corn stalk pretreated with white-rot fungus Trametes hirsute by hot pressing without adhesive. *Bioresource Technology*, 102, 11258–11261. https://doi.org/10.1016/j.biortech.2011.09.097

Xiao, L.-P., Lin, Z., Peng, W.-X., Yuan, T.-Q., Xu, F., Li, N.-C., Tao, Q.-S., Xiang, H., & Sun, R.-C. (2014). Unraveling the structural characteristics of lignin in hydrothermal pretreated fibers and manufactured binderless boards from Eucalyptus grandis. *Sustainable Chemical Processes*, 2(1), 9. https://doi.org/10.1186/2043-7129-2-9

Xu, J., Han, G., Wong, E. D., & Kawai, S. (2003). Development of binderless particleboard from kenaf core using steam-injection pressing. *Journal of Wood Science*, 49(4), 327–332. https://doi.org/10.1007/s10086-002-0485-7

Xu, J., Sugawara, R., Widyorini, R., Han, G., & Kawai, S. (2004). Manufacture and properties of low-density binderless particleboard from kenaf core. *Journal of Wood Science*, 50(1), 62–67. https://doi.org/10.1007/s10086-003-0522-1

Yuan, Y., & Guo, M. (2017). Do green wooden composites using lignin-based binder have environmentally benign alternatives? A preliminary LCA case study in China. *International Journal of Life Cycle Assessment*, 22(8), 1318–1326. https://doi.org/10.1007/s11367-016-1235-1

Zegada-Lizarazu, W., Salvi, S., & Monti, A. (2020). Assessment of mutagenized giant reed clones for yield, drought resistance and biomass quality. *Biomass and Bioenergy*, 134, 105501. https://doi.org/10.1016/j.biombioe.2020.105501

Zhang, D., Zhang, A., & Xue, L. (2015). A review of preparation of binderless fiberboards and its self-bonding mechanism. *Wood Science and Technology*, 49(4), 661–679. https://doi.org/10.1007/S00226-015-0728-6

Zhou, X.-Y., Zheng, F., Li, H.-G., & Lu, C.-L. (2010). An environment-friendly thermal insulation material from cotton stalk fibers. *Energy and Buildings*, 42, 1070–1074. https://doi.org/10.1016/j.enbuild.2010.01.02

Chapter 2. Materials and methods

Chapter content

This Chapter presents the materials and methodology used to produce the fiberboards. The study focuses on the manufacture of high density binderless fiberboard produced from *Arundo donax* L. fibers pretreated with steam explosion. In addition, a preliminary study on medium density fiberboards made with the same material and mixed with softwood fibers is presented and compared with panels made under the same conditions but using pMDI. The steps of the production process are discussed, and their expected role in the final performance of the fiberboard is identified. The equipment used and the methodology of production and characterization are specified in Annex A.

2.1. Materials

2.1.1. *Arundo donax* L.

The *Arundo donax* L. (AD) reeds used were provided by Cañizos Albatera SI and came from Ribarroja de Turia, Valencia (Spain). The reeds are harvested at 2 years of age, they are dried, and have a diameter of 2 to 3 cm, and a height of about 1.70 m (Figure 2.1.). Table 2.1. shows the chemical composition of raw AD.

Table 2.1. *Chemical composition of untreated Arundo donax L.*

Raw Material	Cellulose %	Hemicellulose %	Lignin %	Extractives %	Ash %
Arundo donax	43.1	21.9	22.4	9.3	3.8

Before being treated, the AD reeds are stored in a dry environment to prevent fermentation by fungi and other pests. Before steam explosion (STEX) treatment, the material has a relative humidity (RH) between 8% and 12%.

Figure 2.1. *Picture of Arundo donax L. reeds.*

2.1.2. Wood fibers

Wood fibers (WF) of pine (*Pinus sylvestris* L.) and spruce (*Picea abies* (L.) H.Karst.) at a mixing ratio of 95% to 5% were kindly provided by Gutex® Holzfaserplattenwerk H. Henselmann GmbH and Co. KG (Waldshut-Tiengen, Germany)(Figure 2.2.). Table 2.2. shows the typical chemical composition of softwoods.

Table 2.2. *Chemical composition of softwood (*spruce *Pinus sylvestris L.,* and pine *Picea abies L.).*

Raw material	Cellulose %	Hemicellulose %	Lignin %	Extractives %	Ash %
Spruce	38.2	28.5	25.1	10.7	0.4
Pine	32.1	16.4	36.2	14.2	0.9

2.1.3. pMDI

The pMDI I-Bond WFI 4370 was used as crosslinker and co-binder in Chapter 6 to enhance the bonding between fibers and it was obtained from Huntsman Corporation (Everberg, Belgium). This resin can be used for bonding oriented strand boards, MDF, particleboards, and insulation boards. It contains no added formaldehyde, thus meeting the European standards for formaldehyde emissions.

Figure 2.2. *Picture of wood fibers.*

2.2. Methods for fiberboard production and characterization

The production process here described can be associated with the dry-forming process (DFP) with the difference that the possibility of using any type of adhesive is explored.

2.2.1. Chipping

The first step involves reducing the AD reeds to chips of around 5 cm in length and 2 cm width (Figure 2.3.). The AD reeds are bought whole from Cañizos Albatera SI, and the chipping is necessary for the STEX. This phase involves first manually removing the leaves that have remained attached to the reeds and then the chipping itself. After this, AD chips are stored in bags of 750 g each, the maximum amount placed inside the STEX reactor in order to achieve a homogeneous treatment.

The chipping is carried out immediately prior to STEX, as AD is best preserved in its natural form as reed. Thus, the continuity of the process helps to avoid problems related to the degradation of the raw material sue to the improper storage. Further details about the process phase and the equipment used can be found in Annex A.

Figure 2.3. *Pictures of untreated Arundo donax L. chips.*

2.2.2. Steam explosion pretreatment

STEX equipment is described in more details in the Annex A. This phase involves the introduction of about 750 g of chopped reeds into the batch reactor, for each explosion performed. Here the chips are immersed in saturated steam at 40 bars. After a reaction time (tr) of 9.5 min at the required temperature, the pneumatic valve is opened and the steam pressure released, causing the breakdown of fibers. Several successive explosions are carried out and the material coming from each explosion at the same severity (R_0) was mixed to obtain a higher homogeneity. Pretreatment conditions were changed according to the desired objective, and these will be specified in the following chapters. Either way, from our previous studies, we found that a minimum tr of 9.5 min is necessary to let the steam penetrate the fibers. Therefore, change in R_0 means change in the reaction temperature (Tr). For this reason we will treat the two quantities, i.e., R_0 and Tr, as having the same meaning. The exploded AD was then rinsed in a washing trolley equipped with a 170 mesh sieve to remove the hydrolyzed hemicellulose (Figure 2.4.). After this, the obtained pulp was left to dry in ambient conditions for about 3 weeks (Figure 2.5.).

Figure 2.4. *Pictures of exploded Arundo donax L. in the expansion chamber, and the rinsing step.*

Figure 2.5. *Pictures of exploded Arundo donax L. at different severities (increasing from left to right), during the drying.*

2.2.3. Pulp milling

The exploded AD with a RH of 8-10% is ground to pass a 4 mm sieve (Figure 2.6.). As mentioned, this step is necessary for the enhancement of mechanical properties, especially IB (Velásquez et al., 2002).

2.2.4. Cold and hot pressing

An amount of 28.5 g of ground pulp is weighted to be placed inside a mold and cold pressed in a conventional press to form a mat of 150x50 mm (Figure 2.7.). This amount is calculated considering the RH of the material before the cold pressing (CP), and the desired density and thickness.

After being conditioned in the climatic chamber, the formed mat is hot pressed in a heated press at Tp 205 °C by a three-step procedure:

- Hot pressing (HP) at 1 MPa for 2 min;
- Breathing time of 1 min with no pressing pressure (Pp);
- HP at the desired Pp for 30 s,

The three-step pressure procedure helps to overcome a typical problem in manufacture of fiberboards with HP at high pressing temperature (Tp). This problem consists of the formation of blisters on the surface of the panel, probably due to the uneven moisture in the material, which evaporates quickly during the pressure and creates those vapor blisters.

Figure 2.6. *Pictures of exploded Arundo donax L. before (left) and after (right) the milling step.*

Figure 2.8. shows the appearance of panels where this drawback occurred. The intermediate breathing step allows the vapor to escape. In addition, a steel grid is placed inside the mold that creates a layer between the panel and the hot pressure surface through which the vapor can escape. This results in panels that have no discontinuity on the surface, which is a reason for worsening of the mechanical properties of the panel. Figure 2.9. shows the specimen after cold pressing and after hot pressing. More details concerning the equipment used and the method followed can be found in Annex A.

Figure 2.7. *Pictures of two different molds used for binderless boards cold and hot pressing. From left to right: the mold for smaller thicknesses, the mold for greater thicknesses, and the cold pressing step.*

Figure 2.8. *Pictures of panels with blisters occurred during hot pressing.*

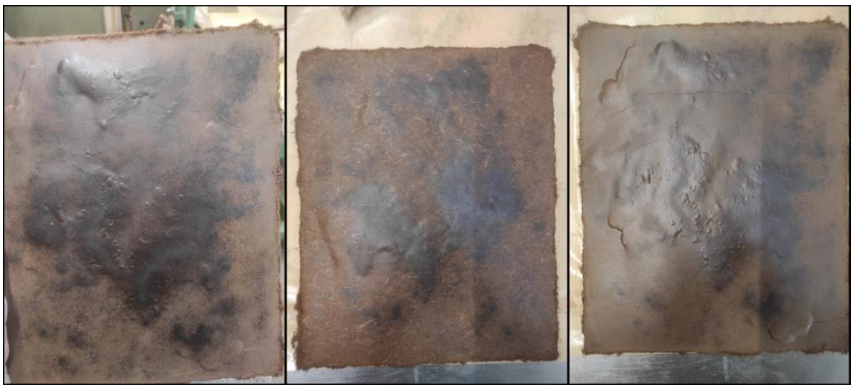

Figure 2.9. *Picture of specimens after cold pressing (right), and after hot pressing (left).*

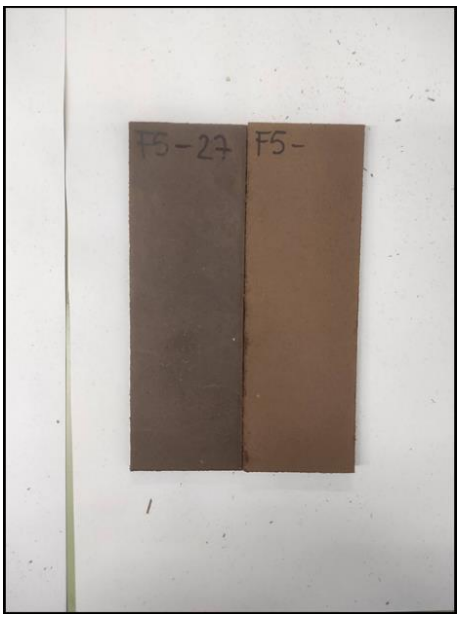

2.2.5. Final heat treatment

Finally, the obtained samples were cured by a final heat treatment (FHT) carried out in an aerated stove at the desired temperature (Tc) for the desired time (tc). The equipment used for this step is specified in Annex A.

The reason for including a FHT stems from the possibility that this last step may improve some of the properties, thus allowing the process to be optimized in its entirety and adjust the parameters of the previous steps according to the effect of this last one. Tc ranging from 165 °C to 180 °C were used for this purpose, for a tc ranging from 0.5 h to 5 h.

2.2.6. Conditioning

The last step before characterization is to condition the specimens in a climate chamber with controlled temperature and RH at 20°C and 65%, respectively (Figure 2.10.). The specimens are repeatedly weighted until the difference between two successive weighing in 24 hours is equal or less than 0.01 %, at this point the specimens are tested.

Figure 2.10. *Picture of specimens being conditioned in the climatic chamber, after the cold pressing step.*

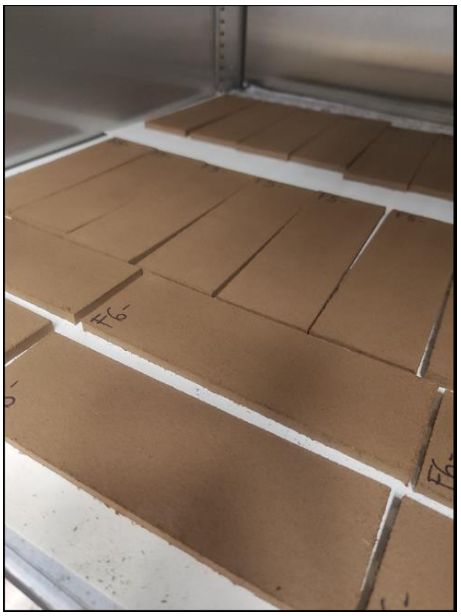

2.2.7. Mechanical and physical characterization

The European Standards were followed in order to characterize the specimens. Modulus of elasticity (MOE) and modulus of rupture (MOR) were measured according to UNE-EN 310:1994, while internal bond (IB) was calculated following UNE-EN 319:1994. Density and thickness swelling (TS) were measured in accordance with UNE-EN 323:1993 and

UNE-EN 319:1994, respectively. MOR, MOE, and IB test was carried out by using the universal testing machine (Annex A). TS and water absorption (WA) were calculated simultaneously by immerging 50x50 mm specimens in a water bath, placed in vertical position (Annex A). The specimens were weighed and measured before and after a 24 h period of the water bath and for some samples also after 2 h, 48 h, and 72 h. Thus, TS and WA were calculated as thickness and weight difference, respectively.

The EN 622-5:2009 was the reference of the mechanical and physical requirements for dry-formed boards (Table 2.3.)

Table 2.3. *Summary of mechanical and thickness swelling requirements depending on the use, according to current European standards (EN 622-5:2009).*

General use in dry conditions (non-structural)			TS (24h) %	IB N mm^{-2}	MOR N mm^{-2}	MOE N mm^{-2}
Thickness range	> 2.5 to 4	mm	35	0.65	23	-
	> 4 to 6	mm	30	0.65	23	-
	> 6 to 9	mm	17	0.65	23	2700
	> 9 to 12	mm	15	0.60	22	2500
General use in wet conditions (non-structural)			TS (24h) %	IB N mm^{-2}	MOR N mm^{-2}	MOE N mm^{-2}
Thickness range	> 2.5 to 4	mm	30	0.70	27	2700
	> 4 to 6	mm	18	0.70	27	2700
	> 6 to 9	mm	12	0.80	27	2700
	> 9 to 12	mm	10	0.80	26	2500
Structural use in dry conditions			TS (24h) %	IB N mm^{-2}	MOR N mm^{-2}	MOE N mm^{-2}
Thickness range	> 2.5 to 4	mm	35	0.70	29	3000
	> 4 to 6	mm	30	0.70	29	3000
	> 6 to 9	mm	17	0.70	29	3000
	> 9 to 12	mm	15	0.65	27	2800
Structural use in wet conditions			TS (24h) %	IB N mm^{-2}	MOR N mm^{-2}	MOE N mm^{-2}
Thickness range	> 2.5 to 4	mm	30	0.70	34	3000
	> 4 to 6	mm	18	0.70	34	3000
	> 6 to 9	mm	12	0.80	34	3000
	> 9 to 12	mm	10	0.80	32	2800

2.2.8. Chemical and morphological characterization

The raw material, the pretreated fibers and the samples obtained from the break surface of IB test were observed by scanning electron microscope (SEM). The samples were mounted on a stub and introduced into the machine to be observed in low vacuum mode (Figure 2.11.). The observation conditions were at acceleration voltages of 15 kV and a distance of approx. 20 mm. All the observations were made at the same magnification of x250 so that different samples could be compared. Prior to observing the pre-treated fibers by SEM, they were dried in the aerated stove at 40 °C for 2 days.

Figure 2.11. *Pictures of samples of exploded Arundo donax L. and binderless boards specimens mounted on the stub for being observed by scanning electron microscope.*

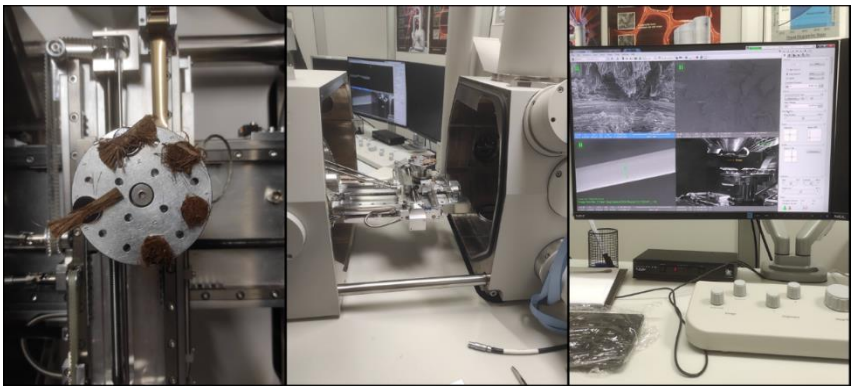

Fourier transform infrared (FT-IR) of untreated AD, steam exploded chips, hot pressed and cured fiberboards were obtained to evaluate possible changes in chemical bonds after each treatment. All spectra were collected in the wavenumber range of 4000–400 cm^{-1} with 4 cm^{-1} resolution, and 32 scans for each of the samples. The assigned bands were obtained by the Spectral Database for Organic Compounds (SDBS), and from literature review (Araújo Junior et al., 2018; Domínguez-Robles et al., 2020; Ferrandez-Villena, Ferrandez-Garcia, Garcia-Ortuño, Ferrandez-Garcia, & Garcia, 2020; Nonaka et al., 2013; Shu et al., 2019), and the bands are reported in Annex A.

Thermogravimetric analysis (TGA) was carried out to determine changes in weight of raw material, and of fiberboards made by exploded fibers, when subjected to a steadily increasing temperature. Approx. 10 mg of material was placed into a polymeric crucible and heated at a heating rate of 10 °C min^{-1} from 30 °C to 600 °C and 800 °C, under nitrogen atmosphere with a gas flow of 50 mL min^{-1}. The degradation steps were identified with reference to other studies on lignocellulosic materials (LM) (Araújo Junior et al., 2018; Asadieraghi et al., 2014; Z. Chen et al., 2015; Zuraida et al., 2017).

Vertical density profiles (VDP) is used to visualize the density distribution along the panel thickness, and from this identify correlations with mechanical properties. VDP were obtained using an X-ray densitometer. The specimen's size was 0x50x10.5±0.5 mm^3, and the density was measured at intervals of 0.01 mm along with the thickness.

2.3. Data analysis

Statistical analysis of physico-mechanical properties was performed by Rstudio software and Excel 2016. Statistical analysis of data is discussed in more details in Annex B.

Boxplots were produced to describe the trend of the results obtained. The standard deviation (St. Dev.) is also calculated.

One-way or two-way ANOVA was used as statistical method to evaluate the significance of the parameters used, at a level of significance α=0.05.

Tukey's honestly significance difference (HSD) was used as post-hoc test to evaluate the difference between the groups.

References

Araújo Junior, C. P., Coaquira, C. A. C., Mattos, A. L. A., de Souza Filho, M. de S. M., Feitosa, J. P. de A., Morais, J. P. S. de, & de Freitas Rosa, M. (2018). Binderless fiberboards made from unripe coconut husks. *Waste and Biomass Valorization*, 9(11), 2245–2254. https://doi.org/10.1007/s12649-017-9979-9

Asadieraghi, M., Ashri, W. M., & Daud, W. (2014). Characterization of lignocellulosic biomass thermal degradation and physiochemical structure: Effects of demineralization by diverse acid solutions. *Energy Conversion and* Management, 82, 71 – 82. https://doi.org/10.1016/j.enconman.2014.03.007

Chen, Z., Hu, M., Zhu, X., Guo, D., Liu, S., Hu, Z., Xiao, B., Wang, J., & Laghari, M. (2015). Characteristics and kinetic study on pyrolysis of five lignocellulosic biomass via thermogravimetric analysis. *Bioresource Technology*, 192, 441 – 450. https://doi.org/10.1016/j.biortech.2015.05.062

Domínguez-Robles, J., Tarrés, Q., Alcalà, M., Mansouri, N.-E. el, Rodríguez, A., Mutjé, P., & Delgado-Aguilar, M. (2020). Development of high-performance binderless fiberboards from wheat straw residue. *Construction and Building Materials*, 232, 117247. https://doi.org/10.1016/j.conbuildmat.2019.117247

Ferrandez-Villena, M., Ferrandez-Garcia, A., Garcia-Ortuño, T., Ferrandez-Garcia, C. E., & Garcia, M. T. F. (2020). Properties of wood particleboards containing giant reed (Arundo donax L.) particles. *Sustainability*, 12(24), 10469. https://doi.org/10.3390/su122410469

Nonaka, S., Umemura, K., & Kawai, S. (2013). Characterization of bagasse binderless particleboard manufactured in high-temperature range. *Journal of Wood Science*, 59(1), 50–56. https://doi.org/10.1007/s10086-012-1302-6

Shu, B., Ren, Q., He, Q., Ju, Z., Zhan, T., Chen, Z., & Lu, X. (2019). Study on mixed biomass binderless composite based on simulated wood. *Wood Research*, 64(6), 1023–1034.

Velásquez, J. A., Ferrando, F., & Salvadó, J. (2002). Binderless fiberboard from steam exploded Miscanthus sinensis: The effect of a grinding process. *Holz Als Roh – Und Werkstoff*, 60(4), 297–302. https://doi.org/10.1007/s00107-002-0304-2

Zuraida, A., Maisarah, T., & Wan-Shazlin-Maisarah, W. M. Y. (2017). Mechanical, physical and thermal properties of rattan fibre-based binderless board. *Journal of Tropical Forest Science*, 29(4), 485–492. https://doi.org/10.26525/jtfs2017.29.4.485492

Chapter 3. High density boards: the effect of steam explosion pretreatment

Chapter content

In this Chapter the effect of steam explosion pretreatment on fiberboards properties is discussed, from both a chemical and physico-mechanical perspective. Specimens measuring 150x50x3 mm^3 were made from hot pressed *Arundo donax* L. chips treated at five different reaction temperatures during steam explosion, without the addition of adhesives. The boards were manufactured following the steps outlined in Chapter 2. Density, mechanical results, and properties related to dimensional stability are compared, along with scanning electron microscope images, Fourier infrared spectroscopy, and thermogravimetric analysis curves. A threshold of 5°C is identified where all properties significantly improve.

3.1. Experimental design and objective

The objective of this Chapter is to explore the effect of various severities (R_0) of steam explosion (STEX) pretreatment carried out on *Arundo donax* L. (AD) fibers with the aim of finding the optimum value beyond which higher R_0 only results in wasted energy as it does not lead to significant improvement in material and fiberboard properties. To achieve the objective, the effect of different R_0 on physical and mechanical properties of binderless fiberboards (BF) were compared, relating them to chemical changes mainly due to the STEX pretreatment and the R_0. Since the reaction time (tr) was always the same, i.e., 9.5 min, for the reasons outlined in Chapter 2, the change in R_0 equals the change in reaction temperature (Tr). Between 9 and 11 specimens were analyzed for each sample, all made by using the condition parameters given in Table 3.1.

Table 3.1. *Parameters used in the manufacturing process of binderless fiberboards from steam exploded Arundo donax L. at five levels of severity.*

Materials	exploded AD		
specimens' size	150x50x3		mm^3
STEX	Tr	187	°C
		190	°C
		195	°C
		200	°C
		204	°C
	tr	9.5	min
milling	Retsch SM 100 mill (4x4 mm^2)		
HP	Pp_1	1	N mm^{-2}
	Pp_2	7.5	N mm^{-2}
	Tp	205	°C
	tp_1	2	min
	tp_2	30	s
FHT	Tc	165	°C
	tc	5	h
Conditioning	T	20	°C
	RH	65	%

3.2. Results and discussion

3.2.1. Physico-mechanical results

The physico-mechanical results of all tested specimens are presented in Table 3.2., while Table 3.3. shows the average values with the corresponding standard deviation (St.Dev.).

***Table 3.2**. Physico-mechanical results of all tested specimens made from steam exploded Arundo donax L. at five levels of severity ($logR_0$).*

Series name	Specimen number	Specimen name	Tr °C	$logR_0$ -	ρ kg m^{-3}	MOE N mm^{-2}	MOR N mm^{-2}	IB N mm^{-2}	TS %	WA %
B	1	3-1			910	703	3.7	0.228	49	81
B	2	3-2			919	1074	5.6	0.440	44	78
B	3	3-3			913	925	4.2	0.421	44	72
B	4	3-4			877	811	3.9	0.218	37	70
B	5	3-5			923	906	4.5	0.220	39	65
B	6	3-6	187	3.52	943	1135	5.5	0.431	40	62
B	7	3-7			927	1026	4.8	0.380	39	75
B	8	3-8			879	680	2.8	0.891	55	80
B	9	3-9			908	694	3.2	0.428	49	72
B	10	4			966	778	5.1	0.489	35	58
B	11	5			922	408	2.5	0.352	15	27
F3	1	1			942	1449	5.7	0.512	26	48
F3	3	R5			948	953	4.9	0.722	31	46
F3	4	8			923	979	5.2	0.678	37	64
F3	5	10			920	915	3.9	0.644	37	61
F3	6	12	190	3.62	912	815	3.6	0.690	45	80
F3	7	14			917	768	3.5	0.523	45	84
F3	8	17			933	1307	5.3	0.376	38	58
F3	9	19			887	738	3.2	0.905	41	66
F3	10	23			930	1278	4.5	0.626	46	77
C	1	3-1			1061	4444	36.2	2.390	13	14
C	2	3-2			1066	4318	32.3	2.046	12	17
C	3	3-3			1088	4896	32.7	3.148	11	16
C	4	3-4			1022	3007	23.1	1.967	13	17
C	5	3-5			981	4289	30.0	2.077	14	17
C	6	3-6	195	3.77	1056	4295	30.8	2.008	11	13
C	7	3-7			1079	4407	33.3	2.703	13	15
C	8	3-8			1053	4370	29.7	2.089	11	14
C	9	3-9			1086	4605	31.9	2.517	11	14
C	10	4			1070	4450	30.8	-	9	11
C	11	5			1027	4343	29.2	-	7	11

Series name	Specimen number	Specimen name	Tr °C	$logR_0$ -	ρ kg m^{-3}	MOE N mm^{-2}	MOR N mm^{-2}	IB N mm^{-2}	TS %	WA %
1	1	1			1102	4639	35.7	3.308	6	8
1	2	5			1097	4621	38.3	4.064	7	9
1	3	8			1105	4694	36.3	4.398	7	9
1	4	10			1052	4762	40.1	4.185	8	10
1	5	R10			1113	4664	32.4	3.808	6	9
1	6	12	200	3.92	1127	4370	31.5	3.644	8	8
1	7	14			1053	4310	33.6	3.541	8	10
1	8	17			1055	4269	32.9	4.585	21	10
1	9	R17			1105	4767	30.5	4.761	8	10
1	10	19			1111	4104	31.8	4.498	7	8
1	11	23			1046	4454	36.7	4.585	10	11
F1	1	1			1078	4393	33.7	2.868	10	13
F1	2	5			1081	4035	29.8	3.178	11	12
F1	3	8			1085	4394	31.3	2.928	11	12
F1	4	10			1066	4067	30.3	1.983	14	15
F1	5	12	204	4.04	1082	4701	35.6	2.535	11	12
F1	6	14			1048	4216	27.8	2.445	11	13
F1	7	17			1087	4144	26.3	3.640	11	12
F1	8	19			1084	4653	33.1	3.276	11	12
F1	9	23			1101	4938	38.3	2.899	9	11

Table 3.3. *Average physico-mechanical results of tested specimens with five levels of severity ($logR_0$: 3.52, 3.62, 3.77, 3.92, 4.04), and the corresponding St.Dev.*

Tr °C	ρ kg m^{-3}	St. Dev. kg m^{-3}	MOE N mm^{-2}	St. Dev. N mm^{-2}	MOR N mm^{-2}	St. Dev. N mm^{-2}	IB N mm^{-2}	St. Dev. N mm^{-2}	TS %	St. Dev. %	WA %	St. Dev. %
187	917	25	831	211	4.2	1.0	0.409	0.187	40	10	67	15
190	923	18	1022	259	4.4	0.9	0.631	0.150	38	7	65	14
195	1053	32	4311	467	30.9	3.3	2.327	0.401	11	2	14	2
200	1088	30	4514	224	34.5	3.1	4.125	0.489	9	4	9	1
204	1079	15	4393	314	31.8	3.8	2.861	0.492	11	1	13	1

Referring to the standard regulation EN 622-5:2010, the results obtained can be divided into two groups delimited by the Tr of 195 °C. Beneath the Tr of 195 °C, the obtained BF did not fulfill the requirements even for general use in dry conditions, while above the Tr of 195 °C the requirements were fulfilled, up to high performance structural use in dry conditions. On the other hand, the high performance structural use in wet conditions need a minimum modulus of rupture (MOR) of 34 N mm^{-2}, and this requirement was not always met. The results which allow this latter usage only belonged to pretreatment at Tr 200 °C. Commercial fiberboards have a modulus of elasticity (MOE) ranging between 2670 and 4299 N mm^{-2}, a MOR of 41.70–42.25 N mm^{-2}, an internal bond (IB) of 0.39–0.47 N mm^{-2}, and a thickness swelling (TS) ranging between 13% and 66% (Domínguez-Robles et al., 2018; Khedari et al., 2004; Ramos et al., 2018; Theng et al., 2015), and the results obtained for series made by the material

exploded at Tr 200°C were very close and even better than those of commercial fiberboards.

All densities exceeded 900 kg/m^3, so all the binderless fiberboards (BF) can be considered high density (Figure 3.1.). ANOVA results (Table 3.4.) revealed the high dependence of density on R_0 since the p-value is much lower than 0.05. Having performed multiple comparisons (Table 3.5.), it was observed that significant differences in the density values occurred between groups of Tr (°C) 195-187, 200-187, 204-187, 195-190, 200-190, 204-190, 200-195, and 204-195, while groups 190-187 and 204-200 did not have a statistically significant difference. As a result, we found that starting from a Tr of 195 °C, the material is more defibrillated and thus more easily compactable. Thanks to this, the fiberboards obtained by treatments at Tr 195°C, 200°C, and 204°C reached higher densities by using the same pressing pressure (Pp).

Table 3.4. *One-way ANOVA for physico-mechanical results of binderless fiberboards from steam exploded Arundo donax L. at five levels of severity, considering Tr as factor.*

Factor	Property		D.f.	R-squared [%]	p-value
Tr	ρ	kg m^{-3}	4	91.09	$<2\cdot10^{-16}$
	MOE	N mm^{-2}	4	97.09	$<2\cdot10^{-16}$
	MOR	N mm^{-2}	4	96.74	$<2\cdot10^{-16}$
	IB	N mm^{-2}	4	93.77	$<2\cdot10^{-16}$
	TS	%	4	86.59	$<2\cdot10^{-16}$
	WA	%	4	90.51	$<2\cdot10^{-16}$

Table 3.5. *Honestly significance difference (HSD) multiple comparison from one-way ANOVA for physico-mechanical results of binderless fiberboards from steam exploded Arundo donax L. at five levels of severity, considering the reaction temperature Tr as factor.*

facTr	t mm	ρ kg m^{-3}	MOE N mm^{-2}	MOR N mm^{-2}	IB N mm^{-2}	TS %	WA %
	p-value	p-value	p-value	p-value	p-value	p-value	p-value
190-187	0.7727	0.9807	0.6493	0.9996	0.6803	0.9141	0.9794
195-187	0.0117	<0.0001	<0.0001	<0.0001	<0.0001	<0.0001	<0.0001
200-187	<0.0001	<0.0001	<0.0001	<0.0001	<0.0001	<0.0001	<0.0001
204-187	0.0075	<0.0001	<0.0001	<0.0001	<0.0001	<0.0001	<0.0001
195-190	0.0006	<0.0001	<0.0001	<0.0001	<0.0001	<0.0001	<0.0001
200-190	<0.0001	<0.0001	<0.0001	<0.0001	<0.0001	<0.0001	<0.0001
204-190	0.0004	<0.0001	<0.0001	<0.0001	<0.0001	<0.0001	<0.0001
200-195	0.1523	0.0219	0.5495	0.0245	<0.0001	0.8307	0.7035
204-195	0.9973	0.1877	0.9762	0.9486	0.0313	0.9999	0.9955
204-200	0.3396	0.9368	0.9090	0.1860	<0.0001	0.8911	0.9173

In Figure 3.2. and Figure 3.3. the boxplots of TS and water absorption (WA) respectively are reported. In both cases, best values were obtained for the pretreatment carried out at Tr 200°C ($\log R_0$ = 3.92) which are 9.22% and 8.68%, respectively. As shown in Table 3.4., R_0 was also statistically significant for dimensional stability and the multiple comparison (Table 3.5.) revealed a statistically significant difference

between groups of Tr (°C) 195-187, 200-187, 204-187, 195-190, 204-190, and 204-190. Again, the Tr of 195°C represented the threshold beyond which properties improved significantly. From Figures 3.2. and 3.3. and the data shown in Table 4.3., we also observed a worsening in fiberboard properties for treatment at Tr 204°C, which could mean that the Tr of 200°C represented the optimum for the pressing and curing conditions considered.

Figure 3.4. and Figure 3.5. show the boxplots of MOE and MOR results, respectively. The R_0 had a significant effect here as well (Table 3.4.), while a multiple comparison (Table 3.5.) showed that significant differences occurred between groups of Tr (°C) 195-187, 200-187, 204-187, 195-190, 200-190, and 204-190 for MOE, and 195-187, 200-187, 204-187, 195-190, 200-190, 204-190, and 200-195 for MOR. The best results were obtained for Tr higher than 195 °C, and particularly for treatment at Tr 200°C.

IB performed similar to MOE and MOR (Figure 3.6.), with values much higher for treatment at conditions Tr 195°C, 200 °C, and 204 °C than 187 °C and 190 °C. Also, the p-value from ANOVA is the same as for the other properties (Table 3.4.). The difference is in the multiple comparison (Table 3.5.) where significant differences between all groups except the ones of Tr (°C) 190-187 were found, thus meaning that changes in Tr were much more significant for IB than the other properties.

Figure 3.1. *Boxplots of density of binderless fiberboards from steam exploded Arundo donax L. made at five levels of severity shown as reaction temperature (Tr), whit the current standard from EN 622-5:2010 (horizontal line).*

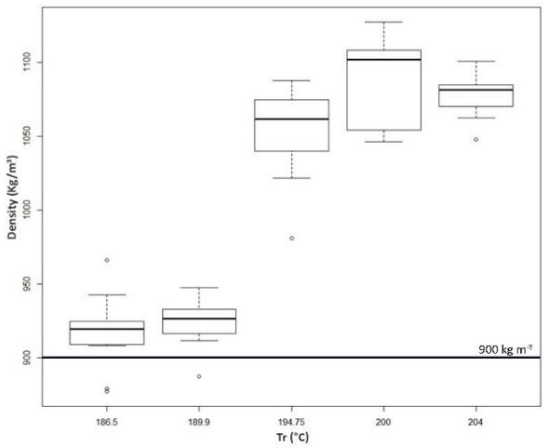

Figure 3.2. *Boxplot of thickness swelling TS of binderless fiberboards from steam exploded Arundo donax L. made at five levels of severity shown as reaction temperature (Tr), whit the current standard from EN 622-5:2010 (horizontal line).*

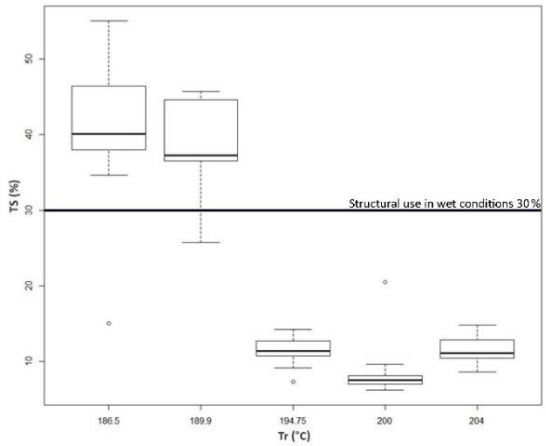

Figure 3.3. *Boxplots of water absorption WA of binderless fiberboards from steam exploded Arundo donax L. made at five levels of severity shown as reaction temperature (Tr), whit the current standard from EN 622-5:2010 (horizontal line).*

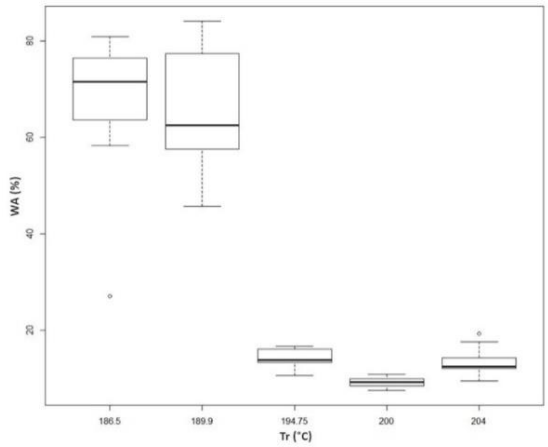

Figure 3.4. *Boxplots of modulus of elasticity MOE of binderless fiberboards from steam exploded Arundo donax L. made at five levels of severity shown as reaction temperature (Tr), whit the current standard from EN 622-5:2010 (horizontal line).*

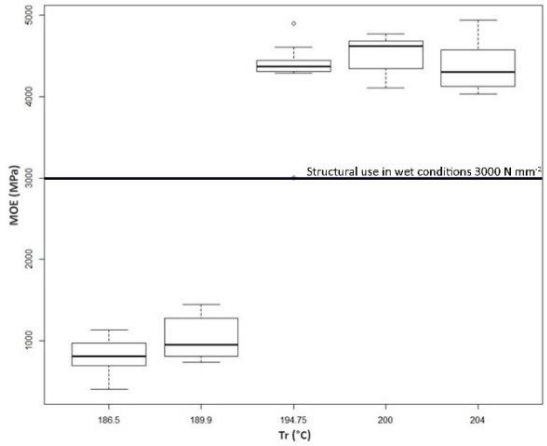

Figure 3.5. *Boxplots of modulus of rupture MOR of binderless fiberboards from steam exploded Arundo donax L made at five levels of severity shown as reaction temperature (Tr), whit the current standard from EN 622-5:2010 (horizontal line).*

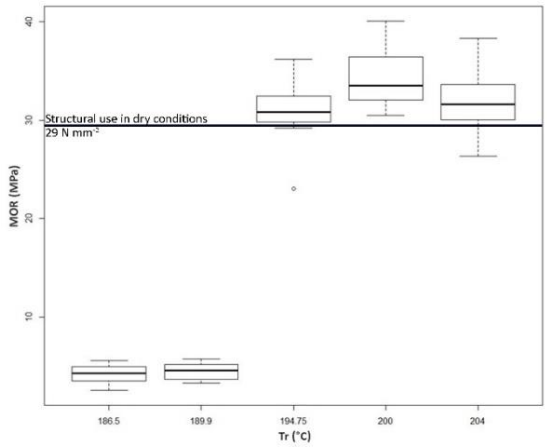

Figure 3.6. *Boxplots of internal bond IB of binderless fiberboards from steam exploded Arundo donax L. made at five levels of severity shown as reaction temperature (Tr), whit the current standard from EN 622-5:2010 (horizontal line).*

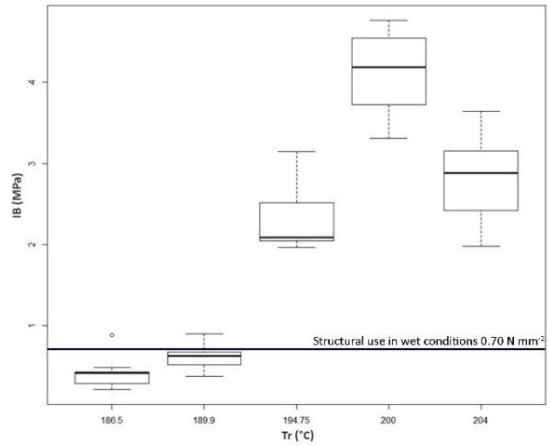

3.2.2. Evaluation of morphological changes by scanning electron microscope (SEM) observation

Color change is a first indicator of chemical changes in the lignocellulosic material (LM) structure. Figure 3.7 shows the appearance of the fibers for each of the treatments considered before grinding, i.e. at Tr 187 °C, 190 °C, 195 °C, 200 °C, and 204 °C, while Figure 3.8. shows 50x50 mm specimens of each sample. The color of the fibers became darker as the R_0 of the STEX increased. This increase in darkness has been related to surface burning and the changes in extractives, lignin, and hemicellulose components (Hidalgo-Cordero et al., 2020; Tuong & Li, 2010), and it has been associated with the improvement in dimensional stability and mechanical properties (Bekhta & Niemz, 2003; Tuong & Li, 2010). From Figure 3.7. can also be observed the difference in the degree of defibrillation of the material: the higher R_0 used the higher the degree of fiber defibrillation, and therefore the more efficient the hot pressing (HP).

Figure 3.7. *Pictures of untreated chips, and steam exploded Arundo donax L. at five levels of reaction temperature Tr*

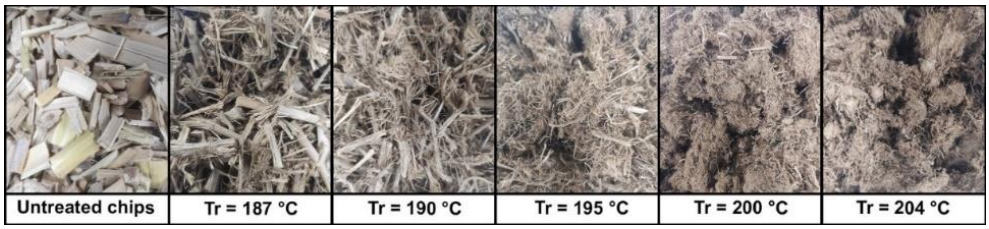

Figure 3.8. *Pictures of 50x50 mm specimens for the five levels of reaction temperature Tr.*

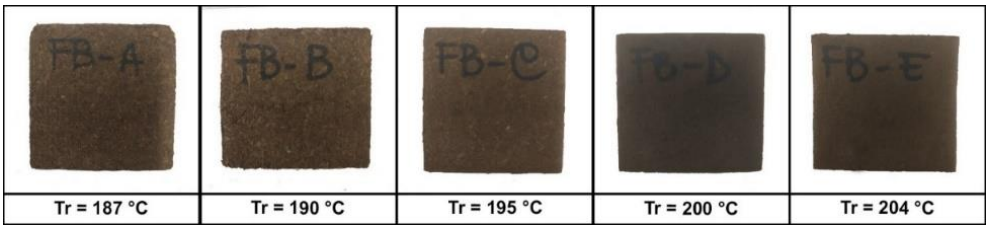

SEM observations supported the above statements. In Figure 3.9.the SEM images of the BF obtained by the exploded AD at the different R_0 are compared. The increase in density by increasing the R_0 was also apparent in SEM images. The increase in density is solely due to the increasing in R_0 since the parameters of the following steps were the same for all the specimens. In Figure 3.9.(a) and Figure 3.9.(b), which correspond to STEX at 187 °C and 190 °C, the fibers appear almost intact. Figure 3.9.(c) shows that the degree of defibrillation started to increase at a Tr of 195 °C, while Figure 3.9.(d) and Figure 3.9.(e) show a completely different morphology of exploded and hot pressed reeds. In order to further explain this evidence, Figure 3.10. shows SEM images of exploded AD at different R_0 before being ground and pressed to form the fiberboards. Comparing the low R_0 treatment in Figures 3.10.(a) and Figure 3.10.(b) with raw material in Figure 3.10.(0), no major differences were observed other than small fractures in the fiber surface, but the fibers appeared mostly unbroken. On the other hand, by increasing the Tr above 195 °C, long and thin fibers were obtained (Figures 3.10.(c), (d), and (e)), as also observed in other studies (Shu et al., 2019). The pretreatment enlarged the contact area between fibers, thus the formation of hydrogen bonds during hot pressing (HP) was enhanced.

The mentioned study, (Shu et al., 2019) associated the decrease of MOR to the amorphous substance deposited on the fiber surface, consisting of degrading hemicellulose and lignin. Here, the same amorphous matter can be observed in SEM images but no decrease in MOR values. This might be due to the rinsing step after STEX as it washed away the residues of hydrolyzed hemicelluloses which could play a major role in the enhancement of the properties of BF. Thus, the amorphous structure may be the lignin that was redistributed between fibers after STEX. Troncoso-Ortega et al., indicated the formation of pseudo-lignin during STEX, and its homogenous relocation onto the fibers surface or in the form of droplets, the abundance of which depends on R_0 (Troncoso-Ortega et al., 2021). In Figures 3.8.(c), (d), and (e), drops of lignin can be identified on the fiber surface. More SEM images can be found in the Annex A.

Figure 3.9. *SEM images of binderless fiberboards made at five levels of reaction temperature Tr*

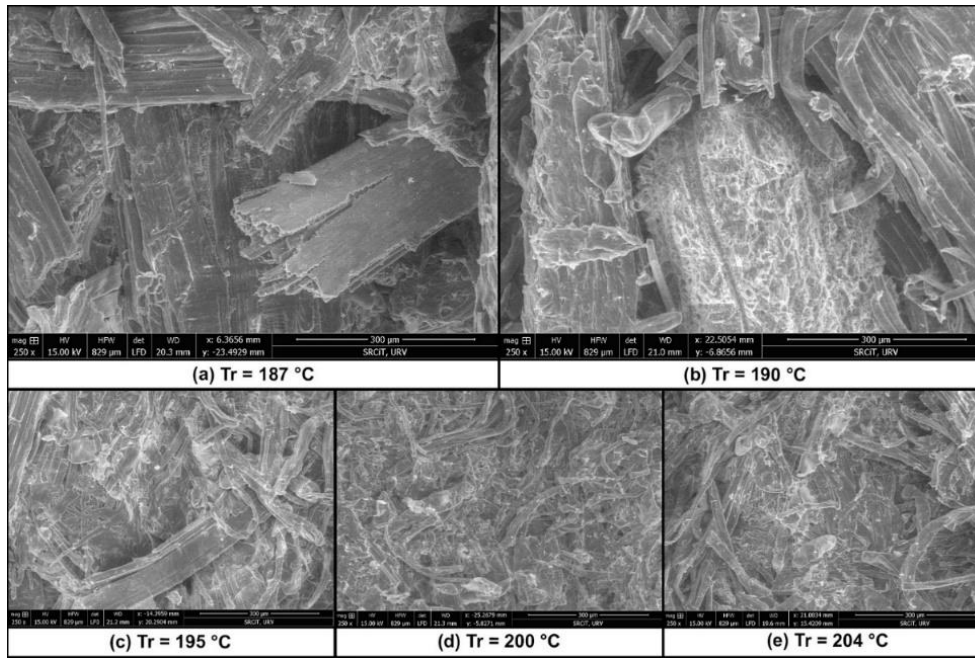

Figure 3.10. *SEM images of raw Arundo donax L. and steam exploded at five levels of reaction temperature Tr*

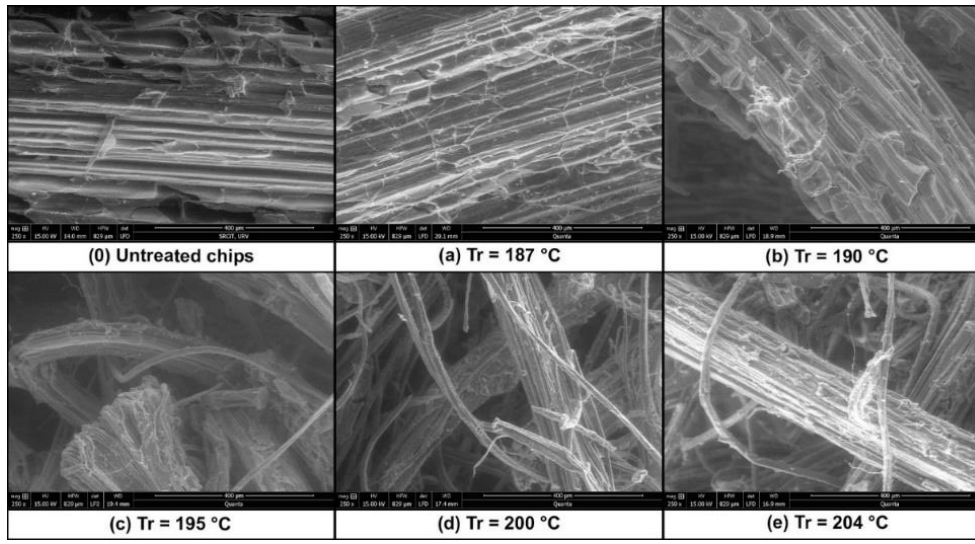

3.2.3. Evaluation of chemical changes by Fourier transform infrared (FT-IR) spectra analysis

FT-IR spectra analysis was carried out, aiming at finding a correspondence between the morphological changes identified through SEM images, and any chemical changes that apparently took place during STEX. Figures 3.11.(a1), (a2), and (b) show FT-IR spectra of raw and exploded material, and spectra of BF. The spectra confirmed that the major chemical changes occurred at the Tr of 195 °C and above: the pretreatments at Tr 195°C, 200°C, and 204°C showed spectra much more similar to those obtained for fiberboards, i.e. after grinding, HP, and final heat treatment (FHT).

The main changes of functional groups after pretreatment were detected in the peak region between 1400-1700 cm^{-1}. At the wavenumber 3415-3421 cm^{-1} the characteristic peak of O-H stretching was reached. The band is associated with hydroxyl groups of lignin which are related to the formation of hydrogen bonds. The bands at the wavenumbers 1200-1110 cm^{-1} are also related to the hydroxyl groups of polysaccharides (i.e., cellulose, and hemicellulose), and showed the same tendency. The hydrogen bonds are associated with the enhancement of IB, and the decreasing in transmittance for the treatment at 204°C may be related with the decreasing of IB. The hydroxyl group peak clearly improved by increasing R_0, being stronger at the Tr of 200°C, while for Tr 204°C a small decrease in absorbance was detected (Figure 3.11. (b)). At the wavenumber 1730-1740 cm^{-1} is the C=O stretching vibration, related to hemicelluloses. The hemicelluloses peak tended to disappear as the Tr increased, due to the hydrolyzation of hemicelluloses (Figure 3.11. (a1), (a2). The band of wavenumbers between 1632 cm^{-1} and 1509 cm^{-1} was associated to the aromatic core of lignin, which became clearly stronger by increasing Tr, indicating a major change in the structure of lignin due to the STEX pretreatment. The two peaks at the wavenumbers 2900 cm^{-1} and 2800 cm^{-1} may be associated with wax substances (Missau et al., 2018) present on the surface of the raw material, which tend to disappear as Tr increases.

Figure 3.11. *FT-IR spectra of untreated and steam exploded Arundo donax L. AD (a1 and a2), and binderless fiberboards (b) made at five levels of Tr.*

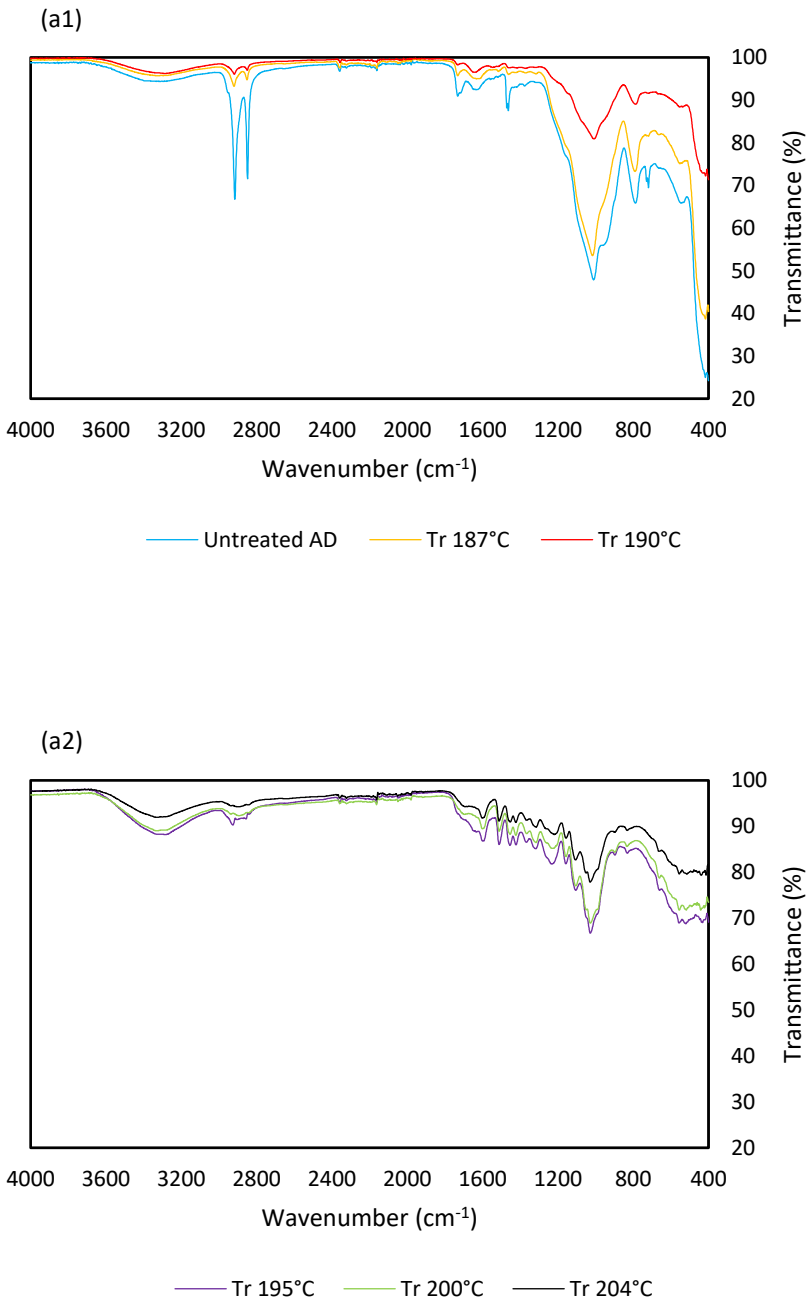

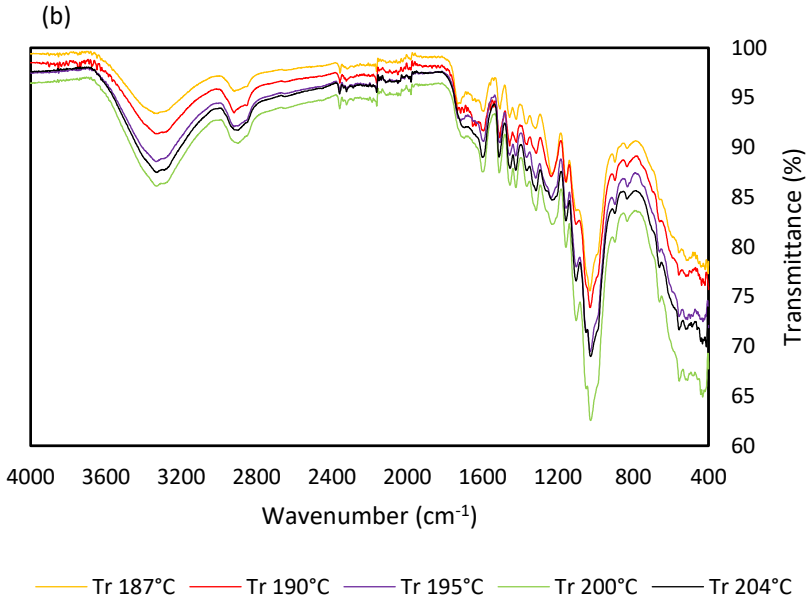

3.2.4. Evaluation of thermal stability by thermogravimetric analysis (TGA) curves

TGA was carried out in order to define the degradation temperatures of chemical components of AD and to verify the benefits that pretreatment may bring in term of thermal stability. Figure 3.12. shows the TGA and dTGA curves of raw untreated AD. The references used for the analysis of the TGA curves were reported in Chapter 2, Section 2.2.7.

Three degradation steps can be clearly identified. The first, occurred between 30 °C and 100 °C and corresponded to the evaporation of water and volatile compounds. The mass loss detected in this step was about 6%. The second step could be associated at the degradation of hemicellulose which starts around 200°C, while the third step corresponded to the degradation of cellulose and lignin, which occurs in the range of 240–350°C and 280–500°C, respectively. The TGA curve in Figure 3.12. shows that the degradation steps of pyrolyzed AD are the same as those found in literature for other LM. Indeed, the major mass loss of the material occurred in the 210–380°C range and can be related to the degradation of the main components of LM, i.e. cellulose, hemicellulose, and lignin.

Figures 3.13.(a) and (b) shows TGA and its first derivative (dTGA) curves of BF obtained by exploded AD. Comparing the curves of the BF with the raw material, a slight shift to the right occurred as the R_0 of the treatment increased. This means a key role of STEX in thermal stability

of each of the specimens. Up to the temperature of 200°C, the weight loss of the specimens is slow and small. Once the degradation temperature of the hemicellulose is reached, the weight loss begins to be significative. For the specimens treated at the lower temperature (i.e., at Tr 187°C), the "ladder" shape is much more clear in the Figure 3.13. (b), and the degradation steps of hemicellulose, cellulose, and lignin are much more differentiated. By increasing the temperature, the first step disappears, due to the hydrolyzation of hemicellulose.

Figure 3.12. *TGA and dTGA curves of untreated Arundo donax L.*

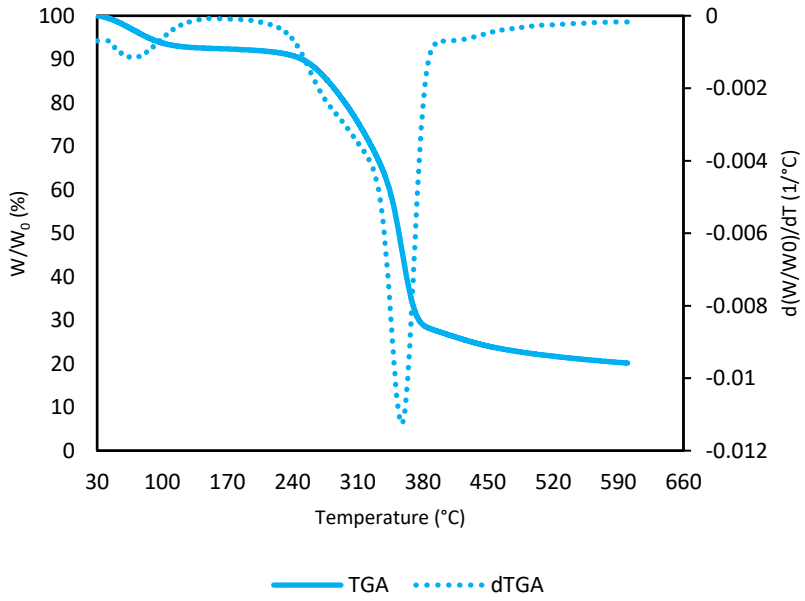

The maximum degradation peaks and the temperature range in which the main weight loss occurred for each of the specimens are shown in Table 3.6. Char residue, or char yield (CY), is presented in Table 3.7. CY was obtained directly from the TGA test as the percentage of the residual mass remaining at the end of pyrolysis at a temperature above 800°C. All samples showed a similar CY, although it seems that STEX produced a small improvement. The CY is related to the limiting oxygen index (LOI) which permits to know the ability of a material to be flame-retardant and self-extinguishing (ISO 4589). The LOI is defined as the minimum O_2 concentration required to maintain combustion and can be calculated by the Van Krevelen and Hoftyzer (Annex A). The minimum LOI for a material to be considered self-extinguishing is 28%. The LOI values of all the specimens were still very close and it seems that the pretreatment produced an increase in CY and in the LOI when comparing samples to raw material. Moreover, although an increase in

R_0 produced a decrease in CY, the CY increased again for the treatment performed at 204°C. The LOI permits a fairly rough knowledge of what the behavior of the material might be when subjected to fire, a topic on which there is a need for further study to draw appropriate conclusions.

Table 3.6. *TGA results: maximum degradation peaks and the temperature range in which the main weight loss occurred for each of the specimens obtained with five levels of severity, and the raw material.*

Sample	Temperature of maximum degradation peak °C	Range temperatures of main weight loss °C
raw	400	230-380
B	335	210-380
F3	345	210-380
C	356	220-380
1	361	220-380
F1	360	240-380

Table 3.7. *Char Yield CY and Limiting Oxygen Index LOI for each of the specimens obtained with five levels of severity, and the raw material.*

Sample	CY 600 °C %	CY 800 °C %	LOI 600°C %	LOI 800°C %
raw	18	16	23	24
B	26	24	28	27
F3	25	23	27	27
C	22	20	26	26
1	22	20	26	25
F1	24	22	27	26

3.3. Conclusions

As a general result, it can be stated that major chemical and morphological changes occurred in STEX AD in a Tr range of 5°C. A minimum Tr of 195°C is necessary for AD BF to obtain physico-mechanical properties which fulfill the requirements. In addition, data analysis shows that the treatment that leads to the best results is the one carried out at 200°C. The treatment at Tr 200 °C is also better from a technological point of view: the material is more defibrillated and occlusions in the equipment are not likely to occur. The optimal conditions parameters in relation to this experimental plan are shown in the Table 4.8.

At 204°C the physical and mechanical properties began to deteriorate, indicating that a further increase in the pretreatment temperature may lead to a further deterioration of properties.

Figure 3.13. *TGA (a) and dTGA (b) of binderless fiberboards made at five levels of reaction temperature Tr.*

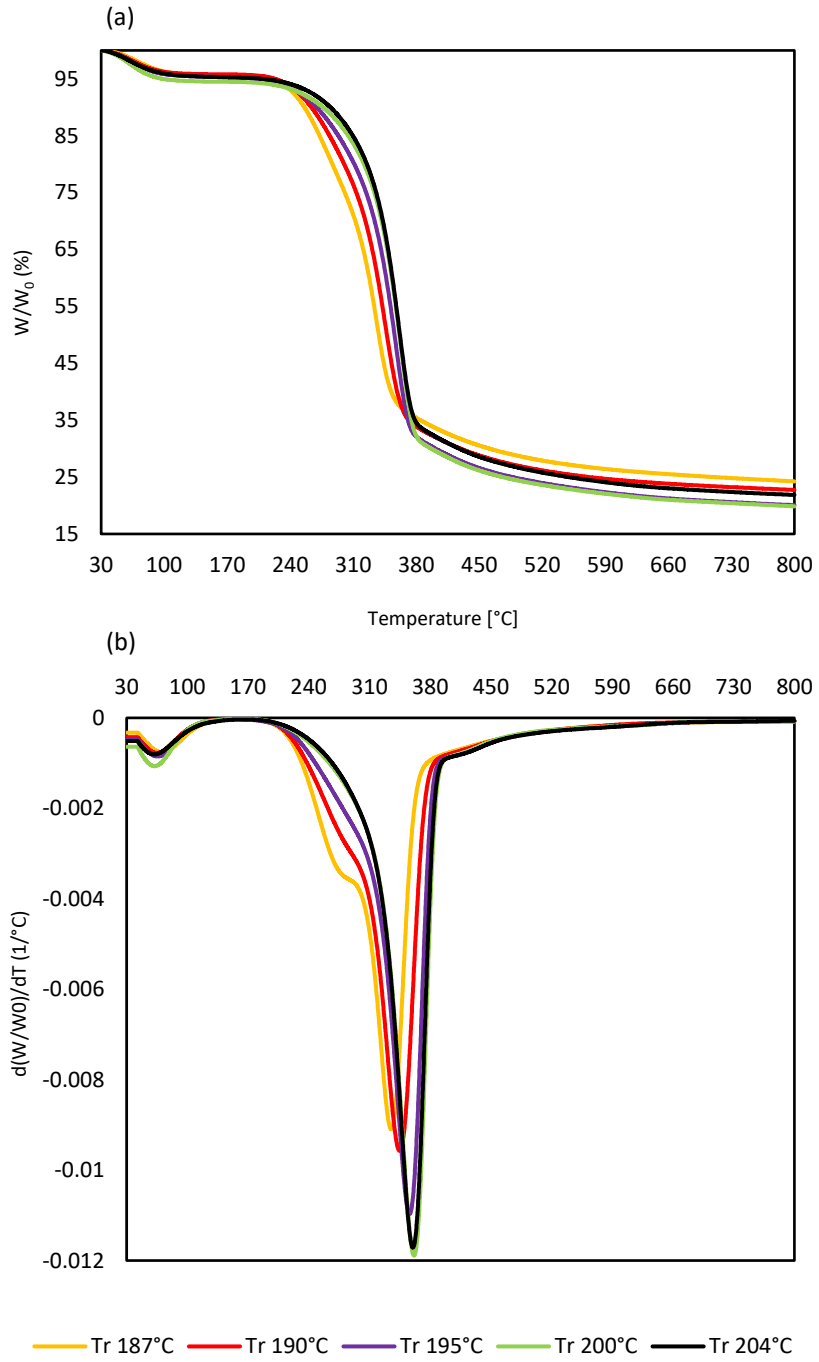

Table 3.8. *Optimal condition parameters for binderless fiberboards found by comparing five levels of severity.*

Materials	exploded AD		
specimens' size	150x50x3		mm^3
STEX	Tr	200	°C
	tr	9.5	min
HP	Pp_1	1	N mm^{-2}
	Pp_2	7.5	N mm^{-2}
	Tp	205	°C
	tp_1	2	min
	tp_2	30	s
FHT	Tc	165	°C
	tc	5	h

SEM images showed the increase in the degree of defibrillation of the AD as the Tr increased, thus obtaining a pulp that can easily be pressed into fiberboards. When comparing the images obtained from each of the samples, a significant change in the morphology of the fibers is noticeable: fibers appear thinner and longer as severity increases. This, combined with the changes in the functional groups visible in the spectroscopy, probably leads to the redistribution of the lignin between the fibers, triggered from the pretreatment Tr of 195°C, which enhanced the bonding of the fibers during HP.

FT-IR reading is in general not easy. Each peak can correspond to different stretches and the identification of the cause of the changes and the changes themselves can be rough. Nevertheless, some conclusions can be drawn from FT-IR results. First, there might be a correlation between the hydroxyl group and the decrease in IB and mechanical properties for samples obtained at Tr 204 °C, as the hydroxyl group is related to the formation of hydrogen bonds between fibers, which enhances the bonding between them. Furthermore, changes in the AD structure were observed: above the Tr of 195°C a spectra of exploded material similar to the HP fiberboards were observed, while for lower Tr no appreciable changes compared to the raw material were remarked. This may mean that pretreatment plays a greater role in activating fiber bonding than HP and FHT.

From the TGA curves, three steps of AD degradation, before and after the treatment, were identified. The same steps were found for other LM, mainly associated with the degradation of cellulose, hemicellulose, and lignin. There is a slight increase in thermal stability of the samples as the Tr increased up to the Tr of 200°C, as the curves shifted lightly to the right. As a result, STEX also has a key role on the thermal stability of the samples.

References

Bekhta, P., & Niemz, P. (2003). Effect of high temperature on the change in color, dimensional stability and mechanical properties of spruce wood. *Holzforschung*, 57(5), 539–546. https://doi.org/10.1515/HF.2003.080

Domínguez-Robles, J., Tarrés, Q., Delgado-Aguilar, M., Rodríguez, A., Espinach, F. X., & Mutjé, P. (2018). Approaching a new generation of fiberboards taking advantage of self lignin as green adhesive. International *Journal of Biological Macromolecules*, 108, 927–935. https://doi.org/10.1016/j.ijbiomac.2017.11.005

Hidalgo-Cordero, J. F., García-Ortuño, T., & García-Navarro, J. (2020). Comparison of binderless boards produced with different tissues of totora (Schoenoplectus californicus (C.A. Mey) Soják) stems. *Journal of Building Engineering*, 27, 100961. https://doi.org/10.1016/j.jobe.2019.100961

Khedari, J., Nankongnab, N., Hirunlabh, J., & Teekasap, S. (2004). New low-cost insulation particleboards from mixture of durian peel and coconut coir. *Building and Environment*, 39(1), 59–65. https://doi.org/10.1016/j.buildenv.2003.08.001

Missau, J., Rocha, J. de G. da, Dotto, G. L., Bertuol, D. A., Ceron, L. P., & Tanabe, E. H. (2018). Purification of crude wax using a filter medium modified with a nanofiber coating. *Chemical Engineering Research and Design*, 136, 734–743. https://doi.org/10.1016/j.cherd.2018.06.031

Ramos, D., Mansouri, N. E. El, Ferrando, F., & Salvadó, J. (2018). All-lignocellulosic fiberboard from steam exploded Arundo donax L. *Molecules*, 23(9), 2088. https://doi.org/10.3390/molecules23092088

Shu, B., Ren, Q., He, Q., Ju, Z., Zhan, T., Chen, Z., & Lu, X. (2019). Study on mixed biomass binderless composite based on simulated wood. *Wood Research*, 64(6), 1023–1034.

Theng, D., Arbat, G., Delgado-Aguilar, M., Vilaseca, F., Ngo, B., & Mutjé, P. (2015). All-lignocellulosic fiberboard from corn biomass and cellulose nanofibers. *Industrial Crops and Products*, 76, 166–173. https://doi.org/10.1016/j.indcrop.2015.06.046

Troncoso-Ortega, E., Castillo, R. D. P., Reyes-Contreras, P., Castaño-Rivera, P., Teixeira Mendonça, R., Schiappacasse, N., & Parra, C. (2021). Effects on lignin redistribution in eucalyptus globulus fibres pre-treated by steam explosion: A microscale study to cellulose accessibility. *Biomolecules*, 11(4), 507. https://doi.org/10.3390/biom11040507

Tuong, V. M., & Li, J. (2010). Effect of heat treatment on the change in color and dimensional stability of acacia hybrid wood. *BioResources*, 5(2), 1257–1267.

Chapter 4. High density boards: the effect of final heat treatment

Chapter content

In this Chapter the effect of the final heat treatment, which serves as the last step of the manufacturing process of fiberboards, is discussed. Specimens were manufactured using steam exploded *Arundo donax* L., following the procedures outlined in Chapter 2: steam explosion of *Arundo donax* L. chips, milling, cold and hot pressing, and final heat treatment. The density, mechanical properties, and dimensional stability (i.e., thickness swelling and water absorption) results are compared with and without the final heat treatment, considering two different temperatures and three different durations of the curing step.

4.1. Experimental design and objective

This Chapter focuses on the effect of the final heat treatment (FHT), which is the last step of binderless fiberboards (BF) production process. FHT can be regarded as a curing treatment, since with this the specimens are exposed to a certain temperature (Tc) for a given time (tc). The objective is to determine the influence of the two parameters on the final properties of the panels, and whether there is an interaction between them and between FHT and the pressing pressure (Pp).

To study the effect of FHT, the optimal steam explosion (STEX) and hot pressing (HP) conditions were first used, i.e., reaction temperature (Tr) 200°C, and second pressing pressure (Pp_2) 7.5 N mm^{-2}. It has been shown that the Tr of 195°C enables good results to be obtained and the standards to be reached. Nevertheless, the *Arundo donax* L. (AD) treated at this Tr still has some non-desfibrated chips that can generate occlusions in the reactor valve, so that the treatment at Tr 200°C is the one that is technologically most convenient and the minimum to avoid this complication. Once the relationship between the two FHT parameters is defined, the results are also analyzed in relation to Pp, comparing the results between high and low pressure, even considering STEX below the 195°C threshold. The parameters used in the manufacturing of these BF series are given in Table 4.1.

Table 4.1. *Parameters used in the manufacturing process of binderless fiberboards from steam exploded Arundo donax L. with different final heat treatment conditions.*

Materials	exploded AD		
specimens' size	150x50x3		mm^3
STEX	Tr	190	°C
		200	°C
	tr	9.5	min
milling	Retsch SM 100 mill (4x4 mm^2)		
HP	Pp_1	1	N mm^{-2}
	Pp_2	7.5	N mm^{-2}
		3.3	N mm^{-2}
	Tp	205	°C
	tp_1	2	min
	tp_2	30	s
FHT	Tc	0	°C
		165	°C
		180	°C
	tc	0	h
		0.5	h
		1	h
		5	h
Conditioning	T	20	°C
	RH	65	%

4.2. Results and discussion

4.2.1. Effect of Final heat treatment and interaction between temperature and time

The physico-mechanical results of all tested specimens are presented in Table 4.2., while Table 4.3. shows the average values with the corresponding standard deviation (St.Dev.). The variables considered in this analysis were only the FHT parameters, i.e., Tc and tc, while STEX and HP conditions were the same for all specimens.

Referring to the EN 622-5:2010 and the average results, the samples with FHT at 165°C for 5h achieved the standards considered for structural use in wet conditions, also exceeding the minimum values.

Table 4.2. *Physico-mechanical results of all tested specimens obtained from steam exploded Arundo donax L. with different final heat treatment conditions.*

Series name	Specimen number	Specimen name	Tc °C	tc h	ρ kg m^{-3}	MOE N mm^{-2}	MOR N mm^{-2}	IB N mm^{-2}	TS %	WA %
F6	1	24	0	0	1017	2684	19.8	1.212	29	51
F6	2	24-1			1017	3121	26.4	1.310	29	53
F6	3	24-2			1011	2612	20.8	1.340	27	48
F6	4	24-3			1008	2530	20.3	1.270	31	58
F6	1	25	180	0.5	1029	3453	28.5	1.782	13	16
F6	2	25-1			1022	3299	27.9	2.262	12	15
F6	3	25-2			1040	3621	29.0	2.310	10	13
F6	4	25-3			1039	2997	25.4	2.133	12	15
F6	1	26	180	1	1023	2726	20.5	1.732	12	15
F6	2	26-1			1019	2879	22.4	1.814	14	17
F6	3	26-2			997	2944	22.1	1.730	13	16
F6	4	26-3			1015	3136	23.5	1.730	14	16
F6	1	1	165	5	1102	4639	35.7	3.308	6	8
F6	2	5			1097	4621	38.3	4.064	7	9
F6	3	8			1105	4694	36.3	4.398	7	9
F6	4	10			1052	4762	40.1	4.185	8	10
F6	5	R10			1113	4664	32.4	3.808	6	9
F6	6	12			1127	4370	31.5	3.644	8	8
F6	7	14			1053	4310	33.6	3.541	8	10
F6	8	17			1055	4269	32.9	4.585	21	10
F6	9	R17			1105	4767	30.5	4.761	8	10
F6	10	19			1111	4104	31.8	4.498	7	8
F6	11	23			1046	4454	36.7	4.585	10	11

Manufacturing conditions: reaction temperature Tr 200°C; second pressing pressure Pp_2 7.5 N mm^{-2}.

The densities ranged from 997 to 1127 kg m^{-3}, with the averages around 1040 kg m^{-3}. Two-way ANOVA revealed a significant influence of both Tc and tc, but their crossed interaction was not significant (Table 4.4.), which means that for the ranges of Tc and tc considered, their effects on the properties can be interpreted separately. By the multiple comparison of the groups for the tc factor, there is no significant

difference between any of the times considered. This may mean that the effect of FHT did not depend on how long the specimens were exposed to Tc, at least in the tc ranges considered. This fact contradicts the observation of the results, without considering the statistical analysis.

Table 4.3. *Average physico-mechanical results of tested specimens with different final heat treatment conditions, and the corresponding St.Dev.*

Tc-tc °C-h	ρ kg m^{-3}	St. Dev.	MOE N mm^{-2}	St. Dev.	MOR N mm^{-2}	St. Dev.	IB N mm^{-2}	St. Dev.	TS %	St. Dev.	WA %	St. Dev.
0-0	1013	5	2737	264	21.8	3.1	1.283	0.055	29	2	52	4
180-0.5	1033	9	3343	265	27.7	1.6	2.122	0.239	12	1	15	1
180-1	1014	12	2921	170	22.1	1.2	1.751	0.042	13	1	16	1
165-5	1088	30	4514	224	34.5	3.1	4.125	0.489	9	4	9	1

Although the R-squared obtained for the model were quite high, the interpretation of the statistical data was not fully comprehensive. For instance, in the case of density, from Figure 4.1. it is clear that there is a difference at least between the 5h treatment and the other tc. This gap may be due to the collinearity of the variables, so it is more appropriate to apply a one-way model considering tc as factor and derive significant differences between the corresponding Tc.

Table 4.4. *Two-way ANOVA for physico-mechanical results considering curing temperature Tc and curing time tc as factors, and their interaction.*

Factor	Property		D.f.	R-squared [%]	p-value
Tc	ρ	kg m^{-3}	1	74.26	0.00476
	MOE	N mm^{-2}	1	93.25	0.00174
	MOR	N mm^{-2}	1	84.36	$7.31 \cdot 10^{-5}$
	IB	N mm^{-2}	1	93.08	$1.35 \cdot 10^{-7}$
	TS	%	1	87.82	$1.02 \cdot 10^{-9}$
	WA	%	1	98.92	$<2 \cdot 10^{-16}$
tc	ρ	kg m^{-3}	1	74.26	$3.39 \cdot 10^{-6}$
	MOE	N mm^{-2}	1	93.25	0.00156
	MOR	N mm^{-2}	1	84.36	$1.57 \cdot 10^{-7}$
	IB	N mm^{-2}	1	93.08	$3.18 \cdot 10^{-11}$
	TS	%	1	87.82	0.00141
	WA	%	1	98.92	$5.88 \cdot 10^{-10}$
Tc:tc	ρ	kg m^{-3}	1	74.26	0.11113
	MOE	N mm^{-2}	1	93.25	0.00198
	MOR	N mm^{-2}	1	84.36	0.00218
	IB	N mm^{-2}	1	93.08	0.0259
	TS	%	1	87.82	0.38534
	WA	%	1	98.92	0.0505

Table 4.5. *Honestly significance difference HSD multiple comparison from two-way ANOVA for physico-mechanical results considering curing temperature Tc and curing time tc as factors.*

facTc	ρ	MOE	MOR	IB	TS	WA
	kg m^{-3}	N mm^{-2}	N mm^{-2}	N mm^{-2}	%	%
	p-value	p-value	p-value	p-value	p-value	p-value
	HSD	HSD	HSD	HSD	HSD	HSD
165-0	0.00	0.00	0.00	0.00	0.00	0.00
180-0	0.74	0.03	0.17	0.02	0.00	0.00
180-165	0.00	0.00	0.00	0.00	0.04	$1.6 \cdot 10^{-6}$
factc	**ρ**	**MOE**	**MOR**	**IB**	**TS**	**WA**
	kg m^{-3}	N mm^{-2}	N mm^{-2}	N mm^{-2}	%	%
	p-value	p-value	p-value	p-value	p-value	p-value
	HSD	HSD	HSD	HSD	HSD	HSD
0.5-0	0.9314	0.5781	0.4719	0.8913	0.9896	0.9225
1-0	0.9314	0.5781	0.4719	0.8913	0.9896	0.9225
5-0	1.0000	1.0000	1.0000	1.0000	1.0000	1.0000
1-0.5	0.6364	0.0780	0.0380	0.5011	0.9261	0.6031
5-0.5	0.8861	0.4203	0.3109	0.8243	0.9819	0.8722
5-1	0.8861	0.4203	0.3109	0.8243	0.9819	0.8722

When it comes to the mechanical characteristics, i.e., modulus of elasticity (MOE), modulus of rupture (MOR), and internal bond (IB) (Figures 4.2.,4.3., and 4.4., respectively), one-way ANOVA (Table 4.6.) revealed pronounced significance of tc, but only differences between groups with tc 0.5-0, 5-0, 5-0.5, and 5-1, were significant (Table 4.7.). This showed that there is actually a significant difference in the mechanical results between the tc of 5h and the other times, but not between 0.5 h and 1 h.

The performance of the mechanical characteristics retraced that of the density. As a general ad well known result, higher density corresponds to higher MOE, MOR, and IB. Therefore, at this point it was not clear whether to associate the mechanical performance to the density and consider instead that the FHT had an effect on the density itself or linking directly the results of MOE, MOR, and IB and the different FHT conditions.

The most interesting results were obtained for the characteristics associated with the dimensional stability, i.e., thickness swelling (TS) and water absorption (WA). Here, the dependence with the density was not so clear, while the improvement due to the FHT was evident from the boxplots in Figure 4.5. and Figure 4.6. The p-value obtained from one-way ANOVA was significant for both TS and WA (Table 4.6.). For TS, multiple comparison (Table 4.7.) revealed that there was no significant difference between the different tc, while the p-value became significant for each of tc with the reference specimens, without FHT. Looking at the average values (Table 4.3.), with only 0.5 h of FHT the TS

was more than halved and similar result was obtained for WA, with the difference being that in the case of WA the differences between all groups were significant, except for 0.5-1 comparison.

To sum up the results obtained from this analysis, with the STEX at Tr 200°C and the Pp_2 at 7.5 N mm^{-2}, the best conditions of FHT were at a lower Tc (165°C) and a longer tc (5 h). The greatest effect of FHT was for TS and WA, although there was any difference between tc 0.5 h and 1 h at 180°C for any of the properties considered.

Figure 4.1. *Boxplots of density for each of the final heat treatment FHT conditions considered (180-05; 180-1; 165-5), and for binderless fiberboards without FHT (0)*

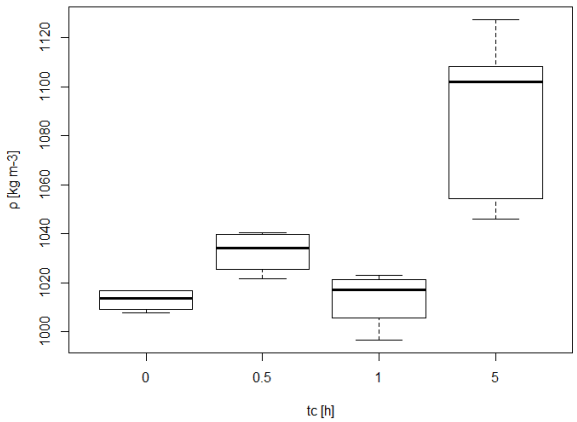

Figure 4.2. *Boxplots of modulus of elasticity MOE for each of the final heat treatment FHT conditions considered (180-05; 180-1; 165-5), and for binderless fiberboards without FHT (0)*

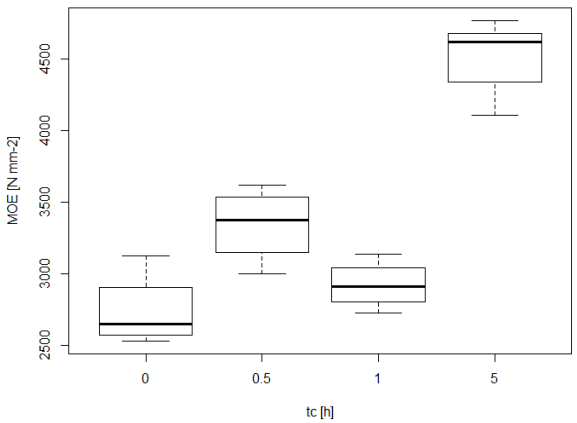

Figure 4.3. *Boxplots of modulus of rupture MOR for each of the final heat treatment FHT conditions considered (180-05; 180-1; 165-5), and for binderless fiberboards without FHT (0)*

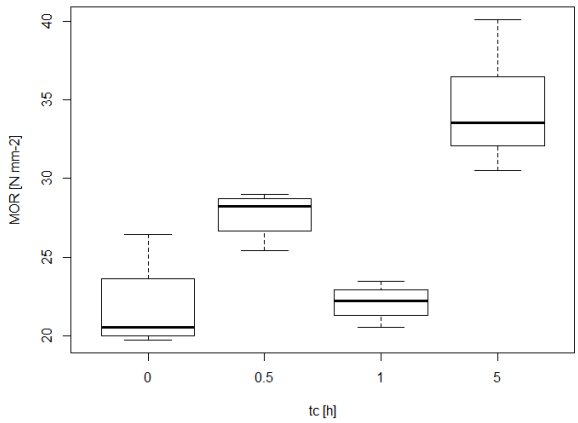

Figure 4.4. *Boxplots of internal bond IB for each of the final heat treatment FHT conditions considered (180-05; 180-1; 165-5), and for binderless fiberboards without FHT (0)*

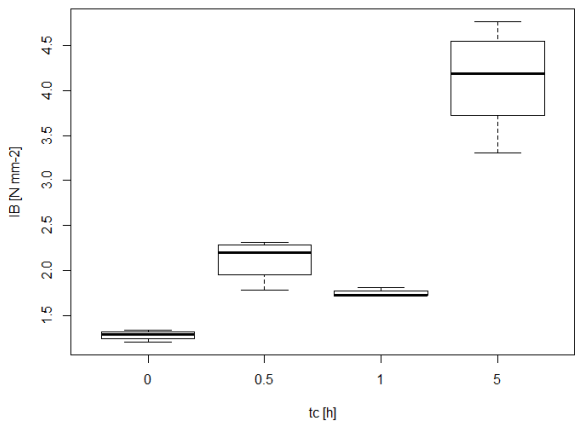

Figure 4.5. *Boxplots of thickness swelling TS for each of the final heat treatment FHT conditions considered (180-05; 180-1; 165-5), and for binderless fiberboards without FHT (0)*

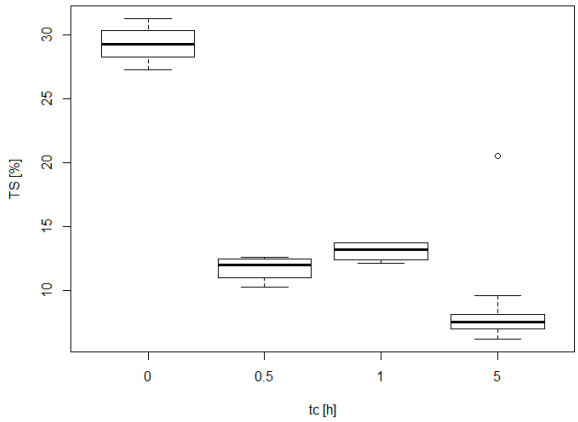

Figure 4.6. *Boxplots of water absorption WA for each of the final heat treatment FHT conditions considered (180-05; 180-1; 165-5), and for binderless fiberboards without FHT (0)*

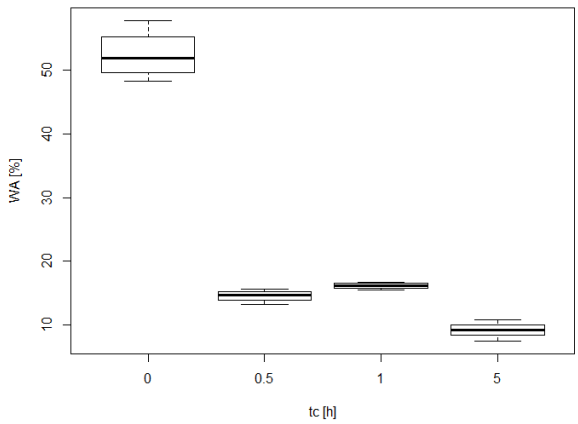

Table 4.6. *One-way ANOVA for physico-mechanical results considering curing time tc as factor.*

Factor	Property		D.f.	R-squared [%]	p-value
tc	ρ	kg m^{-3}	3	74.26	$7.97 \cdot 10^{-6}$
	MOE	N mm^{-2}	3	93.25	$2.65 \cdot 10^{-11}$
	MOR	N mm^{-2}	3	84.36	$7.42 \cdot 10^{-8}$
	IB	N mm^{-2}	3	93.08	$3.33 \cdot 10^{-11}$
	TS	%	3	87.82	$7.02 \cdot 10^{-9}$
	WA	%	3	98.92	$<2 \cdot 10^{-16}$

Table 4.7. *Honestly significant difference HSD multiple comparison from one-way ANOVA for physico-mechanical results considering curing time tc as factor.*

factc	ρ	MOE	MOR	IB	TS	WA
	kg m^{-3}	N mm^{-2}	N mm^{-2}	N mm^{-2}	%	%
	p-value	p-value	p-value	p-value	p-value	p-value
	HSD	HSD	HSD	HSD	HSD	HSD
0.5-0	0.6119	0.0072	0.0274	0.0213	<0.0001	<0.0001
1-0	0.9999	0.6743	0.9986	0.3040	<0.0001	<0.0001
5-0	0.0001	<0.0001	<0.0001	<0.0001	<0.0001	<0.0001
1-0.5	0.6364	0.0780	0.0479	0.5010	0.9260	0.6031
5-0.5	0.0024	<0.0001	0.0017	<0.0001	0.3422	0.0003
5-1	0.0001	<0.0001	<0.0001	<0.0001	0.0988	<0.0001

4.2.2. Final heat treatment and pressing pressure interaction above and below the threshold

Since no significant difference was found in the effect of FHT at tc 0.5 h and 1 h and Tc 180°C, the interaction between FHT and the change in Pp_2 is explored in this subsection, by associating the results of the two tc. The data considered for the analysis are shown in Table 4.8., where there is only the reference to whether there was the FHT or not.

Table 4.8. *Physico-mechanical results of tested specimens with different reaction temperature Tr, second pressing pressure Pp_2, and final heat treatment conditions.*

Series name	Specimen number	Specimen name	Tr	Pp_2	FHT	ρ	MOE	MOR	IB	TS	WA
			°C	N mm^{-2}	-	kg m^{-3}	N mm^{-2}	N mm^{-2}	N mm^{-2}	%	%
F6	1	27	200	3.3	NO	934	1990	13.9	0.965	31	62
F6	2	27-1				926	2180	16.7	0.428	32	60
F6	3	27-2				938	2044	13.3	0.949	33	63
F6	4	27-3				1718	2053	14.3	0.896	30	57
F6	1	24	200	7.5	NO	1017	2684	19.8	1.212	29	51
F6	2	24-1				1017	3121	26.4	1.310	29	53
F6	3	24-2				1011	2612	20.8	1.340	27	48
F6	4	24-3				1008	2530	20.3	1.270	31	58
F6	1	28	200	3.3	YES	962	2462	20.8	0.957	16	21
F6	2	28-1				938	2132	18.5	1.246	15	19
F6	3	28-2				955	2517	20.5	1.328	14	18
F6	4	28-3				930	2456	28.9	1.059	17	23
F6	5	29				950	2706	20.5	1.187	14	18
F6	6	29-1				952	2647	21.5	1.198	13	17
F6	7	29-2				954	2454	18.4	1.053	13	17
F6	8	29-3				967	3121	25.9	2.151	13	17
F6	1	25	200	7.5	YES	1029	3453	28.5	1.782	13	16
F6	2	25-1				1022	3299	27.9	2.262	12	15
F6	3	25-2				1040	3621	29.0	2.310	10	13
F6	4	25-3				1039	2997	25.4	2.133	12	15
F6	5	26				1023	2726	20.5	1.732	12	15
F6	6	26-1				1019	2879	22.4	1.814	14	17
F6	7	26-2				997	2944	22.1	1.730	13	16
F6	8	26-3				1015	3136	23.5	1.730	14	16

Series name	Specimen number	Specimen name	Tr °C	Pp_2 N mm^{-2}	FHT -	ρ kg m^{-3}	MOE N mm^{-2}	MOR N mm^{-2}	IB N mm^{-2}	TS %	WA %
F8	1	24				909	1028	3.7	0.526	92	157
F8	2	24-1				937	1277	4.6	0.408	70	118
F8	3	24-2	190	7.5	NO	947	1301	4.0	0.588	70	122
F8	4	24-3				892	1567	8.1	0.520	65	88
F8	1	27				888	1372	6.3	0.480	57	97
F8	2	27-1	190	3.3	NO	887	1416	7.1	0.380	58	103
F8	3	27-2				870	1572	7.2	0.388	53	86
F8	4	27-3				877	1270	5.6	0.400	63	105
F8	1	28				906	1546	8.3	0.684	29	53
F8	2	28-1				881	1122	5.6	0.440	35	65
F8	3	28-2				856	1277	6.1	0.388	41	80
F8	4	28-3	190	3.3	YES	880	10.54	5.9	0.499	38	69
F8	5	29				879	1089	7.5	0.585	26	34
F8	6	29-1				842	1061	4.9	0.382	26	36
F8	7	29-2				889	1222	5.9	0.509	30	45
F8	8	29-3				876	1098	6.1	0.395	31	54
F8	1	25				912	790	2.7	0.431	53	89
F8	2	25-1				923	999	4.1	0.534	38	82
F8	3	25-2				919	610	3.3	0.340	38	82
F8	4	25-3	190	7.5	YES	952	1941	10.8	0.522	65	88
F8	5	26				942	1178	4.5	0.329	43	77
F8	6	26-1				946	1118	5.7	0.551	30	42
F8	7	26-2				922	1101	5.0	0.304	36	57
F8	8	26-3				927	1530	9.4	0.448	28	49

The results obtained a two different Tr (above and below the threshold), two different Pp_2, and with and without FHT, were compared. The objective is to detect a compensation of FHT to a lowering of Pp or pretreatment Tr. The two series at Tr 200 °C and Tr 190 °C were analyzed separately with a two-way ANOVA model, to compare the significance at a later stage.

4.2.2.1. Final heat treatment and pressing pressure interaction above the threshold

For the results obtained with the Tr 200 °C, the lowest densities were found with the lower Pp_2, although in each case they were all higher than 900 kg m^{-3}, so that they can all be considered as high density (Table 4.9.).

Table 4.9. *Average physico-mechanical results of tested specimens obtained from exploded Arundo donax L. at reaction temperature Tr 200°C, with different pressing pressures, and with and without final heat treatment.*

Pp_2 N mm^{-2}	FHT -	ρ kg m^{-3}	St. Dev.	MOE N mm^{-2}	St. Dev.	MOR N mm^{-2}	St. Dev.	IB N mm^{-2}	St. Dev.	TS %	St. Dev.	WA %	St. Dev.
3.3	NO	937	10	2067	80	14.6	1.5	0.810	0.256	32	1	61	2
3.3	YES	951	12	2562	283	21.9	3.7	1.272	0.374	14	2	19	2
7.5	NO	1013	5	2737	264	21.8	3.1	1.283	0.055	29	2	52	4
7.5	YES	1023	14	3132	305	24.9	3.3	1.937	0.254	12	1	15	1

Referring to the standards EN 622-5:2010, the samples pressed at 7.5 N mm^{-2} and cured with FHT achieved the standards for general use in dry conditions, and none of the sample fulfilled the standards for the structural use in wet conditions, especially because of MOR requirement. Although most of the samples reached the minimum IB and TS for this latter use, i.e., 0.70 N mm^{-2} and 30% respectively, the standard requires a MOR of 34 N mm^{-2}, which was not achieved in any case, despite the improvement in the samples with FHT. It should be noted that with the same pretreatment conditions (Tr 200 °C), and hot pressing conditions (Pp_2 7.5 N mm^{-2}), but with a FHT of 5 h, the MOR standard was reached (see Chapter 3).

As for the density (Figure 4.7.), no significant difference was found for either the Pp factor or FHT, and there was no interaction between the two (Table 4.10.). Both factors were significant for all other properties, while their interaction is only slightly significant for WA. In all other cases, there is no interaction between the factors considered, as the p-value was higher than 0.05.

Analyzing in detail each of the properties, the mechanical ones increased with Pp_2 and FHT, but also with the density.

For the MOE (Figure 4.8.), it is interesting to note that there was no significant difference between the groups 3.3:YES-7.5:NO, i.e., the samples made with Pp_2 3.3 N mm^{-2} with the FHT, and the samples made with Pp_2 7.5 N mm^{-2} without FHT. In the previous subsection, it was clearer the relationship of mechanical properties with density rather than FHT. Whereas, introducing the Pp variable, FHT appeared to actually have an influence on MOE. However, in the multiple comparison shown in Table 4.11. there was no significant difference between the 7.5:YES-7.5:NO groups but there was when it comes to 3.3:YES-3.3:NO groups, which may mean that the effect of FHT is reduced when higher Pp_2 is used.

The influence of FHT was also clear for MOR (Figure 4.9.). Here, as for MOE, there were no significant differences for the groups 3.3:YES:7.5:NO, 7.5:YES-7.5:NO, and 7.5:YES-3.3:YES, confirming the hypothesis that the FHT may compensate for lower Pp_2.

For IB (Figure 4.10.), whether or not there was an effect due to FHT is less clear. The only value that stood out from the others is the one obtained for the sample with Pp_2 7.5 N mm^{-2} and with FHT, while among the other values no significant difference was found. The R-squared obtained for the IB model was more that 70% and the model is therefore considered adequate. As a result, the FHT did not seem to have significant effects on IB except at higher Pp.

For TS (Figure 4.11.) the effect of FHT is clear and did not depend on the pressure: there were no significant differences between the FHT-

treated or untreated groups, regardless of Pp_2. Even just looking at the average values in Table 4.9. the TS was more than halved due to the FHT.

The same result of a strong improvement was obtained for WA (Figure 4.12.), although in this case the differences in all groups were significant. The Pp also had an effect on the water uptake, so that the p-value for the groups 7.5:NO-3.3:NO, and 7.5:YES-3.3:YES, was significant (Table 4.11.). However, it should be noted that the difference between the groups 7.5:YES-3.3:YES, was just below the maximum value, being 0.041, which means that the significance is weak.

To sum up the results of this analysis, there was a more visible effect of FHT on MOE and MOR with respect to the previous subsection, but here also the Pp played a key role: at lower Pp, FHT enhances the mentioned properties while at higher Pp the effect of FHT is milder. On the other hand, it is clear and confirmed the strong effect of FHT on dimensional stability, i.e., TS and WA properties.

Table 4.10. *Two-way ANOVA for physico-mechanical results of binderless fiberboards from steam exploded Arundo donax L. at reaction temperature Tr 200°C, considering pressing pressure Pp and final heat treatment FHT as factors, and their interaction.*

Factor	Property		D.f.	R-squared [%]	p-value
Pp	ρ	kg m^{-3}	1	69.04	0.884
	MOE	N mm^{-2}	1	69.31	$2.17 \cdot 10^{-5}$
	MOR	N mm^{-2}	1	58.53	0.0027
	IB	N mm^{-2}	1	70.29	$4.97 \cdot 10^{-5}$
	TS	%	1	97.43	0.00251
	WA	%	1	98.68	$4.76 \cdot 10^{-5}$
FHT	ρ	kg m^{-3}	1	69.04	0.229
	MOE	N mm^{-2}	1	69.31	0.00105
	MOR	N mm^{-2}	1	58.53	0.00122
	IB	N mm^{-2}	1	70.29	0.000216
	TS	%	1	97.43	$<2 \cdot 10^{-16}$
	WA	%	1	98.68	$<2 \cdot 10^{-16}$
P:FHT	ρ	kg m^{-3}	-	-	-
	MOE	N mm^{-2}	1	69.31	0.67165
	MOR	N mm^{-2}	1	58.53	0.14159
	IB	N mm^{-2}	1	70.29	0.45059
	TS	%	1	97.43	0.75134
	WA	%	1	98.68	0.0339

Table 4.11. *Honestly significance difference HSD multiple comparison from two-way ANOVA for physico-mechanical results of binderless fiberboards from steam exploded Arundo donax L. at reaction temperature Tr 200°C, considering pressing pressure Pp and final heat treatment FHT as factors, and their interaction.*

	MOE	MOR	IB	TS	WA
facPp	N mm^{-2}	N mm^{-2}	N mm^{-2}	%	%
	p-value	p-value	p-value	p-value	p-value
	HSD	HSD	HSD	HSD	HSD
7.5-3.3	$2.17 \cdot 10^{-5}$	0.00	$4.97 \cdot 10^{-5}$	0.00	0.00
	MOE	MOR	IB	TS	WA
facFHT	N mm^{-2}	N mm^{-2}	N mm^{-2}	%	%
	p-value	p-value	p-value	p-value	p-value
	HSD	HSD	HSD	HSD	HSD
YES-NO	0.00	0.00	0.00	0.00	0.00
	MOE	MOR	IB	TS	WA
facP:FHT	N mm^{-2}	N mm^{-2}	N mm^{-2}	%	%
	p-value	p-value	p-value	p-value	p-value
	HSD	HSD	HSD	HSD	HSD
7.5:NO-3.3:NO	0.0104	0.0203	0.1222	0.1424	0.0005
3.3:YES-3.3:NO	0.0320	0.0064	0.0686	<0.0001	<0.0001
7.5:YES-3.3:NO	<0.0001	0.0001	<0.0001	<0.0001	<0.0001
3.3:YES-7.5:NO	0.7146	0.9999	0.9999	<0.0001	<0.0001
7.5:YES-7.5:NO	0.1086	0.4115	0.0066	<0.0001	<0.0001
7.5:YES-3.3:YES	0.0020	0.2553	0.0008	0.0696	0.0407

Figure 4.7. *Boxplots of density of binderless fiberboards from steam exploded Arundo donax L. at Tr 200°C, for each of the Pp-FHT conditions considered. In the x-axis the Pp-FHT conditions were reported, where 0 mean without FHT treatment, while 1 means with FHT treatment.*

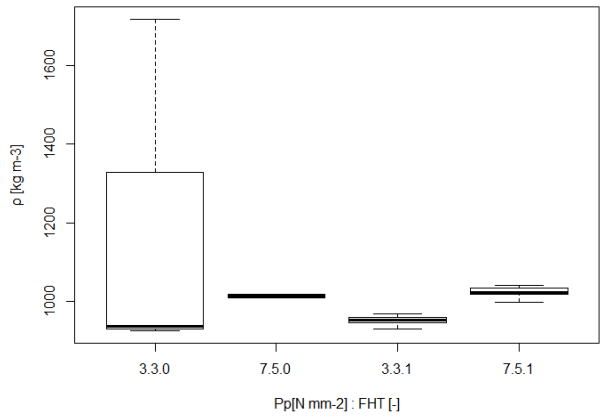

Figure 4.8. *Boxplots of modulus of elasticity MOE of binderless fiberboards from steam exploded Arundo donax L. at Tr 200°C, for each of the Pp-FHT conditions considered. In the x-axis the Pp-FHT conditions were reported, where 0 mean without FHT treatment, while 1 means with FHT treatment.*

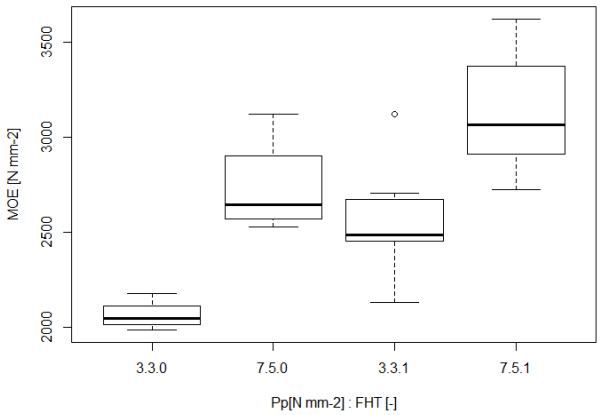

Figure 4.9. *Boxplots of modulus of rupture MOR of binderless fiberboards from steam exploded Arundo donax L. at Tr 200°C, for each of the Pp-FHT conditions considered. In the x-axis the Pp-FHT conditions were reported, where 0 mean without FHT treatment, while 1 means with FHT treatment.*

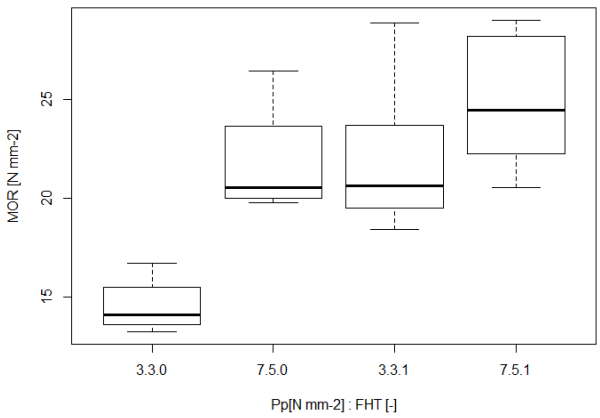

Figure 4.10. *Boxplots of internal bond IB of binderless fiberboards from steam exploded Arundo donax L. at Tr 200°C, for each of the Pp-FHT conditions considered. In the x-axis the Pp-FHT conditions were reported, where 0 mean without FHT treatment, while 1 means with FHT treatment.*

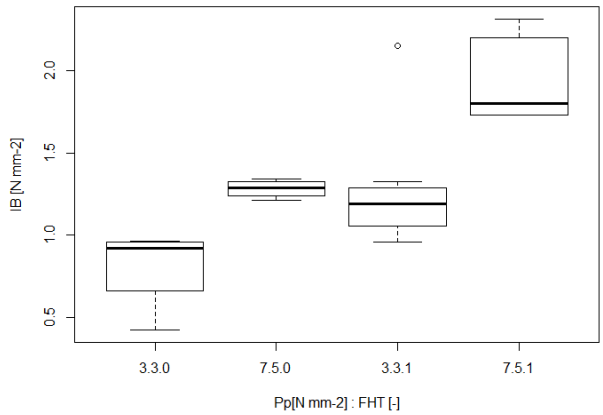

Figure 4.11*. Boxplots of thickness swelling TS of binderless fiberboards from steam exploded Arundo donax L. at Tr 200°C, for each of the Pp-FHT conditions considered. In the x-axis the Pp-FHT conditions were reported, where 0 mean without FHT treatment, while 1 means with FHT treatment.*

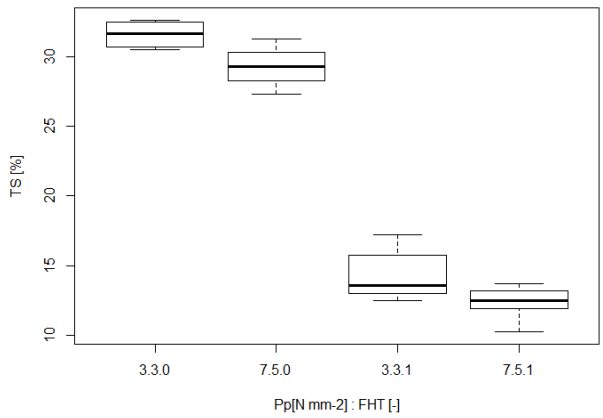

Figure 4.12. *Boxplots of water absorption WA of binderless fiberboards from steam exploded Arundo donax L. at Tr 200°C, for each of the Pp-FHT conditions considered. In the x-axis the Pp-FHT conditions were reported, where 0 mean without FHT treatment, while 1 means with FHT treatment.*

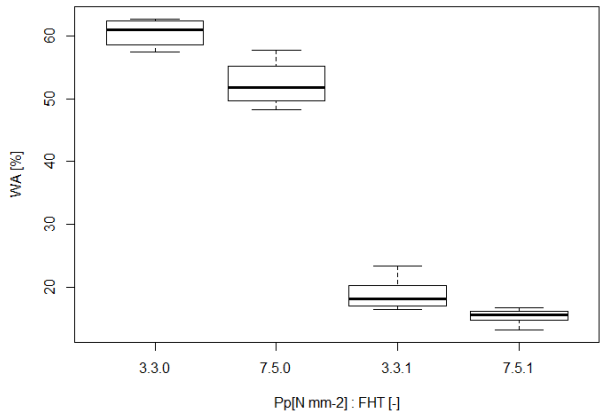

4.2.2.2. Final heat treatment and pressing pressure interaction below the threshold

Also for the results obtained with the Tr 190°C, the lowest densities were found for the lower Pp_2, i.e. 3.3 N mm^{-2}. In this case, the densities were higher than 900 kg m^{-3} just for samples pressed at 7.5 N mm^{-2} (Table 4.12.).

Table 4.12. *Average physico-mechanical results of tested specimens obtained from steam exploded Arundo donax at reaction temperature Tr 190°C, with different second pressing pressures Pp_2, and with and without final heat treatment FHT.*

Pp_2-FHT N mm^{-2}	ρ kg m^{-3}	St. Dev.	MOE N mm^{-2}	St. Dev.	MOR N mm^{-2}	St. Dev.	IB N mm^{-2}	St. Dev.	TS %	St. Dev.	WA %	St. Dev.
3.3-NO	880	9	1408	126	6.5	0.8	0.412	0.046	58	4	98	9
3.3-YES	876	20	1184	166	6.3	1.1	0.485	0.107	32	5	54	16
7.5-NO	921	25	1293	220	5.1	2.0	0.511	0.075	74	12	121	29
7.5-YES	930	15	1158	417	5.7	2.9	0.394	0.172	41	12	70	19

Referring to the standards EN 622-5:2010, none of the samples achieved the requirements even for general use in dry conditions. This result was not surprising given the findings in Chapter 3, in which the threshold of Tr 195°C was identified as the minimum for satisfactory mechanical results. However, it may be useful to analyze the differences with respect to the influence of FHT aiming at obtaining more comprehensive conclusions on the entire process, and at understanding the extent to which FHT may have a significant effect.

As for density (Figure 4.13.), the Pp factor had a significant effect while FHT did not, and there was no interaction between the two (Table 4.13.). The significance of both factors changed slightly from the previously analyzed data, and their interaction was significant only for IB. In all other cases, there is no interaction between the factors considered, as the p-value was higher than 0.05.

For the MOE, MOR, and IB (Figures 4.14., 4.15., and 4.16., respectively), it is interesting to note that there was not significant difference between all the groups. This can be traced back to low Tr and R_0: FHT and Pp are not sufficient to compensate for the lack of chemical and structural changes in the material due to the STEX, which lead to improved properties.

On the other hand, for TS and WA (Figures 4.17., and 4.18, respectively), the result obtained were similar to that obtained with a higher Tr. The TS and WA values were not halved in this case, but greatly reduced, and the significance of multiple comparisons (Table 4.14) indicated that there was always a difference when comparing values with and without FHT, regardless of pressure.

In this case, the effect of FHT is clear only for TS and WA, while the reduced Tr of STEX had such a major influence that FHT cannot compensate for the mechanical results.

Table 4.13. *Two-way ANOVA for physico-mechanical results of binderless fiberboards from steam exploded Arundo donax L. at reaction temperature Tr 190°C, considering pressing pressure Pp and final heat treatment FHT as factors, and their interaction.*

Factor	Property		D.f.	R-squared [%]	p-value
Pp	ρ	kg m^{-3}	1	70.63	$1.12 \cdot 10^{-6}$
	MOE	N mm^{-2}	1	12.11	0.837
	MOR	N mm^{-2}	1	67.66	0.292
	IB	N mm^{-2}	1	15.07	0.592
	TS	%	1	76.01	0.00659
	WA	%	1	66.85	0.0246
FHT	ρ	kg m^{-3}	1	70.63	0.746
	MOE	N mm^{-2}	1	12.11	0.149
	MOR	N mm^{-2}	1	67.66	0.851
	IB	N mm^{-2}	1	15.07	0.6943
	TS	%	1	76.01	$4.57 \cdot 10^{-7}$
	WA	%	1	66.85	$1.01 \cdot 10^{-5}$
P:FHT	ρ	kg m^{-3}	1	70.63	0.398
	MOE	N mm^{-2}	1	12.11	0.508
	MOR	N mm^{-2}	1	67.66	0.626
	IB	N mm^{-2}	1	15.07	0.039
	TS	%	1	76.01	0.39008
	WA	%	1	66.85	0.6607

Table 4.14. *Honestly significance difference HSD multiple comparison from two-way ANOVA for physico-mechanical results of binderless fiberboards from steam exploded Arundo donax L. at reaction temperature Tr 190°C, considering pressing pressure Pp and final heat treatment FHT as factors, and their interaction.*

facPp	ρ kg m^{-3}	MOE N mm^{-2}	MOR N mm^{-2}	IB N mm^{-2}	TS %	WA %
	p-value HSD	p-value HSD	p-value HSD	p-value HSD	p-value HSD	p-value HSD
7.5-3.3	$1.1\cdot10^{-6}$	0.84	0.29	0.59	0.01	0.02
facFHT	ρ kg m^{-3}	MOE N mm^{-2}	MOR N mm^{-2}	IB N mm^{-2}	TS %	WA %
	p-value HSD	p-value HSD	p-value HSD	p-value HSD	p-value HSD	p-value HSD
YES-NO	0.75	0.15	0.85	0.69	$5\cdot10^{-7}$	$1.01\cdot10^{-5}$
facP:FHT	ρ kg m^{-3}	MOE N mm^{-2}	MOR N mm^{-2}	IB N mm^{-2}	TS %	WA %
	p-value HSD	p-value HSD	p-value HSD	p-value HSD	p-value HSD	p-value HSD
7.5:NO-3.3:NO	0.0187	0.9726	0.7347	0.6809	0.0963	0.3175
3.3:YES-3.3:NO	0.9809	0.4342	0.9963	0.7723	0.0010	0.0054
7.5:YES-3.3:NO	0.0008	0.7041	0.8944	0.9955	0.0373	0.1070
3.3:YES-7.5:NO	0.0025	0.7269	0.7666	0.9868	<0.0001	0.0001
7.5:YES-7.5:NO	0.8329	0.9352	0.9616	0.4417	0.0001	0.0012
7.5:YES-3.3:YES	<0.0001	0.9428	0.9317	0.4787	0.2330	0.3363

Figure 4.13. *Boxplots of density of binderless fiberboards from steam exploded Arundo donax L. at Tr 190°C, for each of the Pp-FHT conditions considered. In the x-axis the Pp-FHT conditions were reported, where 0 mean without FHT treatment, while 1 means with FHT treatment.*

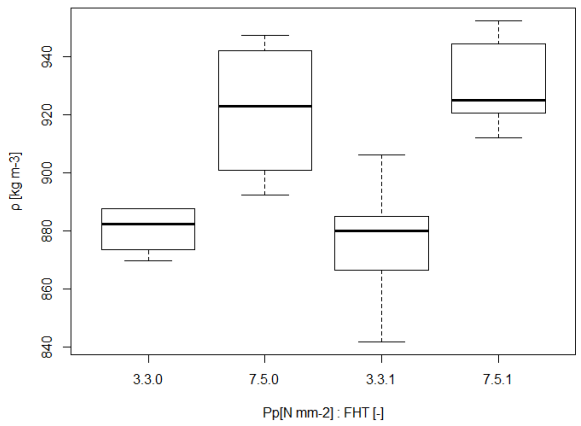

Figure 4.14. *Boxplots of modulus of elasticity MOE of binderless fiberboards from steam exploded Arundo donax L. at Tr 190°C, for each of the Pp-FHT conditions considered. In the x-axis the Pp-FHT conditions were reported, where 0 mean without FHT treatment, while 1 means with FHT treatment.*

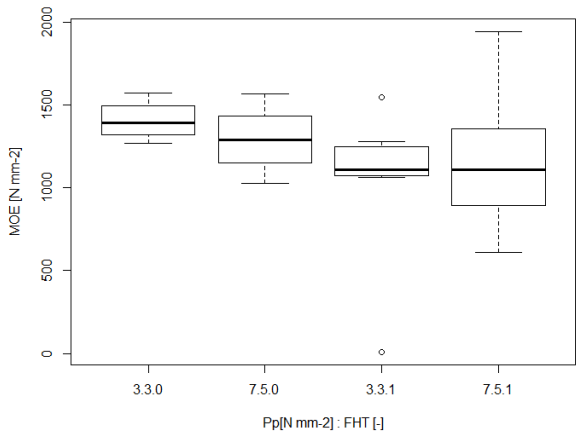

Figure 4.15. *Boxplots of modulus of rupture MOR of binderless fiberboards from steam exploded Arundo donax L. at Tr 190°C, for each of the Pp-FHT conditions considered. In the x-axis the Pp-FHT conditions were reported, where 0 mean without FHT treatment, while 1 means with FHT treatment.*

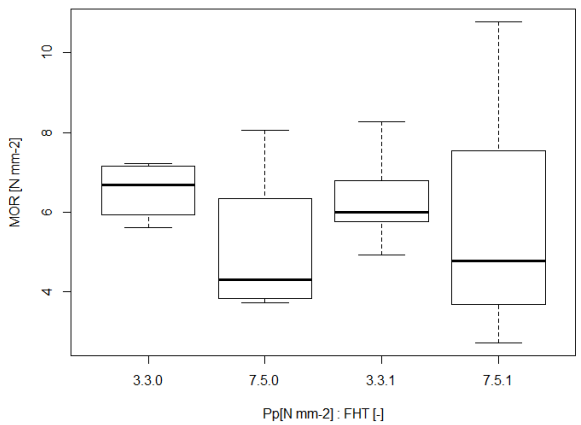

Figure 4.16. *Boxplots of internal bond IB of binderless fiberboards from steam exploded Arundo donax L. at Tr 190°C, for each of the Pp-FHT conditions considered. In the x-axis the Pp-FHT conditions were reported, where 0 mean without FHT treatment, while 1 means with FHT treatment.*

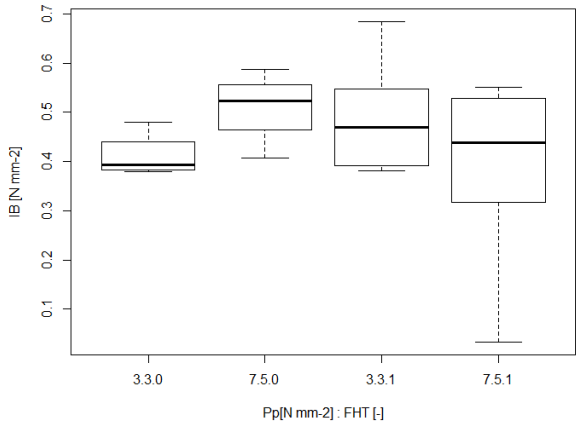

Figure 4.17. *Boxplots of thickness swelling TS of binderless fiberboards from steam exploded Arundo donax L. at Tr 190°C, for each of the Pp-FHT conditions considered. In the x-axis the Pp-FHT conditions were reported, where 0 mean without FHT treatment, while 1 means with FHT treatment.*

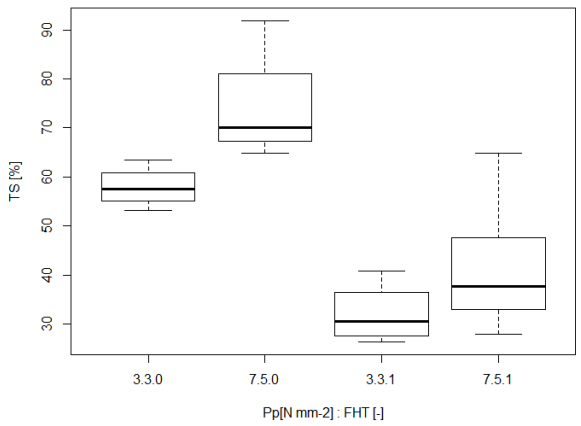

Figure 4.18. *Boxplots of water absorption WA of binderless fiberboards from steam exploded Arundo donax L. at Tr 190°C, for each of the Pp-FHT conditions considered. In the x-axis the Pp-FHT conditions were reported, where 0 mean without FHT treatment, while 1 means with FHT treatment.*

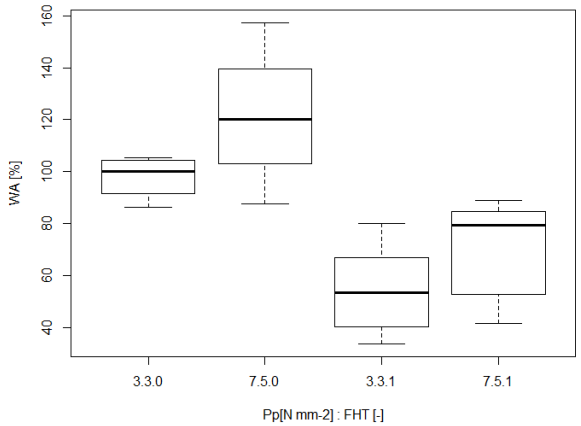

4.3. Conclusions

To combine the results of the different analyses carried out in this Chapter, for the Tc and tc considered, the influence of FHT does not depend on the other conditions of the production process only in the case of TS and WA, although with a Tr below 195 °C the required performance is never achieved.

In general, there is no significance difference between values obtained with low tc deviations (i.e., between 0.5 h and 1 h) at the same Tc, while there is an improvement when tc is much higher, even at lower Tc. In fact, better results were obtained when Tc 165 °C and tc 5 h.

Regardless of whether the results are more or less performing, a scale of importance of production conditions influencing the effect of FHT can be drawn. In doing so, mechanical properties and dimensional stability are considered separately, as the relationships between the variables are quite different for mechanical and physical properties.

As for mechanical properties, the importance of Tr is confirmed. Indeed, from the one hand a low Tr does not lead to the desired results, and from the other hand it limits the effect of FHT, which is instead clearer when Tr rises to 200 °C. For this latter condition, the Pp influences the effect of FHT but in the opposite way: the higher the Pp, the less clear is the influence of FHT on mechanical properties. As a result, it can be concluded that FHT may offset the effect of Pp in

achieving the required characteristics, but only in the case that STEX is carried out at a Tr above the threshold.

For TS and WA the point is quite different and there is always a significant effect of the FHT regardless of Pp and Tr. However, because of the key role of Tr, in this case it can be said that although FHT always has a positive effect on TS and WA, only when Tr is above the threshold, the desired characteristics are achieved, and, for the data analyzed, it can be concluded that a minimum tc of 5 h is necessary for BF to be used also in wet conditions.

Chapter 5. High density boards: the effect of thickness

Chapter content

In this Chapter the effect of thickness as geometric feature on fiberboards properties is discussed. Specimens were manufactured using steam exploded *Arundo donax* L., following the steps outlined in Chapter 2: steam explosion of *Arundo donax* L. chips, milling, cold and hot pressing, and final heat treatment. The effect of three different thicknesses was examined, as well as the interaction with the final heat treatment and whether thickness influenced this step. The effect of thickness is analyzed based on density, mechanical properties, and dimensional stability (i.e., thickness swelling and water absorption) results.

5.1. Experimental design and objective

To study the effect of thickness, we analyzed the results of specimens made with the same steam explosion (STEX) conditions, the same hot pressing (HP) conditions, the same final heat treatment (FHT) conditions, and three different thicknesses, i.e., 3 mm, 6 mm, and 9 mm. Table 5.1 shows the exact conditions used for this series.

Table 5.1. *Parameters used in the manufacturing process of binderless fiberboards from steam exploded Arundo donax L. with different thicknesses.*

Materials	exploded AD		
specimens' size	150x50x3		mm^3
	150x50x6		mm^3
	150x50x9		mm^3
STEX	Tr	190	°C
	tr	9.5	min
milling	Retsch SM 100 mill (4x4 mm^2)		
HP	Pp_1	1	N mm^{-2}
	Pp_2	7.5	N mm^{-2}
	Tp	205	°C
	tp_1	2	min
	tp_2	30	s
FHT	Tc	0	°C
		165	°C
		180	°C
	tc	0	h
		0.5	h
		1	h
		5	h
Conditioning	T	20	°C
	RH	65	%

5.2. Results and discussion

5.2.1. Effect of thickness on mechanical properties

The mechanical results of all tested specimens are presented in Table 5.2., while Table 5.3. shows the average values with the corresponding St.Dev. The variable considered in this analysis was only the thickness, while STEX and HP conditions were the same for all specimens.

From a mechanical point of view, thickness is expected to have a direct effect on modulus of rupture (MOR) and modulus of elasticity (MOE). However, from a technological point of view, with a thicker specimen, the heat during HP takes longer to penetrate to the center, thus also affecting the internal bond (IB), which can be also connected to dimensional stability, especially with the thickness swelling (TS) (Migneault et al., 2011).

Referring to the EN 622-5:2010, the standards report different values depending on the thickness. However, none of the samples achieved the standards even for general, non-structural use in dry conditions. Sample F3 achieved the minimum for IB, but the MOR was about half of the required. Nevertheless, this result can be attributed to the low severity ($logR_0$) of 3.62, and the reaction temperature (Tr) of 190°C.

The R_0 also had an effect of thickness itself. The thicknesses were set at 3, 6, and 9 mm, but all the samples exceeded this target. This, as mentioned in the previous chapters, is due to the low level of defibrillation of the material at this R_0, which makes it more difficult to compact. For ANOVA, the average thickness was considered as factor in a one-way model, as the standard deviation (St.Dev.) was minimal (Table 5.3.).

The densities were all higher than 900 kg m^{-3} (Figure 5.1.). One-way ANOVA revealed a significant influence of thickness on density (Table 5.4.). Overall, density is higher with a greater thickness, which could be due to using more material to achieve the desired thickness. By the multiple comparison of the groups (Table 5.5.), there is no significant difference between 7.6-3.8 thickness groups, while the those of 11.1-3.8 and 11.1-7.6 showed a significance difference, meaning that the greater thickness is the one who led to a higher density, differing from the other two thicknesses.

Table 5.2. *Mechanical results of tested specimens with different thicknesses.*

Series name	Specimen number	Specimen name	Thickness* mm	ρ kg m^{-3}	MOE N mm^{-2}	MOR N mm^{-2}	IB N mm^{-2}
F3	1	1	3.8	942	1449	5.7	0.512
F3	3	R5	3.7	948	953	4.9	0.629
F3	4	8	3.9	923	973	5.2	0.678
F3	5	10	3.9	920	1380	4.6	0.644
F3	6	12	3.9	912	1267	3.6	0.690
F3	7	14	3.9	917	1279	3.5	0.523
F3	8	17	3.8	933	1307	5.3	0.376
F3	9	19	3.6	887	700	3.2	0.905
F3	10	23	3.9	930	1268	4.5	0.626
F3D	1	1	7.6	926	776	3.8	0.089
F3D	2	5	7.6	930	658	4.2	0.200
F3D	3	8	7.8	913	515	3.3	0.150
F3D	4	10	7.7	928	698	4.4	0.242
F3D	5	12	7.6	942	774	5.3	0.304
F3D	6	14	7.6	934	503	3.4	0.354
F3D	7	17	7.6	936	719	4.7	0.481
F3D	8	19	7.6	934	636	4.1	0.335
F3D	9	23	7.6	940	647	4.3	0.459

Series name	Specimen number	Specimen name	Thickness* mm	ρ kg m^{-3}	MOE N mm^{-2}	MOR N mm^{-2}	IB N mm^{-2}
F3T	1	1	11.2	957	647	5.8	0.291
F3T	2	5	11.3	947	538	4.8	0.123
F3T	3	8	11.0	973	498	4.5	0.305
F3T	4	10	11.1	966	611	6.2	0.181
F3T	5	12	11.0	980	696	6.2	0.128
F3T	6	14	11.0	979	637	6.2	0.196
F3T	7	17	11.0	976	647	6.7	0.166
F3T	8	19	11.1	970	691	6.8	0.168
F3T	9	23	11.1	961	468	4.6	0.122

**The average thicknesses considered in the ANOVA were: 3.8 mm for F3; 7.6 mm for F3D; 11.1 mm for F3T.*
Manufacturing conditions: reaction temperature (Tr) 190°C; second pressing pressure (Pp_2) 7.5 N mm^{-2}; curing temperature (Tc) 165°C; curing time (tc) 5h.

Table 5.3. *Average mechanical results (MOE, MOR, and IB) of tested specimens with different thicknesses, and the corresponding St.Dev.*

Series name	thickness mm	St. Dev.	ρ kg m^{-3}	St. Dev.	MOE N mm^{-2}	St. Dev.	MOR N mm^{-2}	St. Dev.	IB N mm^{-2}	St. Dev.
F3	3.8	0.11	923	18	1175	244	4.5	0.9	0.620	0.146
F3D	7.6	0.06	932	9	658	99	4.2	0.6	0.290	0.133
F3T	11.1	0.12	968	11	604	83	5.7	0.9	0.186	0.068

The MOE decreased with increased thickness (Figure 5.2.). From a geometric point of view, this is an expected result, given the MOE formula (Annex A), although the mechanical aspect alone is not exhaustive in explaining the MOE trend. The MOE of the specimens with the smaller thickness was much higher than the other two thicknesses, about twice as high, but with a St.Dev. also higher, probably due to the higher relative error resulting from the measurement of thickness, as further explained in the next section. As well as for the density, for MOE the significance of thickness was also high (Table 5.4.). When it comes to multiple comparison (Table 5.5.), the value of the specimens with the lower thickness stood out and the difference is significant in this case with both other groups, while there was no difference between the latter, i.e., 11.1 and 7.6.

The MOR performed quite different, and it was slightly higher for sample F3T, i.e., with the higher thickness (Figure 5.3.). ANOVA also revealed a significance of the thickness, although weaker with respect to the other properties (Table 5.4.). Besides, there was a significance difference between groups 11.1-3.8 and 11.1-7.6, while the difference for the groups 7.6-3.8 was not significant (Table 5.5.). In this case, was the value obtained with the greater thickness that stood out from the others, indicating that the thickness could have a contrasting role respect to the bending stress applied during the test. Nevertheless, as specified, there was a different level of significance compared to the

other two mechanical properties: here the p-value was about 0.001 (Table 5.4.), which means that the difference between the means is definitely significance but not at the level of the MOE and IB. The R-squared was also lower in this case, being about 40%.

The IB should be the property least affected by the thickness, from a mechanical point of view. Indeed, it is calculated as the ratio between the maximum force applied in N and the breaking surface in mm^2. However, it is an indicator of the internal cohesion of the fibers, which is physically and chemically formed during the HP due to the pressure and heat application. The penetration of the heat in the central layers of the specimens is fundamental for a stronger and more resistant linkage of the fibers (Balea (Paul) et al., 2022; Halvarsson et al., 2008; Pham Van et al., 2021). This is probably the reason why the IB was the property most affected by the thickness. The highest IB was found with the smaller thickness, while for the other two thicknesses the value was halved (Figure 5.4). Moreover, the multiple comparison showed that there was no significant difference between the groups 11.1-7.6.

As a result, mechanical properties were strongly influenced by thickness, especially the MOE and the IB. They decreased with thickness, the former due to a mechanical effect, and the latter due to a technological effect whereby a longer pressure time (tp) would be required to allow the HP heat to reach the center of the panel.

Table 5.4. *One-way ANOVA for mechanical results considering the average thickness as three level factor.*

Factor	Property		D.f.	R-squared [%]	p-value
thickness	ρ	kg m^{-3}	2	70.67	$4.06 \cdot 10^{-7}$
	MOE	N mm^{-2}	2	74.55	$7.37 \cdot 10^{-8}$
	MOR	N mm^{-2}	2	43.90	0.0009
	IB	N mm^{-2}	2	72.53	$1.84 \cdot 10^{-7}$

Table 5.5. *Honestly significance difference HSD multiple comparison from one-way ANOVA for mechanical results (MOE, MOR, and IB) considering the thickness as three level factor.*

facthick	ρ kg m^{-3}	MOE N mm^{-2}	MOR N mm^{-2}	IB N mm^{-2}
	p-value HSD	p-value HSD	p-value HSD	p-value HSD
7.6-3.8	0.3932	<0.0001	0.6606	<0.0001
11.1-3.8	<0.0001	<0.0001	0.0094	<0.0001
11.1-7.6	<0.0001	0.7499	0.0011	0.1817

Figure 5.1. *Boxplots of density for each of the thicknesses considered (3.8, 7.6, and 11.1).*

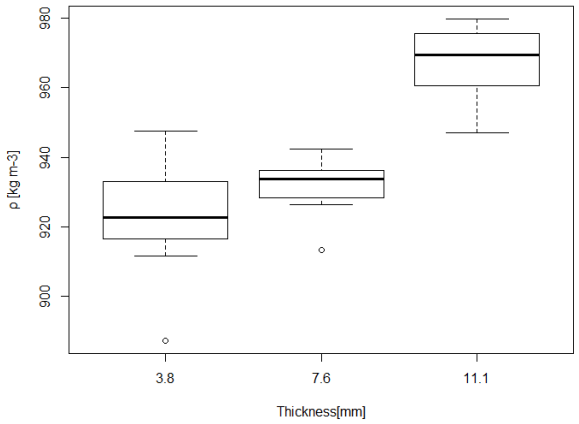

Figure 5.2. *Boxplots of modulus of elasticity MOE for each of the thicknesses considered (3.8, 7.6, and 11.1).*

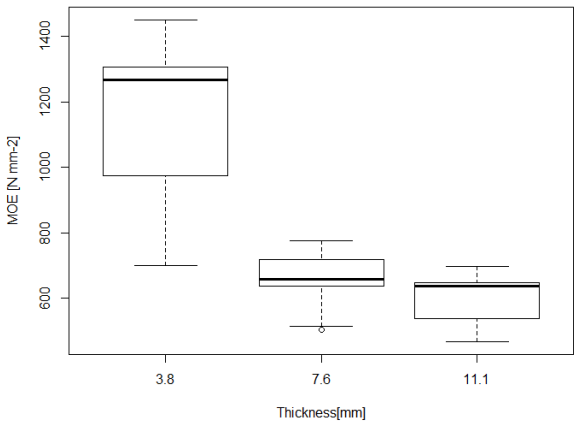

Figure 5.3. *Boxplots of modulus of rupture MOR for each of the thicknesses considered (3.8, 7.6, and 11.1).*

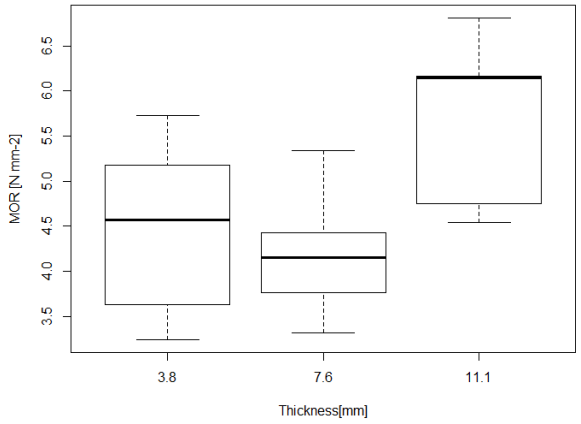

Figure 5.4. *Boxplots of internal bond IB for each of the thicknesses considered (3.8, 7.6, and 11.1).*

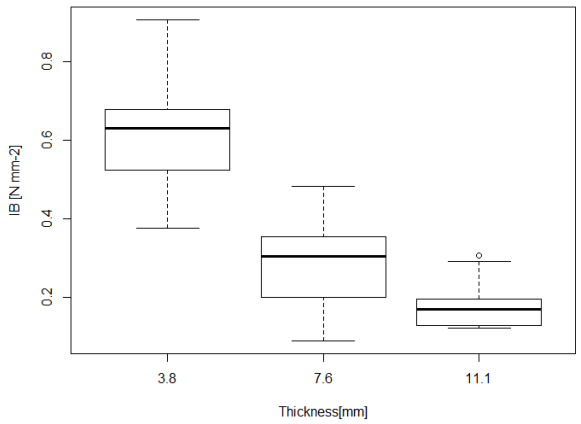

5.2.2. Effect of thickness on dimensional stability

The results of TS and water absorption (WA) of all tested specimens are given in Table 5.6., while Table 5.7. shows the average values with the corresponding standard deviation (St.Dev.). The analysis was carried out with the same methodology used for mechanical properties, i.e., the factor considered in the one-way ANOVA model is the average thickness.

Referring to the EN 622-5:2010, the standards report different values depending on the thickness. For general use in dry conditions, values of 35%, 30%, 17%, and 15% are given, for thicknesses 2.5 to 4

mm, 4 to 6 mm, 6 to 9 mm, and 9 to 12 mm, respectively. Samples F3 and F3D achieved the values, although just for the non-structural use in dry conditions. Nevertheless, this result can be attributed to the low $\log R_0$ of 3.62.

From one-way ANOVA (Table 5.8.), the effect of the thickness is significant for TS, but only between groups 7.6-3.8, and 11.1-3.8 (Table 5.9.). When it comes to WA (Figure 5.6.), the trend is similar to TS and decreased by increasing the thickness. However, from a statistical point of view, there was no significance difference with respect to thickness. The TS improve by increasing the thickness (Figure 5.5.) and this may be related to the higher density, which may indicate fewer and smaller pores through which water can penetrate. Some studies (Migneault et al., 2011; Q. Wu & Piao, 1999), also related TS with IB through the correlation factor (r), thus identifying a close connection between the two properties. Here, an r of 0.99 was found between TS and IB, indicating that they are close correlated.

In general, the WA value is considered much more reliable than TS, even though it is not covered in European standards. This is because thickness measurement is subject to a higher relative error due on the one hand to the instrument itself and on the other hand to the point where the thickness is measured. Homogeneity of the specimens is indeed a challenging goal to achieve at the laboratory level, and even if the thickness is measured at different points and the average is considered, the weight measurement is still more reliable.

As a result, although statistical analysis showed that there was no significant effect of thickness on WA, some consideration must be made about the results. First of all, the coefficient of determination (R-squared) obtained for both models (i.e., TS and WA), was not high, which means that certain predictions cannot be made based on these models. In addition, from the results shown in Table 5.7., there was a decreasing in both TS and WA by increasing the thickness. Although no significance was found from the statistical analysis for WA, this may be due to the fact that in the range of thicknesses considered the effect of thickness is not significant, but, by further increasing the thickness the results might change. Indeed, from Figure 5.6, the trend of WA is clearly downward.

Table 5.6. *Thickness swelling TS and water absorption WA results of tested specimens with different thicknesses.*

Series name	Specimen number	Specimen name	Thickness* mm	ρ kg m^{-3}	TS %	WA %
F3	1	1	3.8	942	26	48
F3	3	R5	3.7	948	31	46
F3	4	8	3.9	923	37	64
F3	5	10	3.9	920	36	61
F3	6	12	3.9	912	45	80
F3	7	14	3.9	917	45	84
F3	8	17	3.8	933	38	58
F3	9	19	3.6	887	41	66
F3	10	23	3.9	930	46	77
F3D	1	1	7.6	926	25	53
F3D	2	5	7.6	930	31	65
F3D	3	8	7.8	913	27	54
F3D	4	10	7.7	928	28	64
F3D	5	12	7.6	942	25	53
F3D	6	14	7.6	934	35	79
F3D	7	17	7.6	936	25	42
F3D	8	19	7.6	934	26	50
F3D	9	23	7.6	940	38	70
F3T	1	1	11.2	957	19	29
F3T	2	5	11.3	947	30	55
F3T	3	8	11.0	973	24	39
F3T	4	10	11.1	966	27	47
F3T	5	12	11.0	980	29	54
F3T	6	14	11.0	979	29	64
F3T	7	17	11.0	976	26	50
F3T	8	19	11.1	970	28	49
F3T	9	23	11.1	961	37	75

**The average thicknesses considered in the ANOVA were: 3.8 mm for F3; 7.6 mm for F3D; 11.1 mm for F3T.*
Manufacturing conditions: reaction temperature (Tr) 190°C; second pressing pressure (Pp_2) 7.5 N mm^{-2}; curing temperature (Tc) 165°C; curing time (tc) 5h.

Table 5.7. *Average thickness swelling TS and water absorption WA results of tested specimens with different thicknesses, and the corresponding St.Dev.*

Series name	thickness mm	St. Dev.	ρ kg m^{-3}	St. Dev.	TS %	St. Dev.	WA %	St. Dev.
F3	3.8	0.11	923	18	38	7	65	14
F3D	7.6	0.06	932	9	29	5	59	11
F3T	11.1	0.12	968	11	28	5	51	13

Table 5.8. *One-way ANOVA for thickness swelling TS and water absorption WA results considering the thickness as three level factor.*

Factor	Property		D.f.	R-squared [%]	p-value
thickness	TS	%	2	43.40	0.0011
	WA	%	2	27.88	0.0941

Table 5.9. *HSD multiple comparison from one-way ANOVA for thickness swelling TS and water absorption WA results considering the thickness as three level factor.*

facthick	TS % p-value HSD	WA % p-value HSD
7.6-3.8	0.0052	0.5872
11.1-3.8	0.0018	0.0782
11.1-7.6	0.9037	0.4171

Figure 5.5. *Boxplots of thickness swelling TS for each of the thicknesses considered (3.8, 7.6, and 11.1).*

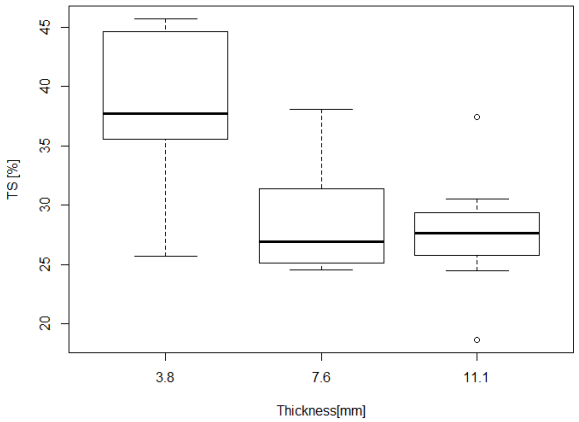

Figure 5.6. *Boxplots of water absorption WA for each of the thicknesses considered (3.8, 7.6, and 11.1).*

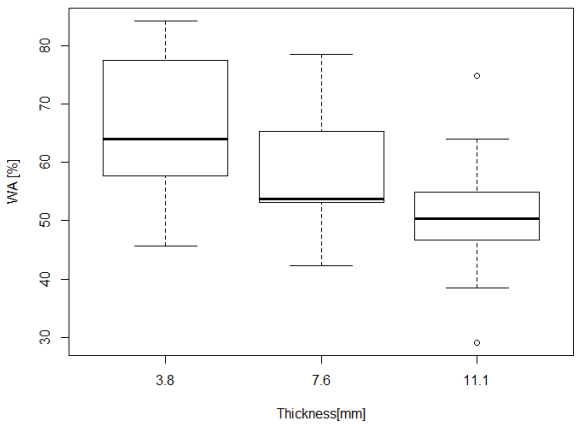

5.2.3. Interaction between thickness and final heat treatment

To complete the analysis of the influence of thickness on physico-mechanical properties, the interaction of thickness with the FHT was considered. In Chapter 4, it was shown that there was no significant difference in the influence of FHT between curing times (tc) 0.5 h and 1 h. Referring back to this assumption, we consider the series made with three different thicknesses, with the same STEX and HP conditions, and with a curing temperature (Tc) of 180 °C, simply indicating whether there was a FHT or not. The full analysis confirming this assumption for this series as well is given in Annex B.

Table 5.10. shows the physico-mechanical results of all tested specimens, while in Table 5.11. the average values with the corresponding St.Dev. are given. The results were analyzed by a two-way ANOVA model, considering the FHT and the thickness as two levels and three levels factors, respectively.

The ANOVA revealed that factor FHT is significant only for TS and WA, while mechanical properties and density were not influenced by the curing step (Table 5.12.). The same result was obtained in the Chapter 4 (Section 4.2.2.2.). On the other hand, the thickness is significant only for density, MOE, and IB. The crossed interaction between the two factors was weakly significant only for TS, being the p-value 0.03.

As for the density (Figure 5.7.), only the difference between groups 11-3.9, and 11-7.6 was significant, while there was no difference between groups 7.6-3.9 (Table 5.13.).

As found in the previous section, the MOE (Figure 5.8.) decreased with thickness. Here again, the value for the smaller thickness stood out and the values of the thickness groups 11 and 7.6 were comparable (Table 5.13.).

In this case, for MOR (Figure 5.9.), neither thickness nor FHT were significant. The values obtained for each thickness, with and without FHT, were comparable, but the R-squared for MOR analysis was lower than for the others, being around 20%. The reason can be identified in the St.Dev. for F3 values, whereby there were some values (specimens 24-3, 25-3, and 26-3) with a significantly higher MOR than the other specimens. Nevertheless, also in the previous section the significance of thickness with respect to MOR was much weaker compared to the other mechanical properties. Indeed, some studies (Martins et al., 2021) reported that MOR depends directly on the strength of face layers, exactly the opposite from IB. Thus, considering that the specimens were all made with the same HP conditions, the biggest difference between the various thicknesses is related to the innermost layers.

Indeed, for IB (Figure 5.10.), a significant difference was found for all thickness groups (Table 5.13). As in the previous section, the value for the smaller thickness was the one that stood out, being the highest. As mentioned, the heat of the HP made the difference, which, with only about 4 mm of thickness had the sufficient time to reach the center of the specimen and activate the adhesion effect between the fibers, giving the specimen a plastic-like appearance and a strong core layer. Moreover, again as previously shown, the difference between the higher thicknesses, i.e., 7.6 and 11, was smaller and many of the significances were weak (Table 5.13.).

***Table 5.10**. Physico-mechanical results of tested specimens with different thicknesses and with or without final heat treatment FHT.*

Series name	Specimen number	Specimen name	FHT -	Thickness* mm	ρ kg m^{-3}	MOE N mm^{-2}	MOR N mm^{-2}	IB N mm^{-2}	TS %	WA %
F3	1	24	NO	4.0	909	962	3.7	0.526	92	157
F3	2	24-1	NO	3.8	937	1719	4.6	0.408	70	118
F3	3	24-2	NO	3.8	947	1200	4.0	0.588	70	122
F3	4	24-3	NO	4.0	892	1567	8.1	0.520	65	88
F3	1	25	YES	4.0	912	772	2.7	0.431	53	89
F3	2	25-1	YES	3.9	923	975	4.1	0.534	38	82
F3	3	25-2	YES	3.9	919	610	3.3	0.340	40	80
F3	4	25-3	YES	3.9	952	1941	10.8	0.522	38	66
F3	1	26	YES	3.8	942	1203	4.5	0.329	43	77
F3	2	26-1	YES	3.7	946	1170	5.7	0.551	30	42
F3	3	26-2	YES	3.8	922	1137	5.0	0.304	36	57
F3	4	26-3	YES	4.0	927	1530	9.4	0.448	28	49
F3D	1	24	NO	7.6	930	667	3.4	0.257	83	138
F3D	2	24-1	NO	7.4	957	684	4.6	0.340	91	144
F3D	3	24-2	NO	7.7	942	801	3.7	0.402	82	135
F3D	1	25	YES	7.6	918	485	3.7	0.319	39	85
F3D	2	25-1	YES	7.7	937	557	3.9	0.449	41	84
F3D	3	25-2	YES	7.6	930	702	4.7	0.201	42	89
F3D	1	26	YES	7.5	918	458	3.6	0.378	24	48
F3D	2	26-1	YES	7.8	911	648	4.6	0.345	22	48
F3D	3	26-2	YES	7.6	915	403	2.8	0.275	29	50
F3T	1	24	NO	10.9	987	635	5.6	0.112	82	131
F3T	2	24-1	NO	11.1	976	608	4.7	0.157	90	140
F3T	3	24-2	NO	10.9	969	681	5.4	0.196	90	141
F3T	1	25	YES	11.1	963	689	6.7	0.218	37	78
F3T	2	25-1	YES	11.1	982	735	5.9	0.160	36	75
F3T	3	25-2	YES	10.8	968	522	5.2	0.117	40	77
F3T	1	26	YES	11.1	958	543	6.4	0.146	27	54
F3T	2	26-1	YES	10.7	980	445	4.9	0.142	27	56
F3T	3	26-2	YES	11.3	966	590	6.1	0.144	19	30

**The average thicknesses considered in the ANOVA were: 3.9 mm for F3; 7.6 mm for F3D; 11 mm for F3T.*

Manufacturing conditions: reaction temperature (Tr) 190°C; second pressing pressure (Pp_2) 7.5 N mm^{-2}.

Table 5.11. *Average physico-mechanical results of tested specimens with different thicknesses and with or without final heat treatment FHT.*

Series name	FHT -	ρ kg m^{-3}	St. Dev.	MOE N mm^{-2}	St. Dev.	MOR N mm^{-2}	St. Dev.	IB N mm^{-2}	St. Dev.	TS %	St. Dev.	WA %	St. Dev.
F3	NO	921	25	1362	344	5.1	2.0	0.510	0.075	74	12	121	29
F3	YES	930	15	1167	420	5.7	2.9	0.432	0.099	38	8	67	17
F3D	NO	943	13	717	73	3.9	0.6	0.333	0.073	85	5	139	5
F3D	YES	922	10	542	116	3.9	0.7	0.328	0.085	33	9	67	21
F3T	NO	977	9	641	37	5.2	0.5	0.155	0.042	87	5	137	6
F3T	YES	970	10	587	108	5.8	0.7	0.154	0.034	31	8	62	19

Table 5.12. *Two-way ANOVA for physico-mechanical results considering the final heat treatment FHT and the thickness as factors, and their interaction.*

Factor	Property		D.f.	R-squared [%]	p-value
FHT	ρ	kg m^{-3}	1	73.67	0.3583
	MOE	N mm^{-2}	1	63.57	0.157
	MOR	N mm^{-2}	1	20.55	0.544
	IB	N mm^{-2}	1	60.92	0.281
	TS	%	1	90.16	$2.09 \cdot 10^{-13}$
	WA	%	1	77.73	$3.51 \cdot 10^{-9}$
Thickness	ρ	kg m^{-3}	2	73.67	$2.62 \cdot 10^{-7}$
	MOE	N mm^{-2}	2	63.57	$3.58 \cdot 10^{-6}$
	MOR	N mm^{-2}	2	20.55	0.787
	IB	N mm^{-2}	2	60.92	$2.16 \cdot 10^{-8}$
	TS	%	2	90.16	0.9862
	WA	%	2	77.73	0.784
FHT:Thickness	ρ	kg m^{-3}	2	73.67	0.0865
	MOE	N mm^{-2}	2	63.57	0.842
	MOR	N mm^{-2}	2	20.55	0.9207
	IB	N mm^{-2}	2	60.92	0.474
	TS	%	2	90.16	0.0315
	WA	%	2	77.73	0.412

For TS (Figure 5.11.) and WA (Figure 5.12.), the significance of FHT was still highly accented, while thickness in this case had a weak influence only on TS, just as in the previous section, being the p-value 0.03. However, looking at the multiple comparison (Table 5.14.), the differences between groups with different thickness but the same FHT, i.e., with FHT (YES) and without FHT (NO), were never significant. Again, as in Chapter 4, TS, and WA for specimens with FHT were less than half of those without FHT.

To sum up, as well as previous sections, thickness had a significant influence on density, MOE, and IB, while FHT only influenced TS and WA. The MOE and the IB decreased with thickness, and the TS an WA significantly improved by carrying out the FHT.

Table 5.13. *Honestly significance difference HSD multiple comparison from two-way ANOVA for physico-mechanical results considering the final heat treatment FHT and the thickness as factors, and their interaction.*

facFHT	ρ	MOE	MOR	IB	TS	WA
	kg m^{-3}	N mm^{-2}	N mm^{-2}	N mm^{-2}	%	%
	p-value	p-value	p-value	p-value	p-value	p-value
	HSD	HSD	HSD	HSD	HSD	HSD
YES-NO	0.36	0.17	0.53	0.27	0.00	0.00
facthick	ρ	MOE	MOR	IB	TS	WA
	kg m^{-3}	N mm^{-2}	N mm^{-2}	N mm^{-2}	%	%
	p-value	p-value	p-value	p-value	p-value	p-value
	HSD	HSD	HSD	HSD	HSD	HSD
7.6-3.9	0.97	0.00	0.10	0.00	1.00	0.77
11-3.9	0.00	0.00	0.98	0.00	0.99	0.98
11-7.6	0.00	1.00	0.09	0.00	0.99	0.88
facFHT:Thick	ρ	MOE	MOR	IB	TS	WA
	kg m^{-3}	N mm^{-2}	N mm^{-2}	N mm^{-2}	%	%
	p-value	p-value	p-value	p-value	p-value	p-value
	HSD	HSD	HSD	HSD	HSD	HSD
YES:3.9-NO:3.9	0.8951	0.8399	0.9936	0.5705	<0.0001	0.0012
NO:7.6-NO:3.9	0.3632	0.0447	0.9429	0.0577	0.5186	0.8199
YES:7.6-NO:3.9	1.0000	0.0010	0.8894	0.0132	<0.0001	0.0020
NO:11-NO:3.9	0.0003	0.0195	0.9999	<0.0001	0.3331	0.8682
YES:11-NO:3.9	0.0002	0.0019	0.9853	<0.0001	<0.0001	0.0006
NO:7.6-YES:3.9	0.7704	0.1714	0.6639	0.4189	<0.0001	0.0001
YES:7.6-YES:3.9	0.8565	0.0029	0.4308	0.1577	0.8522	1.0000
NO:11-YES:3.9	0.0007	0.0761	0.9986	0.0002	<0.0001	0.0001
YES:11-YES:3.9	0.0004	0.0062	0.9999	<0.0001	0.6027	0.9914
YES:7.6-NO:7.6	0.3006	0.9366	1.0000	0.9999	<0.0001	0.0002
NO:11-NO:7.6	0.0674	0.9992	0.9360	0.0844	0.9995	0.9999
YES:11-NO:7.6	0.1298	0.9819	0.6261	0.0326	<0.0001	0.0001
NO:11-YES:7.6	0.0001	0.9946	0.8878	0.0406	<0.0001	0.0002
YES:11-YES:7.6	<0.0001	0.9996	0.4127	0.0076	0.9981	0.9947
YES:11-NO-11	0.9677	0.9997	0.9957	1.0000	<0.0001	0.0001

Figure 5.7. *Boxplots of density of binderless fiberboards from steam exploded Arundo donax L. at reaction temperature Tr 190°C, for each of the FHT-thickness conditions considered. In the x-axis the FHT-thickness conditions are reported, where 0 means without final heat treatment (FHT), while 1 means with FHT.*

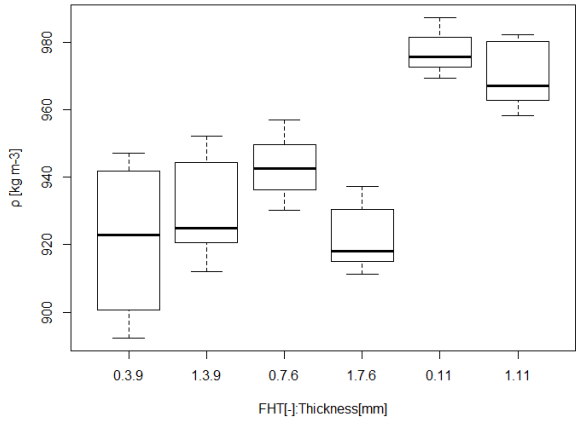

Figure 5.8. *Boxplots of modulus of elasticity MOE of binderless fiberboards from steam exploded Arundo donax L. at reaction temperature Tr 190°C, for each of the FHT-thickness conditions considered. In the x-axis the FHT-thickness conditions are reported, where 0 means without final heat treatment (FHT), while 1 means with FHT.*

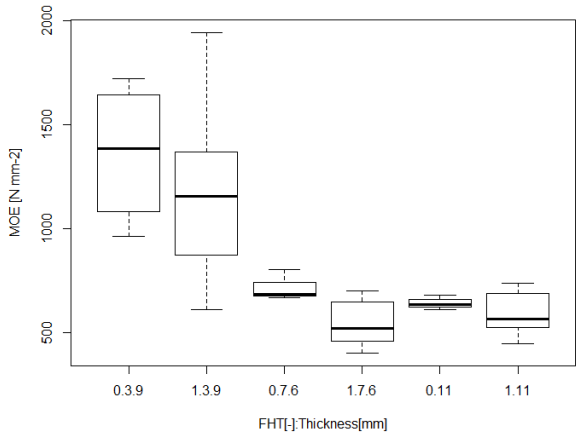

Figure 5.9. *Boxplots of modulus of rupture MOR of binderless fiberboards from steam exploded Arundo donax L. at reaction temperature Tr 190°C, for each of the FHT-thickness conditions considered. In the x-axis the FHT-thickness conditions are reported, where 0 means without final heat treatment (FHT), while 1 means with FHT.*

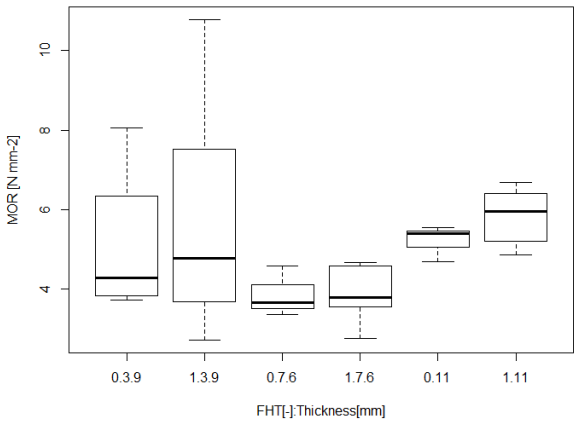

Figure 5.10. *Boxplots of internal bond IB of binderless fiberboards from steam exploded Arundo donax L. at reaction temperature Tr 190°C, for each of the FHT-thickness conditions considered. In the x-axis the FHT-thickness conditions are reported, where 0 means without final heat treatment (FHT), while 1 means with FHT.*

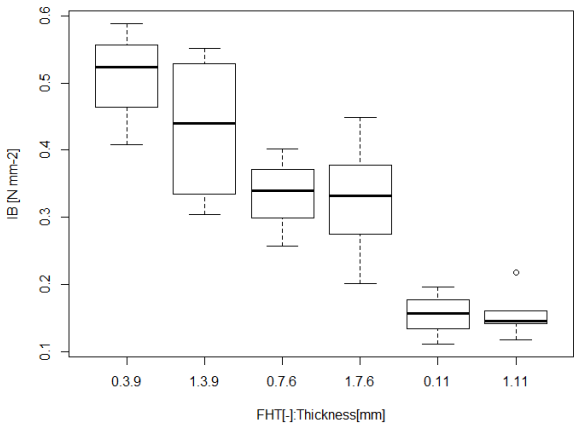

Figure 5.11. *Boxplots of thickness swelling TS of binderless fiberboards from steam exploded Arundo donax L. at reaction temperature Tr 190°C, for each of the FHT-thickness conditions considered. In the x-axis the FHT-thickness conditions are reported, where 0 means without final heat treatment (FHT), while 1 means with FHT.*

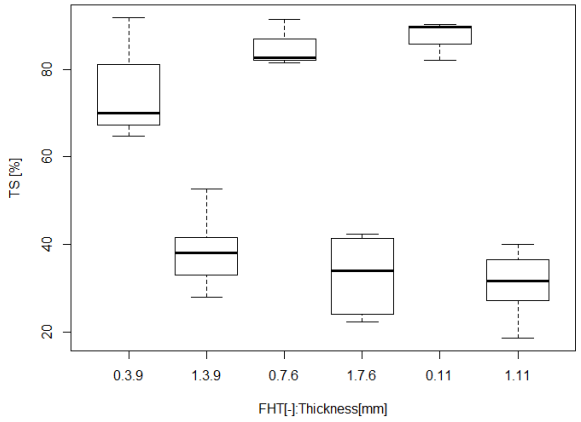

Figure 5.12. *Boxplots of water absorption WA of binderless fiberboards from steam exploded Arundo donax L. at reaction temperature Tr 190°C, for each of the FHT-thickness conditions considered. In the x-axis the FHT-thickness conditions are reported, where 0 means without final heat treatment (FHT), while 1 means with FHT.*

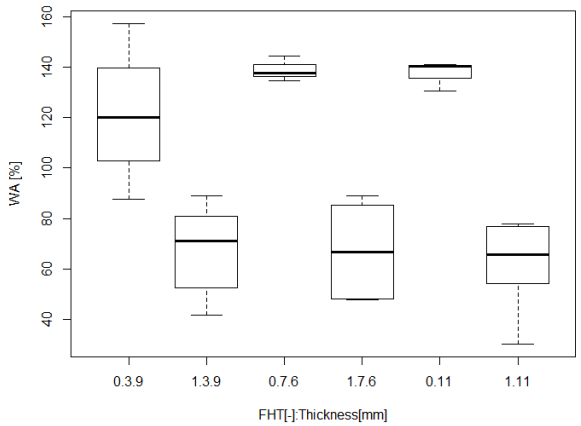

5.3. Conclusions

Considering all the results of the analysis developed in this Chapter, we found that thickness had a significant influence on mechanical properties, while for dimensional stability a progressive, though not significant in the range of the conditions considered, effect can be appreciated. The FHT still had a major influence on dimensional stability, while mechanical properties were not affected by this. This result agrees with the discussion in Chapter 4: the effect of FHT on mechanical properties is clearer when the R_0 is higher, and for this analysis the R_0 used was below the threshold. On the one hand, analyzing the data with a lower R_0 allows the other differences to be seen to a greater extent, but losing in performance on the other hand. No interaction was found between FHT and thickness factors, except in the case of TS for which a p-value of 0.03 was found, thus indicating that there is a weak interaction between them.

Based on statistical analysis, MOE and IB were greatly influenced by thickness. Both of them decreased because of the increasing in thickness, and this result was associated for MOE to a mechanical effect, since the thickness appears cubed in the denominator of the MOE formula, and for IB the result was associated to the HP conditions that should be optimized depending on thickness: a greater thickness needs more time for plate heat to reach the center of the specimen. In any case, for these as well as the other properties, suboptimal results can be related to the low R_0.

For the MOR, the analysis was less clear. In the first analysis the MOR was actually influenced by the thickness, while in the second, when the interaction with FHT was considered, the p-value was higher than 0.05 for both thickness and FHT factors. In both cases the R-squared is quite low, i.e., 40% in the first part and 20% in the second, and this makes the interpretation of the results unclear.

For TS and WA, in agreement with Chapter 4, FHT has a huge influence, and the values were significantly reduced, although, because of the key role of STEX, the values obtained did not fulfill the standards, as well as for mechanical results. Only the IB reached the minimum for general use in dry conditions (IB). However, the main objective was not to achieve the absolute value required by the standards, but to understand the relative effect of FHT and thickness on the properties. It is still clear that the effect of FHT on the dimensional stability of the specimens is consistent.

References

Balea (Paul), G., Lunguleasa, A., Zeleniuc, O., & Coşereanu, C. (2022). Three adhesive recipes based on magnesium lignosulfonate, used to manufacture particleboards with low formaldehyde emissions and good mechanical properties. *Forests*, 13(5), 737. https://doi.org/10.3390/f13050737

Halvarsson, S., Edlund, H., & Norgren, M. (2008). Manufacture of non-resin wheat straw fibreboards. *Industrial Crops and Products*, 29, 437–445. https://doi.org/10.1016/j.indcrop.2008.08.007

Martins, R. S. F., Gonçalves, F. G., Segundinho, P. G. de A., Lelis, R. C. C., Paes, J. B., Lopez, Y. M., Chaves, I. L. S., & Oliveira, R. G. E. de. (2021). Investigation of agro-industrial lignocellulosic wastes in fabrication of particleboard for construction use*. Journal of Building Engineering*, 43, 102903. https://doi.org/10.1016/j.jobe.2021.102903

Migneault, S., Koubaa, A., Riedl, B., Nadji, H., Deng, J., & Zhang, T. (2011). Binderless fiberboard made from primary and secondary pulp and paper sludge. *Wood and Fiber Science,* 43(2), 180 – 193.

Pham Van, T., Schöpper, C., Klüppel, A., & Mai, C. (2021). Effect of wood and panel density on the properties of lightweight strand boards. *Wood Material Science and Engineering*, 16(4), 237–245. https://doi.org/10.1080/17480272.2019.1705906

Wu, Q., & Piao, C. (1999). Thickness swelling and its relationship to internal bond strength loss of commercial oriented strandboard. *Forest Products Journal*, 49, 50–55.

Chapter 6. Medium density boards: comparison between self-bonded and pMDI-bonded boards

Chapter content

In this Chapter the results of two series of medium density fiberboards made by mixing exploded *Arundo donax* L. with traditional wood fibers are presented. The first series compares the results of panels with dimensions of 250x250x11 mm^3, using three different fiber formulations: 100% wood fibers, 50% wood fibers and 50% *Arundo donax* L., and 100% *Arundo donax* L. Both pMDI-bonded and self-bonded panels are manufactured for each fiber formulation to compare the results. The objective of the first series is to study the role of *Arundo donax* L. mixed with wood fibers in the production of self-bonded boards and to determine if the results are comparable to those obtained from panels with the same fiber formulation but pMDI-bonded. For the second series, only self-bonded panels are produced, with an increased minimum percentage of *Arundo donax* L. to 60% and a longer pressure time, double that of the first series. Additionally, the dimensions of the panels are increased to 450x450x11 mm^3. The aim of this series is to improve upon the results obtained for the first series by increasing the pressure time and to simulate an industrial process by manufacturing larger panels. The mechanical and physical properties of these panels are then studied.

6.1. Experimental design and objective

The data in this Chapter refer to the research developed at the Georg-August-Universität Göttingen (Göttingen, Germany), and thus the manufacturing process of the boards has some differences from previous chapters, both in terms of the equipment used (specified in Annex A), and the method. The first difference was the material used: in addition to exploded *Arundo donax* L. (AD), wood fibers (WF) were used, mixed in different percentages, whose composition is presented in Chapter 2. Two series were made: the first with the objective of comparing the results between self-bonded medium density fiberboards (MDF) and MDF with pMDI adhesive at a percentage of 4 wt% (Table 6.1.); the second composed exclusively of binderless panels, changing some parameters compared to the first series such as the percentages of the materials used, the panel size, and the pressing time (Table 6.2.). For both series, the density was set at 780 kg m^{-3}, and the size of the specimens was close to industrial size. For the first series, two panels of size 250x250x10.5 mm^3 were made for each variation, and from these two panels, specimens of the dimensions required by the standard were cut to perform the mechanical and physical tests. Similarly, the specimens for the second series are made from full size panels, the difference being that in this case the full size is 450x450x10.5 mm^3. The steam explosion (STEX) of AD was performed at the optimum conditions found in Chapter 3, i.e., reaction temperature (Tr) 200°C, and reaction time (tr) 9.5 min. The hot pressing (HP) was performed in a single step, due to limitation of the equipment used. Before HP the materials were blended to achieve enough uniformity, and there was no final heat treatment (FHT). For characterization, the specimens were cut from the full size to the dimensions compatible with the testing machine and the standard.

Table 6.1. *Parameters and materials used for the first series of medium density fiberboards with and without pMDI.*

Variations	WF wt%	AD wt%	pMDI wt%
WF0	100	0	0
WF4	96	0	4
WFAD0	50	50	0
WFAD4	48	48	4
AD0	0	100	0
AD4	0	96	4

specimens size	250x250x11		mm^3
STEX	Tr	200	°C
	tr	9.5	min
milling	Electra hammer mill (10 mesh)		
blending	speed	30	round min^{-1}
	time	5	min
HP	Pp	5	N mm^{-2}
	Tp	205	°C
	tp	15	s mm^{-1}
Cutting and sanding	final size	240x240x10.5	mm^3
Conditioning	T	20	°C
	RH	65	%

Table 6.2. *Parameters and materials used for the second series of binderless medium density fiberboards.*

Variations		WF wt%	AD wt%
	WFAD40/60	40	60
	WFAD20/80	20	80
	AD100	0	100

specimens size	460x460x11		mm^3
STEX	Tr	200	°C
	tr	9.5	min
milling	Electra hammer mill (10 mesh)		
blending	speed	30	round min^{-1}
	time	5	min
HP	Pp	5	N mm^{-2}
	Tp	205	°C
	tp	30	s mm^{-1}
Cutting and sanding	final size	450x450x10.5	mm^3
Conditioning	T	20	°C
	RH	65	%

6.2. Results and discussion

6.2.1. First series: comparison between self-bonded and pMDI-bonded boards

6.2.1.1. Density and mechanical properties

The mean density of the samples ranged from 665 to 769 kg m^{-3}, which means that none of the samples reached the target density set at 780 kg m^{-3} (Table 6.3., and Table 6.4.), but they were still in the range of conventional MDF.

Table 6.3. *Density and mechanical results (MOE, MOR, and IB) of tested specimens with different percentages of Arundo donax L., wood fibers, and pMDI.*

Series name	Specimen name	ρ kg m^{-3}	MOE N mm^{-2}	MOR N mm^{-2}	IB* N mm^{-2}
WF0	3-1	618	955	3.9	-
WF0	3-2	732	1859	10.0	-
WF0	4-1	600	1004	3.9	-
WF0	4-2	692	1411	6.5	-
WF0	3-1	693	-	-	**0.009**
WF0	3-2	737	-	-	0.047
WF0	3-3	710	-	-	0.028
WF0	3-4	657	-	-	0.013
WF0	4-1	662	-	-	0.033
WF0	4-2	733	-	-	0.021
WF0	4-3	679	-	-	0.041
WF4	5-1	717	3952	-	-
WF4	5-2	803	5103	34.1	-
WF4	6-1	761	4789	49.7	-
WF4	6-2	791	4143	17.4	-
WF4	5-1	780	-	-	0.244
WF4	5-2	816	-	-	0.389
WF4	5-3	795	-	-	**0.093**
WF4	5-4	756	-	-	**0.095**
WF4	6-1	806	-	-	0.404
WF4	6-2	749	-	-	0.278
WF4	6-3	777	-	-	0.170
WF4	6-4	775	-	-	**0.009**
WFAD0	11-1	688	2221	8.6	-
WFAD0	11-2	766	2884	13.5	-
WFAD0	12-1	699	2181	8.7	-
WFAD0	12-2	755	2574	12.1	-
WFAD0	11-1	737	-	-	0.040
WFAD0	11-2	806	-	-	0.024
WFAD0	11-3	723	-	-	0.033
WFAD0	11-4	622	-	-	0.016
WFAD0	12-1	739	-	-	0.028
WFAD0	12-2	747	-	-	0.027
WFAD0	12-3	731	-	-	0.035
WFAD0	12-4	651	-	-	0.021

Series name	Specimen name	ρ kg m^{-3}	MOE N mm^{-2}	MOR N mm^{-2}	IB* N mm^{-2}
WFAD4	7-1	731	3922	33.5	-
WFAD4	7-2	717	3860	36.1	-
WFAD4	8-1	658	3192	28.6	-
WFAD4	8-2	703	3738	35.0	-
WFAD4	7-1	733	-	-	**0.008**
WFAD4	7-2	727	-	-	0.203
WFAD4	7-3	733	-	-	0.389
WFAD4	7-4	709	-	-	0.348
WFAD4	8-1	705	-	-	**0.007**
WFAD4	8-2	707	-	-	**0.011**
WFAD4	8-3	678	-	-	**0.011**
WFAD4	8-4	683	-	-	0.187
AD0	13-1	708	3473	18.6	-
AD0	13-2	754	4160	25.7	-
AD0	14-1	650	2021	7.9	-
AD0	14-2	814	4486	26.9	-
AD0	13-1	680	-	-	0.047
AD0	13-2	839	-	-	0.217
AD0	13-3	855	-	-	0.012
AD0	13-4	744	-	-	0.045
AD0	14-1	682	-	-	0.041
AD0	14-2	727	-	-	**0.009**
AD0	14-3	794	-	-	0.095
AD0	14-4	810	-	-	**0.007**
AD4	9-1	662	3041	20.9	-
AD4	9-2	712	3854	30.2	-
AD4	10-1	663	2848	20.1	-
AD4	10-2	713	3655	25.3	-
AD4	9-1	710	-	-	0.260
AD4	9-2	721	-	-	0.183
AD4	9-3	712	-	-	0.179
AD4	9-4	679	-	-	**0.023**
AD4	10-1	714	-	-	0.104
AD4	10-2	731	-	-	**0.011**
AD4	10-3	716	-	-	**0.010**
AD4	10-4	706	-	-	0.302

**Values in bold for IB are those removed to perform the statistical analysis.*

Table 6.4. *Average mechanical results (MOE, MOR, and IB) of tested specimens with different percentages of Arundo donax L., wood fibers, and pMDI., and the corresponding St.Dev.*

Series name	ρ kg m^{-3}	St. Dev.	MOE N mm^{-2}	St. Dev.	MOR N mm^{-2}	St. Dev.	IB (all) N mm^{-2}	St. Dev.	IB N mm^{-2}	St. Dev.
WF0	669	54	1307	421	6.1	2.9	0.027	0.014	0.031	0.013
WF4	769	37	4497	540	33.7	16.1	0.210	0.143	0.297	0.099
WFAD0	731	44	2465	331	10.7	2.4	0.028	0.008	0.028	0.008
WFAD4	711	25	3678	333	33.3	3.3	0.146	0.160	0.282	0.102
AD0	740	67	3535	1094	19.8	8.7	0.059	0.070	0.076	0.074
AD4	704	28	3350	481	24.2	4.7	0.134	0.115	0.206	0.077

The highest density was obtained for the sample WF4, followed by AD0, WFAD0, WFAD4, AD4, and WF0 (Figure 6.1.). The AD0 sample was

the one within self-bonded boards with the density closest to the maximum obtained for WF4. This can be explained by the compressibility of AD after STEX, as shown in Chapter 3. Lignocellulosic material (LM) treated by STEX results in a defibrillated pulp for which the fibers are thin and long (Shu et al., 2019; Troncoso-Ortega et al., 2021), thus enhancing the compactness of the boards. Domínguez-Robles et al., also related the increase in density to the decrease of the length and width of the fibers, and to the increase of fine elements as a consequence of the pretreatment, thus observing an improvement in mechanical strength with respect to boards made of untreated fibers (Domínguez-Robles et al., 2020).

The ANOVA were performed by considering the variation as a six level factor and showed that the material formulation had a major influence on density (Table 6.5.). The multiple comparison shows the significance relationships between the groups considered, by comparing the formulations within the groups of self-bonded and pMDI-bonded, and between the same fiber formulation with and without the adhesive. From this, we found that the density values that stand out from the others are those of WF0 and WF4, for being the lowest and highest, respectively. Therefore, the density of WF0 is significantly different from WFAD0, AD0, and WF4, and the density of WF4 is significantly different from WFAD4, AD4, and WF0. On the other hand, the statistically equal densities are WFAD0-AD0, WFAD4-AD4, WFAD0-WFAD4, and AD0-AD4 (Table 6.6.). Thus, comparing the same fiber formulation with and without adhesive, the difference in density was significant only when using only WF, whereas for specimens containing AD there was no difference in density. The analysis of the significant differences with respect to density leads to a better understanding of the differences in mechanical properties, since density is directly related to mechanical performance. Indeed, in the case of self-bonded samples the density increased by adding exploded AD, while in the case of pMDI-bonded samples exactly the reverse occurred, and the density decreased as exploded AD was added. This could indicate low compatibility of the exploded material with this type of adhesive, i.e., pMDI, consequently affecting all other mechanical properties.

Figure 6.2. shows the boxplots of MOE. The highest MOE was obtained for the sample WF4, which reached an average value of 4497 N mm^{-2} (Table 6.4.). As well as density, statistical analysis showed a significant p-value (Table 6.5.). Based on these results, boards made with pMDI showed the highest MOE values except for AD0, which had

an MOE in the same range as WFAD4 and AD4, as also shown by the multiple comparison (Table 6.6.). The increase in MOE can be related to the increase in density, as well as for other mechanical properties, which is connected with the bonding quality and the adhesion between fibers (Bekhta et al., 2021; Buschmann et al., 2021; Hidayat et al., 2022; Li et al., 2010; Luo et al., 2020; Pham Van et al., 2021). This is especially noticeable when comparing self-bonded and pMDI-bonded boards, where MOE showed the same significant differences as density between the groups considered: where there was difference in density, there was difference also in MOE values, which increased for higher density. However, for the pMDI-bonded boards, some differences were found: although there was a significant difference in density between WF4 and the other two groups (WFAD4, and AD4), the samples containing AD did not show any difference in MOE values with WF4. With regard to self-bonded boards, the only deviation with respect to the dependence of MOE on density occurred for the WF0 and WFAD0 groups, whereby there was no significant difference in MOE values while there was for density. Referring to the standard EN 622-5:2010, all the samples made with pMDI met the requirements for structural use both in dry and wet conditions, while for the self-bonded samples only AD0 reached the minimum value required, although sample AD4 was very close to it.

For MOR (Figure 6.3.) the relationship with the presence or absence of adhesive was clearer. Also here the higher average value was found for sample WF4 (Table 6.4.) and the variation had a significant effect on the MOR results, although mostly because of the adhesive (Table 6.5.). Indeed, there were no significant differences between the WF0, WFAD0, and AD0 groups, as well as between the WF4, WFAD4, and AD4 groups, although there were differences for density for some of these groups (Table 6.6.). Whilst for MOE there was the possibility that the percentage of AD had an influence on the values obtained, for MOR it was clear that it depends prevalently on the adhesive in the case where wood fibers were used, while for the AD4 and AD0 groups, not even the presence of the adhesive resulted in differences in the MOR value. Additionally, referring to the standard EN 622-5:2010, only pMDI-bonded samples achieved the required level in terms of MOR.

The IB was very low in each case and none of the samples came to the value set by the standard (Table 6.4.), as the minimum for general use is 0.65 N mm^{-2}. In addition, a large dispersion in values was found, especially for pMDI-bonded samples (Figure 6.4.), maybe due to the low homogeneity of the boards. Previous studies demonstrated the low

uniform distribution of the resin, by adding a fluorescent dye to the adhesive during the blending. This highlighted the non-uniform distribution of the adhesive onto the fibers surface. Indeed, during blending, fiber clusters were formed, and the adhesive was distributed over the surface of these clusters without penetrating into them. Other studies pointed to the same problem (Medved & Grudnik, 2021), concluding that it depends mainly on fiber shape and size, and the adhesive content. In view of the large dispersion of the IB values within the same sample, we decided to eliminate values too far from the mean for each group and perform the statistical analysis on a smaller amount of values. As shown in Figure 6.5., the dispersion of the values was still higher than in the self-bonded samples, but the values were more consistent and so was the statistical analysis, as can be concluded from the higher R-squared (Table 6.5.).

The low values obtained also for pMDI-bonded boards were in line with some works found in literature (Asafu-Adjaye et al., 2020). Overall, the samples showed the same tendency as the MOR, appearing highly dependent on the presence of the adhesive. Indeed, when comparing WF0, WFAD0, and AD0, no significant differences were found, as well as between groups WF4, WFAD4, and AD4. On the other hand, when comparing the same material formulation with and without the adhesive there was a strong significant difference between WF0 and WF4, and between WFAD0 and WFAD4. Conversely, the significant difference between groups AD0 and AD4 were weakly significant, being the p-value 0.03.

Certainly, further studies are needed to improve this property. Comparing these results with other studies found in literature (Fiorelli et al., 2019; Li et al., 2010; Okuda & Sato, 2004), an approach may be using longer pressing times. Indeed, the penetration of the heat of the press into the core layers is essential for a proper bonding and an increased pressure time makes the heat penetrate along the thickness. Other studies also showed the improvement in IB by adding ammonium lignosulphonate or kraft lignin (Hemmilä et al., 2019; Ostendorf et al., 2021; Velásquez et al., 2003), thus obtaining IB values above the threshold.

Table 6.5. *One-way ANOVA for mechanical results (MOE, MOR, and IB) considering the variation as six level factor.*

Factor	Property		D.f.	R-squared [%]	p-value
Variation	ρ	kg m^{-3}	5	35.01	$1.56 \cdot 10^{-9}$
	MOE	N mm^{-2}	5	79.46	$1.18 \cdot 10^{-5}$
	MOR	N mm^{-2}	5	73.26	0.0002
	IB (all)	N mm^{-2}	5	32.19	$1.58 \cdot 10^{-5}$
	IB	N mm^{-2}	5	77.43	$2.80 \cdot 10^{-8}$

Table 6.6. *Honestly significance difference HSD multiple comparison from one-way ANOVA for mechanical results (MOE, MOR, and IB) considering the variation as six level factor.*

fac variation	ρ kg m^{-3}	MOE N mm^{-2}	MOR N mm^{-2}	IB N mm^{-2}
	p-value HSD	p-value HSD	p-value HSD	p-value HSD
WF4-WF0	<0.0001	<0.0001	0.0013	<0.0001
WFAD0-WF0	0.0002	0.1119	0.9393	0.9999
AD0-WF0	<0.0001	0.0006	0.1325	0.8362
WFAD4-WF4	0.0011	0.4070	0.9999	0.9994
AD4-WF4	0.0002	0.1172	0.5347	0.2782
WFAD4-WFAD0	0.7153	0.0876	0.0044	<0.0001
AD0-WFAD0	0.9897	0.1622	0.5107	0.7568
AD4-WFAD4	0.9977	0.9671	0.4998	0.5272
AD4-AD0	0.1397	0.9975	0.9525	0.0334

Figure 6.1. *Boxplots of density for each of the variations considered.*

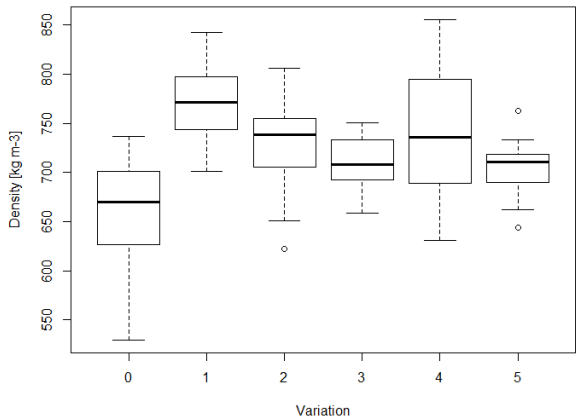

In the x-axis: 0=WF0; 1=WF4; 2=WFAD0; 3=WFAD4; 4=AD0; 5=AD4.

Figure 6.2. *Boxplots of modulus of elasticity MOE for each of the variations considered.*

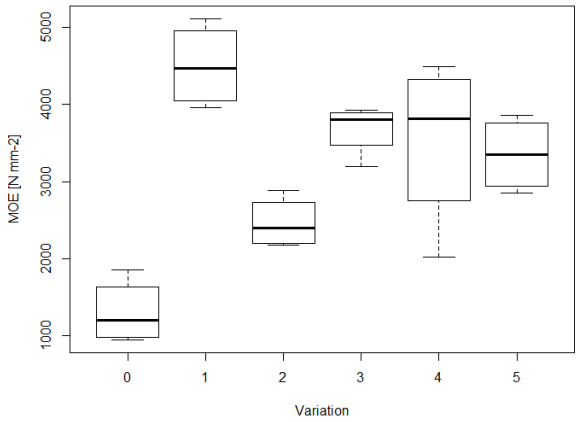

In the x-axis: 0=WF0; 1=WF4; 2=WFAD0; 3=WFAD4; 4=AD0; 5=AD4.

Figure 6.3. *Boxplots of modulus of rupture MOR for each of the variations considered.*

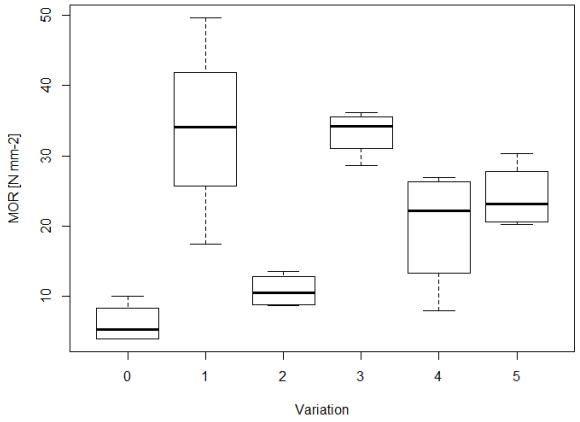

In the x-axis: 0=WF0; 1=WF4; 2=WFAD0; 3=WFAD4; 4=AD0; 5=AD4.

Figure 6.4. *Boxplots of all internal bond results IB for each of the variations considered.*

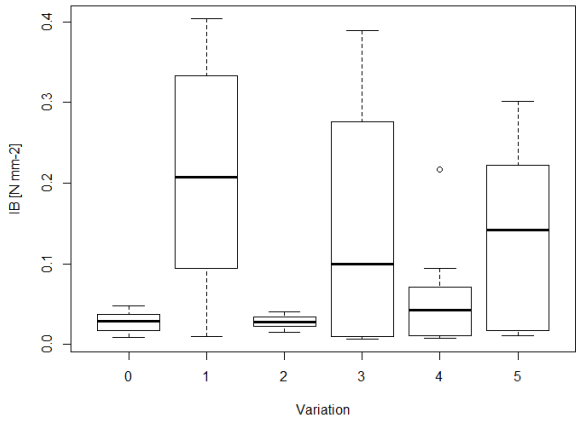

In the x-axis: 0=WF0; 1=WF4; 2=WFAD0; 3=WFAD4; 4=AD0; 5=AD4.

Figure 6.5. *Boxplots of internal bond results IB used for statistical analysis for each of the variations considered.*

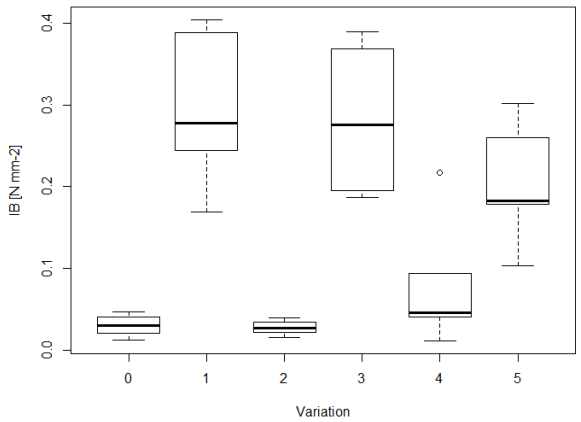

In the x-axis: 0=WF0; 1=WF4; 2=WFAD0; 3=WFAD4; 4=AD0; 5=AD4.

6.2.1.2. Dimensional stability

Thickness swelling (TS) and water absorption (WA) are critical parameters correlated with the dimensional stability, for which it is more difficult to achieve the requirements of the standards when using alternative materials and adhesives (Antov et al., 2021; Li et al., 2010; Syafiqaz et al., 2021; Wistara et al., 2018). Indeed, only version AD4

fulfilled the limit of TS at 24h for general and structural use in dry conditions (Table 6.7., and 6.8.), while for sample WF0 it was not even possible to measure the TS, since the specimens became completely detached after a few minutes of immersion.

Previous studies have proved (Kurokochi & Sato, 2020; Shu et al., 2019) that the STEX prior to the manufacturing of fiberboards has the great advantage of improving dimensional stability. The results obtained showed the improvement of TS and WA values in the samples made with 100% and 50% of steam exploded AD (Table 6.8.). Moreover, the AD as raw material, has a high percentage of lignin (19-24% lignin, 29-43% cellulose, 14-32% hemicellulose). In this way, the combination of AD and STEX is particularly beneficial for TS, since lignin is more hydrophobic than the polysaccharides (Kang et al., 2019).

More specifically, with the STEX pre-treatment, the primary components of the lignocellulosic material are separated, the highly hydrophilic hemicelluloses are mostly hydrolyzed and washed after the treatment, and the lignin is more evenly distributed over the cellulose structure, creating a hydrophobic layer (Kurokochi & Sato, 2020). For TS, as well as for WA, the lowest values at 24h were obtained for the sample AD4 and WFAD4, which were 11% and 16% for TS, and 25% and 33% for WA, respectively. Both TS and WA showed a clear decreasing trend when comparing within the group with pMDI, i.e., WF4, WFAD4, and AD4, as well as the group without pMDI, i.e., WFAD0, AD0 (Figure 6.6., and 6.7.). Although no numerical results are available for sample WF0, the fact that it detached indicates in any case that the addition of AD resulted in an improvement in dimensional stability, although not sufficient to achieve the standard.

The ANOVA results (Table 6.9.) show a high influence of the variation on the properties considered. Through the multiple comparison (Table 6.10.) the differences between the specific groups can be found, and thus whether the significance difference is due to fiber formulation or the presence of the adhesive.

As for TS, there was a significant difference between all groups, except AD4 and WFAD4. There was a clear improvement in swelling thanks to both the addition of AD and pMDI. Indeed, while in the comparison of samples with pMDI the differences were minor (only between WF4 and WFAD4 and with a p-value of 0.03), the difference between WFAD0 and AD0 was much more pronounced, where AD0 has an average value of TS at 24h comparable to WF4.

Table 6.7. *Thickness swelling TS and water absorption WA of tested specimens with different percentages of Arundo donax L., wood fibers, and pMDI, at 2h, 24h, and 48h.*

Series name	Specimen name	ρ kg m^{-3}	TS 2h %	WA 2h %	TS 24h %	WA 24h %	TS 48h %	WA 48h %
WF0	3-5	657	D	D	D	D	D	D
WF0	3-6	737	D	D	D	D	D	D
WF0	3-7	690	D	D	D	D	D	D
WF0	3-8	607	D	D	D	D	D	D
WF0	4-5	635	D	D	D	D	D	D
WF0	4-6	688	D	D	D	D	D	D
WF0	4-7	653	D	D	D	D	D	D
WF0	4-8	530	D	D	D	D	D	D
WF4	5-5	768	10	12	22	34	31	52
WF4	5-6	753	8	12	19	32	24	49
WF4	5-7	738	14	16	27	45	32	58
WF4	5-8	702	8	13	21	37	26	55
WF4	6-5	715	24	31	39	68	42	82
WF4	6-6	737	21	35	40	67	44	77
WF4	6-7	801	8	12	25	38	30	56
WF4	6-8	843	8	9	18	26	23	43
WFAD0	11-5	741	89	158	104	181	105	187
WFAD0	11-6	772	86	145	100	166	105	171
WFAD0	11-7	785	90	151	105	173	108	176
WFAD0	11-8	738	107	182	124	208	129	202
WFAD0	12-5	712	112	196	131	222	135	228
WFAD0	12-6	754	101	178	120	202	123	208
WFAD0	12-7	755	95	159	111	186	115	191
WFAD0	12-8	697	112	214	132	244	139	229
WFAD4	7-5	737	7	13	15	31	18	44
WFAD4	7-6	741	7	13	16	30	20	43
WFAD4	7-7	750	7	12	16	33	21	44
WFAD4	7-8	737	7	12	14	30	17	42
WFAD4	8-5	677	8	16	16	37	21	50
WFAD4	8-6	694	8	16	17	35	20	49
WFAD4	8-7	699	8	14	17	33	20	48
WFAD4	8-8	691	7	13	16	33	19	48
AD0	13-5	695	28	97	31	103	32	105
AD0	13-6	795	24	64	30	77	31	82
AD0	13-7	703	24	93	27	100	28	101
AD0	13-8	631	26	110	30	116	31	115
AD0	14-5	635	24	103	26	110	28	106
AD0	14-6	726	24	87	27	92	27	93
AD0	14-7	786	23	76	28	83	28	84
AD0	14-8	767	26	80	28	87	30	86
AD4	9-5	727	6	13	12	25	14	32
AD4	9-6	763	5	12	11	23	14	31
AD4	9-7	733	5	11	10	22	12	29
AD4	9-8	696	7	15	12	28	15	35
AD4	10-5	686	7	14	12	27	13	32
AD4	10-6	702	7	13	12	25	14	31
AD4	10-7	694	6	13	12	26	14	33
AD4	10-8	644	5	12	10	25	12	31

D = detached

Table 6.8. *Average thickness swelling TS and water absorption WA of tested specimens with different percentages of Arundo donax L., wood fibers, and pMDI., at 2h, 24h, and 48h, and the corresponding St.Dev.*

Series name	TS 2h %	St. Dev.	WA 2h %	St. Dev.	TS 24h %	St. Dev.	WA 24h %	St. Dev.	TS 48h %	St. Dev.	WA 48h %	St. Dev.
WF0	D	-	D	-	D	-	D	-	D	-	D	-
WF4	13	7	17	10	26	9	43	16	32	8	59	14
WFAD0	99	11	173	24	116	13	198	26	120	14	199	22
WFAD4	7	0	14	1	16	1	33	2	20	1	46	3
AD0	25	2	89	15	28	2	96	13	29	2	97	12
AD4	6	1	13	1	11	1	25	2	14	1	32	2

WA results were similar to TS, but there was no difference between the groups with pMDI, i.e., WF4, WFAD4, and AD4, while the TS at 24h of AD0 was about half of WFAD0, and comparable to WF4. Considering the AD0 sample, the anomalous finding was the mismatch between TS and WA: AD0 had a relatively high WA but a relatively low TS, which is not found in the pMDI-bonded samples. The main difference between self-bonded and pMDI-bonded samples was in the initial absorption and swelling (Figure 6.8.): pMDI-bonded boards absorbed water at a slower pace than self-bonded ones, for which the WA and TS at 2h and at 48h were almost the same. Although WF4 and AD0 samples achieved about the same value of TS at 24h, the AD0 sample showed a higher short-term absorption, suggesting that AD0 reached the equilibrium status of saturation in few hours. Indeed, AD0 had already reached its maximum value of TS after 2h. Thus, it remained approximately the same, while WF4 swelling kept increasing to 32% at 48h.

Table 6.9. *One-way ANOVA for thickness swelling TS and water absorption WA considering the variation as six level factor.*

Factor	Property		D.f.	R-squared [%]	p-value
Variation	TS	%	4	97.31	$<2\cdot10^{-16}$
	WA	%	4	95.46	$<2\cdot10^{-16}$

Table 6.10. *HSD multiple comparison from one-way ANOVA for thickness swelling TS and water absorption WA considering the variation as six level factor.*

fac variation	TS % p-value HSD	WA % p-value HSD
WF4-WF0	-	-
WFAD0-WF0	-	-
AD0-WF0	-	-
WFAD4-WF4	0.0307	0.6100
AD4-WF4	0.0009	0.1284
WFAD4-WFAD0	<0.0001	<0.0001
AD0-WFAD0	<0.0001	<0.0001
AD4-WFAD4	0.6967	0.8510
AD4-AD0	0.0002	<0.0001

Figure 6.6. *Boxplots of thickness swelling results TS for each of the variations considered.*

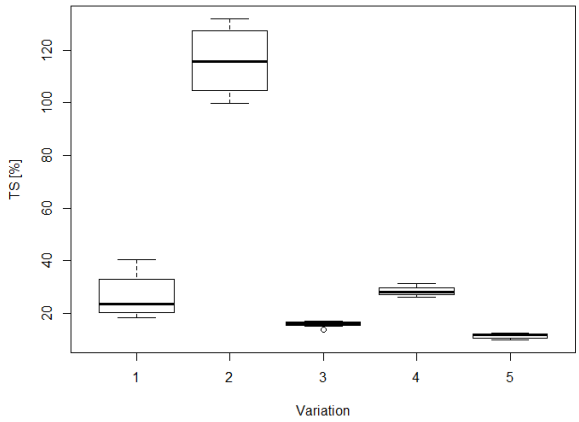

In the x-axis: 0=WF0; 1=WF4; 2=WFAD0; 3=WFAD4; 4=AD0; 5=AD4.

Figure 6.7. *Boxplots of water absorption results WA for each of the variations considered.*

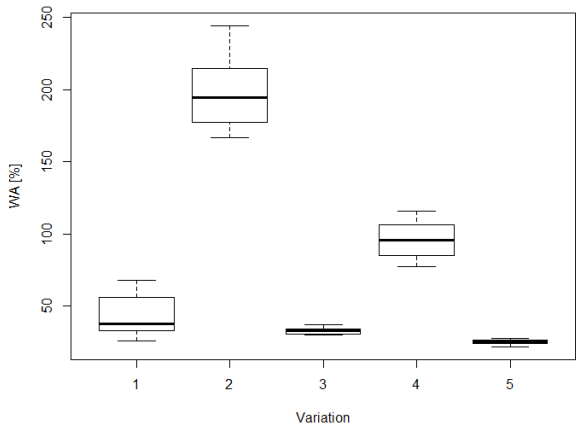

In the x-axis: 0=WF0; 1=WF4; 2=WFAD0; 3=WFAD4; 4=AD0; 5=AD4.

Figure 6.8. *Thickness swelling TS (a) and water absorption WA (b) increasing in 2h, 24h, and 48h of water immersion, for each of the variants considered.*

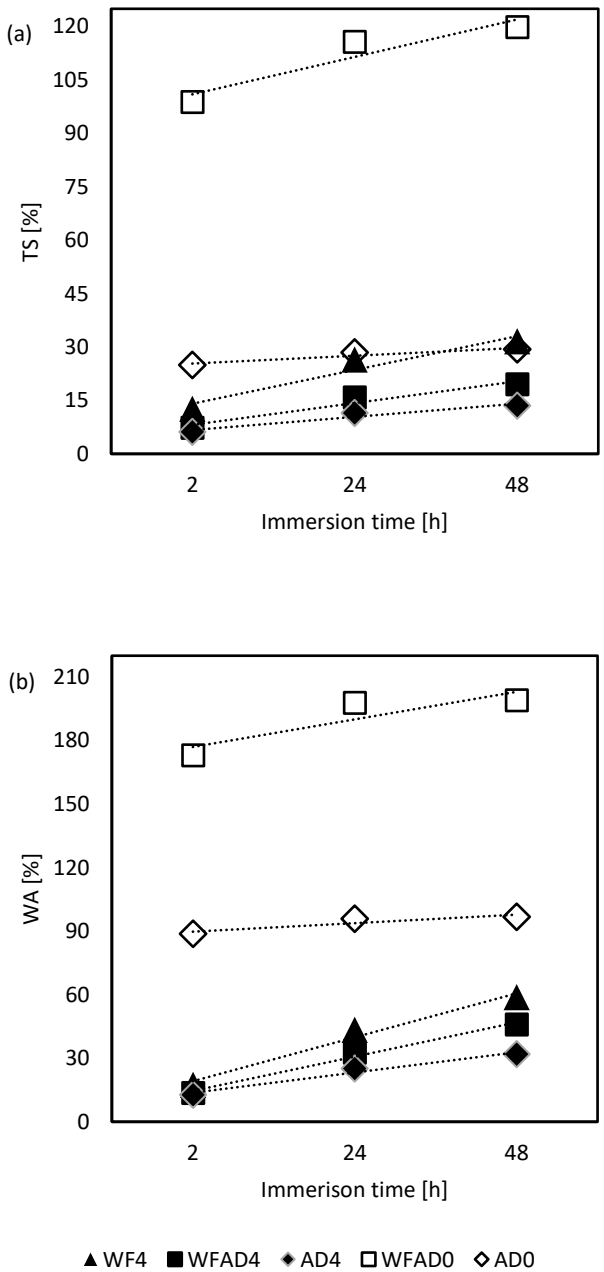

6.2.1.3. Vertical density profiles

Vertical Density profiles (VDP) shows density distribution along the thickness, and they were recorded to find out a correspondence between the densities and the mechanical parameters, especially MOR and IB. Indeed, the IB depends on the bonding of the core layer (Balea (Paul) et l., 2022; Halvarsson et al., 2008; Pham Van et al., 2021), the MOR and the MOE are mostly influenced by the strength of the face layers (Martins et al., 2021), although the MOE depends also on the material itself. A typical MDF density profile presents two peaks at the face layers where the density is the highest, while in the core layer the density drops to its lowest value (Balea (Paul) et al., 2022; Pham Van et al., 2021). This has been associated in other studies with the higher compaction in external regions due to the direct contact with the hot plates, as well as with smaller fiber size and higher resin content (Fiorelli et al., 2019).

Profiles were compared either by pairing the same fiber formulation with and without the adhesive (Figure 6.9.), and by grouping specimens with the adhesive and those without (Figure 6.10.). All samples showed the typical U-shape of MDF, except the WF0, for which the density was about the same along the thickness. This can partly explain the higher MOR of self-bonded boards made with a higher percentage of steam exploded AD, and shows the steam exploded AD gluing ability, activated by the heating during hot pressing (Mahieu et al., 2019). The sanding may have affected the shape of the VDP, especially in the WF0 sample. This may have altered the mechanical properties of WF0, which, after hot pressing, suffered a spring back of the thickness greater than the other samples. Indeed, the sanding probably removed the outermost layers, which are normally the denser ones (Pham Van et al., 2021), and also the ones related to MOE and MOR properties. However, sanding is a step that is normally used at the industrial level, and it is necessary to equalize the surfaces and thicknesses of the panels that will be sold on the market. Thus, considering that the temperature and pressure time were the same for all samples, these results may be due to the steam exploded AD which limited the spring back after pressing, and thus enhanced a better bonding. There may be several reasons for this, among them: the increased presence of fine particles in the exploded material, and the agglomerating effect of lignin distributed on the fiber surface due to the STEX.

The density of self-bonded boards was for each sample, and in every position, lower than pMDI-bonded boards (Figure 6.9. (a), (b), and (c)), a result that can be easily connected with mechanical performance:

both MOR and IB were higher for pMDI-bonded boards, as pMDI led to a better cohesion of the fibers.

Comparing the different formulations with and without adhesive, there was also a match in mechanical properties: the specimens that showed a better profile were WF4 and AD0, which were those that, within their own group, pMDI-bonded and self-bonded respectively, showed the best mechanical performance.

Figure 6.9. *Vertical density profiles of samples WF4-WF0 (a), WFAD4-WFAD0 (b), and AD4-AD0 (c).*

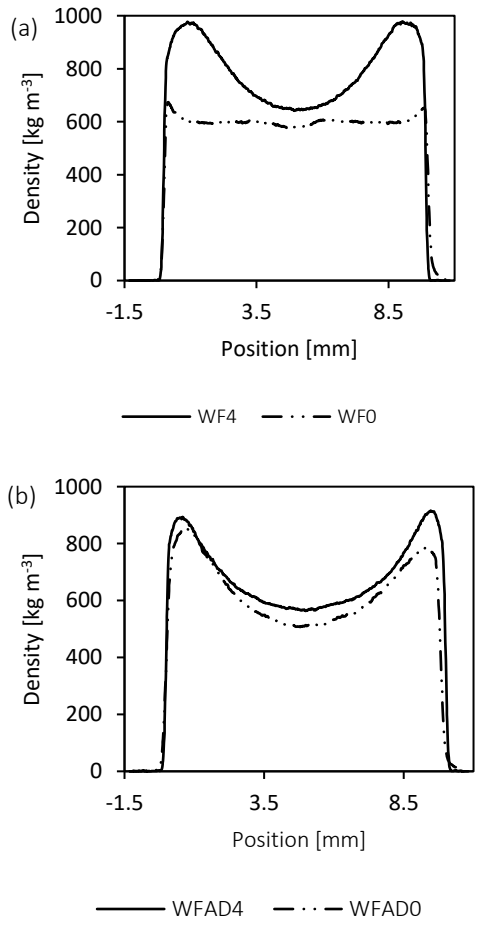

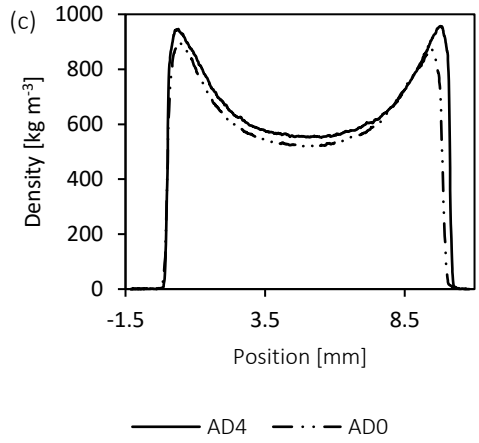

Figure 6.10. *Vertical density profiles of samples with adhesive WF4-WFAD4-AD4 (a), and samples without adhesive WF0-WFAD0-AD0 (b).*

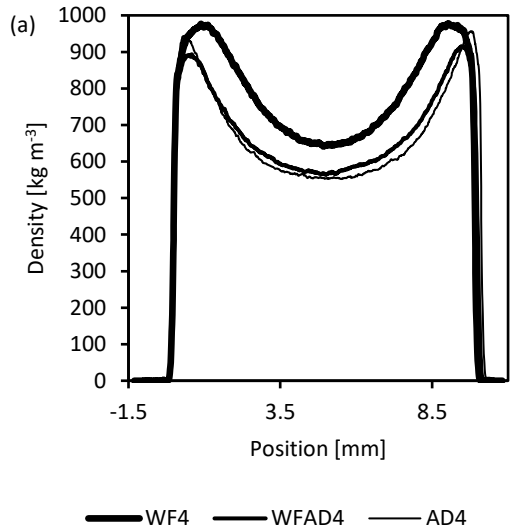

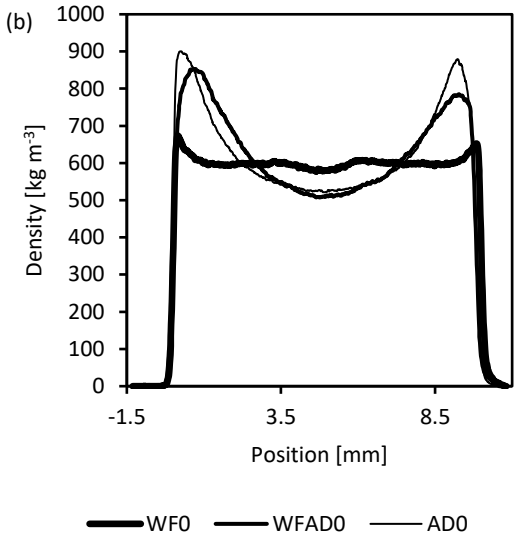

6.2.2. Second series: self-bonded boards

6.2.2.1. Density and mechanical properties

For the second series, exclusively self-bonded panels were manufactured, mixing the wood fibers with the exploded AD here too, but starting from a minimum percentage of AD of 60wt%, and increasing the pressing time (tp) to double compared to the previous series, i.e., 30 s mm^{-1}.

The mean density of the samples ranged from 617 to 667 kg m^{-3}. Compared to the self-bonded boards of the first series, in this case the densities were much lower on average, a result probably due to the larger size of the specimens in this second series, i.e. 450x450x10.5 mm. Indeed, looking at all the results of the specimens (Table 6.11.), there is a greater dispersion in the density values, which in some cases were far away from the target density set at 780 kg m^{-3}, and thus lowering the average (Table 6.12.), due to the greater difficulty in achieving a uniform fiber distribution in a larger mold.

The highest density was obtained for sample AD100, while the sample containing the lower percentage of AD was the one showing the lowest density. As in the previous sections, the increasing in the percentage of AD led to an increasing in the mean density (Figure 6.11.). However, the effect of the non-uniformity of the panels on the density is very large, and the increase in pressing time does not generate any improvement compared to the first series.

Table 6.11. *Density and mechanical results (MOE, MOR, and IB) of tested specimens with different percentages of Arundo donax L., and wood fibers.*

Series name	Specimen name	ρ kg m^{-3}	MOE N mm^{-2}	MOR N mm^{-2}	IB* N mm^{-2}
WFAD40/60	4-1	616	998	3.1	-
WFAD40/60	4-2	592	927	4.0	-
WFAD40/60	4-3	585	899	3.6	-
WFAD40/60	4-4	550	615	2.8	-
WFAD40/60	7-1	688	1247	5.3	-
WFAD40/60	7-2	643	1252	5.8	-
WFAD40/60	7-3	689	1548	6.3	-
WFAD40/60	7-4	641	977	3.5	-
WFAD40/60	4-4	566	-	-	0.011
WFAD40/60	4-7	531	-	-	**0.007**
WFAD40/60	4-8	587	-	-	0.013
WFAD40/60	4-9	657	-	-	0.039
WFAD40/60	4-10	635	-	-	0.021
WFAD40/60	4-11	595	-	-	0.017
WFAD40/60	4-13	554	-	-	0.014
WFAD40/60	4-14	510	-	-	**0.008**
WFAD40/60	7-1	684	-	-	0.013
WFAD40/60	7-2	697	-	-	0.016
WFAD40/60	7-3	715	-	-	0.058
WFAD40/60	7-4	676	-	-	0.014
WFAD40/60	7-5	669	-	-	0.016
WFAD40/60	7-14	636	-	-	0.011
WFAD40/60	7-15	581	-	-	**0.007**
WFAD40/60	7-16	625	-	-	0.020
WFAD20/80	1-1	515	752	1.6	-
WFAD20/80	1-2	583	836	4.2	-
WFAD20/80	1-3	656	1338	6.3	-
WFAD20/80	1-4	746	2546	11.7	-
WFAD20/80	5-1	653	1542	4.5	-
WFAD20/80	5-2	654	1234	4.6	-
WFAD20/80	5-3	617	1177	4.6	-
WFAD20/80	5-4	625	1002	3.2	-
WFAD20/80	1-5	491	-	-	0.012
WFAD20/80	1-7	550	-	-	**0.008**
WFAD20/80	1-8	557	-	-	**0.009**
WFAD20/80	1-11	625	-	-	0.018
WFAD20/80	1-12	586	-	-	0.018
WFAD20/80	1-18	756	-	-	0.060
WFAD20/80	1-20	829	-	-	0.082
WFAD20/80	1-21	699	-	-	0.017
WFAD20/80	5-4	640	-	-	0.016
WFAD20/80	5-5	719	-	-	0.033
WFAD20/80	5-6	703	-	-	0.019
WFAD20/80	5-7	602	-	-	0.025
WFAD20/80	5-8	674	-	-	0.013
WFAD20/80	5-9	582	-	-	**0.009**
WFAD20/80	5-10	548	-	-	0.018
WFAD20/80	5-11	588	-	-	0.024

Series name	Specimen name	ρ kg m^{-3}	MOE N mm^{-2}	MOR N mm^{-2}	IB* N mm^{-2}
AD100	2-1	609	951	3.7	-
AD100	2-2	606	1056	3.8	-
AD100	2-3	620	1273	6.3	-
AD100	2-4	574	875	3.5	-
AD100	6-1	653	1805	7.2	-
AD100	6-2	741	2804	11.5	-
AD100	6-3	709	2552	13.0	-
AD100	6-4	748	2505	14.1	-
AD100	2-1	575	-	-	**0.024**
AD100	2-3	662	-	-	0.092
AD100	2-5	683	-	-	0.097
AD100	2-6	622	-	-	0.051
AD100	2-8	576	-	-	0.065
AD100	2-12	823	-	-	0.097
AD100	2-15	495	-	-	**0.021**
AD100	2-16	530	-	-	**0.019**
AD100	6-5	747	-	-	0.083
AD100	6-12	700	-	-	0.087
AD100	6-13	674	-	-	0.047
AD100	6-15	674	-	-	0.103
AD100	6-16	833	-	-	0.102
AD100	6-17	779	-	-	0.060
AD100	6-18	760	-	-	0.108
AD100	6-21	599	-	-	**0.025**

**Values in bold for IB are those removed to perform the statistical analysis.*

Table 6.12. *Average mechanical results (MOE, MOR, and IB) of tested specimens with different percentages of Arundo donax L., and wood fibers, and the corresponding St.Dev.*

Series name	ρ kg m^{-3}	St. Dev.	MOE N mm^{-2}	St. Dev.	MOR N mm^{-2}	St. Dev.	IB (all) N mm^{-2}	St. Dev.	IB N mm^{-2}	St. Dev.
WFAD40/60	617	56	1058	283	4.3	1.3	0.018	0.013	0.020	0.014
WFAD20/80	627	80	1303	565	5.1	3.0	0.024	0.020	0.027	0.021
AD100	667	84	1728	796	7.9	4.4	0.068	0.033	0.083	0.021

The statistical analysis showed a significant p-value (Table 6.13.), and a significant difference only between the specimens with 60% AD and with 100% AD (Table 6.14.). Nevertheless, the R-squared was very low, the lowest found until now, and in every sample, regardless of the percentage of AD, there were values ranging from less than 500 kg m^{-3} to more than 800 kg m^{-3}.

The R-squared was low also for MOE and MOR. The effect of the AD percentage was slightly significant only for MOE (Table 6.13.), being the p-value 0.03, but with no differences between the various percentages (Table 6.14.). In general, both MOE and MOR increased slightly as the percentage of AD increases (Figures 6.12., and Figure 6.13., respectively). Again, the variation of the values within each sample was high, especially for the AD100 sample. Therefore, the main problem was the uniform distribution of fibers in the mold at the time of pressing the

panel, a problem that stemmed from the industrial sizes made in this series and that was not faced with laboratory-sized specimens.

As for IB (Figure 6.14., and 6.15.), the R-squared was slightly higher and increased further by removing outliers from the mean. In this case, the effect of AD percentage was very significant (Table 6.13.). The groups with 60% and 80% of AD did not differ from each other (Table 6.14.). On the other hand, AD100 had a higher mean IB value than the other groups, thus latter differing significantly from both others. As the first series, the results obtained for IB needs to be improved: they are almost identical to those obtained for the self-bonded boards in the first series, which means that the increase in tp did not have the desired effect, and that, to obtain improvements, tp must be further increased.

As a result, beyond the trends in density and each of the mechanical properties, the main problem faced was the difficulty in the uniform distribution of the material when increasing the size of the panels to the industrial level. Indeed, this resulted in large variations in the values of the mechanical properties, thus lowering the overall average. Future studies must therefore focus on this problem to try to bring the laboratory level closer to the industrial one.

Table 6.13. *One-way ANOVA for mechanical results (MOE, MOR, and IB) considering the Arundo donax L. percentage (%AD) as three level factor.*

Factor	Property		D.f.	R-squared [%]	p-value
%AD	ρ	kg m^{-3}	2	8.02	0.0075
	MOE	N mm^{-2}	2	20.25	0.0296
	MOR	N mm^{-2}	2	21.42	0.0796
	IB	N mm^{-2}	2	69.99	7.11·10^{-10}

Table 6.14. *HSD multiple comparison from one-way ANOVA for mechanical results (MOE, MOR, and IB) considering the Arundo donax L. percentage (%AD) as three level factor.*

fac %AD	ρ kg m^{-3}	MOE N mm^{-2}	MOR N mm^{-2}	IB N mm^{-2}
	p-value HSD	p-value HSD	p-value HSD	p-value HSD
80-60	0.8092	0.6851	0.8744	0.6136
100-60	0.0086	0.0806	0.0818	<0.0001
100-80	0.0465	0.3365	0.2007	<0.0001

Figure 6.11. *Boxplots of density for each of the variations considered.*

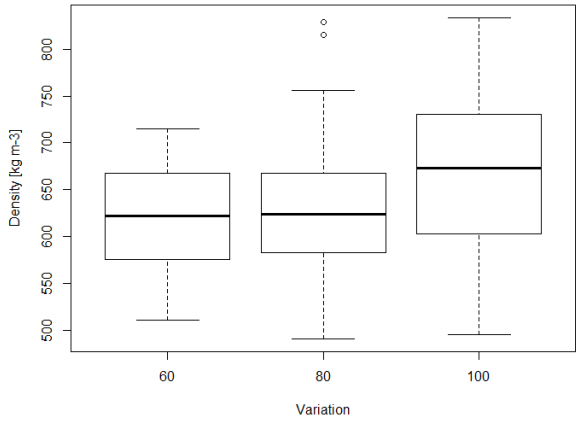

In the x-axis the percentage of steam exploded Arundo donax L. is reported. The corresponding variations are: 60 = WFAD40/60, 80 = WFAD20/80, and 100 = AD100.

Figure 6.12. *Boxplots of modulus of elasticity MOE for each of the variations considered.*

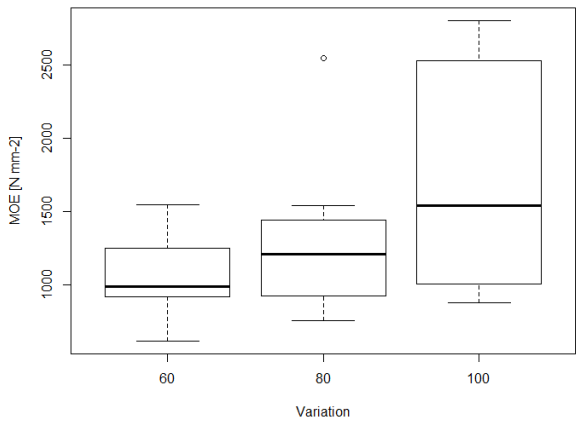

In the x-axis the percentage of steam exploded Arundo donax L. is reported. The corresponding variations are: 60 = WFAD40/60, 80 = WFAD20/80, and 100 = AD100.

Figure 6.13. *Boxplots of modulus of rupture MOR for each of the variations considered.*

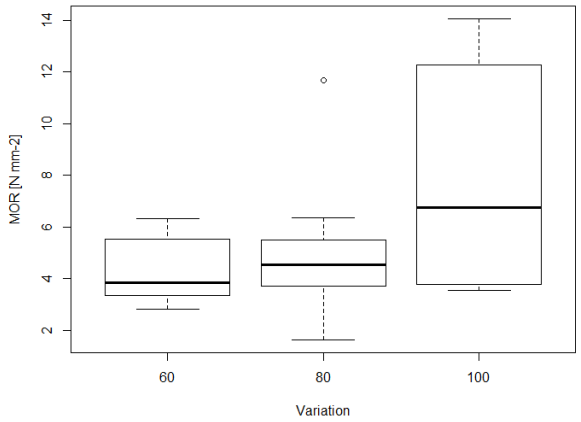

In the x-axis the percentage of steam exploded Arundo donax L. is reported. The corresponding variations are: 60 = WFAD40/60, 80 = WFAD20/80, and 100 = AD100.

Figure 6.14. *Boxplots of all internal bond results IB for each of the variations considered.*

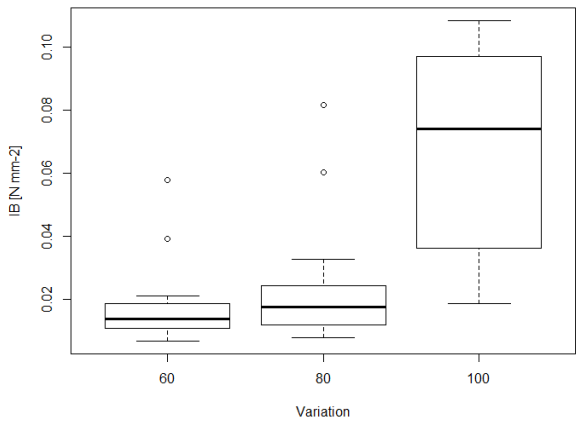

In the x-axis the percentage of steam exploded Arundo donax L. is reported. The corresponding variations are: 60 = WFAD40/60, 80 = WFAD20/80, and 100 = AD100.

Figure 6.15. *Boxplots of internal bond results IB used for statistical analysis for each of the variations considered.*

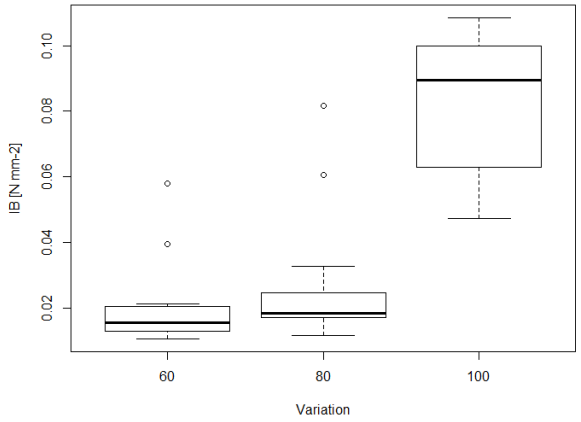

In the x-axis the percentage of steam exploded Arundo donax L. is reported. The corresponding variations are: 60 = WFAD40/60, 80 = WFAD20/80, and 100 = AD100.

6.2.2.2. Dimensional stability

The results obtained for dimensional stability, although not achieving the standard, confirmed the improving effect due to AD treatment (Table 6.15., and 6.16.).

Considering the values at 24h, the TS is almost halved between samples WFAD40/60 and WFAD20/80, and further reduced for AD100 (Figure 6.16.). Statistical analysis validated the great influence of the percentage of exploded AD on TS (Table 6.17.), and a significant difference between all percentages considered (Table 6.18.). In this case the dispersion of the values is very small, and the standard deviation is low, especially for the higher percentages of AD. This is probably related to a lower influence of the density on the dimensional stability, as well as to the great waterproofing effect that the STEX gave to the material, already outlined in the previously (Subsection 6.2.1.2.).

WA also improved by increasing the exploded AD percentage (Figure 6.17.), and statistically, the influence of the AD percentage was even higher that for TS (Table 6.17.), with a significant difference between all the percentages considered (Table 6.18.). As found previously, here too the mismatch between TS and WA was confirmed, and to a relatively low TS corresponded a relatively high WA, especially for WFAD20/80 and AD100. Again, the WA showed the same linear pattern and high short-term sorption as the self-bonded boards of the first series (Figure

6.18.). Compared to the first series, the panels made with 100% exploded AD were slightly higher, and this could be an effect of the lower density obtained for the second series.

As a result, the effect of the STEX on the dimensional stability is high, but the increasing in tp did not produce any beneficial effect when comparing with the first series, perhaps also due to the different size of the specimens. Further improvements in dimensional stability could be achieved by further increasing the tp or, based on the findings of Chapter 4, by applying a final heat treatment.

Table 6.15. *Thickness swelling TS and water absorption WA of tested specimens with different percentages of Arundo donax L., and wood fibers, at 2h, 24h, and 72h.*

Series name	Specimen name	ρ	TS 2h	WA 2h	TS 24h	WA 24h	TS 72h	WA 72h
		kg m^{-3}	%	%	%	%	%	%
WFAD40/60	4-12	579	98	273	113	307	117	314
WFAD40/60	4-15	553	104	320	124	361	130	372
WFAD40/60	4-16	582	97	278	116	314	123	328
WFAD40/60	4-17	619	88	234	102	267	107	275
WFAD40/60	4-18	571	88	269	100	303	109	317
WFAD40/60	4-19	560	97	295	114	333	115	346
WFAD40/60	4-20	523	96	323	109	360	118	376
WFAD40/60	4-21	526	108	358	127	399	133	419
WFAD40/60	7-8	630	72	197	89	227	94	230
WFAD40/60	7-9	666	66	173	81	200	87	207
WFAD40/60	7-10	697	68	164	82	192	87	199
WFAD40/60	7-11	685	62	161	76	184	80	188
WFAD40/60	7-12	677	61	160	74	185	81	192
WFAD40/60	7-17	611	74	222	90	256	94	257
WFAD40/60	7-18	640	73	190	89	218	92	218
WFAD40/60	7-21	645	76	211	92	239	98	243
WFAD20/80	1-1	533	50	184	61	210	67	218
WFAD20/80	1-2	523	45	186	54	209	59	221
WFAD20/80	1-3	525	41	179	52	201	54	210
WFAD20/80	1-4	508	45	195	55	207	59	213
WFAD20/80	1-15	624	53	160	64	177	69	188
WFAD20/80	1-16	677	47	128	56	152	60	160
WFAD20/80	1-17	731	46	109	54	123	59	131
WFAD20/80	1-19	815	43	92	53	105	62	117
WFAD20/80	5-12	661	41	130	50	146	53	155
WFAD20/80	5-13	607	39	143	48	162	51	171
WFAD20/80	5-16	641	42	139	50	157	54	165
WFAD20/80	5-17	609	39	148	49	164	51	173
WFAD20/80	5-18	587	42	155	50	174	55	183
WFAD20/80	5-19	594	39	150	48	168	52	178
WFAD20/80	5-20	624	36	137	46	151	48	162
WFAD20/80	5-21	642	44	145	54	159	58	170

Series name	Specimen name	ρ kg m^{-3}	TS 2h %	WA 2h %	TS 24h %	WA 24h %	TS 72h %	WA 72h %
AD100	2-4	632	31	117	35	133	37	138
AD100	2-10	662	29	105	34	119	34	125
AD100	2-11	697	28	99	33	109	34	114
AD100	2-13	669	31	108	36	119	39	126
AD100	2-18	546	27	141	31	154	34	161
AD100	2-19	583	27	133	32	143	34	150
AD100	2-20	587	28	135	33	146	35	154
AD100	2-21	536	32	163	35	172	38	181
AD100	6-2	689	28	99	33	110	35	114
AD100	6-6	673	24	96	30	110	33	115
AD100	6-7	683	31	95	36	113	39	119
AD100	6-8	679	26	101	31	111	33	117
AD100	6-10	775	25	75	28	85	31	91
AD100	6-11	767	23	75	29	84	30	89
AD100	6-19	805	24	68	30	79	30	83
AD100	6-20	721	29	90	36	101	36	106

Table 6.16. *Average thickness swelling TS and water absorption WA of tested specimens with different percentages of Arundo donax L., and wood fibers, at 2h, 24h, and 72h, and the corresponding St.Dev.*

Series name	TS 2h %	St. Dev. %	WA 2h %	St. Dev. %	TS 24h %	St. Dev. %	WA 24h %	St. Dev. %	TS 72h %	St. Dev. %	WA 72h %	St. Dev. %
WFAD40/60	83	64	239	64	99	17	271	70	104	17	280	74
WFAD20/80	43	4	149	28	53	5	166	30	57	6	176	30
AD100	28	3	106	26	33	3	118	26	34	3	124	27

Table 6.17. *One-way ANOVA for thickness swelling TS and water absorption WA considering the percentage of Arundo donax L. (%AD) as three level factor.*

Factor	Property		D.f.	R-squared [%]	p-value
%AD	TS	%	2	67.14	$1.34 \cdot 10^{-11}$
	WA	%	2	88.37	$<2 \cdot 10^{-16}$

Table 6.18. *HSD multiple comparison from one-way ANOVA for thickness swelling TS and water absorption WA considering the percentage of Arundo donax L. (%AD) as three level factor.*

fac %AD	TS % p-value HSD	WA % p-value HSD
80-60	<0.0001	<0.0001
100-60	<0.0001	<0.0001
100-80	0.0132	<0.0001

Figure 6.16. *Boxplots of thickness swelling results TS for each of the variations considered.*

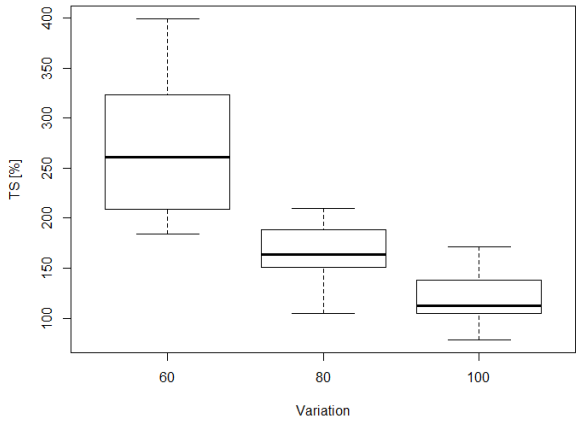

In the x-axis the percentage of steam exploded Arundo donax L. is reported. The corresponding variations are: 60 = WFAD40/60, 80 = WFAD20/80, and 100 = AD100.

Figure 6.17. *Boxplots of water absorption results WA for each of the variations considered.*

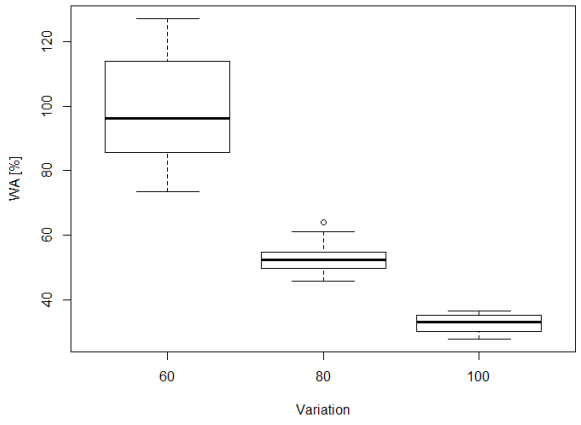

In the x-axis the percentage of steam exploded Arundo donax L. is reported. The corresponding variations are: 60 = WFAD40/60, 80 = WFAD20/80, and 100 = AD100.

Figure 6.18. *Thickness swelling TS (a) and water absorption WA (b) increasing in 2h, 24h, and 72h of water immersion, for each of the variants considered, compared with self-bonded boards of the first series.*

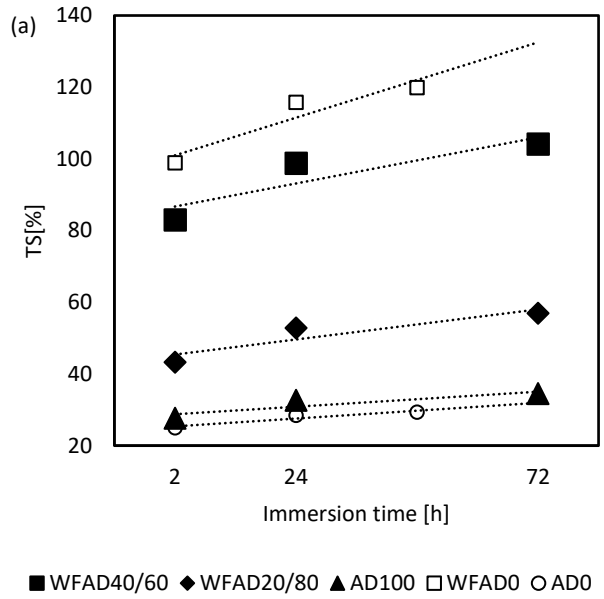

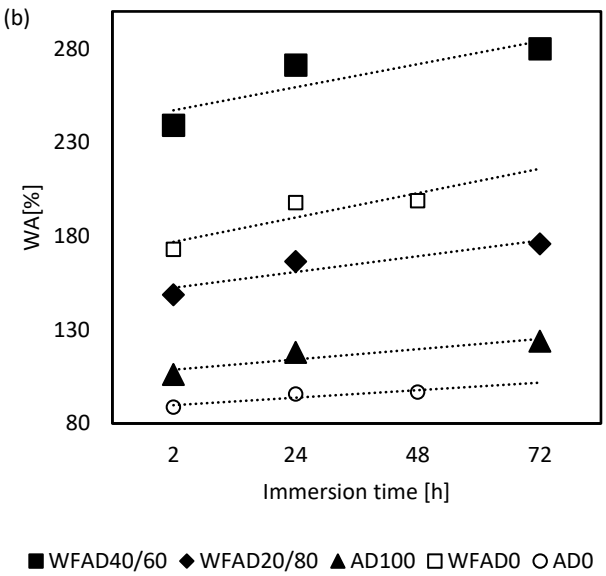

6.2.2.3. Vertical density profiles

VDP were recorded for several specimens of each variation, chosen depending on the density. Figure 6.19. reports the density profiles of the specimen with the maximum and minimum density of each sample, while the densities of the samples are reported in Table 6.19, with the corresponding IB, which was the property tested on these specimens.

Profiles highlight how within the same panel the density was very different. In addition, for the higher density profiles, the typical U-shape was much more evident, while for the lower density profiles, this was almost constant along the thickness. The greatest inhomogeneity in the results was obtained for the specimens containing AD, probably due to the inhomogeneity of the material itself. This inhomogeneity, as mentioned, affects the final average result especially of mechanical properties, including IB (Table 6.19).

As a result, once again, the optimization of results must start from working on the final homogeneity of the boards to avoid large differences in the properties of the same panel.

Table 6.19. *Density and internal bond of the specimens used for recording the vertical density profiles.*

Series name	Specimen number	ρ kg m^{-3}	IB N mm^{-2}
WFAD40/60	4-9	657	0.039
	4-14	510	0.008
WFAD20/80	1-20	829	0.081
	1-5	491	0.012
AD100	2.12	829	0.097
	2-15	495	0.021

6.4. Conclusions

The results presented in this Chapter, both from first and second series, represent a first exploration both in terms of the material used and the method. The performance obtained did not reach the expected standard, but it can be considered as a starting point to identify the critical points for further optimization.

One of the critical point for both series is identified in the low homogeneity of the panels, due to the strain in evenly distributing the material with laboratory tools over a larger panel area than the specimens made for the series of the other chapters, and explored here for the first time. Indeed, the low homogeneity of the specimens results in a high standard deviation, especially for mechanical properties, and, consequently, unclear interpretation of the results obtained. This is

particularly evident when comparing the two series: although the second series was made with twice the pressure time of the first, this did not produce any improvement in performance, probably because of the larger size of the panels, and thus even less homogeneity.

Regardless of the lower performance than the standard, a result from the first series is that the combination of exploded AD with pMDI does not produce the same effect as the combination of WF with pMDI: WF are much more compatible with this type of adhesive than AD. Indeed, when comparing WF0 and WF4 he differences are much higher in both mechanical properties and dimensional stability. On the other hand, for AD0 and AD4 there is only a small difference in IB, for mechanical properties, while the differences are high for dimensional stability, as the synthetic adhesive has better hydrophobic properties.

In any case, for both the first series and the second series, increasing the percentage of AD improves the behavior against water. However, even the use of 100% AD did not lead to results that meet the standard, and for this reason further improvements, both in mechanical properties and dimensional stability, must be sought in the manufacturing process.

Given that homogeneous material distribution can be more easily reached at industrial level, the improvement of properties can be achieved by further increasing the pressing time on the one hand, and by increasing the target density on the other hand. The first approach would give more time for the heat to penetrate along the thickness, thus improving the IB, while the second would produce an improvement of the other mechanical properties. Furthermore, in Chapter 5, it was already observed that the specimens with the best properties were manufactured with a thickness of 3 mm, against the other two thicknesses studied (i.e., 6 mm and 9 mm). Consequently, lowering the thickness would produce an improvement in the properties, but at the same time limiting the production to specific geometric characteristics.

To conclude, in the previous chapters it was shown that the FHT has an enormous positive effect on the dimensional stability, halving the values of TS and WA. Hence, a further approach to improve the water uptake could be to repeat the series including this step.

Figure 6.19. *Vertical density profiles of samples WFAD40/60 (a), WFAD20/80 (b), and AD100 (c), comparing the maximum and minimum density obtained for each sample.*

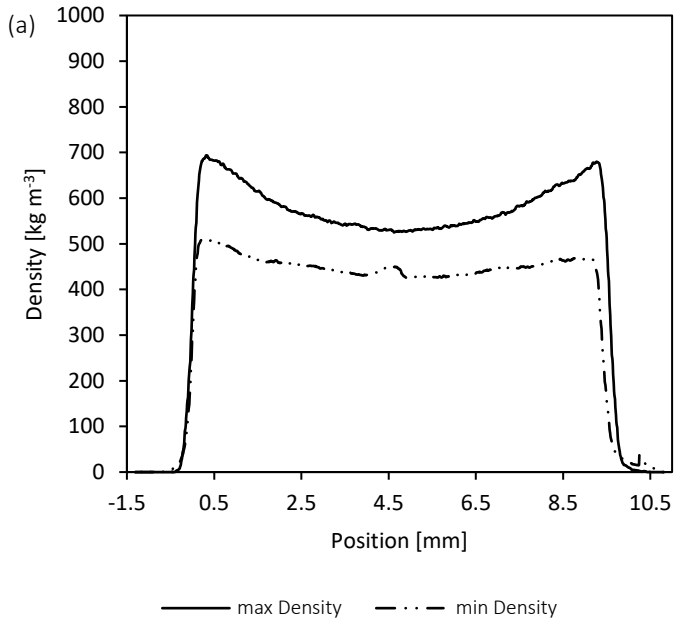

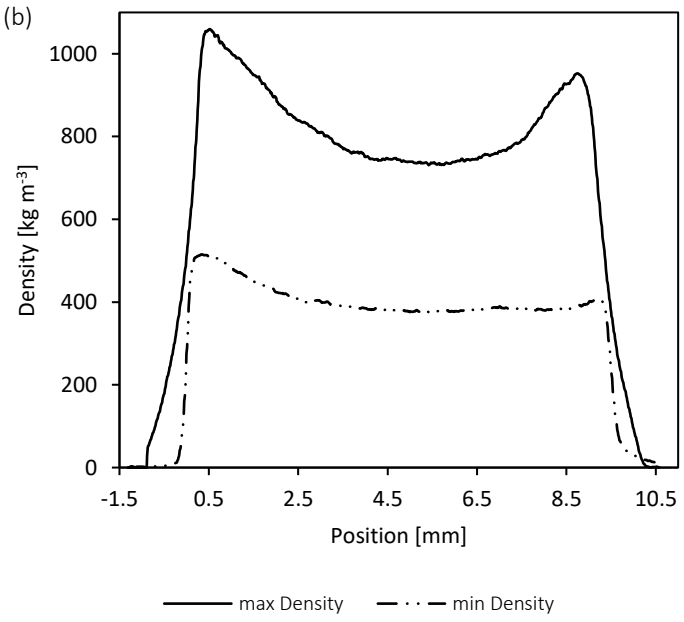

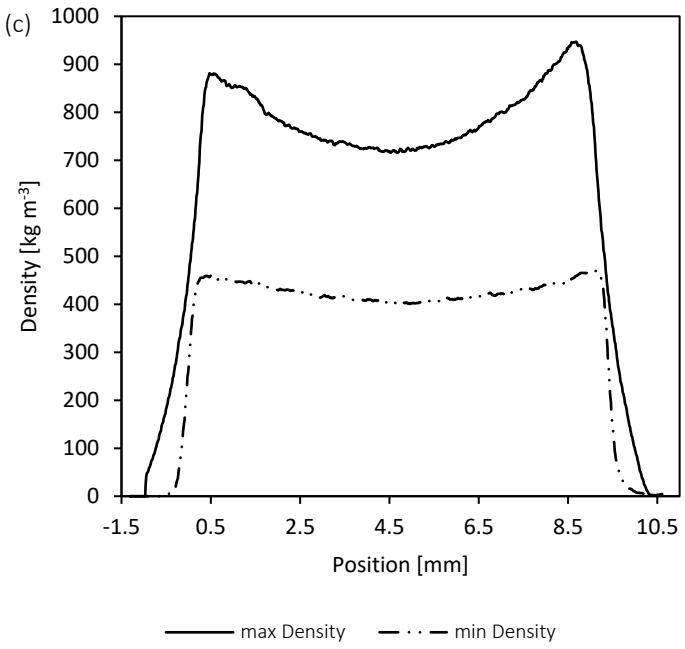

References

Antov, P., Krišťák, L., Réh, R., Savov, V., & Papadopoulos, A. N. (2021). Eco-friendly fiberboard panels from recycled fibers bonded with calcium lignosulfonate. *Polymers*, 13(4), 1–14. https://doi.org/10.3390/polym13040639

Asafu-Adjaye, O., Via, B., & Banerjee, S. (2020). Soy flour substitution in polymeric methylene diphenyl diisocyanate resin for composite panel applications. *Forest Products Journal*, 70(3), 350–355. https://doi.org/10.13073/FPJ-D-20-00014

Balea (Paul), G., Lunguleasa, A., Zeleniuc, O., & Coşereanu, C. (2022). Three adhesive recipes based on magnesium lignosulfonate, used to manufacture particleboards with low formaldehyde emissions and good mechanical properties. *Forests*, 13(5), 737. https://doi.org/10.3390/f13050737

Bekhta, P., Noshchenko, G., Réh, R., Kristak, L., Sedliačik, J., Antov, P., Mirski, R., & Savov, V. (2021). Properties of eco-friendly particleboards bonded with lignosulfonate-urea-formaldehyde adhesives and PMDI as a crosslinker. *Materials*, 14(17), 4875. https://doi.org/10.3390/ma14174875

Buschmann, B., Henke, K., Talke, D., Saile, B., Asshoff, C., & Bunzel, F. (2021). Additive manufacturing of wood composite panels for individual layer fabrication (Ilf). *Polymers*, 13(19), 3423. https://doi.org/10.3390/polym13193423

Domínguez-Robles, J., Tarrés, Q., Alcalà, M., el Mansouri, N.-E., Rodríguez, A., Mutjé, P., & Delgado-Aguilar, M. (2020). Development of high-performance binderless fiberboards from wheat straw residue. *Construction and Building Materials*, 232, 117247. https://doi.org/10.1016/j.conbuildmat.2019.117247

Fiorelli, J., Bonilla Bueno, S., & Cabral, R. (2019). Assessment of multilayer particleboards produced with green coconut and sugarcane bagasse fibers. *Construction and Building Materials* , 205, 1–9. https://doi.org/10.1016/j.conbuildmat.2019.02.024

Halvarsson, S., Edlund, H., & Norgren, M. (2008). Manufacture of non-resin wheat straw fibreboards. *Industrial Crops and Products*, 29, 437–445. https://doi.org/10.1016/j.indcrop.2008.08.007

Hemmilä, V., Adamopoulos, S., Hosseinpourpia, R., & Ahmed, S. A. (2019). Ammonium lignosulfonate adhesives for particleboards with pMDI and furfuryl alcohol as crosslinkers. *Polymers*, 11(10). https://doi.org/10.3390/polym11101633

Hidayat, W., Aprilliana, N., Asmara, S., Bakri, S., Hidayati, S., Banuwa, I. S., Lubis, M. A. R., & Iswanto, A. H. (2022). Performance of eco-friendly particleboard from agro-industrial residues bonded with formaldehyde-free natural rubber latex adhesive for interior applications. *Polymer Composites*, 43(4), 2222–2233. https://doi.org/10.1002/PC.26535

Kang, X., Kirui, A., Dickwella Widanage, M. C., Mentink-Vigier, F., Cosgrove, D. J., & Wang, T. (2019). Lignin-polysaccharide interactions in plant secondary cell walls revealed by solid-state NMR. *Nature Communications*, 10(1), 347. https://doi.org/10.1038/s41467-018-08252-0

Kurokochi, Y., & Sato, M. (2020). Steam treatment to enhance rice straw binderless board focusing hemicellulose and cellulose decomposition products. *Journal of Wood Science*, 66(1), 1–8. https://doi.org/10.1186/s10086-020-1855-8

Li, X., Cai, Z., Winandy, J. E., & Basta, A. H. (2010). Selected properties of particleboard panels manufactured from rice straws of different geometries. *Bioresource Technology*, 101, 4662–4666. https://doi.org/10.1016/j.biortech.2010.01.053

Luo, P., Yang, C., Li, M., & Wang, Y. (2020). Manufacture of thin rice straw particleboards bonded with various Polymeric methane diphenyl diisocyanate/urea formaldehyde resin mixtures. *BioResources*, 15(1), 935–944.

Mahieu, A., Alix, S., & Leblanc, N. (2019). Properties of particleboards made of agricultural by-products with a classical binder or self-bound. *Industrial Crops and Products*, 130, 371 – 379. https://doi.org/10.1016/j.indcrop.2018.12.094

Martins, R. S. F., Gonçalves, F. G., Segundinho, P. G. de A., Lelis, R. C. C., Paes, J. B., Lopez, Y. M., Chaves, I. L. S., & Oliveira, R. G. E. de. (2021). Investigation of agro-industrial lignocellulosic wastes in fabrication of particleboard for construction use. *Journal of Building Engineering*, 43, 102903. https://doi.org/10.1016/j.jobe.2021.102903

Medved, S., & Grudnik, J. (2021). Influence of resin content on the surface covered with adhesive. *International Journal of Adhesion and Adhesives*, 104, 102698. https://doi.org/10.1016/j.ijadhadh.2020.102698

Okuda, N., & Sato, M. (2004). Manufacture and mechanical properties of binderless boards from kenaf core. *Journal of Wood Science*, 50(1), 53–61. https://doi.org/10.1007/s10086-003-0528-8

Ostendorf, K., Ahrens, C., Beulshausen, A., Tayo, J. L. T., & Euring, M. (2021). On the feasibility of a pMDI-reduced production of wood fiber insulation boards by means of kraft lignin and ligneous canola hulls. *Polymers*, 13(7). https://doi.org/10.3390/polym13071088

Pham Van, T., Schöpper, C., Klüppel, A., & Mai, C. (2021). Effect of wood and panel density on the properties of lightweight strand boards. *Wood Material Science and Engineering*, 16(4), 237–245. https://doi.org/10.1080/17480272.2019.1705906

Shu, B., Ren, Q., He, Q., Ju, Z., Zhan, T., Chen, Z., & Lu, X. (2019). Study on mixed biomass binderless composite based on simulated wood. *Wood Research*, 64(6), 1023–1034.

Syafiqaz, N., Arman, N., Chen, S., & Ahmad, S. (2021). Review of state-of-the-art studies on the water absorption capacity of agricultural fiber-reinforced polymer composites for sustainable construction. *Construction and Building Materials*, 302, 124174. https://doi.org/10.1016/j.conbuildmat.2021.124174

Troncoso-Ortega, E., Castillo, R. D. P., Reyes-Contreras, P., Castaño-Rivera, P., Teixeira Mendonça, R., Schiappacasse, N., & Parra, C. (2021). Effects on lignin redistribution in eucalyptus globulus fibres pre-treated by steam explosion: A microscale study to cellulose accessibility. *Biomolecules*, 11(4). https://doi.org/10.3390/biom11040507

Velásquez, J. A., Ferrando, F., & Salvadó, J. (2003). Effects of kraft lignin addition in the production of binderless fiberboard from steam exploded Miscanthus sinensis. *Industrial Crops and Products*, 18, 17–23. https://doi.org/10.1016/S0926-6690(03)00016-5

Wistara, N. J., Starini, W., Febrianto, F., Pari, G., & Kehutanan, J. I. (2018). Binderless MDF from Hydroxymethylated Kenaf Pulp MDF Tanpa Perekat dari Pulp Kenaf Terhidroksimetilasi. *Journal of Forest Science*, 12, 3–13. https://jurnal.ugm.ac.id/jikfkt

Chapter 7. Environmental footprint and life cycle assessment of binderless high density boards

Chapter Content

This Chapter focuses on the environmental impact of binderless board made by following the steps outlined in Chapter 2. A life cycle assessment is conducted with the two main objective. Firstly, to compare the environmental impact of adhesive-free panels with conventional ones, and secondly, to identify any critical points in the production process that could be optimized in the future from an environmental perspective. The assessment follows the guidelines provided by ISO 14040 and ISO 14044. It begins with the identification of material flows and inputs within the system boundaries defined for the study. Subsequently, environmental indicators are calculated using the ReCiPe method, both at the mid-point and end-point level.

7.1. Life cycle assessment methodology and objective

7.1.1. Goal, scope, and system boundaries

The environmental impact generated by fully bio-based products is believed to be less than products using fossil raw materials, which in this case can be associated with the adhesive normally used in the wood-based panels (WBP) industry. Indeed, many studies (Bovea & Vidal, 2004; Çınar, 2004; González-García et al., 2009) that deal with life cycle assessment (LCA) of WPB, pointed out that much of the impact comes from the raw materials used, whether this is due to the production and preparation of the material itself or its transportation. However, in defining the environmental impact of binderless fiberboards (BF), the difference in the production process must be considered and evaluated. Actually, the production process is the part that allows for a performing product without the addition of fossil adhesives. As much as research has moved in identifying a LCA of new and eco-friendly WBP, there are no studies concerning the production process presented in this manuscript.

Hence, the main goal is to analyze the manufacture of BF from an LCA perspective in order to define the environmental impact of the process. At this point of the product development stage, the LCA can be useful from two points of view:

- in order to have the tools necessary to further optimize the process with a view to sustainability;
- in order to compare the environmental impact of the production process proposed with the conventional one, to decide whether it is worth it from an environmental point of view or not.

For the purpose, 1 m^3 of the finished board is considered as functional unit. The system model chosen considers the stages of the process from gate to gate. The wood raw material is considered pre-processed and already collected in the form of chips, leaving further consideration of the chipping stage of material to future work. Therefore, step identification was done based on the process described in Chapter 2, and on the database related to conventional hardboard production in Ecoinvent.

With the gate to gate model, the system boundaries (SB) were identified by dividing the process into two main subsystems (SS):

- Wood chips preparation
- Board manufacturing.

Within each SS, different steps were identified in order to obtain a specific inventory of inputs and outputs to each phase (Figure 7.1.).

7.1.1.1. Subsystem description: wood chips preparation

The steps identified for the first SS of wood chips preparation were the following:

- *Steam explosion pre-treatment (STEX)*: the collected wood chips are placed inside the reactor to be treated with STEX. Through STEX, a pulp is obtained that can be pressed into panels without the addition of any adhesive. The STEX condition considered are the optimal ones according to our studies (reaction temperature Tr 200°C to 204°C). The production of the steam required for the wood chips treatment is considered in-house, through a biomass-fired boiler that allow the reuse of the waste produced during the process;
- *Pulp rinsing*: the material from STEX is washed with tap water. The main objective of rinsing is to remove the residual hydrolyzed hemicellulose that affects dimensional stability (i.e. thickness swelling (TS) and water absorption (WA));
- *Pulp drying*: the washed material is dried at a temperature of 35°C to a relative humidity (RH) of about 10% by dry weight;
- *Milling*: the dry material is shredded to obtain a maximum size of 4 mm.

7.1.1.2. Subsystem description: boards manufacturing

The steps identified for the second SS of boards manufacturing were:

- *Cold pressing* (CP): the dried and milled fibers are placed into a cold press to form a mat. This step lasts a few seconds and a pressure of 16 MPa is considered;
- *Hot pressing* (HP): the obtained mat from cold pressing is placed in the hot press to finally obtain the board. A maximum pressure of 7.5 MPa and a maximum temperature of 205°C were considered in this stage. For simplicity, a one-step HP were considered;
- Final heat treatment (FHT): after pressing, the boards are cured with a FHT that improve physical properties. The maximum temperature considered is 180°C.

Figure 7.1. *System boundaries for binderless fiberboards manufacturing from gate to gate.*

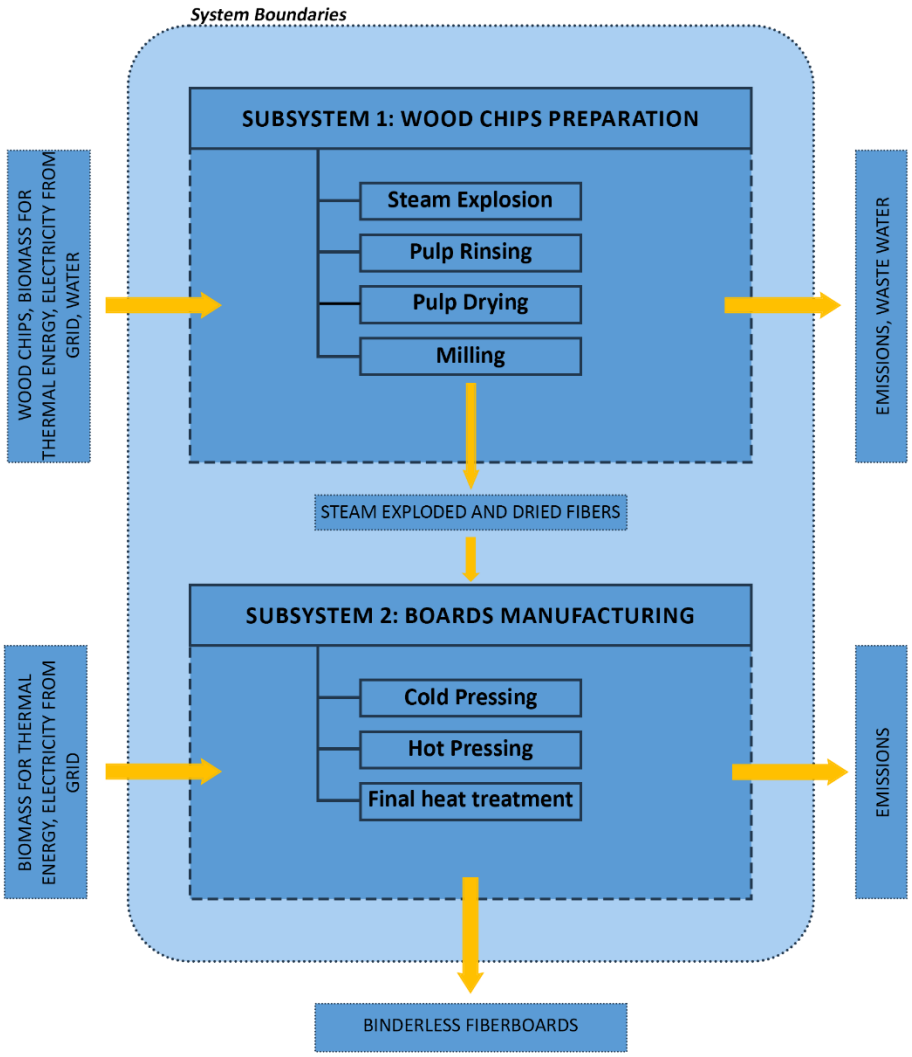

7.1.2. Life cycle inventory

Life cycle inventory (LCI) data for the system described above is the result of calculation that simulate the operation of an industrial plant (Annex C). The calculation in this study, through which the inputs and outputs of each step were obtained, refers to the process parameters optimized and developed during the group's years of work and experience (Anglès et al., 1999; Anglés et al., 2001; Mancera et al., 2008; Ramos et al., 2017, 2018, 2020; Velásquez et al., 2002; Vitrone, Ramos, Ferrando, et al., 2022; Vitrone, Ramos, Vitagliano, et al., 2022). Direct reference is made to the Ecoinvent 3.8 database only for certain steps and for the traditional boards, used as reference. In addition, literature research of recent years was conducted to get a complete picture of the available data and the most widely used process methodology. Table 7.1. shows the studies deemed valuable for comparison with the present one.

7.1.3. Life cycle impact assessment

The method for the life cycle impact assessment (LCIA) used was the ReCiPe 2016 (Huijbregts et al., 2017) at a hierarchical level (H), which considers a time period of 50 years. Both mid-point and end-point impact categories were considered. The categories addressed to the ReCiPe methos are eighteen, described in Annex C, and summarized in Table 7. 2..

The LCA interpretation of the results dealt with the hotspot analysis aiming to identify opportunities in the manufacturing of boards to improve the environmental impact. To this aim, an eco-efficiency indicator was also considered, by combining relevant physical-mechanical properties with the environmental impacts. The eco-efficiency factor (Ecoef) was defined by Uemura Silva et al. as follows:

$$Ecoef = \frac{MOR\ [N\ mm^{-2}]}{GWP\ [kg\ CO_2^{eq}]}$$ (Uemura Silva et al., 2021)

Where MOR is the average modulus of rupture obtained with the conditions outlined in the previous sections, and GWP is the global warming potential obtained by the LCA study. The higher the MOR the higher the Ecoef, and the lower the GWP the higher the Ecoef. The main features of the BF considered are shown in Table 7.3.

Table 7.1. *Summary of selected LCI and LCA studies on wood-based boards.*

Application	Material	Scope	Functional unit	Approach	Refecernce
Particleboard	Wood waste	Generate a comprehensive life cycle inventory for resin bonded wood particleboards.	1 m^3	LCI	Rivela et al. (2006)
Medium density fiberboard	Wood chips	Generate a comprehensive life cycle inventory for medium density fiberboard.	1 m^3	LCI	Rivela et al. (2007)
Hardboard	Lignocellulosic fibers	Analyze the manufacture of hardboard to detect the environmental hot spot to improve the environmental performance.	1 m^3	cradle-to-gate LCA	González-García et al. (2009)
Hardboard	Lignocellulosic fibers	Analyze the manufacture of green hardboard to detect the environmental hot spot to compare the results with conventional hardboard.	1 m^3	cradle-to-gate LCA	González-García et al. (2011)
Medium density particleboard	Wood particles	Presents LCA of medium density particleboards produced in Brazil and suggest improvement opportunities.	1 m^3	cradle-to-gate LCA	Aparecido Lopes Silva et al. (2013)
Particleboard	Sugarcane bagasse and Pine wood residues	Identify the main environmental aspects and impacts related to production of the particleboards, enabling improvements to be made.	1 m^2	Laboratory scale LCA	Dos Santos et al. (2014)
Medium density fiberboard	Pine and Eucalyptus shavings	Propose ways of improving the environmental life cycle of MDF panel by means of a LCA study.	1 m^3	cradle-to-gate LCA	Piekarski et al. (2017)
Medium density and high density particleboard	Pine and Eucalyptus shavings	Propose the assessment of particleboards based on the circular economy approach, in which wood wastes and bio resins are used to produce circular construction materials and compare them with conventional panels made of synthetic polymers and virgin wood particles.	1 m^3	cradle-to-gate LCA	Uemura Silva et al. (2021)

Table 7.2. *Environmental indicators for ReCiPe mid-point method, with the corresponding category and unit.*

Indicator	Category	Unit
ALOP	agricultural land occupation	m^2a
GWP500	Climate change	kg CO_2-Eq
FDP	fossil depletion	kg oil-Eq
FETPinf	freshwater ecotoxicity	kg 1,4-DC
FEP	freshwater eutrophication	kg P-Eq
HTPinf	human toxicity	kg 1,4-DC
IRP_HE	ionizing radiation	kg U_{235}-Eq
METPinf	marine ecotoxicity	kg 1,4-DC
MEP	marine eutrophication	kg N-Eq
MDP	metal depletion	kg Fe-Eq
NLTP	natural land transformation	m^2
ODPinf	ozone depletion	kg CFC-Eq
PMFP	particulate matter formation	kg PM_{10}-Eq
POFP	photochemical oxidant formation	kg NMVOC
TAP500	terrestrial acidification	kg SO_2-Eq
TETPinf	terrestrial ecotoxicity	kg 1,4-DC
ULOP	urban land occupation	m^2
WDP	water depletion	m^3

Table 7.3. *Main features of binderless boards obtained from steam exploded chips.*

Board thickness		3-4	mm
Density	1088	± 30	kg m^{-3}
MOE	4514	± 224	N mm^{-2}
MOR	34.5	± 3.1	N mm^{-2}
IB	4.125	± 0.489	N mm^{-2}
TS	9	± 4	%

7.2. Results and discussion

7.2.1. Life cycle inventory

The inventory data of the subsystems of wood chips preparation, and board manufacturing are shown in Table 7.4., as well as the total amount of inputs for the entire process. The inputs considered refers to the functional unit of 1 m^3 of finished board and to the Ecoinvent dataset related to hard fiberboard production. Compared to the dataset, the same source and quantity of wood chips were considered, whose primary amount, i.e., before STEX, was calculated considering the weight and material loss that is normally found in this process, which is about 20% of the initial weight, on dry basis. The sources of wood chips considered by the dataset are diverse: most of the raw material is virgin wood chips, while a small portion is residual wood. In order to focus the comparison on the use or non-use of adhesive and thus on the differences in the production process, the same percentage of virgin and waste material was considered. However, it is worth specifying that the STEX process allows for good quality included using only waste materials, or alternative materials to wood, such as *Arundo*

donax L., thus presumably lowering the final footprint, as is also the case in the studies presented in Table 7.1.

Table 7.4. *Binderless boards manufacturing inventory for 1 m³ of finished board.*

SUBSYSTEM 1: WOOD CHIPS PREPARATION			
Steam explosion			
Input:			Reference:
Wood chips (d.m.)	1075.50	kg	Ecoinvent
Biomass (boiler)	45.03	kg	This study
Energy from boiler	648.47	MJ	This study
Pulp rinsing			
Input:			
Wood pulp (d.m.)	860.40	kg	Ecoinvent
Water	8604.00	kg	This study
pulp drying			
Input:			
Wood pulp (with moisture)	1720.80	kg	Ecoinvent
Biomass (boiler)	148.22	kg	This study
Energy from boiler	2134.33	MJ	This study
Milling			
Input:			
wood pulp (d.m.)	860.40	kg	Ecoinvent
Electricity (from grid)	56.05	MJ	Ecoinvent
	(15.57	kWh)	
SUBSYSTEM 2: BOARDS MANUFACTURING			
Cold pressing			
Input:			
Wood pulp (d.m.)	860.40	kg	Ecoinvent
Electricity (from grid)	15,23	MJ	This study
	(4.23	kWh)	
Lubricants	0.02	kg	Ecoinvent
Hot pressing			
Input:			
Mat (cold pressed wood pulp)	860.40	kg	Ecoinvent
Electricity (from grid)	3.60	MJ	This study
	(1.00	kWh)	
Biomass (boiler)	0.83	kg	This study
Energy from boiler	11.92	MJ	This study
Final heat treatment			
Input:			
Fiberboard	1	m^3	
Biomass (boiler)	18.00	kg	This study
Energy from boiler	264.13	MJ	This study
TOTAL INPUTS			
Wood chips (d.m.)	1075.50	kg	Ecoinvent
Heat (from biomass boiler)	3058.85	MJ	This study
Electricity, from grid	74.88	MJ	This study
	20.80	kWh	
tap water	8604.00	kg	This study
Lubricating oil	0.30	kg	Ecoinvent
Diesel (internal transport)	41.60	MJ	Ecoinvent
DIRECT EMISSIONS			
wastewater, to be treated	8.29	m^3	This study

The total amount of energy needed to produce 1 m^3 of BF is 870.48 kWh, of which the 97% is thermal energy, expressed in MJ in the Table 7.4., and produced within the plant. The biomass needed to produce this amount of thermal energy is about 194 kg, and the parameters used for the transformation of the MJ used into kg of biomass are given in Annex C. Of all thermal energy produced, about 91% is used within the first subsystem of wood chips preparation, and in particular the most energy consuming stage is the pulp drying. For electricity, on the other hand, we considered the use of energy from the public grid. Here again, most of electricity is used in the first subsystem, for the milling step.

Comparing the thermal energy consumption with the Ecoinvent dataset and some of the studies presented in the Table 7.1., it was comparable or lower. For instance, Rivela et al. presented a LCI of medium density fiberboards and reported a total amount of energy consumed of 1120.65 kWh (Rivela et al., 2007). González-García et al., on the other hand, reported a value of 1395.56 kWh for thermal energy, and 476.39 kWh for electricity, in the manufacturing of hardboard (González-García et al., 2009). Our total value of 870.48 kWh of heat and electricity is not perfectly comparable with either of the two cited references: in the first case the study dealt with boards with a lower density, and in the second with hardboards, which are produced with a wet process. Despite this, they can be taken as reference values together with that indicated by the Ecoinvent dataset, according to which energy consumption is around 1460 kWh, considering heat and electricity together.

A crucial point in the inventory was found in water consumption. This consumption is due to the rinsing step through which a large amount of water is used, which was calculated based on assumptions derived from the real amount of water consumed at the laboratory level. This is the major drawback at this point, when comparing with conventional panels, as it increased the consumption of natural resources. Besides, this step generates the production of wastewater that needs to be treated because it contains the material hydrolyzed from STEX, in addition to the initial amount of water used. As a result, the rinsing step represents a key point for future process optimizations from the environmental point of view.

7.2.2. Life cycle impact assessment and interpretation of the results

7.2.2.1. Mid-point ReCiPe indicators

BF were less impactful than the reference boards in most of the categories, except for some points for which the indicator is slightly higher, although in the same order of magnitude (Table 7.5.).

Table 7.5. *Impact assessment results for 1 m^3 of binderless boards and reference boards, according to ReCiPe mid-point method.*

Indicator	Unit	Binderless board	Reference board
ALOP	m^2a	925.51	3112.76
GWP500	kg CO_2-Eq	142.33	867.27
FDP	kg oil-Eq	93.35	233.38
FETPinf	kg 1,4-DC	7.79	15.64
FEP	kg P-Eq	0.10	0.68
HTPinf	kg 1,4-DC	141.87	440.49
IRP_HE	kg U_{235}-Eq	35.13	91.54
METPinf	kg 1,4-DC	7.14	14.60
MEP	kg N-Eq	0.15	0.36
MDP	kg Fe-Eq	**56.38**	**24.47**
NLTP	m^2	-0.02	-0.06
ODPinf	kg CFC-Eq	**$4.05 \cdot 10^{-5}$**	**$3.37 \cdot 10^{-5}$**
PMFP	kg PM_{10}-Eq	3.33	2.00
POFP	kg NMVOC	1.80	4.89
TAP500	kg SO_2-Eq	1.31	5.24
TETPinf	kg 1,4-DC	0.13	0.56
ULOP	m^2	15.22	35.38
WDP	m^3	3.81	4.64

The two indicators that are higher for BF are metal depletion (MDP), and ozone depletion (ODPinf), both related to the use of raw material (wood chips). Indeed, compared to reference panels, a 20% material plus is considered because of the dry weight loss due to pretreatment, which in the case of reference panels does not occur. The difference for the ODPinf category is really minimal, while, in the case of MDP, the indicator raised to twice that of the reference.

SS1 is the one that contributed the most in each impact category (Figure 7.2.), a result that was already predictable from the LCI phase, and that is also found in other studies (Table 7.1.). It is also interesting to consider the contribution of individual inputs, beyond the subsystem, to each impact category (Figure 7.3.). The input that affects all categories the most is the wood chips, and it can be assumed that the use of a greater percentage or total percentage of waste material may change its contribution positively. It is also clear that the MDP category is greatly affected by the use of wood chips, along with heat, which are the inputs whose contribution is most visible for MDP indicator. As a result, raw material (wood chips) and thermal energy, are the two most

impactful elements on all categories, while water consumption and treatment have a substantial impact on only few categories.

Based on mid-point categories, and in particular on global warming potential (GWP), the eco-efficiency factor (Ecoeff) were calculated. For MOR value, the minimum standard indicated by the EN 622-5:2010 was used (i.e., 34 N mm^{-2}), and the results show that the Ecoeff is much higher for BF (Figure 7.4.).

Figure 7.2. *Relative contribution (%) of wood chips preparation subsystem (Subsystem 1), and boards manufacturing subsystem (Subsystem 2) for each impact category.*

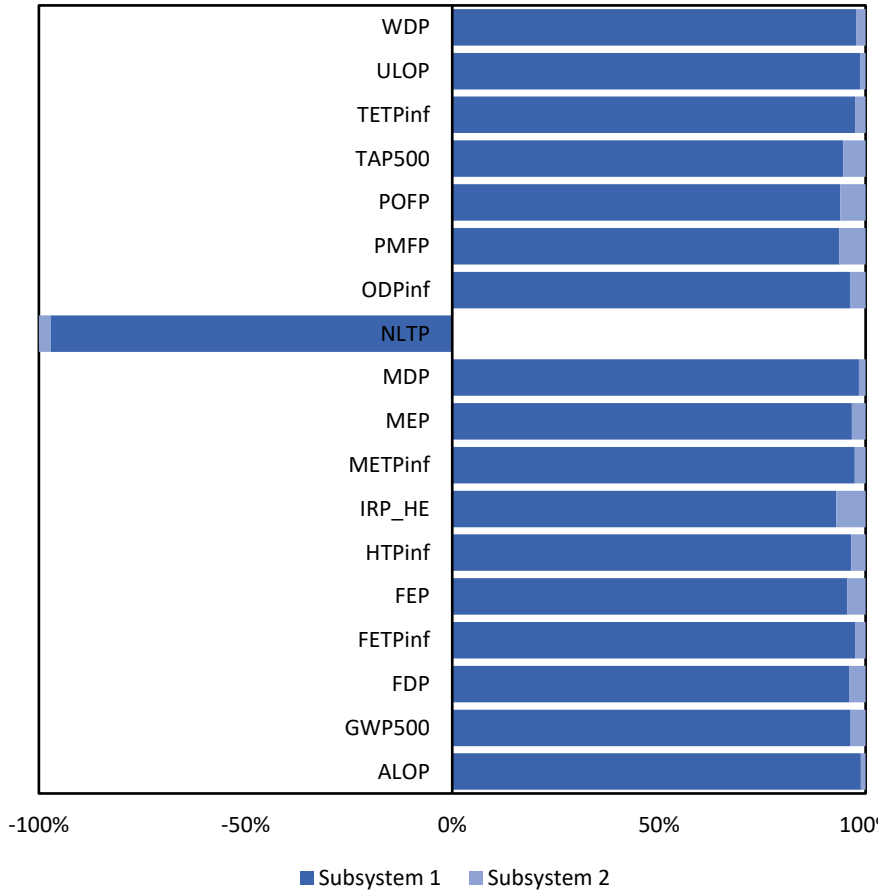

Figure 7.3. *Relative contribution (%) of each input considered in the inventory of 1 m³ of finished binderless fiberboard, for each impact category.*

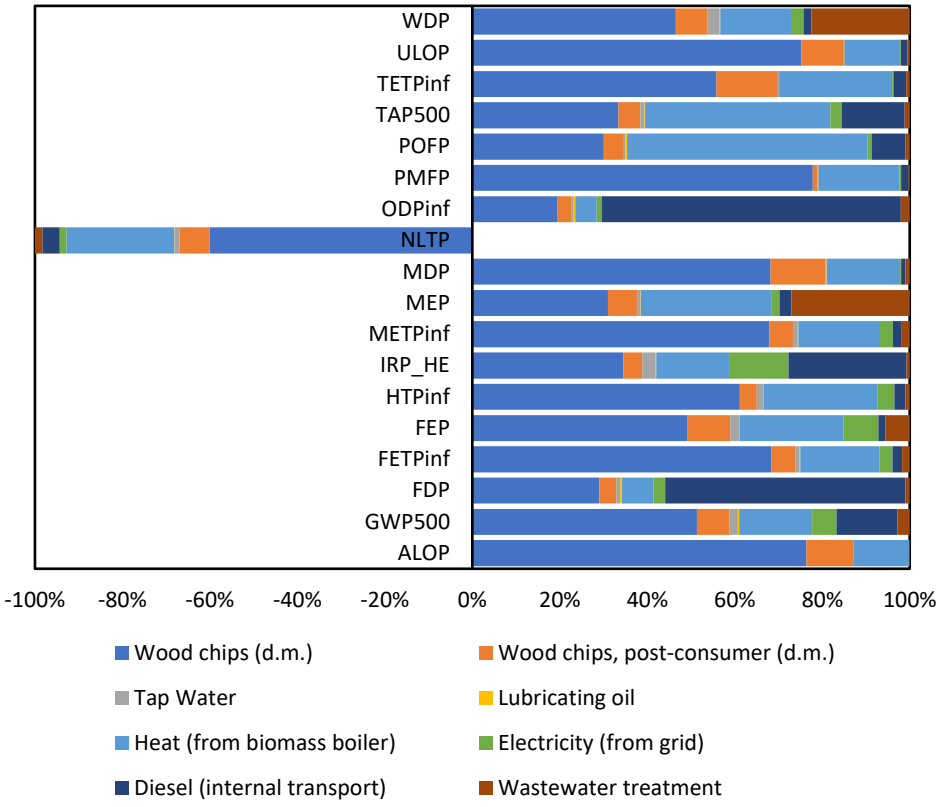

Figure 7.4. *Combining MOR with GWP as normalization factors to calculate eco-efficiency of the binderless board and reference board: adapted from* (Uemura Silva et al., 2021).

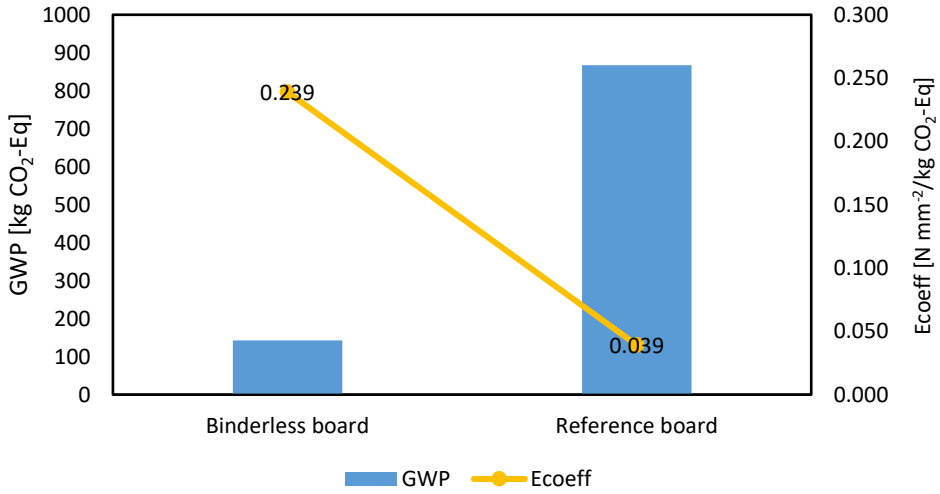

7.2.2.2. End-point ReCiPe indicators

The end-point categories allow the translation of environmental impact into harm to human health, damage to the ecosystem (terrestrial, freshwater, and marine), and consumption of resources. The reference board has a higher impact on all categories, probably due to the use of synthetic adhesives (Table 7.6.).

Table 7.6. *Impact assessment results for 1 m^3 of binderless boards and reference boards, according to ReCiPe end-point method.*

	Human Health	Terrestrial Ecosystem	Freshwater Ecosystem	Marine Ecosystem	Resources
	DALY m^{-3}	Species.yr m^{-3}	Species.yr m^{-3}	Species.yr m^{-3}	UDS2013 m^{-3}
Binderless board	1.14	0.59	$2.76 \cdot 10^{-7}$	$3.35 \cdot 10^{-8}$	2616904
	Human health (HH)		Ecosystem depletion (ED)		Resource depletion (RD)
	1.14		0.59		2616904
Reference board	6.56	1.98	$1.14 \cdot 10^{-6}$	$6.88 \cdot 10^{-8}$	6542366
	HH		ED		RD
	6.56		1.98		6542366

In Figure 7.5. the impact of the two boards are compared for each end-point category. As a result, considering the end-point categories that are more realizable indicators of the damage caused by a product, BF are definitely more sustainable. In addition, some strategies could be implemented for further optimization:

- Further reduction in the amount of water used: this would reduce the residual water to be treated by an equal amount;
- Consider that the same mechanical performance can be achieved with residual or alternative material, such as *Arundo donax* L.

Then, further research, may involve the same analysis but with these modification, which likely lead to an even smaller footprint.

For all other categories, BF has a lower impact and is therefore a better alternative from an environmental point of view. The damage to human health of BF is about 20% of the damege of conventional panels, the resource consumption is about 40%, and the total ecosystem damage is about 30% of the one of conventional boards, mainly due to the freshwater ecosystem. Indeed, considering individually the categories that contribute to the ecosystem damage, the last mentioned is the only one where BF has a greater impact, while for all others, i.e., terrestrial, and marine, BF is still a more eco-friendly alternative than conventional panels (Figure 7.5.).

7.3. Conclusions

The comparison between BF, obtained by the production process described in the previous chapters, and conventional panels, showed that overall BF has a lower impact than conventional panels in almost all impact categories considered.

The points in favor of BF depend mainly on the use of less total energy and the use of materials, since conventional panels use adhesives.

Global warming potential, which represent the carbon footprint, is far lower for BF when comparing with conventional panels. Thus, the eco-efficiency factor, calculated as the ratio of MOR and the GWP, is much higher for BF.

As a conclusion, it has been shown that BF are much more sustainable than conventional panels. Moreover, the footprint of BF can be further reduced by using only alternative or residual materials, and further reducing the use of tap water.

Figure 7.5. *Relative contribution of binderless board and reference board for human health (a), terrestrial ecosystem (b), freshwater ecosystem (c), marine ecosystem (d), and resources (e).*

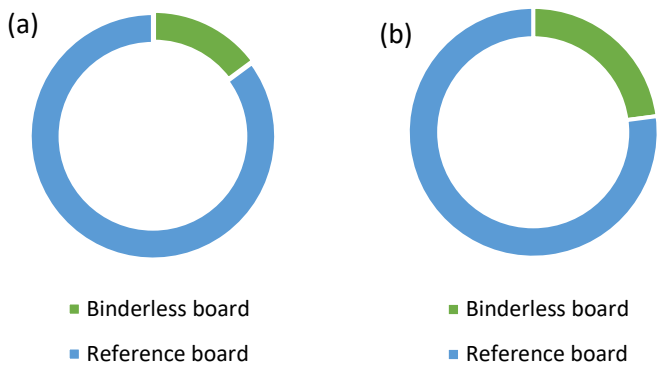

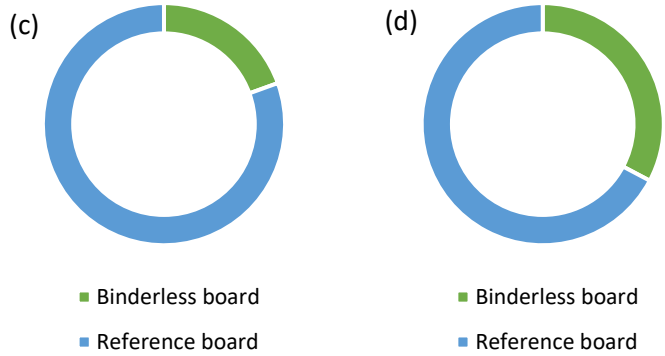

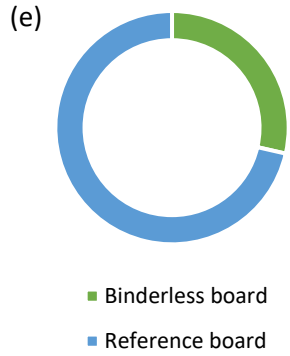

References

Anglés, M. N., Ferrando, F., Farriol, X., & Salvadó, J. (2001). Suitability of steam exploded residual softwood for the production of binderless panels. Effect of the pre-treatment severity and lignin addition. *Biomass and Bioenergy*, 21, 211–224.

Anglès, M. N., Reguant, J., Montané, D., Ferrando, F., Farriol, X., & Salvadó, J. (1999). Binderless composites from pretreated residual softwood. *Journal of Applied Polymer Science*, 73(12), 2485–2491. https://doi.org/10.1016/S0961-9534(01)00031-9

Aparecido Lopes Silva, D., Antonio Rocco Lahr, F., Pinheiro Garcia, R., Miguel Cereja Seixas Freire, F., & Roberto Ometto, A. (2013). Life cycle assessment of medium density particleboard (MDP) produced in Brazil. *International Journal of Life Cycle Assessment*, 18, 1404–1411 . https://doi.org/10.1007/s11367-013-0583-3

Bovea, D., & Vidal, R. (2004). Materials selection for sustainable product design: a case study of wood based furniture eco-design. *Materials and Design*, 25, 111–116. https://doi.org/10.1016/j.matdes.2003.09.018

Çınar, H. (2004). Eco-design and furniture: Environmental impacts of wood-based panels, surface and edge finishes. *Forest Products Journal*, 55(11), 27–33.

Dos Santos, F. M. N., Battistelle, A. G., Stolte Bezerra, B., & Varum, H. S. A. (2014). Comparative study of the life cycle assessment of particleboards made of residues from sugarcane bagasse (Saccharum spp.) and pine wood shavings (Pinus elliottii). *Journal of Cleaner Production*, 64, 345–355. https://doi.org/10.1016/j.jclepro.2013.06.039

González-García, S., Feijoo, G., Heathcote, C., Kandelbauer, A., & Moreira, M. T. (2011). Environmental assessment of green hardboard production coupled with a laccase activated system. *Journal of Cleaner Production*, 19(5), 445–453. https://doi.org/10.1016/j.jclepro.2010.10.016

González-García, S., Feijoo, G., Widsten, P., Kandelbauer, A., Zikulnig-Rusch, E., & Moreira, M. T. (2009). Environmental performance assessment of hardboard manufacture. *International Journal of Life Cycle Assessment*, 14(5), 456–466. https://doi.org/10.1007/s11367-009-0099-z

Huijbregts, M. A. J., Steinmann, Z. J. N., Elshout, P. M. F., Stam, G., Verones, F., Vieira, M. D. M., Hollander, A., Zijp, M., & van Zelm, R. (2017). ReCiPe 2016 v1.1 A harmonized life cycle impact assessment method at midpoint and endpoint level. *RIVM Report*. www.rivm.nl/en

Mancera, C., Ferrando, F., & Salvadó, J. (2008). Cynara cardunculus as raw material for the production of binderless fiberboards: Optimization of pretreatment and pressing conditions. *Journal of Wood Chemistry and Technology*, 28(3), 207–226. https://doi.org/10.1080/02773810802347024

Piekarski, C. M., de Francisco, A. C., da Luz, L. M., Kovaleski, J. L., & Silva, D. A. L. (2017). Life cycle assessment of medium-density fiberboard (MDF) manufacturing process in Brazil. *Science of the Total Environment*, 575, 103–111. https://doi.org/10.1016/j.scitotenv.2016.10.007

Ramos, D., Ferrando, F., Farriol, X., & Salvadó, J. (2020). Optimization of the production factors of boards obtained from Arundo Donax L. Fibers without added adhesives. *Molecules*, 25(7). https://doi.org/10.3390/molecules25071660

Ramos, D., Mansouri, N. E. El, Ferrando, F., & Salvadó, J. (2018). All-lignocellulosic fiberboard from steam exploded Arundo donax L. *Molecules*, 23(9). https://doi.org/10.3390/molecules23092088

Ramos, D., Salvadó, J., & Ferrando, F. (2017). High Mechanical Performance Boards Made from Fibers of Arundo donax without Added Adhesives. *BioResources*, 12(3), 5383–5394.

Rivela, B., Hospido, A., Moreira, M. T., & Feijoo, G. (2006). Life cycle inventory of particleboard: A case study in the wood sector. *International Journal of Life Cycle Assessment*, 11(2), 106–113. https://doi.org/10.1065/lca2005.05.206

Rivela, B., Moreira, M. T., & Feijoo, G. (2007). Life cycle inventory of medium density fibreboard. *International Journal of Life Cycle Assessment*, 12(3), 143–150. https://doi.org/10.1065/lca2006.12.290

Uemura Silva, V., Fátima Nascimento, M., Oliveira, P. R., Panzera, T. H., Oliveira Rezende, M., Aparecido, D., Silva, L., Borges De Moura Aquino, V., Antonio, F., Lahr, R., & Christoforo, A. L. (2021). Circular vs. linear economy of building materials: A case study for particleboards made of recycled wood and biopolymer vs. conventional particleboards. *Construction and Building Materials*, 285, 122906. https://doi.org/10.1016/j.conbuildmat.2021.122906

Velásquez, J. A., Ferrando, F., & Salvadó, J. (2002). Binderless fiberboard from steam exploded Miscanthus sinensis: The effect of a grinding process. *Holz Als Roh - Und Werkstoff*, 60(4), 297–302. https://doi.org/10.1007/s00107-002-0304-2

Vitrone, F., Ramos, D., Ferrando, F., & Salvadó, J. (2022). The influence of thickness and final heat treatment on mechanical properties and dimensional stability of binderless fiberboards from steam exploded Arundo donax L. *Materials Today: Proceedings*. https://doi.org/10.1016/J.MATPR.2021.12.481

Vitrone, F., Ramos, D., Vitagliano, V., Ferrando, F., & Salvadó, J. (2022). All-lignocellulosic fiberboards from giant reed (Arundo donax L.): Effect of steam explosion pre-treatment on physical and mechanical properties. *Construction and Building Materials*, 319, 126064. https://doi.org/10.1016/j.conbuildmat.2021.126064

General Conclusions and perspectives

This last section details the general conclusions from each of the objectives outlined at the beginning, and presents some perspectives for future work, based on the results achieved.

General conclusions

The main objective was to test whether it was possible to manufacture binderless fiberboards (BF) from steam exploded *Arundo donax* L. (AD).

The results obtained were remarkable, in many cases meeting the current standards, indicating that AD is a feasible material for the production of BF. However, the pretreatment and production process conditions have a significant effect on the final performance, and at the current stage of the investigation, arrangements are necessary to achieve good results. They are reported below, in the following subsections.

Conclusions on the effects of steam explosion

Given that pretreatment of the material is necessary to achieve good results in the production of fiberboards without adhesives, steam explosion (STEX) proved its effectiveness because it generally led to good quality panels.

In general, it was already known from previous work that the pretreatment has a significant effect on all properties considered. In the case of AD, the novelty with respect to previous works is that it was found that a minimum reaction temperature (Tr) of 195°C, with a reaction time (tr) of 9.5 min, is necessary to achieve the minimum required standards. The results obtained, both mechanical results and dimensional stability, increase considerably in the temperature range between 190°C and 195°C. This means that the Tr of 195°C is the temperature that triggers the chemical and morphological changes in the fibers that lead to better quality bonding.

Furthermore, the optimal Tr is set at 200°C for reasons of both technology and the results obtained. Indeed, with this Tr the best mechanical results are achieved with the same pressure and final heat treatment (FHT) conditions, even reaching the standards for structural use. On the other hand, from a technological point of view, when the

pretreatment is carried out at 200 °C, the material is sufficiently defibrillated to avoid occlusions in the reactor valve.

To conclude, it can be stated that the best STEX conditions for the pretreatment of AD are at a Tr of 200°C for a tr of 9.5 min.

Conclusions on the effects of final heat treatment

FHT was added to the production process relatively recently, as a curing step with the aim on the one hand of further improving the properties, and on the other hand of compensating for any lowering of the pressing pressure (Pp) or the Tr.

In general, the effect of FHT is significant both on the mechanical performance and on the dimensional stability. However, its effect on mechanical characteristics depends on the conditions of the other process steps, especially the pretreatment. It has a positive effect only on samples manufactured with a Tr above the threshold of 195°C . On the contrary, for dimensional stability and the characteristics of thickness swelling (TS) and water absorption (WA), the effect of FHT is always clear and very significant, even halving the values obtained.

The two parameters of FHT studied are curing temperature (Tc) and curing time (tc). The results obtained from the analysis lead to conclude that small variations in tc do not produce significant variations in the results, while for a much longer tc the results improve considerably even at a slightly lower temperature. In fact, the combination of Tc(°C)-tc(h) conditions tested were 180-0.5, 180-1, and 165-5, and the best results were obtained with the last combination.

Conclusions on the effects of panel size

The dimensions can have a large effect on the final properties of the fiberboards, both for mechanical and technological reasons. The previous sections (in particular Chapter 5 and Chapter 6) both the effect of the thickness on small specimens and the effect of the increasing of the panel size on the final characteristics were studied, obtaining some conclusions which may be useful for future improvements.

The thickness has a significant effect on the mechanical properties, but not on the dimensional stability within the range of thicknesses considered, although there is a progressive improving effect. Among the mechanical properties, the internal bond (IB) is the property most affected: by thickness, with a progressive decrease as the thickness increases. This is likely due to a technological effect where the heat of the press needs more time to reach the center of the specimen and improve bonding between the fibers. Indeed, the optimal properties for

IB are obtained for a thickness of 3 mm, and could be improved by increasing the pressing time (tp) for greater thicknesses.

The effect of the panel size is also a technological problem. The increase in panel size results in a higher standard deviation of the properties, especially density and mechanical characteristics. This is due to the difficulty of homogenous distribution of the material over a larger surface, a problem which causes notable differences in performance in specimens cut from the full size, as well as difficulties of interpretation. Thus, future studies must develop a method for achieving uniform material distribution, so that the properties of the panels can be studied on a larger scale.

Conclusions on the relationships between the main steps of production process

In many cases, the conditions of each phase are interconnected, and the conditions set for one of them can influence the effect of the others on the boards properties. In particular, the parameters of STEX are those which make any other phase more or less effective. Focusing on AD, it was found that a minimum Tr of 200 °C with a tr of 9.5 min is needed for hot pressing (HP) and FHT to have the desired effect.

The pressing pressure (Pp) is studied in this manuscript only in relation to FHT, as previous studies explored its influence on the individual characteristics separately. Given that it is necessary to carry out the HP into three steps, it turns out that above the indicated threshold of STEX pretreatment (i.e., Tr 195°C), the second optimal pressure (Pp_2) is 7.5 N mm^{-2}, even if remarkable results are also obtained with a pressure of 3.3 N mm^{-2}.

The FHT, as mentioned, shows a compensation of the lowering of the Pp_2 both from a mechanical point of view and from a water absorption point of view, even if in general it has been shown that FHT has a huge positive effect on water absorption. However, this effect is clear only when working at Tr above the threshold.

To sum up, STEX is the phase that influences the performance the most, followed by HP and FHT.

Conclusions on the environmental impact of the manufacturing process

Fully bio-based fiberboards are commonly associated with a lower environmental impact, as synthetic adhesives are typically derived from petroleum resources and have a substantial environmental impact. However, to obtain BF, pretreatments are required. They involve phases that have a different impact than the process for conventional panels,

and it is necessary to verify their sustainability through a life cycle analysis (LCA).

The LCA was performed based on a gate to gate model, by considering wood chips as the row material entering the system. From the LCA results, favorable environmental impact indicators are obtained for fiberboards made with steam explosion and without adhesives, when compared with conventional panels whose impact is provided by the Ecoinvent database. The BF have a lower impact in almost all the categories considered, probably due to a lower total energy and the lack of the adhesive. As a result, BF are much more sustainable than conventional panels and their footprint can be further reduced by using only alternative or residual materials, and further reducing the use of tap water.

Perspectives and Future work

Based on the results obtained in the present work, further studies could focus on different possibilities reported below.

Continuing in the research line on AD, which proved to be a good raw material for BF manufacturing, there is a need to explore more production conditions of both HP and FHT. Indeed, just as a threshold was found for STEX, exploring different conditions for the other two phases can help define the upper and lower bounds of each of them, to find the optimum.

Besides, the threshold was found for the STEX of AD, and can be verified on other materials to understand if it depends on modifications of the main components of the lignocellulosic material or not, and if it can therefore be generalized.

Furthermore, the life cycle analysis reported in this study does not contemplate the use of steam exploded AD, a study that would certainly be useful to compare the results with those reported in this manuscript and understand the environmental impact of the use of this material.

Conclusions i perspectives generals

En aquest darrer apartat es detalla la conclusió general de cadascun dels objectius plantejats al principi, i es presenten algunes perspectives de treball futur, a partir dels resultsts assolits.

Conclusions generals

Lobjectiu principal era provar si era possible fabricar taulers de fibra sense aglutinant a partir de l'explosió de vapor d'*Arundo donax* L.

Com a resultat, es van obtenir resultats notables, en molts casos complint amb els estàndards actuals, de manera que es pot concloure que l'*Arundo donax* L. és un material que es pot utilizar per a la producció de tauler sense aglutinant. No obstant això, les condicions del procés de pretractament i producció tenen un efecte significatiu en el rendiment final i, en l'etapa actual de la investigació, són necessaris certs arranjaments per aconseguir bons resultats. Aquests s'expliquen a continuació.

Conclusions sobre els efectes de l'explosió de vapor

Atès que el pretractament del material és necessari per aconseguir bons resultats en la producció de taulers de fibra sense adhesius, l'explosió de vapor va demostrar la seva eficàcia perquè generalment condueix a taulers de bona qualitat.

En general, per treballs anteriors ja se sabia que el pretractament té un efecte significatiu en totes les proprietats considerades. En el cas de l'*Arundo donax* L., la novetat respecte a treballs anteriors és que s'ha constatat que és necessaria una temperatura mínima de reacció (Tr) de 195 °C, amb un temps de reacció (tr) de 9.5 min, per aconseguir els restàndards mínims exigits. Els resultats obtinguts, tant els mecànics com l'estabilitat dimensional, augmenten considerablement en el rang de temperatures entre 190 °C i 195 °C. Això vol dir que el Tr de 195°C és la temperatura que activa els canvir químics i morfológics de les fibres que condueixen a una unió de millor qualitat.

A més, la Tr òptima s'estableix a 200 °C tant per raons tecnològiques com pels resultats obtinguts. De fet, amb aquesta Tr s'aconsegueixen els millors resultats mecànics amb les mateixes condicions de pressió i tractament tèrmic final, arribant fins i tot als estàndards d'ús estructural. D'altra banda, des del punt de vista tecnólogic, quan el pretractament es realitza a 200 °C, el material està prou desfibril·lat per evitar oclusió a la vàlvula del reactor.

Per concloure, es pot afirmar que les millors condicions de l'explosió de vapor per al pretractament de l'*Arundo donax* L. es troben a un Tr de 200 °C durant un tr de 9.5 min.

Conclusions sobre els efectes del tractament tèrmic final

El tractament tèrmic final es va afegir al procés de producció fa relativament poc temps, com a pas de curat amb l'objectiu d'una banda de millorar encara més les proprietats, i de l'altra de compensar qualsevol reducció de la pressió de premsat (Pp) o del Tr.

En general, l'efecte del tractament tèrmic final és significatiu tant en el rendiment mecànic com en l'estabilitat dimensional. Tanmateix, en el cas de les característiques mecàniques, el seu efecte està lligat a les condicions de les altres etapes del procés, i en particular al pretractament: només té un efecte positiu en mostres fabricades amb un Tr superior al umbral de 195 °C. Per contra, per a l'estabilitat dimensional i les característiques d'inflament de gruix (TS) i d'absorció d'aigua (WA), l'efecte del tractament tèrmic final és sempre clar i molt significatiu, fins i tot reduint a la meitat els valors obtinguts.

Els dos paràmetres del tractament tèrmic final estudiats són la temperatura de curat (Tc) i el temps de curat (tc). Els resultats obtinguts de l'anàlisi porten a concloure que petites variacions de tc no produeixen variacions significatives en els resultats, mentre que durant una tc molt més llarga els resultats milloren considerablement fins i tot a una temperatura lleugerament inferior. De fet, les condicions Tc(°C)-tc(h) provades van ser 180-0.5, 180-1, i 165-5, i els millors resultats es van obtenir amb l'última combinació.

Conclusions sobre els efectes de la mida del tauler

Les característiques geomètriques poden tenir un gran efecte sobre les proprietats finals dels taulers de fibra, tant per motius mecànics com tecnològics. En els capítols anteriors (en particular el Capítol 5 i el Capítol 6) s'ha estudiat tant l'efecte del gruix en mostres petites com l'efecte de l'augment de la mida del tauler sobre les característiques finals, obtenint algunes conclusions que poden ser útils per a futures millores.

El gruix té un efecte significatiu només sobre les proprietats mecàniques. Pel que fa a l'estabilitat dimensional, hi ha un efecte progressiu de millora, però no significatiu en el rang de gruixos considerat. Entre les proprietats mecàniques, l'enllaç intern (IB) és el més afectat: a mesura que augmenta el gruix, l'IB disminueix progressivament. Això probablement es deu a un efecte tecnològic, ja que el calor de la premsa necessita més temps per arribar al centre de

la mostra i millorar la unió entre les fibres. De fet, les proprietats òptimes per a IB s'obtenen per a un gruix de 3 mm, i la millora de l'IB per als gruixos més grand es podria aconseguir augmentant el temps de premsat (tp).

L'efecte de la mida del tauler també és un problema tecnològic. L'augment de la mida dels taulers comporta una desviació estàndard més alta de les propietats, especialment de la densitat i les característiques mecàniques. Això es deu a la dificultat de distribució homogènia del material sobre una superfície més gran, un problema que provoca diferències notables en el rendiment de les mostres tallades de la mida completa, així com dificultats d'interpretació. Així, els estudis futurs han de proporcionar un mètode de distribució uniforme del material, de manera que es puguin estudiar les propietats dels panells a gran escala.

Conclusions sobre les relacions entre les principals fases del procés de fabricació

En molts casos està clar que les condicions de cada fase estan interconnectades i que les condicions establertes per a una d'elles influeixen en l'efecte de les altres. En particular, els paràmetres de l'explosió de vapor són els que fan que qualsevol altra fase sigui més o menys efectiva. Centrant-se en *l'Arundo* donax L., es va descobrir que es necessita un mínim de Tr de 200 °C amb un tr de 9,5 min per aconseguir que la premsa en calent i el tractament tèrmic final tinguin l'efecte desitjat.

La Pp s'estudia en aquest document només en relació amb el tractament tèrmic final, ja que estudis anteriors van explorar la seva influència en les característiques individuals per separat. Donat que és necessari dur a terme el premsat en tres passos, es descobreix que per sobre del umbral indicat del pretractament (i.e., Tr 195°C), la segona pressió òptima (Pp_2) és de 7,5 N mm^{-2}, tot i que també s'obtenen resultats destacables amb una pressió de 3,3 N mm^{-2}.

Com es va esmentar, el tractament tèrmic final mostra una compensació de la disminució de Pp_2 tant des del punt de vista mecànic com des del punt de vista de l'absorció d'aigua, tot i que en general s'ha demostrat que el tractament tèrmic final té un enorme efecte positiu en l'absorció d'aigua. No obstant això, aquest efecte és clar només quan es treballa a Tr per sobre del llindar. Per resumir, l'explosió de vapor és la fase que més influeix en el rendiment, seguida per el premsat en calent i el ytractament tèrmic final.

Conclusions sobre l'impacte ambiental del procés de fabricació

Comunament, es relaciona una menor petjada ecològica amb els taulers de fibra totalment biobasats, ja que els adhesius sintètics solen provenir de recursos petrolífers que tenen un impacte ambiental substancial. No obstant, per obtenir taulers sense adhesius, són necessaris tractaments previs. Aquests implican fases que tenen un impacte diferent del procés per a taulers convencionals i és necessari verificar la seva sostenibilitat a través d'un anàlisi de cicle de vida (ACV).

L'ACV es va dur a terme basant-se en un model porta a porta, considerant que les xips de fusta són la matèria primera que entra al sistema. A partir dels resultats de l'ACV, s'obtenen indicadors favorables d'impacte ambiental per als taulers fabricats amb explosió de vapor i sense adhesius, comparats amb els taulers convencionals, el seu impacte es proporciona per la base de dades Ecoinvet. Els taules sense adhesius tenen un impacte menor en gairebé totes les categories considerades, probablement a causa d'una energia total més baixa i la falta d'adhesiu. Per tant, són molt més sostenibles que els taulers convencionals i la seva petjada pot reduir-se encara més utilitzant només materials alternatius o residuals, i reduint encara més l'ús d'aigua de l'aixeta.

Perspectives i treballs futurs

Basant-se en els resultats obtinguts en aquest treball, futurs estudis podrien centrar-se en les diferents possibilitats que es detallen a continuació.

Continuant en la línia de recerca sobre AD, que es va demostrar que és una bona matèria primera per a la fabricació de taulers sense adhesiu, és necessari explorar més les condicions de producció de premsat i tractament tèrmic final. De fet, tal com es va trobar un umbral per a l'explosió de vapor, explorar diferents condicions per a les altres dues fases pot ajudar a definir els límits superiors i inferiors de cada una d'elles, per trobar l'òptima.

A més, es va trobar el umbral per a l'explosió de vapor de l'*Arundo donax* L., i això es pot verificar en altres materials per comprendre si depèn de modificacions dels components principals del material lignocel·lulòsic o no, i si per tant es pot generalitzar.

A més a més, l'anàlisi del cicle de vida realitzada en aquest estudi no contempla l'ús d'*Arundo donax* L., un estudi que sens dubte seria útil per comparar els resultats amb els que es van informar en aquest manuscrit i comprendre l'impacte ambiental de l'ús d'aquest material.

Annexes

This section includes:

- Annex A. Equipment and methods for boards manufacturing and characterization;
- Annex B. Methods for data analysis
- Annex C. Life cycle assessment methodologies, and data collection

Annex A. Equipment and methods for boards manufacturing and characterization

Annex content

This annex provides a description of the equipment and method employed for the production of the panels and specimens, as well as the characterization techniques utilized. It covers various aspects such as fiber pretreatment, panel formation via cold and hot pressing, post-treatment, and the tools used for sample manufacturing and characterization. Additionally, it includes additional electron microscope images of both pretreated and untreated material and specimens, which are relevant to Chapter 4.

A.1. Equipment and methods for raw material preparation

A.1.1. Wood chipper

The chipping was carried out with an electrical chipper, namely Gartenhäcksler Model LH 280 A (Ahien, Germany) (Figure A.1.). After chipping, *Arundo donax* L. (AD) chips are stored in bags of 750 g each, the maximum amount placed inside the steam explosion (STEX) reactor.

Figure A.1. *Picture of electrical chipper Gartenhäcksler LH 280 A.*

A.1.2. Steam boiler

The steam for STEX pretreatment was provided by an electrical Boreal boiler of 380 V/82 KW. The water comes from a 500 VA Millipore deionization equipment and is equipped with a Milli-RX 45 water purification system.

A.1.3. Steam explosion batch reactor

STEX equipment was made by the Justinox company, and the whole equipment was realized in stainless steel. It consisted of a 16 L cylindrical reactor at the top and a 100 L expansion chamber at the bottom, connected by a pneumatic valve, by which the sudden expansion occurs (Figure A.2.). A second valve is placed at the top of the reactor and allows to feed the lignocellulosic material (LM) to be treated. The whole equipment is provided by an autonomous control system, as well as the steam boiler for which the resistors stop every two hours. The reactor is also equipped with a jacket connected to the steam network that enables better temperature control. The expansion chamber can be opened by a exhaust port that covers the entire diameter, and it is equipped by two valves: one at the top for the removal of vapor to reduce the pressure inside the chamber, and one

at the bottom for the easy liquid outflow, obtained after the treatment. The amount of steam needed was estimated to be 0.2 kg of steam per kg of dry raw material.

Figure A.2. *Picture of steam explosion reactor and expansion chamber (Justinox company).*

A.1.4. Washing trolley

When the treated material is extracted from the expansion chamber, it is immediately washed using a washing trolley (Figure A.3.) equipped with a 170 mesh sieve to remove the products of the treatment including the hydrolyzed hemicellulose. An estimated amount of water of 10 L/kg of dry material was considered for the rinsing step.

After being washed the material is transported to a plat to be thoroughly distributed, and here it is left to dry for about 3 weeks, until it reaches a relative humidity (RH) of 8-10%.

Figure A.3. *Pictures of washing trolley and rinsing step.*

A.1.5. Miller

The dried pulp is ground with an electrical miller, namely Retsch SM 100 mill (Düsseldorf, Germany). The miller has the possibility of sieving using different sieve lights but, for this study it was equipped with a 4 mm sieve to control the maximum particle size (Figure A.4.).

Figure A.4. *Pictures of electrical miller Retsch SM 100.*

The results presented in the Chapter 6 were obtained during a research stay in the University George-August in Göttingen, Germany and the equipment used from this point forward of the process differs from the other chapters. In this case and Electra hammer mill (Poudenas, France) (Figure A.5.) was used.

Figure A.5. *Picture of the Electra hammer mill, used for grinding of steam exploded Arundo donax L. in Chapter 6.*

A.2. Equipment and methods for boards manufacturing

A.2.1. Drum blender

The results presented in the Chapter 6 were obtained by mixing the fibers (wood fibers WF and exploded AD fibers) with different percentage of pMDI, and water. The mixing was obtained by blending the fibers in a rotating drum blender (Figure A.6.) for 5 min at a speed of 30 round/min, spraying pMDI for the adhesive bonded samples, and water to adjust the moisture content from the initial 8% to 11% (necessary to ensure the formation of polyurea adhesive from pMDI) and homogenous mixing of the fibers both with and without the binder.

Figure A.6. *Picture of the drum blender used for mixing the fibers with pMDI and water (Chapter 6).*

The material required to achieve the desired thickness is weighed on the basis of relative humidity (Figure A.7.), from which the amount of water and pMDI in g to be used are derived. After blending, the weighed material is then placed inside a wooden molde, ready to be cold pressed.

Figure A.7. *Pictures of relative humidity measurement, weighting, and material inside the blender.*

A.2.2. Conventional press

The ground material was weighted with a balance and 28.5 g of milled pulp was placed into a mold of 150x50xthickness mm^3 (Figure A.8.) to be first cold pressed with a conventional press (MEGA-30 AN, Berriz, Spain) and then hot pressed with a Servitec Polystat 300 S (Wustermark, Germany).

Figure A.8. *Pictures of cold pressing process: weighing, mold preparation, and pressing.*

The cold hydraulic press (CP) that runs on compressed air and has a table on which the mold rests and a cylinder put into action with a knob that opens a valve for compressed air to pass through (Figure A.9.). For even distribution of the pressure over the surface of the mat, aluminum pieces of the same size as the molde were used.

Figure A.9. *Pictures of the cold press and the molds used for pressing the specimens.*

The hot press (HP) has an integrated hydraulic system to allow high pressure through an operation cylinder which moves the lower plate vertically. The hydraulic system runs under oil and allows a press force of 450 kN. The press is equipped with a control panel that allows the temperature of both plates to be set, and long-life heating cartridges made of aluminum provides an equal heating distribution. The press is also equipped of a cooling system, which allows a quick cooling under pressure achieved with flowing water inside the plates themselves. The set temperature is achieved through electrical power of 8 kW in each plate, which insure a temperature gradient of 10°/min and a maximum temperature of 300 °C. From the control panel also the pressure can be controlled. The pressure is reached manually through a lever on the side of the panel. The cold pressed specimen is placed into a mold equipped by a special piece that is inserted inside the mold to distribute the pressure (Figure A.10.). Furthermore, there is an additional layer between the panel and the aluminum piece, composed of a steel mesh which allows the vapors to escape.

Figure A.10. *Pictures of hot press and the mold used for manufacturing the specimens.*

For the results presented in the Chapter 6, the HP used was Joos LAP 40, Pfalzgrafenweiler, Germany for the first series, and the Joos HP-200 lab for the second series (Figure A.11.).

For the first series, the mixture of WF, exploded AD, and pMDI was first prepressed (Figure A.11.) into a mat and then placed in the HP at 205°C for 15 s/mm with a pressure of 5 N/mm^2, to form a board of 250x250x11 mm^3. On the other hand, the second series was made by changing the tp (30 s/mm), and the size (450x450x11 mm^3).

Figure A.11. *Pictures, from left to right, of: Cold press, Joos LAP 40 hot press, and Joos HP-200 lab hot press (Chapter 6).*

A.2.3. Sander and cutter

For the results presented in Chapter 6, the cooling of the specimens after hot pressing is followed by two more steps before conditioning: sanding and cutting of the specimens. The sanding step was included to equalize the thicknesses and surface finish of the panels. The sander used is from the brand Kundis (Werkstatt, Büsgenweg 4). The panels are then cut by an industrial cutter from the brand Felder (Figure A.12.).

Figure A.12. *Pictures of Kundis sander, and Felder cutter (Chapter 6).*

A.2.4. Aerated stove

After pressing the panels, in most cases they are further treated with a curing treatment, namely the final heat treatment (FHT). The treatment is carried out by using an electrical aerated stove of 1600 W, made by the brand JP Selecta SA (Abrera, Barcelona) (Figure A.13.). The parameters are set via a control panel that allows to set the desired time (tc) and temperature (Tc).

Figure A.13. *Picture of electrical aerated stove JP Selecta SA (1600 W).*

A.2.5. Cutter

For panels made already to specimen size for mechanical properties (for all chapters except Chapter 6), cutting is done to make IB, TS, and WA tests, resulting in specimens of size 50x50xthickness mm^3.

For smaller thicknesses, a small cutter (TÜVRheinland) was used, and for larger thicknesses, the Holzkraft HBS 431 was used (Figure A.14.).

Figure A.14*. Pictures of TÜVRheinland and Holzkraft HBS 431 cutters.*

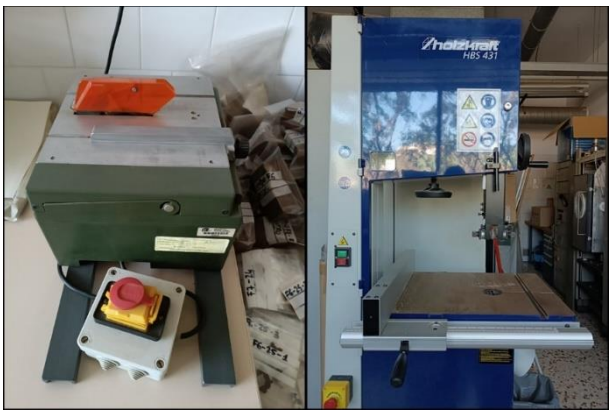

A.2.6. Climatic chamber

After being manufactured, the panels are stored in a climatic chamber Asis 10 (Figure A.15.) at the desired conditions until the difference in weight between two successive weighing in 24 h is equal or less than 0.01. The weight is measured with an electrical precision scale (Figure A.15.).

Figure A.15. *Pictures of the climatic chamber, the samples during conditioning, and the precision scale used for weighing.*

A.3. Equipment and methods for boards characterization

A.3.1. Mechanical characterization

MOE and MOR were tested simultaneously according to the EN 310:1993, by using the universal testing machine HOUNSFIELD H10KS (Figure A.16.), and for the results presented in the Chapter 6, Zwick-Roell Z010 (Zwic-Roell, Ulm, Germany) was used (Figure A.16.).

Figure A.16. *Pictures of the universal testing machine HOUNSFIELD H10KS, and Zwick-Roell Z010.*

The specimens are tested in the full size produced, i.e. 150x50xthickness and they are supported in two point at the edges and the charge is applied in the center of the specimen to determine the

resistance and the elasticity under flexural load. The two supports are parallel and made by two cylindrical rollers whose distance can be set as desired. The force is applied through a central cylinder equidistant from the two supports, with a speed such that the maximum force is reached in 60±30 s.

The MOE is expressed in N mm^{-2} and it is calculated according to the equation:

$$MOE = \frac{[l_1^3(F_2 - F_1)]}{[4bt^3(a_2 - a_1)}$$

Where:

l_1 is the distance between the two cylindrical supports

b is the width of the specimen in mm

t is the thickness of the specimen in mm

$F_2 - F_1$ is the increment in N of the charge in the linear section of the load-deformation curve

F_1 is approx. considered as a 10% of the F_{max}, while F_2 is approx. equal to a 40% of the F_{max}.

$a_2 - a_1$ is the increment in mm of the deformation in the center of the specimen corresponding to F_2 and F_1, respectively.

For each sample the MOE is indicated as the average of the values of each specimen, and the standard deviation (St.Dev.).

The MOR is expressed in N mm^{-2} and it is calculated as follow:

$$MOR = \frac{3F_{max}l_1}{2bt^2}$$

Where:

F_{max} is the maximum charge in N

l_1, b, and t are the same values used for MOE and expressed in mm

For each sample the MOR is indicated as the average of the values of each specimen, and the St.Dev.

The IB was tested according to EN 319:1993 using the same universal testing machine used for MOE and MOR, by changing the supports. The IB is the tensile strength perpendicular to the faces and it is a measure of the internal cohesion of the boards. The specimens used for the IB test have a size of 50x50xthickness mm^3 and they are cut from the full size specimens (150x50xthickness mm^3) after the flexural failure test. These specimens are glued with epoxy resin onto T-shaped metal supports, taking care to leave the side surface of the specimen free of any glue residue so that this does not affect the result (Figure A.17.).

Figure A.17. *Pictures of internal bond test.*

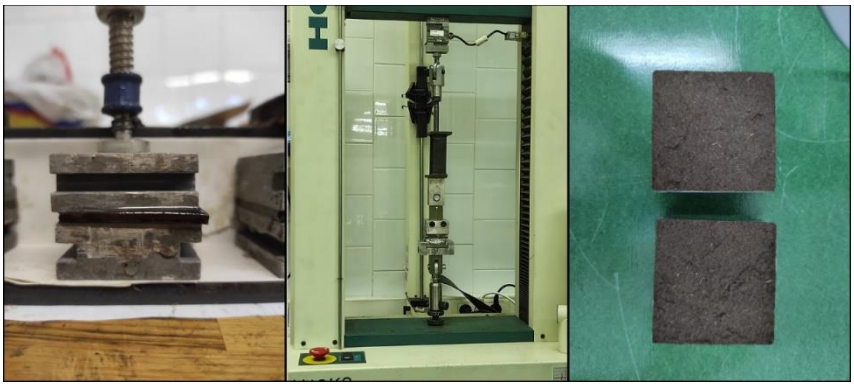

The specimens glued onto the T-shaped supports are the placed in the universal testing machine equipped with grip blocks to hook the specimen. The force is applied with constant speed such that the maximum force is reached in 60±30 s.

The IB is expressed in N mm^{-2} according the following formula:

$$IB = \frac{F_{max}}{axb}$$

Where:

F_{max} is the breaking load in N

a, b are the length and width in mm

In the case where some specimens exhibit a non-uniform rupture, i.e. they detached from the support and do not break approx. in the central plane, the results are either discarded or are corrected by considering the actual area, depending on the extent of the area detached (Figure A.18.).

For each sample the IB is indicated as the average of the values of each specimen, and the St.Dev.

Figure A.18. *Pictures of detached specimens during the internal bond test.*

A.3.2. Physical characterization

Density was calculated according to the EN 323:1993 on specimen measuring approx. 150x50xthickness mm^3 and conditioned at 20°C and 65% RH.

Density is expressed in kg m^{-3} as the ratio between mass and volume:

$$\rho = \frac{m}{b_1 x b_2 x t}$$

Where:

m is the mass of the specimen in kg

b_1, b_2, t are the length, the width, and the thickness, respectively, in m

The weight is measured by a precision scale (Figure A.19.) with a precision of 0.001 g, while the exact size of the specimen is obtained by a digital scale for length and width (Figure A.19.), and a digital micrometer for the thickness (Figure A.18.), both with a precision of 0.01 mm. The thickness is measured in 5 points, i.e., the 4 corners and the center; the length in measured on both longer edges, and the width is measured on the two edges and on the center.

For each sample the density is indicated as the average of the values of each specimen, and the St.Dev.

WA and TS are tested simultaneously, the latter according to the EN 37:1993 on specimens have a size of 50x50xthickness mm^3.

The TS measure the swelling of the board as the percentage (%) of the ratio of the change in thickness due to water absorption in a given period of time, to the initial thickness:

$$TS = \frac{t_2 - t_1}{t_1} \; x \; 100$$

Where:

t_1 is the initial thickness in mm

t_2 is the thickness after the water bath in mm

On the other hand, WA measure the change in weight expressed as the percentage (%) of the ratio of the change in weight due to the water absorption in a given period of time, to the initial weight:

$$WA = \frac{m_2 - m_1}{m_1} \; x \; 100$$

Where:

m_1 is the initial weight in g

m_2 is the weight after the water bath in g

Figure A.19. *Pictures of the precision scale, the digital scale, and the digital micrometer.*

The weight is measured with a precision scale before and after the water bath (Figure A.19.) with a precision of 0.001 g, while the thickness is measured by a digital micrometer (Figure A.19), with a precision of 0.01 mm, in 5 points, i.e., the 4 corners and the center. The water bath consists of deionized water in which the specimens are immersed in a vertical position. The measurement is mainly done after 24 h, but for some series also at 2 h, 48 h, and 72 h, by first removing the excess water from the specimens (Figure A.20.).

Figure A.20. *Pictures of thickness swelling and water absorption test (Chapter 6).*

A.3.3. Chemical and morphological characterization

FT-IR is an analytical method used to analyze the structure of individual molecules or the composition of molecular mixtures. It determines a semi-quantitatively chemical structure using energy modulated in the infrared band to study a sample. Infrared light is absorbed at specific frequencies that correspond directly to the vibrational energy levels of the bonds between atoms in the molecule. In this study, Spectroscopy id used aiming at understanding the changes in the structure after various steps in the production process (specifically STEX, HP, and FHT), thus obtaining important information

to optimize the process. The FT-IR spectra are obtained using a FT-IR 6700 Jasco spectrometer, by pressing the sample on the diamond surface of an ATR probe. 32 scans in a frequency range of 400 to 4000 cm^{-1} at a resolution of 4 cm^{-1} were made for the raw material, the exploded material, and the finished boards. The absorption bands were assigned as follows (Table A.1.).

Table A.1. *Characteristic bands assigned in FT-IR spectra (SDBS database)*

Wavenumber [cm^{-1}]	Band origin	Assigned compound
875	glycosidic linkage	hemicellulose
930	glycosidic linkage	cellulose, hemicellulose
990	C-O valence vibration	cellulose
1110-1035	C-O, C=C, C-C-O stretching	cellulose, hemicellulose, lignin
1160	C-O-C asymmetrical stretching	cellulose, hemicellulose
1200	O-H bending	cellulose, hemicellulose
1215	C-C+C-O stretch	lignin (wood)
1270	aromatic ring vibration	guiacyl lignin
1280	C-H bending	crystalline cellulose
1310	CH2 wagging	cellulose, hemicellulose
1327	C-O of syringyl ring	lignin (wood)
1335	C-H vibration, O-H in plane bending	cellulose, hemicellulose, lignin
1380	C-H bending	cellulose, hemicellulose, lignin
1425	C-H in plane deformation	lignin (wood)
1440	O-H in plane bending	cellulose, hemicellulose
1465	C-H deformation	lignin
1500-1510	aromatic ring vibration	lignin
1595	aromatic ring vibration+C=O stretch	lignin
1632-1682	C=O stretching (unconjugated)	lignin (wood)
1730-1740	ketone/aldehyde C=O stretch	hemicellulose
1750	free ester	hemicellulose
2840-2937	C-H stretching	lignin (wood)
3415-3421	O-H stretching	lignin (wood)
	NH groups	urethane bonds

TGA is an analytical technique that measures weight changes in a material when subjected to a gradual and controlled increase in temperature. The weight of the specimen is monitored continuously as a function of temperature or time while the specimen is subjected controlled temperature program in a controlled atmosphere. Therefore, TGA determines a quantitative analysis of the composition of a specimen without directly identifying the nature of the components. Identification of the components can still be made on the basis of preliminary data on the nature of the specimen, laboratory experience, and data from the literature.

In this case, the test was carried out by means of a Mettler TGA/SDTA 851e thermobalance (Columbus, OH, USA), and consists of placing a small amount of material, between 8 and 10 mg, inside the crucible that

is subjected to the controlled increase in temperature, from ambient temperature up to 800°C, in inert atmosphere (nitrogen atmosphere). As a result, a stepped curve is obtained where each step represent a weight loss due to the evaporation/degradation of the components of the specimen being analyzed, thus obtaining information about the composition of the specimen and its thermal stability. The weight of the sample at the end of the test is the so-called char yield (CY). The CY is related to the Limiting Oxygen Index (LOI), defined as follow:

$$LOI = 17.5 + 0.4CY$$

LOI is defined as the minimum concentration of oxygen in a mixture of oxygen and nitrogen that is needed to support the flaming combustion of a material. It was first proposed in 1966 by Fenimore and Martin (Koncar, 2019) to indicate the relative flammability of materials, and was then standardized internationally (ISO 4589). The LOI is relatively unsophisticated method today because of the development and standardization of more elaborated methods, but it remains one of the most important screening and quality control methods used mainly in the plastics and related industries.

Electron microscopy is a technique that exploit the interaction between an electron beam and the atoms that make up the specimen under examination, and allows images to be generated at high magnification. Therefore, SEM consists of few essential elements: the electron source from which the electron beam is generated; a column of several lenses which allow the beam to be controlled; a series of detectors that collect the signal generated as a result of the interaction between the beam and the specimen, which allow the reconstruction of the image; a stage on which the sample is placed; a vacuum system which ensure a vacuum level to prevent the beam or the signals from encountering obstacles, with which they would interact resulting in a noisier image and less accurate analysis.

In this case, SEM images were obtained by using FEI ESEM Quanta 600. The specimens were first dried in the aerated stove at 40°C for 2 days. They were mounted on an adhesive stub and then observed in low vacuum mode with acceleration voltage of 15kV, distance of approx. 20 mm, and magnification of x250. Some additional SEM images related to Chapter 4 are reported in the following section.

VDP were obtained using an X-ray densitometer (DAX, Fagus-Grecon GmbH & Co. KG, Alfeld, Germany). The specimens were cut from the full size to a dimension of 50x50xthickness mm^3 and put inside the densitometer in the armored compartment. The X-ray equipment was

calibrated for continuous thickness scanning of the specimens by the X-ray beam and the scanning was at intervals od 0.01 mm. As a result, information on the uniformity of specimens were obtained, as well as a more comprehensive view of the dependence of mechanical properties on density.

A.4. Additional SEM images related to Chapter 4.

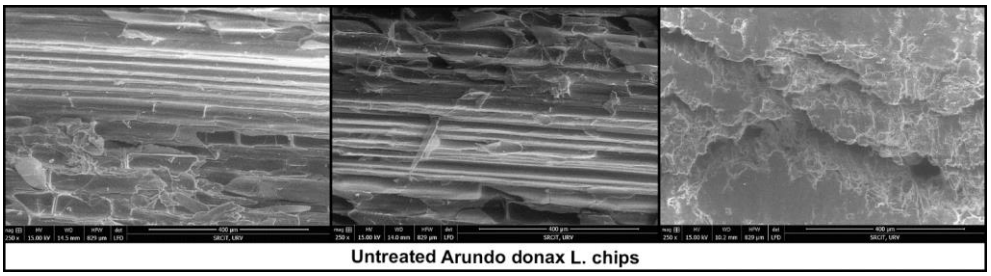

Untreated Arundo donax L. chips

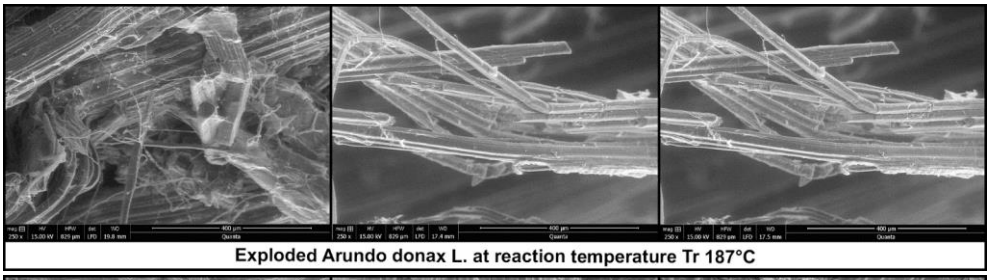

Exploded Arundo donax L. at reaction temperature Tr 187°C

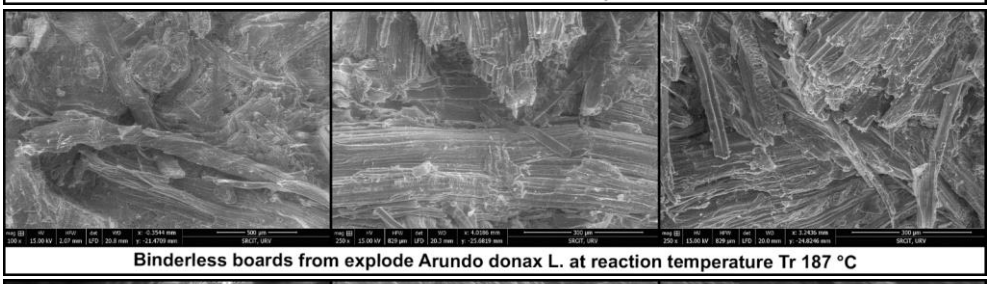

Binderless boards from explode Arundo donax L. at reaction temperature Tr 187 °C

Exploded Arundo donax L. at reaction temperature Tr 190°C

Binderless boards from explode Arundo donax L. at reaction temperature Tr 190 °C

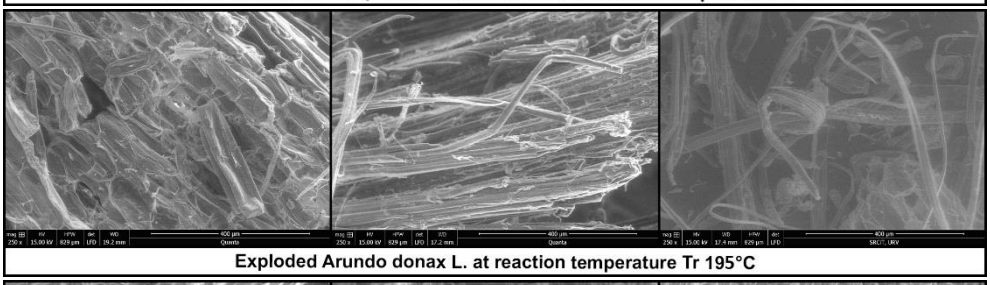

Exploded Arundo donax L. at reaction temperature Tr 195°C

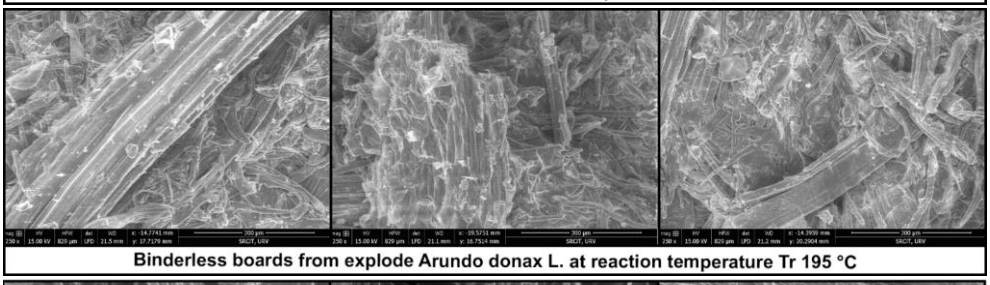

Binderless boards from explode Arundo donax L. at reaction temperature Tr 195 °C

Exploded Arundo donax L. at reaction temperature Tr 200°C

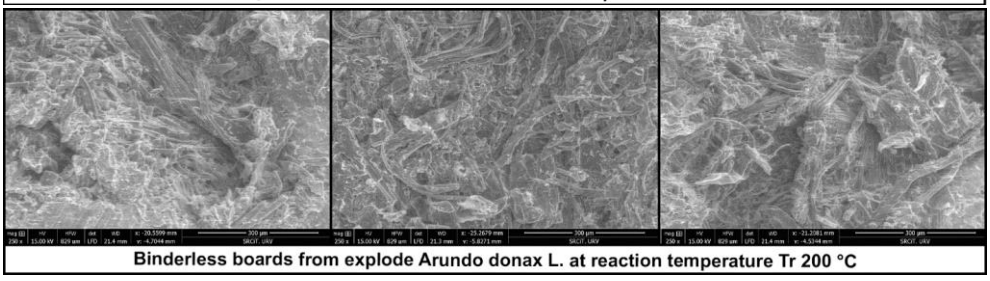

Binderless boards from explode Arundo donax L. at reaction temperature Tr 200 °C

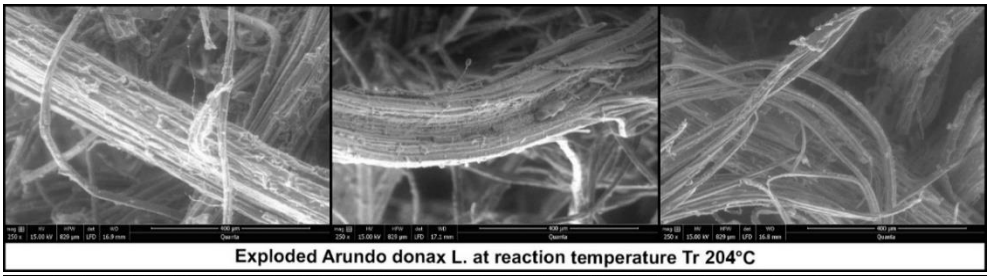

Exploded Arundo donax L. at reaction temperature Tr 204°C

Binderless boards from explode Arundo donax L. at reaction temperature Tr 204 °C

Annex B. Methods for data analysis

Annex content

This annex provides the description of the statistical analysis methods employed for the data. Firstly, it briefly describes statistical tools such as boxplot, analysis of variance, and Tukey's multiple comparison. Secondly, it presents specific details regarding the data analysis for each chapter, including a summary of the method used and the resulting outcome.

B.1. Methods for statistical analysis

B.1.1. Box and whiskers plot

A boxplot is a statistical graph illustrating the distribution of data, serving as a visual tool for checking normality or identifying possible outliers. It contains information about:

- The minimum value;
- The first quartile (25th percentile);
- The median (50th percentile);
- The third quartile (75th percentile);
- The maximum value.

Thus, the graph presents the width of the middle half of the distribution: the height of the box coincides with the interquartile range and it contains the observations made that lie between the first and third quartiles, and the median represented by the line inside the box. The two segments extending upward and downward from the box are the "whiskers" and express the dispersion of values below the first quartile and above the third quartile not labeled as outliers. In the presence of outliers, they appear in the boxplot as isolated points either above and/or below the whiskers of the distribution.

In Rstudio the code used to produce a boxplot is:

```
> boxplot(dependent_variable$indipendent_variable)
```

B.1.2. Analysis of variance (ANOVA)

ANOVA is a statistics tool used to compare the variances between the means of different groups. It is used to determine the influence that independent variables have on the dependent variable in a regression study. The analysis returns an F-value equal to the ratio between the mean sum of squares due to the treatment, and the mean sum of squares due to error. The p-value related to the F-statistic is calculated on the basis of the degrees of freedom of the considered variable and the residuals, and is the most important value of the analysis to understand what the effect of the treatment (independent variable) considered is.

There are two types of ANOVA that are commonly used, the one-way ANOVA and the two-way ANOVA, depending on the number of independent variables. In the case, the independent variables considered are the conditions of the production process, while the dependent variables, whose response is studied, are the mechanical (MOE, MOR, and IB) and physical (density, TS, and WA) characteristics of the binderless boards.

The limitation of ANOVA is that it can exclusively indicate whether there is a significant difference between the means of at least two groups, but it cannot explain which pair differs. For this reason, ANOVA is used in combination with other statistical methods, such as multiple comparison methods.

B.1.2.1. One-way ANOVA

One-way ANOVA compares the variance in the group means within a samples by considering only one independent variable or factor. In a one-way ANOVA there are two possible hypothesis:

- The null hypothesis (H0): there is no difference between the groups and the means are equal;
- The alternative hypothesis (H1): there is a difference between the means and groups.

The assumptions needed to perform one-way ANOVA include the normally distribution of the data, the homogeneity of the variance, and the independence of the observations from each other.

The code used in R to develop the ANOVA is reported below, with the corresponding verification of the assumptions.

```
#separation of the variables
> attach(dataset)
#normality test: if p-value>0.05 the normality is verified
> shapiro.test(dependent_variable)
#homoscedasticity test: if p-value>0.05 the homogeneity of the
variance is verified
> levene.Test(dependent_variable~fac)
#creating ANOVA model
>model = aov(dependent_variable~fac)
#displaying the model
>summary(model)
Output:
            Df     Sum Sq        Mean Sq       Fvalue        Pr(>F)
factor
Residuals
Signif. Codes: 0 ‘***’ 0.001 ‘**’ 0.01 ‘*’ 0.05 ‘.’     0.1 ‘ ’
1
```

Where:

Df (factor): degrees of freedom of the independent variable calculated as #groups-1.

Df (residuals): degrees of freedom of the residuals (errors) calculated as #total pbservations-#groups.

Sum Sq (factor): sum of squares of the dependent variable considered.

Sum Sq (residuals): sum of squares of the residuals of the variable considered

Mean Sq (factor): mean sum of squares associated with the variable considered, calculated as the Sum Sq divided for the Df of the variable.

Mean Sq (residuals): mean sum of squares associated with the residuals of variable considered, calculated as the Sum Sq divided for the Df of the residuals.

F-value: the overall F-statistic of the ANOVA model, calculated as the Mean Sq of the variable divided for the Mean Sq of the residuals.

Pr(>F): the p-value related to the F-statistic, and the Df of the variable and the residuals.

B.1.2.2. Two way ANOVA

Two-way ANOVA compares the variance in the group means within a samples by considering two factors. Hence, the two-way ANOVA examines the effects of two factors, and whether they affect each other to influence the dependent variable.

In a two-way ANOVA there are three pairs of null and alternative hypothesis. Considering the two factor as 1st factor and 2nd factor:

- H0: the means of all 1st factor groups are equal;
- H1: the means of at least one of 1st factor group is different.

- H0: the means of all 2nd factor groups are equal;
- H1: the means of at least one of 2nd factor group is different.

- H0: there is no interaction between 1st and 2nd factor;
- H1: there is interaction between 1st and 2nd factor.

The assumptions needed to perform two-way ANOVA are the same of the one-way model, and the two independent variables must be in two separate, categorical, independent groups.

The code used in R to develop the ANOVA is reported below, with the corresponding verification of the assumptions.

```
#separation of the variables
> attach(dataset)
#normality test: if p-value>0.05 the normality is verified
> shapiro.test(dependent_variable)
#homoscedasticity test: if p-value>0.05 the homogeneity of the variance is verified
>levene.Test(dependent_variable~interaction(1stfac, 2ndfac)
#creating ANOVA model
>model = aov(dependent_variable~1stfac*2ndfac)
#displaying the model
>summary(model)
Output:
            Df     Sum Sq        Mean Sq       Fvalue Pr(>F)
1st fac
2nd fac
1st fac : 2nd fac
Residuals
Signif. Codes: 0 '***' 0.001 '**' 0.01 '*' 0.05 '.' 0.1 ' ' 1
```

Where:

Df (factor): degrees of freedom of the independent variable calculated as #groups-1.

Df (residuals): degrees of freedom of the residuals (errors) calculated as #total pbservations-#groups.

Sum Sq (factor): sum of squares of the dependent variable considered.

Sum Sq (residuals): sum of squares of the residuals of the variable considered

Mean Sq (factor): mean sum of squares associated with the variable considered, calculated as the Sum Sq divided for the Df of the variable.

Mean Sq (residuals): mean sum of squares associated with the residuals of variable considered, calculated as the Sum Sq divided for the Df of the residuals.

F-value: the overall F-statistic of the ANOVA model, calculated as the Mean Sq of the variable divided for the Mean Sq of the residuals.

Pr(>F): the p-value related to the F-statistic, and the Df of the variable and the residuals.

B.1.3. Multiple comparison

As mentioned, ANOVA cannot provide information on differences among the groups considered, or on combination of them. Further tests, called post hoc test are necessary to fully comprehend the groups' differences. These tests are conducted on subset of data previously tested by ANOVA, and they are the multiple comparison analysis tests.

Tukey's multiple comparison test was the one reported for the statistical analysis of the data reported in this manuscript, and it is also called Tukey's honestly significance difference (HSD).

Tukey's test is performed when ANOVA reveals that the group means differ, to investigate which of them are different. Indeed, the test compare the difference between each pair of means, showing the results in a matrix in which the p-value for each pair is presented. As it is a post hoc test performed after ANOVA, it has the same assumptions of ANOVA: normal distribution of the population, and homoscedasticity.

Assuming that a one-way ANOVA was performed, with a three level factor consisting of three categorical groups (1,2,and 3), the code used in R to develop the Tukey HSD is reported below.

```
> TukeyHSD(model)
Output:
          diff          lwr          upr          p adj
2-1
3-1
3-2
```

Where:

2-1;3-1;3-2 are all the possible pairs for comparison, for a three level factor.

diff is the difference in means.

lwr is the lower value of the confidence interval.

upr is the upper value of the confidence interval.

p adj is the adjusted p-value for each pair.

B.2. Data analysis specification

B.2.1. Data analysis Chapter 3

The data analysis in Chapter 3 focuses on exploring the effects of the severity (R_0) of steam explosion (STEX) pretreatment on *Arundo donax* L. fibers and binderless fiberboards. To study the effect of R_0, five samples are made, each of 9 to 11 specimens, at different R_0. The severity indicates the combined intensity of the reaction time (tr) and reaction temperature (Tr), and in this case, we choose to change only the Tr and leave the tr unchanged for all samples. The analysis model chosen is a one-way ANOVA, given that the factor considered (i.e., Tr) is unique and at five levels, i.e., the five R_0. Table B.1. summarizes methods, factors, and results from the data analysis.

Table B.1. *Summary of methods, factors, and results of the data analysis from Chapter 3.*

ANOVA method		one-way
number of independent variables (factor)		1
factor(s) name		Tr
number of factor levels		5
names of factor levels		187;190;195;200;204
number of dependent variables		6
p-value		
	Density	***
	MOE	***
	MOR	***
	IB	***
	TS	***
	WA	***
Multiple comparison method		Tukey HSD
Highlighted results of Tukey HSD		Optimum at Tr 200°C Threshold between 190°C and 195°C

Significance codes: * for values ≤ 0.01; ** for values ≤ 0.001; *** for values ≤ 0.0001

B.2.2. Data analysis Chapter 4

Data analysis in Chapter 4 focuses on exploring the effect of final heat treatment (FHT) parameters, i.e., curing temperature (Tc), and curing time (tc). The analysis takes place on two levels. The first part analyzes the effect of time with a one-way analysis, setting tc as the independent variable (Table B.2.). This analysis shows that there is no

statistically significant difference between the two times 0.5 h and 1 h, both with a Tc of 180°C. Therefore, the second part of the analysis combines the results of these two times into one group (FHT YES), to study the effect of FHT and its interaction with the second pressing pressure (Pp_2), both used as factors in the analysis. Indeed, this second part is developed with a two-way model and the analysis is repeated with the same method for both the results obtained below the threshold, i.e., at Tr 190 °C (Table B.3.), and the results obtained above the threshold, i.e., 200 °C (Table B.4.).

Table B.2. *Summary of methods, factors, and results of the data analysis from Chapter 4, related to the first part of the analysis: one-way analysis with tc factor.*

ANOVA method		one-way
number of independent variables (factor)		1
factor(s) name		tc
number of factor levels		4
names of factor levels		0;5;0.5;1
number of dependent variables		6
p-value		
	Density	***
	MOE	***
	MOR	***
	IB	***
	TS	***
	WA	***
Multiple comparison method		Tukey HSD
Highlighted results of Tukey HSD		tc 0.5 h ≈ tc 1 h Optimum at tc 5 h and Tc 165 °C

Significance codes: * for values ≤ 0.01; ** for values ≤ 0.001; *** for values ≤ 0.0001

Table B.3. *Summary of methods, factors, and results of the data analysis from Chapter 4, related to the second part of the analysis: two-way analysis for results above the threshold, i.e., at Tr 200 °C.*

ANOVA method		two-way	
number of independent variables (factor)		2	
factor(s) name		FHT	
		Pp_2	
number of factor levels		2	
		2	
names of factor levels		YES;NO	
		3.3;7.5	
number of dependent variables		6	
p-value		FHT	Pp_2
	Density	>0.05	>0.05
	MOE	**	***
	MOR	**	**
	IB	***	***
	TS	***	**
	WA	***	***
Multiple comparison method		Tukey HSD	
Highlighted results of Tukey HSD		FHT and Pp_2 influence both mechanical results (MOE, MOR, and IB), and dimensional stability (TS, and WA)	
		No interaction between FHT and Pp_2	
		FHT compensates the lower Pp_2	

Significance codes: * for values ≤ 0.01; ** for values ≤ 0.001; *** for values ≤ 0.0001

Table B.4. *Summary of methods, factors, and results of the data analysis from Chapter 4, related to the second part of the analysis: two-way analysis for results below the threshold, i.e., at Tr 190 °C.*

ANOVA method		two-way	
number of independent variables (factor)		2	
factor(s) name		FHT Pp_2	
number of factor levels		2 2	
names of factor levels		YES;NO 3.3;7.5	
number of dependent variables		6	
p-value		FHT	Pp_2
	Density	>0.05	***
	MOE	>0.05	>0.05
	MOR	>0.05	>0.05
	IB	>0.05	>0.05
	TS	***	**
	WA	***	***
Multiple comparison method		Tukey HSD	
Highlighted results of Tukey HSD		FHT and Pp_2 only influence dimensional stability (TS, and WA) No interaction between FHT and Pp_2 FHT cannot compensate the lower Pp_2	

Significance codes: * for values ≤ 0.01; ** for values ≤ 0.001; *** for values ≤ 0.0001

B.2.3. Data analysis Chapter 5

Data analysis in Chapter 5 focuses on exploring the effect of thickness on final properties of binderless boards. Here again, the analysis takes place on two levels. The first part analyzes the effect of three different thicknesses with a one-way analysis, setting the thickness as the independent variable (Table B.5.). This analysis shows that thickness has a major influence on mechanical properties. With the second part of the analysis, we wanted to study the effect of FHT and its interaction with the thickness, both used as factors in the two-way analysis (Table B.6.).

Table B.5. *Summary of methods, factors, and results of the data analysis from Chapter 5, related to the first part of the analysis: one-way analysis with thickness as factor.*

ANOVA method		one-way
number of independent variables (factor)		1
factor(s) name		thickness
number of factor levels		3
names of factor levels		3.8;7.6;11.1
number of dependent variables		6
p-value		
	Density	***
	MOE	***
	MOR	***
	IB	***
	TS	**
	WA	>0.05
Multiple comparison method		Tukey HSD
Highlighted results of Tukey HSD		Thickness has a major effect on mechanical properties (MOE, MOR, and IB) Optimum at thickness ≈ 3 mm

Significance codes: * for values ≤ 0.01; ** for values ≤ 0.001; *** for values ≤ 0.0001

Table B.6. *Summary of methods, factors, and results of the data analysis from Chapter 5, related to the first part of the analysis: one-way analysis with thickness as factor.*

ANOVA method		two-way	
number of independent variables (factor)		2	
factor(s) name		FHT thickness	
number of factor levels		2 3	
names of factor levels		YES;NO 3.8;7.6;11.1	
number of dependent variables		6	
p-value		FHT	thickness
	Density	>0.05	***
	MOE	>0.05	***
	MOR	>0.05	>0.05
	IB	>0.05	***
	TS	***	>0.05
	WA	***	>0.05
Multiple comparison method		Tukey HSD	
Highlighted results of Tukey HSD		FHT influences mainly dimensional stability (TS, and WA) Thickness influences mainly mechanical properties (MOE, and IB) No interaction between FHT and thickness Optimum at thickness ≈ 3 mm	

Significance codes: * for values ≤ 0.01; ** for values ≤ 0.001; *** for values ≤ 0.0001

In particular, the second part of the analysis is based on one of the results obtained in the previous chapters, namely, that there is no significant difference between tc 0.5 h and 1 h. The demonstration of the validity of this assumption for this case too is given below:

```
   > modeldensity=aov(DENSITY~factor(tc)+factor(thick),
data = data5)
   > summary(modeldensity)
                Df Sum Sq Mean Sq F value   Pr(>F)
   factor(tc)    2    194      97   0.409    0.669
   factor(thick)  2  12288    6144  25.920 8.02e-07 ***
   Residuals     25   5926     237
   > TukeyHSD(modeldensity)
     Tukey multiple comparisons of means
       95% family-wise confidence level
   factor(tc)`
              diff       lwr      upr p adj
   0.5-0 -4.236077 -21.38607 12.91391 0.81
   1-0   -6.072966 -23.22296 11.07702 0.65
   1-0.5 -1.836889 -18.98688 15.31310 0.96

   > modelMOE=aov(MOE~factor(tc)+factor(thick), data =
   data5)
   > summary(modelMOE)
                Df  Sum Sq Mean Sq F value   Pr(>F)
   factor(tc)    2  144450   72225   1.029    0.372
   factor(thick)  2 2851337 1425669  20.310 5.77e-06 ***
   Residuals     25 1754888   70196
   > TukeyHSD(modelMOE)
     Tukey multiple comparisons of means
       95% family-wise confidence level
   factor(tc)`
            diff       lwr      upr p adj
   0.5-0 -153.63 -448.7603 141.5003 0.41
   1-0   -139.79 -434.9203 155.3403 0.47
   1-0.5   13.84 -281.2903 308.9703 0.99

   > modelMOR=aov(MOR~factor(tc)+factor(thick), data =
   data5)
   > summary(modelMOR)
                Df Sum Sq Mean Sq F value Pr(>F)
   factor(tc)    2   1.40   0.700   0.228 0.7974
   factor(thick)  2  18.01   9.005   2.937 0.0715 .
   Residuals     25  76.65   3.066
   > TukeyHSD(modelMOR)
     Tukey multiple comparisons of means
       95% family-wise confidence level
   factor(tc)`
           diff       lwr      upr p adj
   0.5-0 0.3262 -1.624271 2.276671 0.90
   1-0   0.5241 -1.426371 2.474571 0.78
   1-0.5 0.1979 -1.752571 2.148371 0.96

   > modelIB=aov(IB~factor(tc)+factor(thick), data =
   data5)
   > summary(modelIB)
                Df Sum Sq Mean Sq F value   Pr(>F)
   factor(tc)    2 0.0098 0.00490   0.828    0.449
   factor(thick)  2 0.4748 0.23738  40.085 1.59e-08 ***
   Residuals     25 0.1480 0.00592
   > TukeyHSD(modelIB)
     Tukey multiple comparisons of means
       95% family-wise confidence level
   factor(tc)`
             diff        lwr        upr p adj
```

```
0.5-0 -0.02133 -0.1070516 0.06439161 0.81
1-0   -0.04427 -0.1299916 0.04145161 0.41
1-0.5 -0.02294 -0.1086616 0.06278161 0.78

> modelTS=aov(TS~factor(tc)+factor(thick), data =
data5)
> summary(modelTS)
             Df Sum Sq Mean Sq F value   Pr(>F)
factor(tc)    2  15414    7707 127.336 7.78e-14 ***
factor(thick)  2      2       1   0.016    0.984
Residuals     25   1513      61
> TukeyHSD(modelTS)
  Tukey multiple comparisons of means
    95% family-wise confidence level
factor(tc)`
            diff       lwr        upr p adj
0.5-0 -41.00987 -49.67602 -32.343712 0.00
1-0   -52.92016 -61.58632 -44.254005 0.00
1-0.5 -11.91029 -20.57645  -3.244137 0.06
```

B.2.4. Data analysis Chapter 6

Data analysis in Chapter 6 focuses on exploring the effect of material formulation on the final properties of medium density fiberboards (MDF). Data from two series are analyzed: the first made by mixing AD and wood fibers (WF), with and without pMDI; the second made by mixing WF and AD in different percentages, and without any adhesive.

For the first series the means are compared on two levels (Table B.7.): on the one hand between the specimens made with the same fiber formulation (AD, WF, and their combination) with and without adhesive (e.g. WF0-WF4); on the other hand between the specimens with different fiber formulation within the same self-bonded or pMDI-bonded group, indicated with the numbers 0 and 4, respectively (e.g. WF0-AD0). For the second series the one-way analysis is performed by using the variation as a three level factor (Table B.8.).

Table B.7. *Summary of methods, factors, and results of the data analysis from Chapter 6, related to the first series by one-way analysis with variation as factor.*

ANOVA method	one-way
number of independent variables (factor)	1
factor(s) name	variation
number of factor levels	6
names of factor levels	WF0;WF4;WFAD0;WFAD4;AD0;AD4
number of dependent variables	6
p-value	
Density	***
MOE	***
MOR	***
IB	***
TS	***
WA	***
Multiple comparison method	Tukey HSD
Highlighted results of Tukey HSD	pMDI improves the properties STEX AD improves properties, especially dimensional stability AD0 shows the best performance for self-bonded boards WF4 shows the best performance for pMDI-bonded boards

Significance codes: * for values ≤ 0.01; ** for values ≤ 0.001; *** for values ≤ 0.0001

Table B.8. *Summary of methods, factors, and results of the data analysis from Chapter 6, related to the second series by one-way analysis with variation as factor.*

ANOVA method	one-way
number of independent variables (factor)	1
factor(s) name	variation
number of factor levels	3
names of factor levels	WFAD40/60;WFAD20/80;AD100
number of dependent variables	6
p-value	
Density	**
MOE	*
MOR	>0.05
IB	***
TS	***
WA	***
Multiple comparison method	Tukey HSD
Highlighted results of Tukey HSD	STEX AD percentage improves the properties, especially dimensional stability WFAD40/60 ≈ WFAD20/80 for mechanical properties AD100 shows the best performance

Significance codes: * for values ≤ 0.01; ** for values ≤ 0.001; *** for values ≤ 0.0001

Annex C. Life cycle assessment methodologies and data collection

Annex content

This annex refers to Chapter 7, relating to the environmental impact of the production process of binderless fiberboards. Here, the life cycle assessment is explored, presenting the most common methods used, with particular attention to the ReCiPe method, which is the one used in Chapter 7. In addition, the input calculation presented in the Chapter are outlined in this annex.

C.1. Introduction and regulations

LCA is a methodology aiming at evaluating the environmental effects of a product over its entire life. This method has been standardized internationally by ISO-14040, and ISO-14044, both actualized in 2006. The first international standard refers to principles and framework of LCA, while the second defines some guidelines for the development of a LCA study. The ISO also provide a unique definition of LCA, namely:

"Compilation and evaluation of the inputs, outputs, and the potential environmental impacts of a product system throughout its life cycle"

As defined by the cited standards, as part of the analysis of a product's environmental impact, LCA can assist in identifying the opportunities to improve the footprint as it addresses the environmental aspects and potential impact throughout a product's life cycle, from the raw material acquisition, through production, use, end-of-life, recycling, and disposal.

LCA is defined as a relative and iterative approach structured by defining the functional unit, which defines what is being studied and to which all the inputs and outputs are related. According to the cited ISO, it must follow four steps to define the environmental impact:

- Goal and scope definition, including the system boundary and level of detail;
- Inventory analysis (LCI), a collection of input and output data of the system being studied;
- Impact assessment (LCIA), which helps to assess LCI results aiming at a deeper understanding the environmental significance of the data collected;
- Interpretation of the results, which summarizes and discusses the results of LCI and LCIA.

C.2. Life cycle assessment methodologies

C.2.1. Goal and scope

In general, the goal of an LCA states the intended application, the reason motivating the analysis, and the audience to which the study is intended to be communicated. Goal and scope definition step concerns first the characterization of the system to be studied and the system boundary, as well as the functional unit.

The functional unit must be a defined and measurable unit because its primary purpose is to provide a reference to which the data collected are normalized.

The system boundary determines the unit processes of the whole process considered and their inter-relationships. The characterization

of the product system allows the identification input and output that should be traced to the environment. The system characterization encompasses the selection of material and energy inputs and outputs associated with each of the unit processes. In this step the data can be collected by using recognized data sources or published studies.

The goal and scope definition also provide the determination of the LCIA method used and the relative impact categories and indicators.

The data selected also depend on the goal and scope of the study and they can be collected as a combination of measured, calculated, or estimated data.

C.2.2. Life cycle inventory analysis

Inventory analysis involves data collection and calculation procedures, which quantifies relevant inputs and outputs of the defined product system. The data for each unit process can be classified in four main categories:

- Energy, raw material, ancillary, and other physical inputs;
- Products, co-products, and waste;
- Emissions to air, water, and soil;
- Other environmental aspects.

C.2.3. Life cycle impact assessment

LCIA focuses on evaluating the potential environmental impacts using the LCI results. This step involves associating the collected data with specific impact indicators. However, LCIA addresses only the environmental impacts specified in the goal and scope, thus representing a partial assessment on the environmental issues of the product system being studied. Actually, it is a relative approach based on a functional unit. The ISO-14044 defines the mandatory elements for LCIA:

- The selection of impact categories, category indicators and characterization models;
- Assignment of LCI results to the selected impact category;
- Calculation of category indicator results.

Moreover, for each impact category, the necessary components of the LCIA includes:

- The identification of the category endpoints;
- The definition of the category indicator for given category endpoints;
- The identification of appropriate LCI results that can be assigned to the impact category;

- The identification of the characterization model and the characterization factors.

As general recommendations, the ISO 14044 suggests the use of impact categories internationally accepted. The set of impact categories depends on the LCIA method implemented. Several LCIA methods are available and widely used, some newer and some others older but continuously being updated. A brief description of some of them follows:

CML

This method was developed in 2001 by the University of Leiden in the Netherlands and contains more than 1700 flows. The method is divided in baseline, the most common, and non-baseline. The impact category groups held in the CML baseline method are:

- Acidification potential;
- Climate change;
- Depletion of abiotic resources;
- Ecotoxicity;
- Eutrophication;
- Human toxicity;
- Ozone layer depletion;
- Photochemical oxidation.

On the other hand, the non-baseline CML method encompassed some more category groups, in addition to these:

- Ionizing radiation;
- Land use;
- Odor.

CED (Cumulative Energy Demand)

This method was created on the basis of the method published by the Ecoinvent center. The primary aim of this method is to quantify the energy usage throughout the life cycle, and it is structured in eight impact categories, divided in two groups:

- Non-renewable resource: fossil, nuclear, and primary forest;
- Renewable resources: biomass, geothermal, solar, wind, and water.

ECO-INDICATOR 99

This method replaced the Eco-indicator 95, which was the first endpoint assessment method. The advantage of this method is that it allows the expression of the environmental impact in a single score. It analyzes human health, ecosystem quality, and resources damage.

ECOLOGICAL SCARCITY METHOD 2006

This method focuses on the calculation of environmental impacts as pollutant emissions and resource consumption. It consists in applying eco-factors that depends on the substance, derives from standard targets, and it is expressed in eco-points. The only impact category group is the depletion of abiotic resources.

ILCD 2011

This method was developed by the Joint Research Center through a project of the European Commission, which aim was to analyze several LCIA methods and define the recommended one for each environmental topic. It consists of eleven impact category groups, all of them grouped into three areas of protection (human health, resource depletion, and ecosystem):

- Acidification;
- Climate change;
- Depletion of abiotic resources;
- Ecotoxicity;
- Eutrophication;
- Human toxicity;
- Ionizing radiation;
- Land use;
- Ozone depletion;
- Particulate matter;
- Photochemical oxidation.

TRACI 2.1

This method was developed by EPA specifically for US, using input parameters with US locations for the following impact category groups:

- Acidification;
- Ecotoxicity;
- Eutrophication;
- Climate change;
- Human toxicity;
- Ozone layer depletion;
- Photochemical oxidation;
- Resource depletion.

USEtox

This method focuses mainly in identifying human and eco-toxicological impacts of chemicals, and it consists of two impact category groups only:

- Ecotoxicity;
- Human toxicity.

C.2.4. Life cycle interpretation

The interpretation step puts together the finding from LCI and LCIA to provide a complete presentation of the results and to draw conclusions. As described in the ISO-14044 it may include:

- The identification of the crucial issues with reference to the LCI and LCIA;
- The evaluation of the results;
- Conclusions, limitations, and recommendations.

This phase is strictly connected to the goal and scope definition and must consider also the appropriateness of the system boundary, and the functional unit.

C.3. ReCiPe approach

This method combines the Eco-indicator 99 and the CML method in an updated version. It distinguishes two level of indicators (midpoint and endpoint) and provides a "recipe" to calculate the impact category indicators. The acronym represents also the initials of the contributors: RIVM and Radboud University, CML, and PRé Consultants.
The midpoint level embraces eighteen impact categories:

- Climate change;
- Ozone depletion;
- Terrestrial acidification;
- Freshwater eutrophication;
- Marine eutrophication;
- Human toxicity);
- Photochemical oxidant formation;
- Particulate matter formation;
- Terrestrial ecotoxicity;
- Freshwater ecotoxicity;
- Marine ecotoxicity;
- Ionizing radiation;
- Agricultural land occupation;
- Urban land occupation;
- Natural land transformation;
- Water depletion;
- Metal depletion;
- Fossil depletion.

Table C.1. *Overview of the midpoint categories and characterization factors of the ReCiPe method.*

Impact category name	Characterization factor name	Abbr.	Unit	Emission
Climate change (CC)	Global warming potential	GWP	kg CO_2	to air
Ozone depletion (OD)	Ozone depletion potential	ODP	kg CFC-11	to air
Terrestrial acidification (TA)	Terrestrial acidification potential	TAP	kg SO_2	to air
Freshwater eutrophication (FE)	Freshwater eutrophication potential	FEP	kg P	to water
Marine eutrophication (ME)	Marine eutrophication potential	MEP	kg N	to water
Human toxicity (HT)	Human toxicity potential	HTP	kg 1,4DB	to air
Photochemical oxidant formation (POF)	Photochemical oxidant formation potential	POFP	kg NVOC	to air
Particulate matter formation (PMF)	Particulate matter formation potential	PMFP	kg PM_{10}	to air
Terrestrial ecotoxicity (TET)	Terrestrial ecotoxicity potential	TETP	kg 1,4DB	to soil
Freshwater ecotoxicity (FET)	Freshwater ecotoxicity potential	FETP	kg 1,4DB	to water
Marine ecotoxicity (MET)	Marine ecotoxicity potential	METP	kg 1,4DB	to water
Ionizing radiation (IR)	Ionizing radiation potential	IRP	kg U^{235}	to air
Agricultural land occupation (ALO)	Agricultural land occupation potential	ALOP	m^2 x yr	-
Urban land occupation (ULO)	Urban land occupation potential	ULOP	m^2 x yr	-
Natural land transformation (NLT)	Natural land transformation potential	NLTP	m^2	-
Water depletion (WD)	Water depletion potential	WDP	m^3	-
Mineral resource depletion (MRD)	Mineral resource depletion potential	MDP	kg Fe	-
Fossil fuel depletion (FD)	Fossil fuel depletion potential	FDP	kg oil	-

The endpoint level aggregates the impact categories of the midpoint level into three categories:

- Damage to human health (HH);
- Damage to ecosystem diversity (ED);
- Damage to resource availability (RA).

Table C.2. *Overview of the endpoint categories and indicators of the ReCiPe method.*

Impact category name	Indicator name	Unit
Damage to human health (HH)	Disability-adjusted life years (DALY)	yr
Damage to ecosystem diversity (ED)	Loss of species during a year	yr
Damage to resource availability (RA)	Increased cost	$

The quantitative connection between the two levels depends on the perspective, whether it is individualist (I), hierarchist (H), or egalitarian (E).

Table C.3. *Overview of the relation between midpoint and endpoint impact categories with the environmental impact.*

Environmental impact	Midpoint category	Endpoint category
Climate change	CC	HH, ED
Ozone depletion	OD	HH, ED
Acidification	TA	ED
Eutrophication	FE, ME	-
Toxicity	HT, TET, FET, MET	HH, ED
Human health	POF, PMF	HH
Ionizing radiation	IR	HH
Land use	ALO, ULO, NLT	ED
Water depletion	WD	-
Mineral resource depletion	MRD	RA
Fossil fuel depletion	FD	RA

C.3.1. Climate change

CC impact category in the ReCiPe method considers the effect of CO^2 and other greenhouse gases (GHG), and it is measured as kg of CO^2 equivalent. Generally, climate change is the change in global temperature caused by the GHG released by human activities. The raise in global temperature is expected to cause climatic disturbance, desertification, and rising sea levels, among other effects. The characterization factor for climate change is the GWP, calculated for a substance in a time horizon.

The selection of the time horizon depends on the perspective chosen. The perspective can be:

- Hierarchist (100 years);
- Egalitarian (500 years);
- Individualist (20 years).

CC has effects on the temperature, human health, and ecosystem diversity, which also are the three groups of the ReCiPe method collecting all the impact categories. In the midpoint level, temperature, human health, and ecosystem diversity are calculated as factors to

define the climate change, while the endpoint level combines the temperature and ecosystem factors.

IMPACT CATEGORY	CLIMATE CHANGE	
Definition	Alteration of global temperature caused by GHG	
LCI results	GHG, CFCs	
Midpoint indicator	CC	kg CO^2 eq.
Endpoint indicator	HH, ED	yr

C.3.2. Ozone depletion

OD impact category describe the potential contribution to the so-called "ozone hole" and occurs when the rate of ozone destruction increases due to anthropogenic substances (ODS) which persists in the atmosphere. CFCs (chlorine atoms in chlorofluorocarbons) are the major cause of ozone depletion. Indeed, persisting in the atmosphere, they have the ability to destroy the ozone molecules, thus reducing the ability of the layer to prevent ultraviolet light (UV).

The ODP is a relative measure of the ozone depletion capacity of an ODS using CFC-11 as a reference, thus the unit id kg CFC-11 equivalent. Only damage to human health is addressed to this impact category, as the reduced protection from UV can cause skin cancer, and UV induced cataract.

IMPACT CATEGORY	OZONE DEPLETION	
Definition	Destruction of ozone molecules by ODS	
LCI results	ODS: CFCs	
Midpoint indicator	OD	kg CFC-11 eq.
Endpoint indicator	HH	yr

C.3.3. Terrestrial acidification

TA impact category describe the potential increase of the acidity in soil system. Acid gases such as SO_2 react with water in atmosphere and cause the so-called "acid rains". These cause the damage of the ecosystems even at a considerable distance from the gas source. TAP is expressed in kg SO_2 equivalent, but also considers the NOx emissions, thus including the acidification due to fertilizers.

IMPACT CATEGORY	ACIDIFICATION	
Definition	Reduction of the pH of the soils due to anthropogenic emissions	
LCI results	NOx, NH_3, SO_2	
Midpoint indicator	TA	kg SO_2 eq.
Endpoint indicator	ED	yr

C.3.4. Freshwater and marine eutrophication

Eutrophication is the nutrient enrichment that cause an excessive growth of some species and a decrease in the ecosystem quality. For FE and WE impact categories the reference ecosystem is the aquatic one

that can be damaged by emissions of ammonia, nitrates, N, and P. FE and WE are expressed in kg P equivalent, and kg N equivalent, respectively. An excessive presence of N and P in the aquatic environment can cause a disproportionate growth of algae, thus affecting the water quality and animal population.

IMPACT CATEGORY	EUTROPHICATION	
Definition	Excess of nutrients in aquatic environment	
LCI results	N, P compounds	
Midpoint indicator	FE	kg P eq.
	ME	kg N eq.
Endpoint indicator	ED	yr

C.3.5. Human toxicity and Ecotoxicity

HT, TET, FET, and MET impact categories are characterized by the persistence in the environment (i.e., fate), and accumulation in the human food chain (i.e., exposure), and toxicity (i.e., effect) of a chemical. The emissions of some chemicals, such as heavy metals, have a great impact on the ecosystem. The toxicity potentials, both for human and environment, are calculated considering the fate, the exposure, and the effect and using the reference unit kg 1.4DB (dichlorobenzene) equivalent.

IMPACT CATEGORY	TOXICITY	
Definition	Toxic effect of chemicals on human health and ecosystem	
LCI results	several toxic substances	
Midpoint indicator	HT	kg 1.4DB eq.
	TET	kg 1.4DB eq.
	FET	kg 1.4DB eq.
	MET	kg 1.4DB eq.
Endpoint indicator	HH, ED	yr, m^2 yr

C.3.6. Photochemical oxidant formation and particulate matter formation

POF and PMF impact categories are connected with the releasing to air of non-methane volatile organic compound (NMVOC) and particulate matter with a size of 10 um (PM_{10}). Thus, the reference unit are kg NMVOC equivalent, and kg PM_{10} equivalent, respectively.

PM affects the human health. It is a complex mixture of extremely small particles that contribute to the air pollution. They can be acids, organic chemicals, metals, and soil or dust particles, and cause human health problems, especially affecting the respiratory system. The potential is expressed in kg PM_{10} equivalent.

POF deals with the damaging of human health, and the ecosystem quality. The effect is the so-called “ground level ozone”, which is toxic to humans and is due to the reaction of NMVOC and NO. the reference unit is kg NMVOC equivalent, or kg C_2H_4 equivalent.

IMPACT CATEGORY	PARTICULATE MATTER AND NMVOC	
Definition	Suspended small particles and smog created from anthropogenic processes	
LCI results	PM_{10}, NH_3, SO_2, NOx, NMVOC	
Midpoint indicator	POF	kg NOVOC eq.
	PMF	kg PM_{10} eq.
Endpoint indicator	HH	yr

C.3.7. Ionizing radiation

IR impact category is related to the damage of human health and ecosystem due to the releases of radioactive material to the environment. These emissions can be related to the use of nuclear power as electricity source, even mixed with other sources. The potential related to IR is expressed in kg U^{235} (uranium-235).

IMPACT CATEGORY	IONISING RADIATION	
Definition	Type of emission connected to radioactive molecules	
LCI results	radionuclides	
Midpoint indicator	IR	kg U235
Endpoint indicator	HH	yr

C.3.8. Agricultural and Urban land occupation, and natural land transformation

ALO, ULO, and NLT impact categories reflect the damage to the ecosystem caused by the occupation and transformation of lands. The damage deal with the potentially disappeared fraction (PDF) of species and they are expressed in m^2 yr and m^2, respectively. Many production processes need a certain area of land in some unit of the process, due to for example to the cultivation/production of the raw material, or to the installation used for the manufacturing. During the period that an area is occupied, there are two main effects: on the one hand the regional effect, and on the other hand the local effect. The secondo refers to the occupied area itself, while the first enlarges the area of interest.

IMPACT CATEGORY	LAND USE	
Definition	Impact on the land due to occupation and transformation during processes	
LCI results	land occupation and transformation	
Midpoint indicator	ALO	m^2 yr
	ULO	m^2 yr
	NLT	m^2
Endpoint indicator	ED	yr

C.3.9. Water, mineral resource, and fossil fuel depletion

WD, MRD, and FD impact categories are referred to the consumption of non-biological resources. The value of the resource consumption depends on the scarcity of the substance itself. Practically, it is the

amount of the resource depleted, expressed in kg for mineral resources and fossil fuels, and in m^3 for water.

IMPACT CATEGORY	RESOURCE DEPLETION	
Definition	Use of non-biological resources, i.e. water, minerals, and fossil fuels	
LCI results	freshwater use, extraction of minerals and fossil fuels	
Midpoint indicator	WD	m3
	MD	kg (Fe)
	FD	kg (oil)
Endpoint indicator	RC	$

C.4. Inventory data calculation for the production process

Energy quantity calculations are carried out on a 1000 kg feedstock base, with 10% moisture content (MC) and considering the use of a biomass boiler for all steps involving thermal energy use.

C.4.1. Steam Explosion

First, the amount of steam required per kg of raw material is calculated.

The available data are as follows:

$$Total\ mass = 1\ kg\ (10\%\ MC) = \begin{cases} 900\ g\ dry\ mass \\ 100\ g\ water \end{cases}$$

$$Specific\ heat\ capacity\ of\ biomass\ (30°C \div 207°C) = c_p^b = 1.61\ [\frac{kJ}{kgK}]$$

$$Specific\ heat\ capacity\ of\ water = c_p^w = 4.184\ [\frac{kJ}{kgK}]$$

$$Temperature\ increment = \Delta T = 205°C - 25°C = 180\ [°C\ o\ K]$$

The energy E required for 1 kg of raw material to go from 25°C to 205°C is calculated as follow:

$$E = \left(0.9\ kg\ x\ c_p^b\ x\ \Delta T\right) + \left(0.1\ kg\ x\ c_p^w\ x\ \Delta T\right) = 336.13\ kJ$$

The following data are considered to calculate the amount of steam required:

$$Pressure = P = 30\ [bar]$$
$$Temperature = T = 234\ [°C]$$
$$Steam\ enthalpy = h_s = 2803\ \left[\frac{kJ}{kg}\right]$$
$$Hot\ water\ enthalpy = h_w = 1008\ \left[\frac{kJ}{kg}\right]$$
$$\Delta h = 1795\ [\frac{kJ}{kg}]$$

The amount of steam is obtained by the energy balance:

$$q_s\ x\ \Delta h = E$$
$$q_s \cong 0.2\ [kg]$$

Assuming the use of a biomass boiler, the energy consumed by the process per 1000 kg of feedstock is calculated below. Therefore, the following data are considered:

$$Steam\ pressure = P_s = 30\ [bar]$$

$Maximum\ temperature = T_s = 234\ [°C]$

$Steam\ enthalpy = h_s = 2803\ \left[\frac{kJ}{kg}\right]$

$Hot\ water\ enthalpy = h_w = 1008\ \left[\frac{kJ}{kg}\right]$

$Temperature\ of\ water = T_w = 25\ [°C]$

$Water\ enthalpy\ at\ 25°C = h_{w25} = 90\ \left[\frac{kJ}{kg}\right]$

The Δh of water heating is:

$$\Delta h_w = 918\ [\frac{kJ}{kg}]$$

Whereby, for 1 kg of water at 25 °C transformed into 1 kg of steam at 235 °C and 30 bar, the required enthalpy is calculated:

$$\Delta h_w + (h_s + h_w) = 2713\ [\frac{kJ}{kg}]$$

Th amount of steam necessary for 1000 kg of raw material is:

$$q_s = 0.2\ x\ 1000 = 200\ [kg]$$

Thus, the Energy consumption for the aforementioned quantity is:

$$E_s = 200\ kg\ x\ 2713 \frac{kJ}{kg} = 542600\ [kJ] = 542.6\ [MJ]$$

To calculate the amount of biomass used by the boiler to produce the calculated amount of stem, it is first necessary to consider the heating value of the biomass used, and the yield of the boiler. For the first, a generic low heating vale (LHV) is taken, related to a biomass with a RH of 10% and an ash content <10%. The second was set considering the typical values of biomass boilers:

$$LHV = 16000\ [\frac{kJ}{kg}]$$

$$\eta = 90\ [\%]$$

This way, the amount of biomass is calculated as an energy balance:

$$q_b\ x\ LHV\ x\ \eta =\ \Delta h_w\ x\ q_s$$

Therefore, the amount of biomass is:

$$q_b = \frac{\Delta h_w\ x\ q_s}{\eta\ x\ LHV} = 38\ [kg]$$

C.4.2. Rinsing

The actual amount of water used to wash the material after STEX is very difficult to estimate and can only be based on assumptions and sensitivity analysis.

Considering 1000 kg of raw material at 10% MC, 900 kg of dry material and 100 kg of water enter the STEX reactor. During the treatment, the material loses about 20% by dry weight, so at the reactor outlet there will be:

720 kg dry material
100 kg initial moisture

180 kg steam
180 kg hydrolyzed material
Total = 1180 kg

The MC at this point raised to 64%. Assuming that the RH after rinsing rises further to 100%, the following can be calculated:

$$\begin{cases} 720\ kg\ dry\ material \\ 460\ kg\ water \end{cases} \rightarrow \quad rinsing\ 7200\ kg\ water \quad \rightarrow \quad \begin{cases} 720\ kg\ dry\ material \\ 1180 + 7200 - 720 = 7760\ kg\ water \end{cases}$$

From the last value of the total water after rinsing, the residual water can be obtained by subtracting the moisture of 100%:

$$7760\ kg - 720\ kg = 6940\ [kg]$$

C.4.3. Drying

The material that comes to the drying step has a MC of 100%, so there are 720 kg of dry material, and 720 kg of water. The objective of the drying step is to reach a 10% MC, so 648 kg of water has to be evaporated. The data available on the air characteristics at ambient condition are:

T_{a25} = 25 °C
RH_{25} = 65%
$AH_{25} = 13.2\ \frac{g}{kg}\ dry\ air$
$h_{a25} = 57.5\ \frac{kJ}{kg}\ dry\ air$

Setting a maximum temperature of 35 °C, the available data on the heated air characteristics are:

T_{a35} = 35 °C
RH_{35} = 38%
$AH_{35} = 13.2\ \frac{g}{kg}\ dry\ air$
$h_{a35} = 69.5\ \frac{kJ}{kg}\ dry\ air$

An isenthalpic process up to RH 90% is considered. At these conditions, air characteristics are:

T_{a90} = 24.5 °C
RH_{90} = 90%
$AH_{90} = 17.5\ \frac{g}{kg}\ dry\ air$
$h_{a90} = 69.5\ \frac{kJ}{kg}\ dry\ air$

From these data, the kg of water evaporated froe ac kg of dry air can be calculated by the formula:

$$AH_{90} - AH_{35} = 4.3\ [\frac{kg_w}{kg_{dry\ air}}]$$

The enthalpy variation is:

$$h_{a35} - h_{a25} = 12\ [\frac{kJ}{kg}]$$

Which represents the energy used to heat the air from 25°C to 35°C. The quantity of dry air is calculated as follow:

$$q_a = \frac{648\ kg\ x\ 1000}{4.3\ \frac{g}{kg\ dry\ air}} = 150697.7\ [kg\ dry\ air]$$

The amount of biomass used by the boiler is derived as follow:

$$q_b\ x\ LHV\ x\ \eta = \ q_a\ x\ (h_{a35} - h_{a25})$$

Thus, the amount of biomass is:

$$q_b = 104,65\ kg$$

C.4.4. Cold and Hot pressing

For CP, only the electrical energy is considered, calculated on the basis of the assumed linear relationship of the maximum pressure, set at 16 N/mm^2, and the change in thickness, assuming that at each step the thickness halves. The calculation is here made on laboratory size of the specimen (150x50x3 mm^3), and then carried over to the required measurement. Available data are, then:

t_i = 0.0132 m
t_f = 0.0066 m
V_i = 0.000099 m^3
V_f = 0.0000495 m^3
$|\Delta V|$ = 0.0000495 m^3
P_{max} = 16 N/mm^2

The work is calculated as the area under the curve of the P-V plot:

$$W_{CP} = \frac{1}{2}\ x\ 16000000\frac{N}{m^2}\ x\ 0.0000495\ m^3 = 396\ [J] = 9.86\ kWh$$

For HP, both electrical and thermal energy were considered. The first one is calculated as for the CP. The data are:

t_i = 0.0066 m
t_f = 0.0033 m
V_i = 0.0000495 m^3
V_f = 0.00002475 m^3
$|\Delta V|$ = 0.00002475 m^3
P_{max} = 7.5 N/mm^2

Therefore, the work is:

$$W_{HP} = \frac{1}{2}\ x\ 7500000\frac{N}{m^2}\ x\ 0.00002475\ m^3 = 92.81\ [J]$$

Considering 1000 kg of material, the works are:

W_{CP} = 3.86 kWh
W_{HP} = 0.912 kWh

To calculate the thermal energy for HP, the temperature increases between 25 °C and 205 °C is considered. The following data are necessary for the calculation:

T_0 = 20 °C
T_f = 205 °C
Plates material → Iron
Plate dimension = 30x30x40 cm^3
Plate volume = V_p = 0.009 m^3
Plates number = n_p = 2

Iron density = ρ = 7850 kg/m^3
Iron specific heat = c = 456 J/kg°C

The energy applied to heat the plates from 20 °C to 205 °C is:

$$Q = m\ x\ c\ x\ \Delta T = (\rho V)\ x\ c\ x\ (T_f - T_0) = 5960.034\ [kJ]$$

Therefore, the amount of biomass for the boiler to produce heat is calculated from the energy balance:

$$q_b\ x\ LHV\ x\ \eta = Q$$
$$q_b = 0.4\ [kg]$$

This value is considered doubled for the heating of two plates.

C.4.5. Final heat treatment

A heat treatment lasting 5 h at a temperature of 170°C is considered as example. The data considered are then:

T_0 = 25 °C
T_f = 170 °C
t_c = 18000 s
Air heat capacity = cp = 1.012 kJ/kgK
Air flow = fl = 0.1 kg/s

The energy is calculated as:

$$E = c_p\ x\ fl\ x\ t_c\ x\ \Delta T = 246132\ kJ = 73.84\ kWh$$

Then, the energy balance for the amount of biomass calculation is:

$$q_b\ x\ LHV\ x\ \eta = E$$
$$q_b = 18\ [kg]$$